FORMULATION AND EVALUATION OF NANOSIZED DRUG FORMULATIONS AS NOVEL DELIVERY SYSTEM FOR DRUGS WITH LOW BIOAVAILABILITY

A thesis submitted to

THE MAHARAJA SAYAJIRAO UNIVERSITY OF BARODA

For the award of the degree of

DOCTOR OF PHILOSOPHY
in
PHARMACY

By

SANDIP SHIVAJI CHAVHAN

Under the guidance of

PROF. KRUTIKA K. SAWANT

सत्यं शिवं सुन्दरम्

Pharmacy Department,
Faculty of Technology and Engineering,
The M. S. University of Baroda,
Vadodara-390 001

DECEMBER 2011

DECLARATION

In accordance with University ordinance number ACED-309 Ph.D., I, the undersigned states that, the work presented in this thesis entitled "Formulation and evaluation of nanosized drug formulations as novel delivery system for drugs with low bioavailability" comprises independent investigations carried out by me. Wherever references have been made to the work of others, it has been clearly indicated with the source of information under the title of references at end of each chapter.

Date:

Place: Vadodara   (Sandip Shivaji Chavhan)

Certified by and forwarded through research guide,

Prof. Krutika K. Sawant,
Pharmacy Department,
Faculty of Technology and Engineering,
The Maharaja Sayajirao University of Baroda,
Vadodara- 390 001

<u>CERTIFICATE</u>

This is to certify that the thesis entitled "Formulation and evaluation of nanosized drug formulations as novel delivery system for drugs with low bioavailability" submitted for the Ph. D. Degree in Pharmacy by Mr. Sandip Shivaji Chavhan incorporates the original research work carried out by him under my supervision and no part of this work has been previously submitted for any degree.

Guide   Head

Prof. Krutika. K. Sawant   Pharmacy Department

DEAN

Faculty of Technology & Engineering,

The M.S. University of Baroda,

Vadodara -390 001

DEDICATION

I wish to dedicate this thesis to my late mother,

Saraswati

She taught me to persevere and prepared me to face the challenges with faith and humility. She was constant source of inspiration to my life. Although she is not here to give me strength and support I always feel her presence that used to urge me to strive to achieve my goals in life.

And

My father

Who always had confidence in me and offered me encouragement and support in all my endeavors

Acknowledgements

INDEX

LIST OF FIGURES

LIST OF TABLES

LIST OF ABBREVATIONS

ABPR -Automated back pressure regulator

DLS -Dynamic Light Scattering

DSC -Differential Scanning Calorimetry

ENE - Entacapone nanoemulsion

ENS -Entacapone nanosuspension

ENT-Entacapone

E-SDPs- Entacapone Solid dispersion particles

HPH –High pressure homogenization

NE-Nanoemulsions

NS-Nanosuspensions

PCS -Photon correlation spectroscopy

PD-Plain drug suspension

PIT -Phase inversion temperature

RESS -Rapid Expansion of Supercritical Solutions

RSM -Response Surface Methodology

SAS -Supercritical Anti Solvent process

SCF -Supercritical fluid

SDP -Solid dispersion particles

SEM -Scanning Electron Microscopy

SIM -Simvastatin

SNE -Simvastatin nanoemulsion

SNS -Simvastatin nanosuspension

TEM- Transmission Electron Microscopy

XRD-X-ray diffraction

1.1 Introduction

An important fraction (~40%) of the new drug candidates emerging from drug discovery programs has poor water solubility and this trend is not expected to change in the future [Stegemann et al; 2007]. Nowadays, large portion of new molecules come from combinatorial chemistry which focuses on target-receptor geometry, target identification and lead candidate generation. However, candidates emerging from these screens invariably have high molecular mass and high Log P, which contribute to insolubility. Also, high affinity and high specificity binding to molecular targets generally entails some degree of hydrophobic interactions which leads to solubility constraints. The major problem of many newly developed pharmaceutical drugs is their poor solubility in water and simultaneously in organic media. The basic challenges associated with poorly soluble drugs are low bioavailability and/or erratic absorption. In case of poor bioavailability after oral administration, many times parenteral administration cannot solve this problem. Available strategies for poorly water soluble drugs include; aqueous mixtures with an organic solvent (e.g. water-ethanol), solubilization, formation of complexes e.g. using β-cyclodextrin, solid dispersions, co crystallization, exploiting the effects of pH or salt form. But, these approaches have certain limitations such as side effects associated with co-solvents, need for sufficient ionizing groups for salt formation, need for possessing sufficient solubility in oils or other hydrophobic media, need for having a suitable molecular size and shape to incorporate in the cyclodextrin ring etc. Hence, identification of some novel formulation approaches for drugs having poor water solubility is the mainstay of drug delivery research throughout the world.

The oral route is by far the most convenient one for drug administration. However, for oral administration, the low concentration gradient between the gut and blood vessel due to the poor solubility of the drug leads to a limited transport, consequently influencing its oral absorption. The pharmacological effect for any orally-administered drug relies on involved mechanism of transport from the site of entry into the body to the site of action [Klueglich et al; 2005]. Recent drug delivery research mainly focuses on nanotechnology based strategies for poorly water soluble drugs in order to improve their therapeutic performance. Nanoparticulate technology has proven its competence for numerous drugs

for large number of applications. The versatility, flexibility and adaptability of the nanoparticulate delivery systems have proven their potential to fulfill the need for improved health care and better patient compliance. Nanoparticulate delivery systems include polymeric nanoparticles, solid lipid nanoparticles, nanoemulsions, liposomes, nanostructured lipid carriers, nanogels and drug nanoparticles. The oral delivery of poorly water soluble drugs presents a major challenge because of their low aqueous solubility. For such compounds, the absorption rate from the gastrointestinal (GI) lumen is controlled by dissolution [Amidon et al; 1995]. In recent years, much attention has focused on particle size engineering and lipid based formulations to improve the oral bioavailability of poorly water soluble drug compounds. Nicolaos et al reported that the bioavailability of cefpodoxime proxetil increased from 50 to 98 % when using submicronic emulsions for oral administration [Nicolaos et al; 2003]. Some investigations show that the dissolution rate of griseofulvin particles with sizes in the range of 200 nm was about two-fold higher than for the conventional micronized material [Turk et al; 2002]. There are many reports available which prove that these approaches are very successful for drugs having low bioavailability. Particulate drug delivery systems offer great promise to increase drug absorption at intestine.

Pure drug nanoparticles are nowadays considered as a viable formulation route for the oral administration of drugs having poor dissolution rate and/or aqueous solubility [Kessisoglou et al; 2007]. The ability to formulate poorly-water soluble compounds as nanometer sized particles can have a dramatic effect on performance, such as enhancing bioavailability, eliminating food effects, allowing for dose escalation and hence improving efficacy and safety. The potential of nanosized particles to alter tissue distribution after intravenous dosing should always be a consideration. Nanosizing technology (nanonization) has also been applied to reduce variability in pharmacokinetic behavior of oral dosage forms [Shono et al; 2010]. Nanosizing drug or formulating drug as a nanoparticulate system results in better dissolution and solubilization of drug due to increase in surface area and saturation solubility. Since this approach has been adopted to handle milligram quantities of drug substance, this technology provides an avenue for the research scientist to improve screening efforts without having to deal with solubility-

related performance issues. The utility of this technology has been proven from the number of marketed/available products based on these techniques. Also, for marketed products that have performance issues related to poor solubility of the active, reformulation into nanosized dosage forms can offer the possibility of adding new life to old compounds while improving efficacy and patient compliance.

The two main approaches used for nanosizing drug or formulating drug nanoparticles are top down and bottom up approaches. Top down approach is widely used and generally referred to as nanosizing. This approach is based on use of mechanical force to convert large crystalline particles to nanosized drug particles. Bottom up approach involves controlled precipitation i.e. drug is dissolved in one solvent and then it is precipitated by addition of antisolvent in a controlled manner. One top down (media milling) and one bottom up (supercritical technique) are gaining wide acceptability now days. Media milling is a widely used top down approach for nanonization of the drug. Among all methods reported for nanosizing drug particles in pharmaceutical industry, media milling technique is considered to be the leader with highest commercial applicability. In this technique, the drug particles are subjected to media milling wherein the high-energy shear forces generated as a result of impaction of the milling media with drug provide energy to disintegrate drug micro-particles to nanosized drug particles. In this method, the milling chamber is charged with milling pearls, dispersion medium (e.g. water), drug powder and stabilizer. The pearls are rotated at a very high speed to generate strong shear forces which disintegrate the drug powder into nanoparticles [Merisko-Liversidge et al; 2003].

Supercritical fluid (SCF) technologies have revealed great potential in particle engineering and have emerged as an alternate to most of the existing techniques. SCF technology has been used to manufacture fine particles of medicinal substances by a build-up process i.e. in contrast to conventional bottom up technique; this involves growing of the particles in controlled fashion to attain desired morphology. For particle size reduction of neat drug particles, two SCF technologies are generally used, Rapid Expansion of Supercritical Solutions (RESS) and Supercritical Anti Solvent (SAS) process. In the SAS method, the solid material (drug) is dissolved in an organic solvent and a supercritical fluid is then forced by means of pressure to dissolve in it. In this way, the volume of the system is expanded, thus

lowering the density, and therefore the solubility of the material of interest is also decreased. As a result, the material precipitates out of the solution as a solid with a very small particle diameter. In the case of RESS, the supercritical fluid is used to dissolve the solid material (drug) under high pressure and temperature, thus forming a homogeneous supercritical phase. Thereafter, the solution is expanded through a nozzle and drug nanoparticles are formed. Recently, the SAS process has been proposed as an alternative for formulating coprecipitates that may be smaller in particle size and lower in residual organic solvent. Solid dispersion particles (SDP) of felodipine with enhanced solubility and dissolution rate were prepared by SAS method using HPMC (Won et al; 2005).

Nanoemulsion drug delivery system is one of the promising technologies, which is being applied to enhance the oral bioavailability of the poorly soluble drugs. Nanoemulsions are a class of emulsions with a droplet size between 20 and 500 nm [Tadros; 1983]. Nanoemulsions are transparent or translucent systems mostly covering the size range 50–200 nm [Nakajima; 1997]. A nanoemulsion has fundamental difference from microemulsions. Microemulsions are equilibrium systems (i.e. thermodynamically stable), while nanoemulsions are non-equilibrium systems with a spontaneous tendency to separate into the constituent phases. Nevertheless, nanoemulsions may possess a relatively high kinetic stability [Gutierrez et al; 2008]. In addition, high kinetic stability, low viscosity and optical transparency make them very attractive systems for industrial applications in the pharmaceutical field as drug delivery systems [Taha et al; 2004].

Many deadly diseases are treated with first line drugs that are having problem of poor bioavailability. There is need of suitable delivery systems for such drugs. Cardiovascular diseases (CVD) are the most prevalent cause of death and disability in both developed as well as developing countries. CVD is usually due to atherosclerosis of large and medium sized arteries and dyslipidemia has been found to be one of the most important contributing factors. Dyslipidemias, including hyperlipidemia (hypercholesterolemia) and low levels of high-density-lipoprotein cholesterol (HDL-C), are major causes of increased atherogenic risk. Hyperlipidemia is a major cause of atherosclerosis and atherosclerosis-associated conditions, such as coronary heart disease (CHD), ischemic cerebrovascular disease, and peripheral vascular disease. The statin class of drugs that lower cholesterol

levels are among the most commercially successful drugs. Simvastatin is a first line option for treatment of hyperlipidemia but suffers from problem of low solubility and poor bioavailability.

Simvastatin (SIM) is a lipid-lowering agent that is derived synthetically from a fermentation product of Aspergillus terreus. SIM, an inactive lactone, is hydrolyzed to the corresponding hydroxyacid form after oral administration. It is a potent inhibitor of 3-hydroxy-3-methylglutaryl-coenzyme A (HMG-CoA) reductase. This enzyme catalyzes the conversion of HMG-CoA to mevalonate, which is an early and rate-limiting step in the biosynthesis of cholesterol. SIM, a crystalline powder, is practically insoluble in water and poorly absorbed from the gastro-intestinal (GI) tract. It is a BCS class II drug (Graeser et al; 2008) and shows poor bioavailability due to limited dissolution rate [Jun et al; 2007]. Therefore, improvements in solubility and/or dissolution rate of this poorly water-soluble drug may lead to enhancement in their bioavailability [Yamamura and Rogers; 1996].

Parkinson's disease (PD) is major neurodegenerative disease characterized by progressive degeneration of the dopaminergic nigrostriatal pathways, which results in marked loss of cerebral dopamine. Worldwide there are likely to be more than 6 million people with PD. The prevalence of PD is about 0.3% of the whole population in industrialized countries. PD is more common in the elderly and prevalence rises from 1% in those over 60 years of age to 4% in the population over 80. The mean age of onset is around 60 years, although 5–10% of cases, classified as young onset, begin between the ages of 20 and 50. However, due to so many people with Parkinson's disease remaining undiagnosed, there may be millions more. There is no cure for Parkinson's disease, but medications, surgery and multidisciplinary management can provide relief from the symptoms.

Entacapone (ENT) is an inhibitor of catechol-O-methyltransferase (COMT), used in the treatment of Parkinson's disease as an adjunct to levodopa/carbidopa therapy. The aqueous solubility of Entacapone increases with increased pH. Its bioavailability after oral administration is low (29–46%) and is characterized by large inter individual variation [Keranen et al; 1994]. The reason for poor bioavailability may be poor aqueous solubility in GI fluids, poor membrane permeation and first pass effect. Entacapone as per BCS

classification is a class IV drug (Kalantri; 2010). Nanosized formulations are reported to improve aqueous solubility, permeability and avoiding first pass effects. Thus, improving the solubility and dissolution rate could lead to improved bioavailability and therapeutic activity of Entacapone.

1.2 Aims & objectives:

The present investigation was aimed at the development of nanoparticulate delivery system for oral administration of Simvastatin and Entacapone with following objectives:

- To formulate nanoparticulate delivery systems such as drug nanoparticles and nanoemulsions with improved solubility, dissolution rate and improved permeability which ultimately will increase absorption and hence bioavailability of the poorly water soluble drugs
- To evaluate the prepared formulation for in vitro and in vivo parameters
- To prove the utility of nanosizing approaches in improving oral bioavailability of drugs with poor water solubility
- To compare the prepared nanoparticulate systems with respect to ease of formulation, improvement in solubility and dissolution rate, in vitro characteristics, stability and in vivo performance viz. pharmacokinetic and pharmacodynamic studies.

1.3 Plan of Work:

- Literature survey, procurement of APIs and excipients
- Preformulation studies – Screening of excipients and characterization of API
- Formulation of Nanoparticulate systems for Simvastatin and Entacapone: Nanosuspension, nanoemulsion and nanoparticles by SAS method
- Optimization of process and formulation variables for each formulation by factorial design.
- In vitro characterization and drug release studies of these formulation in comparison with plain drug suspension
- Stability studies – Short term stability studies
- In vivo pharmacokinetic and pharmacodynamic studies of Simvastatin formulations.
- In vivo pharmacokinetic studies of Entacapone formulations.

1.4 References

- Amidon GL, Lennernas H, Shah VP, Crison JR. A theoretical basis for a biopharmaceutical drug classification: the correlation of in vitro drug product dissolution and in vivo bioavailability. Pharm Res. 12, 1995, 413–420.

- Graeser KA, Strachan CJ, Patterson JE, Gordon KC, Rades T. Physicochemical Properties and Stability of Two Differently Prepared Amorphous Forms of Simvastatin. Cryst Growth Des. 2008, 8(1), 128–135.

- Gutierrez JM, Gonzalez C, Maestro A, Sole I, Pey CM, Nolla J. Nano-emulsions: New applications and optimization of their preparation. Curr Opin Colloid Int Sci. 13, 2008, 245–251.

- Jun SW, Kim MS, Kim JS, Park HJ, Lee S, Woo JS. Preparation and characterization of Simvastatin/hydroxypropylbeta-cyclodextrin inclusion complex using supercritical antisolvent (SAS) process. Eur J Pharm Biopharm. 66, 2007, 413–421.

- Kalantri MR. Pharmaceutical compositions of Entacapone. United States Patent. US 2010/ 0104634, Apr 29, 2010.

- Keranen T, Gordin A, Karlsson M, Korpela K, Pentikainen PJ, Rita H, Schultz E, Seppala L, Wikberg T. Inhibition of soluble catechol catechol-O-methyltransferase and single-dose pharmacokinetics after oral and intravenous administration of Entacapone. Eur J Clin Pharmacol. 46, 1994, 151–157.

- Kessisoglou F, Panmai S, Wu Y. Nanosizing - Oral formulation development and biopharmaceutical evaluation. Adv drug deliv Rev. 59, 2007, 631-644.

- Klueglich M, Ring A, Scheuerer S, Trommeshauser D, Schuijt C, Liepold B, Berndl G. Ibuprofen extrudate, a novel, rapidly dissolving ibuprofen formulation: relative bioavailability compared to ibuprofen lysinate and regular ibuprofen and food effect on all formulations. J Clin Pharmacol. 45, 2005, 1055–1061.

- Merisko-Liversidge E, Liversidge GG, Cooper ER. Nanosizing: a formulation approach for poorly water-soluble compounds. Eur J Pharm Sci. 18, 2003, 113–120.

- Nakajima H, in: Solans C, Konieda H, (Eds.), Industrial Applications of Microemulsions, Marcel Dekker, 1997. pp. 175-197.

- Nicolaos G, Crauste-Manciet S, Farinotti R, Brossard D. Improvement of cefodixim poxetil oral absorption in rats by an oil-in-water submicron emulsion. Int J Pharm. 263, 2003, 165–171.

- Shono Y, Jantratid E, Kesisoglou F, Reppas C, Dressman JB. Forecasting in vivo oral absorption and food effect of micronized and nanosized aprepitant formulations in humans. Eur J Pharm Biopharm. 76, 2010, 95–104.

- Stegemann S, Leveiller F, Franchi D, de Jong H, Linden H. When poor solubility becomes an issue: from early stage to proof of concept. Eur J Pharm Sci. 31, 2007, 249–261.

- Tadros T, in: Becher P. (Ed.), Encyclopedia of Emulsion Technology, vol. 1, Marcel Deckker, New York, 1983, pp. 129–285.

- Taha EI, Al-Saidan S, Samy AM, Khan MA. Preparation and in vitro characterization of self nanoemulsified drug delivery system (SNEDDS) of all trans-retinol acetate. Int J Pharm. 285, 2004, 109-119.

- Turk M, Hils P, Helfgen B, Schaber K, Martin HJ, Wahl MA. Micronization of pharmaceutical substances by rapid expansion of supercritical solutions (RESS): a promising method to improve bioavailability of poorly soluble pharmaceutical agents. J Supercrit Fluids 22, 2002, 75–84.

- Won D, Kim M, Lee S, Park J, Hwang S. Improved physicochemical characteristics of felodipine solid dispersion particles by supercritical anti-solvent precipitation process. Int J Pharm. 301, 2005, 199–208.

- Yamamura S, Rogers LA. Characterization and dissolution behaviour of nifedipine and phosphatidylcholine binary systems. Int J Pharm. 130, 1996, 65-73.

The interest in the preparation and application of nanometer sized materials is increasing due to their tremendous potential as a drug delivery system with wide range of applications. Recently, nanoscale systems have gained much interest to resolve solubility issues due to their cost effectiveness and technical simplicity as compared to liposomes and other colloidal drug carriers. Two major nanoscale systems pure drug nanoparticles prepared by nanosizing and nanoemulsions. Both systems are gaining much attention in recent times for improving the oral bioavailability of poorly soluble drugs.

Nanosizing approaches include size reduction by high energy methods and by supercritical technology. Nanosizing approaches have proved to be a better alternative over other approaches currently available for improving bioavailability of a number of poorly soluble drugs. These approaches have been extensively developed for a wide range of drugs and evaluated for *in vitro* and *in vivo* applications by various routes like parenteral, oral, pulmonary, topical, and also for drug targeting.

The oral bioavailability of poorly water-soluble, lipophilic drugs may be enhanced when co-administered with a meal rich in fats. This realization has led to increased interest in formulation of poorly water-soluble drugs in lipids as a means to enhance drug solubilisation in the gastrointestinal tract (GIT). For some drug candidates, lipid-based drug delivery systems provide an effective and practical solution to the problem of formulating drugs where low solubility in the fluids of the GIT limits drug exposure. Nanoemulsions have all been used to enhance the oral bioavailability of many poorly water soluble drugs and are gaining more attention in recent period. Nanoemulsions have been extensively developed for a wide range of drugs and showed applications by various routes like parenteral, oral, pulmonary, topical, and drug targeting.

2.1 Nanosizing approaches

Poorly-water soluble compounds are known to comprise a significant and growing percentage of the industrial drug development pipeline and historically they have been viewed as highly risky development candidates (Krishnaiah; 2010). Poorly water-soluble drugs with poor bioavailability often result in higher cost to the consumer, inefficient treatment and increased risk of toxicity. Thus, there is urgent need of formulation

strategies for these classes of drugs which include molecules in BCS classification II (poorly soluble and permeable) and Class IV (poorly soluble and impermeable).

Nanoparticulate technology has proven its competence for numerous drugs for large number of applications. The nanoparticulate delivery systems have proven their potential to fulfill the need for improved health care and better patient compliance due to their versatility, flexibility and adaptability. Nanoparticulate delivery systems include polymeric nanoparticles, solid lipid nanoparticles, nanoemulsions, liposomes, nanostructured lipid carriers, nanogels and drug nanoparticles. Nano-drug formulations have been developed to enhance dissolution and bioavailability of drugs with poor aqueous solubility [Kesisoglou et al; 2007).

Pure drug nanoparticles are nowadays considered as a viable formulation route for the oral administration of drugs having poor dissolution rate and/or aqueous solubility (Kesisoglou et al; 2007). The ability to formulate poorly-water soluble compounds as nanometer sized particles can have a dramatic effect on their performance, such as enhancing bioavailability, eliminating food effects and allowing for dose escalation, thereby improving their efficacy and safety (Merisko-Liversidge and Liversidge 2011). The potential of nanosized particles to alter tissue distribution after intravenous dosing should always be a consideration. For pure drug nanoparticles, tissue distribution by intravenous dosing depends upon the particle size and surface properties. However, solubility of the compound in blood is the primary attribute that determines its tissue distribution. If the compound is soluble in blood, the pure drug nanoparticles' formulation will have a pharmacokinetic profile similar to a solution and if the compound has poor solubility in blood, the formulation will behave similarly as other nanoparticulate formulation [Merisko-Liversidge and Liversidge 2011]. Nanosizing technology (nanonization) has also been applied to reduce variability in pharmacokinetic behavior of oral dosage forms (Shono et al; 2010]. Nanosizing drug or formulating drug as a nanoparticulate system results in better dissolution and solubilization of drug due to increase in surface area and saturation   solubility. Pure drug nanoparticles have an edge over liposomes, microemulsions and polymeric nanoparticles in terms of commercialization, drug loading capacity, site-specific delivery, cost efficacy, carrier associated side effects, local delivery

and delivery of poorly water and lipid soluble drugs (Date and Patravale; 2004). Since this approach has been adapted to handle milligram quantities of drug substance, this technology provides an avenue for the research scientist to improve screening efforts without having to deal with solubility-related performance issues. The utility of this technology has been proven from the number of marketed/available products based on these techniques. Also, for marketed products that have performance issues related to poor solubility of the active, reformulation into nanosized dosage forms can offer the possibility of adding new life to old compounds while improving efficacy and patient compliance.

2.1.1 Mechanism of solubility enhancement by nanonization

Nanonization of drug particles leads to an increase in the surface area, resulting in increased dissolution rate, according to Noyes–Whitney equation (Eq. 1.1).

$$\frac{dX}{dt} = \frac{D.S}{h}\left(Cs - \frac{Xd}{V}\right) \qquad (1.1)$$

Where, dX/dt is dissolution rate, Xd is amount dissolved, D is diffusion coefficient, S is particle surface area, V is volume of fluid available for dissolution, Cs is saturation solubility, h is effective boundary layer thickness.

The equation shows that the dissolution rate of drug is proportional to the surface area available for dissolution. This principle has been extensively used in micronization of drugs for improving their oral bioavailability. Obviously, decrease in particle size to nanometer range will further increase the dissolution rate due to significant increase in effective particle surface area. As per Prandtl equation (Eq. 1.2), nanonization results in the decrease of the diffusion layer thickness surrounding the particles and an increased concentration gradient between the surface of the particle and bulk solution, which facilitates particle dissolution by increasing dissolution velocity.

$$h_H = k.\left(\frac{L^{\frac{1}{2}}}{V^{\frac{1}{2}}}\right) \qquad (1.2)$$

h_H- hydrodynamic boundary layer thickness, k- constant, V- relative velocity of the flowing liquid against a flat surface, L- length of the surface in the direction of flow.

It is clear from Eqs. 1.1 & 1.2 that nanosizing is a suitable approach for increasing bioavailability of poorly soluble drugs, where dissolution is the rate limiting step in systemic absorption (Sharma et al; 2010)

Another important aspect of nanonization is increase in saturation solubility, which can be explained by the Kelvin-Gibbs (Eq. 1.3) and the Ostwald–Freundlich (Eq. 1.4) equations.

As per Kelvin equation, the vapor pressure increases with increasing curvature of the droplet of a liquid in gas. If this is extended to a solid, it implies that the dissolution pressure increases with decrease in particle size.

According to Ostwald-Freundlich equation, the increased saturation solubility is due to creation of high energy surfaces when disrupting the more or less ideal drug microcrystal to nanoparticle (Muller and Peters; 1998).

$$\frac{P_r}{P_\infty} = \frac{2\gamma M}{rRT\rho} \qquad (1.3)$$

$$S = S_\infty \exp\left(\frac{2\gamma M}{r\rho RT}\right) \qquad (1.4)$$

Where, P_r is the dissolution pressure of a particle with radius r, $P\infty$ is the dissolution pressure of infinitely large particle, S is saturation solubility of the nanosized drug, $S\infty$ is saturation solubility of an infinitely large drug crystal, γ is the crystal medium interfacial tension, M is the compound molecular weight, r is the particle radius, ρ is the density, R is a gas constant and T is the temperature.

The theoretical backgrounds of Kelvin, Ostwald-Freundlich and Prandtl equations support the fact that below a size of approximately 1-2µm, the saturation solubility is a function of the particle size.

Nanosized particles also possess increased adhesiveness due to increased contact area of these particles as compared to micro-particles. The actual interpretation of this is depicted in Fig. 2.1.

1. dissolution pressure $(\Delta p \sim 1/r)$ $\longrightarrow$ $Cs_N > Cs_M$

substance layer
(flat surface)

large particle
(slight curvature)

nanosuspension
(strong curvature)

2. increased dissolution velocity dc/dt (~ Cs, ~ 1/h)

concentration gradient

Cx - concentration in
surrounding medium

large
microparticle
(app. 40 - 1000 μm)
e.g. "normal"
powder

h_M

Cs_M - layer of saturated solution
on the surface

larger
concentration gradient

nanosuspension

h_N

$$\Rightarrow \frac{Cs_N - Cx}{h_N} >> \frac{Cs_M - Cx}{h_M}$$

$Cs_N > Cs_M$
$h_N < h_M$

Fig. 2.1: Mechanisms of increasing saturation solubility (Cs) and dissolution velocity in nanosuspensions. (Δp, dissolution pressure; Cs_N, saturation solubility nanoparticles; Cs_M, saturation solubility microparticles; h_M, diffusional distance microparticles; h_N, diffusional distance nanoparticles (Muller et al; 1998).

2.1.2 Formulation theory:

Nanoparticles can be formed by building particles up from the molecular state, as in precipitation, or by breaking larger micron-sized particles down, as in milling. In either case, a new surface area, ΔA, is formed, which necessitates a free-energy (ΔG) cost as defined by $\Delta G = \gamma s/l \cdot \Delta A$, in which $\gamma s/l$ is the interfacial tension. This arises because water molecules incur fewer attractive forces with other water molecules when located at a free surface. The system prefers to reduce this increase in surface area by either dissolving incipient crystalline nuclei, in the case of precipitation, or by agglomerating small particles,

regardless of their formation mechanism. This tendency is resisted by the formulator through the addition of surface-active agents, which reduce the γs/l and therefore the free energy of the system (Fig. 2.2).
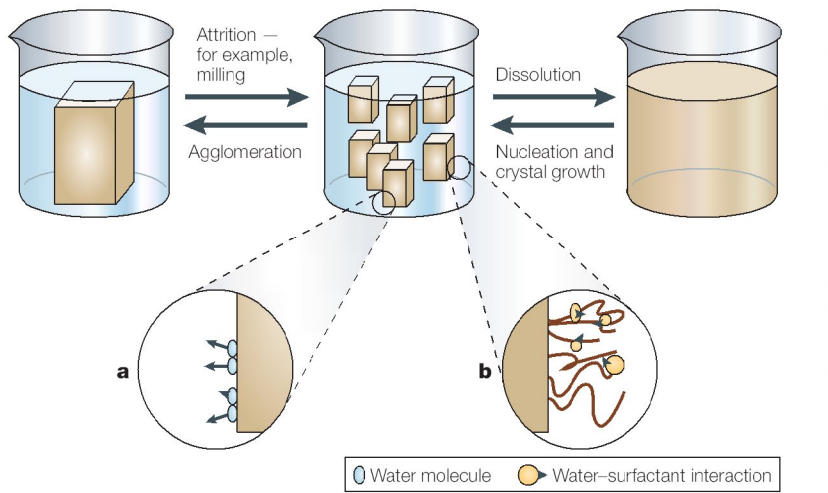
Fig. 2.2 Creation and stabilization of nanoparticles, from the perspective of surface energetics.

a)   In the case of unfavorable energetics, hydrophobic crystal surface directly contacting water molecules leads to crystal agglomeration, because water molecules are energetically driven to leave the surface, as shown by the arrows.

b)   A surfactant stabilized crystal surface reduces interfacial tension by allowing attractive water surfactant interactions. The crystal surface is stabilized and shows reduced tendency to agglomerate.

These agents confer immediate protection and are more effective when present at the time of creation of the new, fresh surface than if added afterwards. By virtue of their complementary properties, surfactants of two classes are utilized: charged or ionic surfactants, which effect an electrostatic repulsion among the particles; and non-ionic polymers, which confer a steric repulsion that is, they resist compression. If the particles approach each other too closely, they will agglomerate. This must be prevented to ensure a stable system. Energetically, this requires the placement of a sufficiently high energy barrier at relatively long separation distances, to prevent the particles coming too close together. Therefore, a non-ionic polymeric surfactant is also used that coats the surface with a hydrophobic chain, and permits a hydrophilic tail to project into the water.

Compression of the polymeric coating, as by the approach of a similarly coated particle, causes loss of entropy and is therefore unfavorable. This provides the necessary repulsive barrier between two neighboring particles. The polymeric coating performs a dual role: inhibiting crystal growth and reducing particle size (Ziller K H; 1990)

Both electrostatic and steric mechanisms are enabled by combining polymers and ionic surfactants, which therefore complement each other. Entropic steric interactions are inherently more sensitive to temperature fluctuations than is electrostatic repulsion. Therefore, temperature cycling could disrupt a suspension stabilized only by polymer. To prevent this, ionic surfactants are used as well. There is a synergy between the two, because adding a neutral polymer to a surface stabilized with an ionic surfactant permits greater coverage by the ionic surfactant. This occurs because self-repulsion of the charged surfactant molecules is minimized, which therefore permits closer packing.

The repulsive energy of two similarly charged particles is given by the equation

$$VR = (\varepsilon a \psi 0 / \kappa 2) \ln [1 + \exp(-\kappa Ho)]$$

Where,

a is the particle radius,

H_0 is the distance of separation between the two particles,

ε is the dielectric constant of the medium,

$\psi 0$ is the electrostatic surface potential, and

K is related to the thickness of the diffuse electric double layer.

The net repulsive energy decreases with separation of the particles (FIG. 2.3). At shorter distances of separation, there is an attractive force between the two particles due to van der Waals forces. The superposition of both these forces results in an attractive potential, provided the particles can overcome an energy barrier.

Therefore, regardless of the nature of the bulk particles, colloidal stability is determined primarily by the choice of surfactants, which affects the repulsive potentials. This does not mean that there is no effect of drug on the stability of suspensions; the drug affects the nature of the surface to which the surfactant must bind.

The design of a stable formulation for nanosuspensions can differ from that used for suspensions of larger particle size. The latter often strives for weak flocculation, which corresponds to the secondary minimum, Vs, (Fig. 2.3) and yields readily dispersible particles after agitation. This is designed to prevent slow settling, which promotes tight packing and consequent caking of the suspensions, which are then no longer dispersible (Tabibi and Rhodes; 1996)
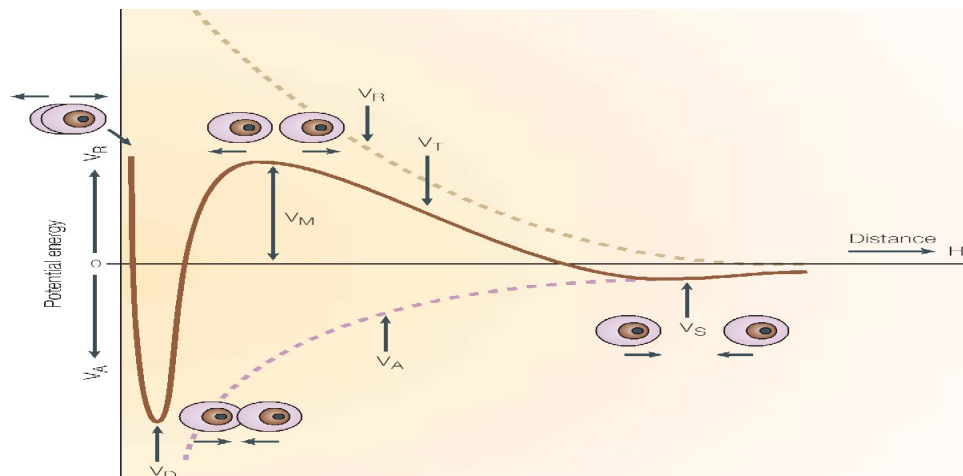
Fig. 2.3 Potential energy curve for approach of two nanoparticles. The total potential energy curve V is a superposition of an attractive curve VA and a repulsive curve VR. As two particles approach, they can overcome the energy barrier VM, leading to attractive aggregation of the closely packed particles. To prevent this for microparticulate suspensions, one can formulate as a weak floc, making use of the secondary minimum (Vanderhoff JW; 1996).

2.1.3 Current Nanonization Strategies

The two main approaches used for nanosizing drugs or formulating drug nanoparticles are top down and bottom up approaches. Top down approach is widely used and generally referred to as nanosizing. This approach is based on use of mechanical force to convert large crystalline particles to nanosized drug particles. Bottom up approach involves controlled precipitation i.e. drug is dissolved in one solvent and then it is precipitated by addition of antisolvent in a controlled manner. Some of the widely employed technologies are briefly described herewith.

2.1.3.1 Media milling:

This is a widely used top down approach for nanonization of the drug. Among all methods reported for nanosizing drug particles in pharmaceutical industry, media milling technique is considered to be the leader with highest commercial applicability. In this technique, the drug particles are subjected to media milling wherein the high-energy shear forces generated as a result of impaction of the milling media with drug provide energy to disintegrate drug micro-particles to nanosized drug particles. In this method, the milling chamber is charged with milling pearls, dispersion medium (e.g. water), drug powder and stabilizer. The pearls are rotated at a very high speed to generate strong shear forces which disintegrate drug powders into nanoparticles (Merisko-Liversidge et al; 2003). The schematic diagram of the nanosizing process using media milling technology is shown in Fig. 2.4.
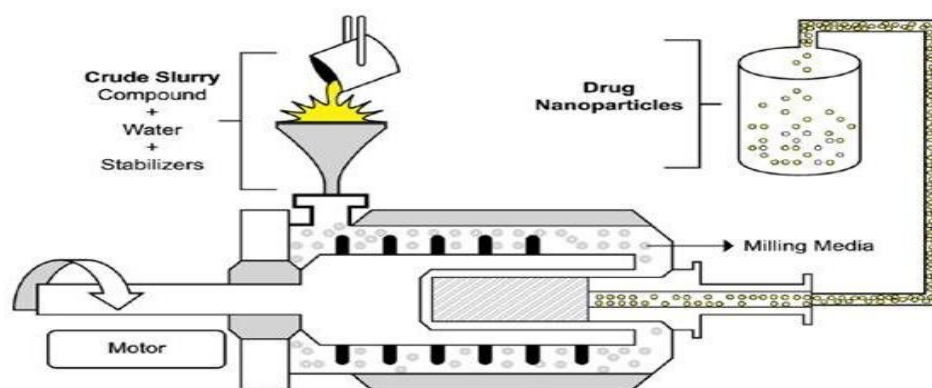
Fig. 2.4: Schematic diagram of nanosizing process using media milling (Merisko-Liversidge and Liversidge; 2011)

Physical characteristics of the resulting nanoparticles depend on the number of milling pearls, milling time, speed, temperature and the amount of drug and stabilizer. The milling time usually varies from few hours to days based on properties of the compound and extent of particle size reduction needed to achieve the desired product performance while milling media generally include glass, zirconium oxide or highly cross-linked polystyrene resin. Salt assisted milling was used for nanosizing of fenofibrate recently (Mochalin et al; 2009).

Media milling technique has been utilized from laboratory to small scale and finally for large scale i.e., the processing of drug from few milligrams to 500–1000 kg of active per batch in a reproducible manner is possible. One important aspect to be considered in such particle size reduction method is the increase in surface energy due to which the nanoparticles tend to aggregate. Thus, surface stabilization is essential to avoid aggregation of nanoparticles. Stabilization of drug nanoparticles is generally achieved by steric, electrostatic or a combination of both types of interactions. Surfactants are generally used to stabilize the particle and selection of the stabilizer is a crucial parameter. In addition to stabilizing the drug nanoparticles against aggregation, care must be taken to avoid or control Ostwald ripening. Ostwald ripening is a result of enhanced solubility of small nanosized particles which may solubilize or re-crystallize onto larger particles in the formulation. The most effective means of detecting the Ostwald ripening is by particle size analysis wherein particle size growth is observed with time while processing and during storage. Performing basic solubility testing on the drug compound at various pH conditions and in stabilizer solutions can help to detect Ostwald ripening. In addition to its shelf stability, it is also important to ensure compatibility of nanosized formulation in the appropriate biological fluid. Very recently, Emerisko Liversidge and GG Liversidge have detailed the applications of wet media milling technology for nanosizing of poorly water soluble compounds [Merisko-Liversidge and Liversidge; 2011].

The advantages of media milling method include, applicability for drugs having poor solubility in water as well as organic solvents, capacity to handle very dilute to highly concentrated suspensions, flexibility to handle large quantity of drugs, easy scale up, reproducibility and narrow size distribution. Some limitations include, contamination of the final product by milling media due to erosion occurred during milling and time and energy consuming process. The problem of microbial contamination may occur if the processing time is too high and the scale up may get affected if the quantity of milling media required is too high.

2.1.3.2 High pressure homogenization:

The second approach for production of drug nanoparticles via the top-down disintegration mechanism is high-pressure homogenization (HPH). As an advanced nanonization strategy,

HPH offers an excellent choice for producing high-quality drug nanoparticles on an industrial scale. Two homogenization principles are applied; Piston gap fluidization and microfluidization.

In the first method, the suspension of a drug and surfactant is forced under pressure through a nanosized aperture valve of a high pressure homogenizer and particle size reduction is based on the cavitation principle. Particle size is also reduced due to high shear forces and the collision of the particles against each other. In this method, major concern is the need for drug particles to be in a micronized state before loading and the number of homogenization cycles required (Chingunpituk; 2007). The size of the drug nanocrystals which can be achieved depends mainly on power density of the homogenizer, number of homogenization cycles and temperature. The particles/crystals break during nanonization preferentially at weak points, i.e. imperfections and number of imperfections reduces with decreasing particle size. Thus, the force required to break the crystals increases with decreasing particle size.

The second method, microfluidization, is based on a jet stream principle. In this method, the drug suspension is accelerated and passes with a high velocity in a specially designed homogenization chamber (either Z shape or Y shape), leading to reduction in particle size of the drug due to collisions between particles and shear forces generated.

HPH is carried out in either water or a non-aqueous media. For water sensitive drugs, non-aqueous media is suitable. Nanopure® is a new homogenization technique in which homogenization of drug particles is carried out in non-aqueous media (e.g. propylene glycol) or mixtures of water with water miscible liquids (e.g. PEG, glycerol). Nanoedge® technique uses combination of homogenization and precipitation to avoid the growth of drug nanoparticles during precipitation.

The advantages of HPH method include, applicability for drugs having poor solubility in water as well as organic solvents, capacity to handle very dilute to highly concentrated suspensions, industrial scale up feasibility, allows aseptic production, low risk of product contamination etc. The limitations of this method include, prerequisite for drug to be in micronized state before homogenization, high cost of instrument, high number of homogenization cycles and possible contamination by metal ions from homogenizer.

2.1.3.3 Precipitation:

Precipitation method has been applied to prepare small particles for many years, but was used for preparation of nanoparticles for drug delivery in 1980s (Siostromet al; 1993). In this method, the formation of crystalline or semi crystalline drug nanoparticles occurs by nucleation and growth of drug crystals. This process takes advantage of difference in solubility of the drug in two miscible solvents. Here, the drug is dissolved in a solvent (generally organic solvent), and this solution is then added into a miscible antisolvent (generally aqueous phase). Due to this addition, sudden high super saturation occurs which results in rapid nucleation and precipitation. The mixing step is very crucial as super saturation of the solution is the driving force for nanoprecipitation. The nanoparticles formed after precipitation have tendency to agglomerate as there is drastic increase in the free energy of the system. Hence, stabilizers are added to the aqueous phase to modify the surface of the precipitated nanoparticles and lower the interfacial tension, thereby inhibiting crystal growth. The drug nanoparticles can be processed further to remove the solvent, and the dried drug nanoparticles can be obtained by suitable technique. The choice of solvents and stabilizers and the mixing process are key factors to control the size and stability of the drug nanocrystals. The parameters which affect the process performance include, volume ratio of antisolvent to solvent, stirring rate, drug content and temperature. The challenge in the liquid precipitation process is that most small-molecule drugs tend to form relatively large crystals within the range of 10-100 μm (Kashchiev; 2000).

Recently, sonoprecipitation approach is reported for nanosizing to avoid the problem of formation of aggregates as a result of poor mixing. Here, ultrasound mixing provides uniform conditions throughout the vessel during anti-solvent process. Ultrasound intensifies the mass transfer when it propagates through a liquid medium, and initiates cavitation. Cavitational bubbles are formed during the negative-pressure period of the sound wave and when it implodes, a localized hot spot with a high temperature and pressure is formed releasing a powerful shock wave. Seconds after ultrasound is applied, the solvent and anti-solvent are mixed homogeneously, reaching maximum supersaturation so that primary nucleation and crystal growth are implemented rapidly (Dhumal et al; 2008). These effects bring considerable benefits to crystallization process,

such as induction of primary nucleation, reduction of crystal size, inhibition of agglomeration and manipulation of crystal size distribution (Louhi-Kultanen et al; 2006).

Another innovative method that has been reported for the generation of nanoparticles by precipitation is high gravity reactive precipitation or Highee technology. The method generates nanomaterials by employing high gravity mixing of reactants on the molecular level with the help of rotating packed bed (RPB). The high gravity micromixing helps in enhancing the mass transfer and heat transfer between the reactants by several magnitudes, thus inducing rapid nucleation of the final product while suppressing the crystal growth. As the reactants enter the rotating packed bed, they are spread or split into very thin films or nanodroplets under the high shear created by the high gravity. An intense micromixing and centrifugal force together helps in enhanced mass transfer resulting in the production of nanoparticles (Chen et al; 2004).

The advantages of precipitation process include simplicity, low cost equipments, easy scale up, avoids use of high energy such as disintegration (which prevents denaturation of drug) (Zhong et al; 2005) and possible formation of amorphous state enabling increase in solubility (Kipp; 2004). Its limitations are; necessity of drug to be soluble in one of the solvents, the need for the solvent to be miscible with the nonsolvent and removal of the residual solvent at the end of the process.

2.1.3.4 Supercritical Methods:

The application of Supercritical fluid (SCF) technology in preparation of microparticles and microparticulate drug delivery system is well established and the current focus is on nanomaterials. SCF technologies have revealed great potential in particle engineering and have emerged as an alternative to most of the existing techniques. SCF technology has been used to manufacture fine particles of medicinal substances by a build-up process i.e. in contrast to conventional bottom up technique; this involves growing of the particles in controlled fashion to attain desired morphology. A SCF is defined as a substance that is at a pressure and temperature greater than its critical point (Subramaniam et al; 1997). Supercritical fluids are gases or liquids at temperatures and pressures above their critical points (Tc – critical temperature; Pc – critical pressure). Above these points, the SCF exists as a single phase with several advantageous properties of both liquids and gases. The

properties that make supercritical fluids particularly attractive to produce nanomaterials are: gas-like diffusivities, the continuously tunable solvent power/selectivity and the possibility of complete elimination at the end of the process (Reverchon and Adami; 2006)

The most widely used SCF for pharmaceutical applications is carbon dioxide because of its low critical temperature (31.18 °C), attractiveness for heat sensitive materials including products sourced from biologicals, as well as being non-flammable, non-toxic, GRAS ('generally regarded as safe') status and inexpensive. Supercritical Carbon dioxide (CO_2), due to its excellent thermodynamic and transport properties, creates very rapid, uniform, and extremely high supersaturation in the solution which leads to formation of nanoparticles/microparticles with narrow particle size distribution.

Various SCF particle design processes using supercritical CO_2 have been investigated for production of micro/nanoparticles. For particle size reduction of neat drug particles, two SCF technologies are generally used, Rapid Expansion of Supercritical Solutions (RESS) and Supercritical Anti Solvent (SAS) process (Fig. 2.5). The first process uses supercritical fluid as solvent while the latter uses supercritical fluid as antisolvent. Other SCF techniques are based on slight modification to these systems. In the case of RESS, the supercritical fluid is used to dissolve the solid material (drug) under high pressure and temperature, thus forming a homogeneous supercritical phase. Thereafter, the solution is expanded through a nozzle and drug nanoparticles are formed. At the rapid expansion point right at the opening of the nozzle, there is a sudden pressure drop that forces the dissolved material to precipitate out of the solution.

In the SAS method, the solid material (drug) is dissolved in an organic solvent and a supercritical fluid is then forced by means of pressure to dissolve in it. In this way, the volume of the system is expanded, thus lowering the density, and therefore the solubility of the material of interest is also decreased. As a result, the material precipitates out of the solution as a solid with a very small particle diameter. The factors that affect the particle properties include solubility of material, pre-expansion conditions, spray device, solvent extraction and mass transfer.
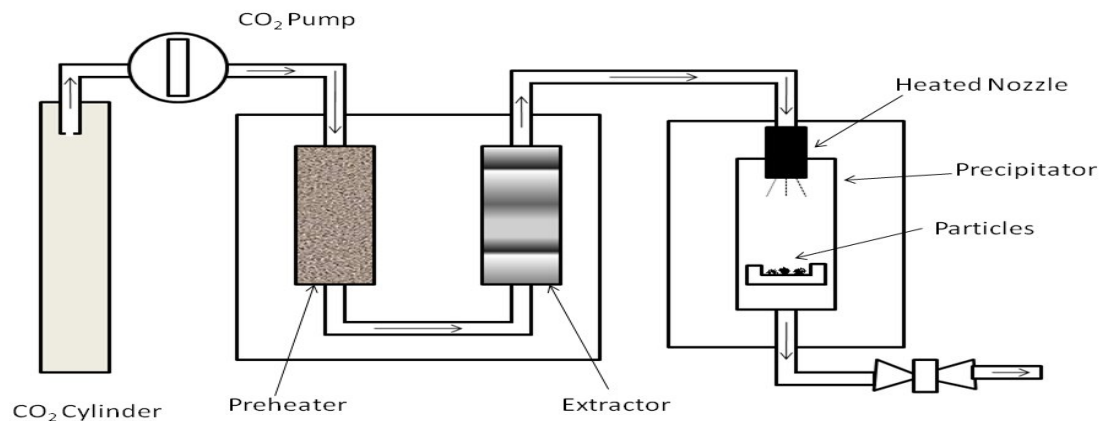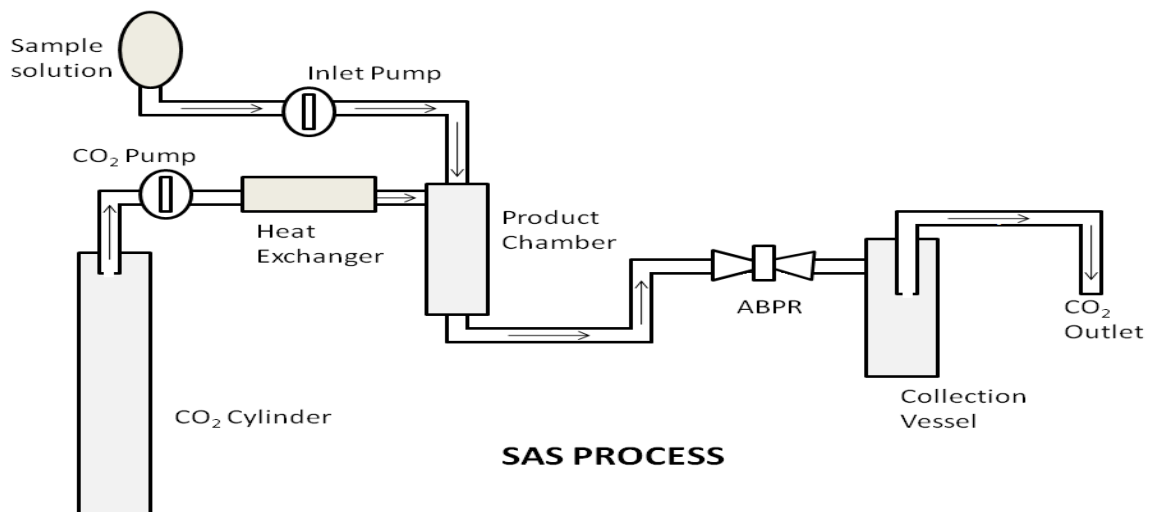
Fig. 2.5: Schematic of RESS and SAS process

A new technique, the supercritical antisolvent with enhanced mass transfer (SAS-EM), which is a modification of SAS was introduced for improving mass transfer between solution and antisolvent. This process generates ultrasound field which enhances mass transfer and thus leads to formation of particles smaller than those from SAS (Chattopadhyay and Gupta; 2001). Recently, an improved system using both supercritical antisolvent precipitation and rapid expansion from supercritical to aqueous solution (RESAS) was used for production of drug nanoparticles (Tozuka et al; 2010).

The advantages of supercritical method include better control over the process, mild operating conditions, and production of solvent free particles. The supercritical methods are also single step process, suitable for variety of compounds and are considered as green alternative i.e. have potential of being GMP compliant (York; 1999) and the product need not be subjected to any further post-treatment. The major limitation of the supercritical methods is equipment cost and poor understanding of the particle formation phenomenon.

Recently, the supercritical anti-solvent (SAS) process has been proposed as an alternative for formulating coprecipitates such as solid dispersion particles that may be smaller in particle size, lower in residual organic solvent, and have better flowability.

The term 'solid dispersion' has been utilized to describe a family of dosage forms whereby the drug is dispersed in a biologically inert matrix, usually with a view to enhancing oral bioavailability. Initially, first generation solid dispersions were prepared using crystalline carriers such as urea and sugars. In the late sixties it was observed that solid dispersions, where the drug was maintained in the crystalline state, might not be as effective as the amorphous, because the former were more thermodynamically stable. Therefore, a second generation of solid dispersions appeared, containing amorphous carriers instead of crystalline. Indeed, the most common solid dispersions do not use crystalline carriers but amorphous. In the latter, the drugs are molecularly dispersed in an irregular form within an amorphous carrier, which are usually polymers.

Polymeric carriers have been the most successful for solid dispersions, because they are able to originate amorphous solid dispersions. They are divided into fully synthetic polymers and natural product-based polymers. Fully synthetic polymers include povidone (PVP), polyethyleneglycols (PEG) and polymethacrylates. Natural product based polymers are mainly composed by cellulose derivatives, such as hydroxypropylmethylcellulose (HPMC), ethylcellulose or hydroxypropylcellulose or starch derivates, like cyclodextrins.

Amorphous solid suspensions occur when the drug has limited carrier solubility or an extremely high melting point. Drugs with a high melting point are candidates for producing an amorphous solid suspension. Molecularly, the obtained dispersion does not have a homogeneous structure, but is composed of two phases. Small drug particles, when

dispersed in polymeric carriers, are able to provide an amorphous final product (Vasconcelos et al; 2007).

The dispersions have traditionally been formed by heating mixes of the drug and carrier to the molten state (although whether this molten mix is a suspension or solution is usually not defined) followed by resolidification via cooling. Alternative methods involve dissolving the components in a mutual volatile solvent followed by evaporation or dissolving the drug in a solvent. These methods are classified as Fusion method, hot melt extrusion, solvent evaporation and supercritical methods (Dhirendra et al; 2009). The physical nature of the dispersion was not clear in many cases. However, some possibilities were suggested. These include eutectic systems, whereby on cooling the molten mix the system forms a microfine dispersion of the two components with a concomitant decrease in melting point. The second common explanation is that of a solid solution, whereby the drug is present as a molecular dispersion within the carrier. Thirdly, the drug may be present as dispersion in a glassy matrix. Overall, therefore, there still remain numerous questions regarding the physical nature of solid dispersions, despite the chemical simplicity of these systems.

While a number of potential and realised advantages of solid dispersions have been described in the literature, the single most widely cited consideration is the improvement in dissolution rate, with concomitant implications for improving the bioavailability of poorly water-soluble drugs. Various mechanisms have been proposed for describing the improvement in dissolution rate by solid dispersion. The currently accepted range of possible mechanisms of enhanced dissolution are i) particle size reduction & reduced agglomeration and ii) increased solubility or dissolution rate of drug (Craig; 2002).

Management of the drug release profile using solid dispersions is achieved by manipulation of the carrier and solid dispersion particles properties (Vasconcelos et al; 2007). If these properties are properly controlled, improvement in bioavailability can be obtained. The major advantages of solid dispersion are summarized as follows:

Particles with reduced particle size: Molecular dispersions, as solid dispersions, represent the last state on particle size reduction, and after carrier dissolution the drug is molecularly dispersed in the dissolution medium. Solid dispersions apply this principle to

drug release by creating a mixture of a poorly water soluble drug and highly soluble carriers. A high surface area is formed, resulting in an increased dissolution rate and, consequently, improved bioavailability.

Particles with improved wettability: A strong contribution to the enhancement of drug solubility is related to the drug wettability improvement verified in solid dispersions. It was observed that even carriers with or without any surface activity improved drug wettability. Moreover, carriers can influence the drug dissolution profile by direct dissolution or co-solvent effects.

Particles with higher porosity: Particles in solid dispersions have been found to have a higher degree of porosity. The increase in porosity also depends on the carrier properties, for instance, solid dispersions containing linear polymers produce larger and more porous particles than those containing reticular polymers and, therefore, result in a higher dissolution rate. The increased porosity of solid dispersion particles also hastens the drug release profile.

Drugs in amorphous state: Poorly water soluble crystalline drugs, when in the amorphous state tend to have higher solubility. The enhancement of drug release can usually be achieved using the drug in its amorphous state, because no energy is required to break up the crystal lattice during the dissolution process.

If the above parameters are successfully controlled improvements in dissolution will be observed which lead to enhanced bioavailability. Solid dispersion particles (SDP) prepared by SAS method using PEG 8000, PVP K17, Poloxamer 188 and 407 and showing improved dissolution characteristics have been reported for oxeglitazar (Badens et al; 2009). Solid dispersion particles (SDP) of felodipine with enhanced solubility and dissolution rate were prepared by SAS method using HPMC (Won et al; 2005). Thus, solid dispersion particles prepared using SAS method with nanometer size range could have improved dissolution characteristics which may be due to nanonization of the drug.

2.1.3.5 Aerosol flow reactor method:

Aerosol flow reactor method is a simple and efficient one-step continuous process for engineering drug nanoparticles with narrow particle size distribution. In this method, drug is dissolved in a suitable biocompatible volatile solvent and atomized with the help of

pressurized inert carrier gas into nanodroplets by means of an atomizer. Then the nanodroplets suspended in the inert carrier gas are passed through a heated tubular laminar flow reactor maintained at a temperature sufficient to evaporate the solvent. The drug nanoparticles are formed due to instantaneous evaporation of the solvent which induces supersaturation of the drug in the inert gas. The parameters which affect the process performance include temperature, drug solubility, solution concentration, type of atomizer and atomizing efficiency. The advantages of this method include; formation of dried nanoparticles with unimodal size distribution and better control over size and morphology of particles.

2.1.3.6 Microemulsion template technology:

The use of partially water-miscible, biocompatible organic solvents through microemulsion as a template has been described for engineering drug nanoparticles (Trotta et al; 2003⬚). These systems are applicable for drugs that are soluble in either volatile organic solvents or partially water miscible solvents. In this technique, an organic solvent or mixture of solvents loaded with the drug is added slowly to an aqueous medium with stirring at a high speed that leads to formation of small droplets (containing drug dissolved in organic solvent) emulsified in the aqueous vehicle. As the stirring progresses at high speed, the droplet size is further reduced. The process is also accompanied by slow evaporation of the organic solvent from the droplets. Once the organic solvent is evaporated completely, pure drug particles stabilized by surfactant are left behind, suspended in the aqueous vehicle. The advantages of this technique are: high drug solubilization, long shelf life, ease of production by controlling the emulsion droplet and easy scale-up. The limitations are use of hazardous solvents and high amount of surfactants.

2.1.4 Characterization of Nanosuspensions

The unique qualities and performance of nanoparticulate systems as device for drug delivery arises directly from their physicochemical properties. Hence, determining such characteristics is essential in achieving the mechanistic understanding of their behaviour. A good understanding allows prediction of in vivo performance as well as allowing particle designing, formulation development and process troubleshooting to be carried out in a rational fashion. Nanosuspensions are generally characterized for the following parameters

- Particle size
- Surface charge (Zeta potential)
- Crystalline state
- Saturation solubility
- Surface morphology
- Stability

Particle size

The most basic and important property of any nanoparticulate system is its size. The saturation solubility, dissolution velocity, physical stability and even biological performance of these systems depend on their particle size. Saturation solubility and dissolution velocity showed considerable variation with change in particle size of the drug (Muller and Peters; 1998). The most frequently used techniques for particle size measurement of nanosized systems are dynamic light scattering techniques, static light scattering techniques and microscopy. Each method has its own advantages as well as disadvantages. The mean size and width of distribution (polydispersity index) is typically determined by photon correlation spectroscopy (PCS). This technique can be used for rapid and accurate determination of the mean particle diameter of nanosuspensions (Muller; 1984). It records the variation in the intensity of scattered light on the microsecond time scale (Pecora; 2000). The measuring range of PCS is limited to approximately 3 nm–3mm. Therefore, Laser Diffractometry (LD) is also used to detect any particles in the micrometer range or aggregates of drug nanoparticles. For nanosuspension intended for intravenous use, particle size determination by coulter counter is also essential as few particles with

particle size more than 5 μm may cause problem of blockage of blood vessels. Depending on the type of equipment employed, the measuring size range is approximately 0.01–80 μm. The instrument and the material to be analyzed are important parameters which will affect the accurate particle size measurement. The stability of the sample during analysis is the most important requisite for correct and reproducible results (Keck; 2010). Thus, all above things must be considered during selection of appropriate technique for particle size determination for a particular sample.

Surface charge (Zeta potential)

Particle charge is a stability determining parameter in aqueous nanosuspensions. It is measured by electrophoresis and typically expressed as phoretic mobility [(mm/S) / (V/cm)] or zeta potential (mV). Zeta potential is used as surrogate for surface charge, and is often measured by observing the oscillations in signal that result from light scattered by particles located in an electric field (Yang and Zhu; 2002). There are a number of instrumental configurations with different approaches implemented in different equipments, with mostly used Doppler shift. The zeta potential of a nanosuspension is governed by both the surfactant and the drug itself. For a physically stable nanosuspension solely stabilized by electrostatic repulsion, a zeta potential of ±30 mV is required as minimum. In case of a combined electrostatic and steric stabilization, ±20mV is sufficient as a rough guideline (Muller and Jacobs; 2002).

Crystalline state

Drug particles in amorphous form are likely to be generated when nanosuspensions are prepared. Hence, it is essential to investigate the extent of amorphous drug particles generated during production of nanosuspensions. The crystalline status of the nanosuspension can be assessed by differential scanning calorimetry (DSC) (Muller at al; 2001). This is particularly very important when the drug exhibits polymorphic forms. The changes in the physical state of the drug particles as well as extent of amorphous fraction can be determined by X-ray diffraction analysis (Muller and Grau; 1998) and can be supplemented by DSC studies (Shanthakumar et al; 2004). The assessment of the crystalline state and particle morphology together helps in understanding the polymorphic and morphological changes that a drug undergoes when subjected to nanosizing.

Saturation solubility

The increase in saturation solubility and consequently an increase in dissolution rate of the compound decide its applications. Though saturation solubility is defined as a compound specific, temperature dependent constant, it also depends on particle size.

The saturation solubility of the drug in different physiological buffers as well as at different temperature should be assessed using different methods described in literature. For example, the saturation solubility can be determined at different temperatures by shaking experiments till equilibrium has reached. The improvement in dissolution rate of nanosuspension as compared to conventional formulations reflects the advantages achieved by nanosizing. Apart from adhesiveness, increased dissolution velocity and increased saturation solubility are the special benefits of nanosuspensions. These two parameters mainly determine the in vivo fate of nanosuspensions.

Surface morphology

Nanoparticles can be directly observed by Scanning Electron Microscopy (SEM) and Transmission Electron Microscopy (TEM) with the former method being better for morphological examinations (Molpeceres et al; 2000). TEM has a smaller size limit of detection and provides structural information via electron diffraction, but staining is usually required. Researchers must be cognizant of the statistically small sample size and the effect of applied vacuum on the particles during analysis. Very detailed images can be obtained from freeze fracture approach in which a cast is made of the original sample (Mosqueira et al; 2001). Sample corruption resulting from the extensive sample preparation is always a possibility, though lower vacuum instrumentation reduces this manipulation, albeit at the loss of some resolution (Nizri at al; 2004). Atomic force microscopy (AFM) microscopy can also be used to confirm the size and shape of nanosized particles. AFM is capable of scanning the surfaces in controlled environmental conditions and is a complementary to SEM imaging.

Stability

Physical stability is crucial in formulation of drug nanosuspension. As nanosuspensions have mean particle diameter in nanometer range, they are prone to aggregation of the particles. The aggregation may be due to Ostwald ripening which occurs due to different

saturation solubilities in the vicinity of very small and larger particles. Nanosizing results in creation of additional surface area and/or interfaces which lead to change in free energy and become thermodynamically unstable and will tend to agglomerate to minimize the free energy (Gonzales-Caballero et al; 2000). Hence, stabilizers like surfactants or polymeric macromolecules are required to stabilize the nanoparticles against inter-particulate forces and prevent them from aggregation. Surfactants are used to minimize the free energy and stabilize the system. The stabilization provided by the stabilizers is by steric, electrostatic or combination of these two processes. Steric stabilization is achieved by adsorbing surfactants/polymers onto the particle surface while electrostatic stabilization is obtained by adsorbing charged molecules, which can be ionic surfactants or charged polymers, onto the particle surface. Generally, steric stabilization alone is sufficient to provide stability to the nanosized particles but electrostatic stabilization is often combined with it as an additional measure.

Beside physical stability (Ostwald ripening), another important issue is chemical stability of the active in nanosuspension which is affected in some cases due to possible hydrolysis of the compound. The active content of the nanosuspension formulation must be studied as some drugs have low stability in aqueous medium. However, some examples exist which showed that formulation of nanosuspension prevents hydrolysis of drug as compare to solution (Muller et al; 2006). Thus, drug content of the formulation must be studied immediately after preparation to check the chemical stability of the drug. Formation of impurities due to process and formulation parameters must be studied. The impurities could be identified by various techniques such as infrared spectroscopy (IR), high performance liquid chromatography (HPLC) and mass spectroscopy (MS). Additionally, impurities related to the process must also be tested, e.g. possibility of zirconium content in the formulation if media milling method using zirconium oxide beads was used for preparation.

Beside characterization of above properties, additional characterization of the nanosuspension is required if surface modification is done for particles. The parameters for which surface modified nanosuspensions are evaluated include adhesion properties, surface hydrophilicity/hydrophobicity and interaction with body proteins. The

adhesiveness of the drug nanoparticles is considered to be a major factor contributing towards increasing the bioavailability and reducing variability of absorption. Surface hydrophobicity determines the interaction with the cells prior to phygocytosis and is relevant parameter for adsorption of plasma proteins. It is considered as important parameter affecting *in vivo* organ distribution after i.v. injection. Separation by Hydrophobic Interaction Chromatography (HIC) depends on the reversible adsorption of biomolecules according to their hydrophobicity. HIC is widely used for the separation and purification of proteins in their native state (Hofstee; 1976). HIC technique is used for determination of surface hydrophilicity/hydrophobicity. Hydrophobicity of nanoparticles is characterized by HIC in which hydrophilic particles pass the column faster while elution of hydrophobic particles is retarded (Stolnik et al; 1994).

2.1.5 Applications of Nanosuspensions

Nanosuspensions are used to advantage in diverse dosages forms. Their small size and increased surface area leads to increased dissolution rate and increased bioavailability. On the other hand, their particulate nature can lead to targeting of monocyte phygocytic system (MPS), with unusual pharmacokinetic consequences. Nanosuspensions can play a critical role as an enabling technology for poorly water-soluble and/or poorly permeable molecules having significant activity observed in *in vitro* studies. These molecules may pose problems at any or both of the following stages during new drug development processes:

■ Formulation of an intravenously injectable product for preclinical *in vivo* evaluation to measure its toxicity and other pharmacokinetic characteristics.

■ Improving absorption of the drug candidate from the GIT which showed poor bioavailability during preclinical as well as clinical development studies.

As the particle size of nanosuspension is the range of 1-1000 nm, these formulations are suitable for application through various routes of administration like parenteral, oral topical, pulmonary and targeted drug delivery system.

Oral: Oral drug delivery is the most widely preferred route of administration of drugs. But, some drugs possess the problem of limited bioavailability due to poor solubility and absorption which ultimately reduces its efficacy. In such cases, nanosuspension can solve

the problem as it helps in improving the dissolution rate and absorption due to increased surface area and enhanced adhesiveness. Nanosuspension can lead to increased mucoadhesion which can increase gastrointestinal transit time and lead to increased bioavailability. Administration of atovaquone as a nanosuspension resulted in a 2.5-fold increase in oral bioavailability as compared to the micronized drug. The enhancement in oral bioavailability can be attributed to increased surface area, saturation solubility and the adhesiveness of the drug nanosuspension (Scholer et al; 2001). Taste masking of particulate system is also easily possible. Nanosuspension was also reported to enhance oral bioavailability of BMS-488043 in dogs as compared to a conventional formulation containing the micronized crystalline drug substance (Fakes et al; 2009). Nanosuspension formulation also helps in avoiding the food effect on absorption as observed for EMEND formulation in a study (Majumdar et al; 2006).

Parenteral: Nanosuspensions can be used to transform poorly soluble non-injectable drugs into a formulation suitable for intravenous administration. Although the production of nanosuspension for parenteral use is critical, current developments in this technology have proved its utility as injectable formulations. The methods used for preparation of nanosuspension are now precisely controlled, and are able to produce uniform particles with better control over maximum particle size. Various research reports are available which emphasize the applicability of nanosuspensions for parenteral administration. Injectable formulation of nimodipine nanosuspension proved better than commercial product (ethanol based) in terms of local irritation and phlebitis risks (Xiong et al; 2008).

Ocular delivery: Nanosuspension can prove to be a boon for drugs that exhibit poor solubility in lachrymal fluids. Nanosuspensions represent an ideal approach for ocular delivery of hydrophobic drugs due to their inherent ability to improve saturation solubility of drugs. Kassem et al have developed nanosuspension delivery system for certain glucocorticoid drugs (Kassem et al; 2007).

Pulmonary: Nanosuspensions can be advantageous for delivering drugs that exhibit poor solubility in pulmonary secretion. Currently available approaches for pulmonary delivery such as aerosols or dry powder inhalers possess certain disadvantages such as limited diffusion at required site, less residence time etc, which can be overcome by

nanosuspensions. Fluticasone and budesonide have been successfully formulated as nanosuspension for pulmonary delivery (Yang et al; 2008).

Dermal: The nanocrystalline form possesses increased saturation solubility resulting in enhanced diffusion of the drug into the skin. Nanocrystals also exhibit various properties such as increased penetration into a membrane, enhanced permeation and bioadhesiveness which could be very useful for dermal application. Piao et al showed increased permeability of diclofenac sodium nanosuspension across the skin compared to the control for transdermal delivery (Piao et al; 2008).

Targeting: The uptake of drug nanoparticles depends on their particle size. By changing the surface properties of the nanoparticles, their *in vivo* behavior can be altered and can be used as targeted delivery system. The phagocytotic uptake of nanocrystals can be avoided by preparing stealth nanocrystals or by preparing smart crystals i.e. drug particles below particle size of 100nm, which can be used as a targeted drug delivery system. Due to method simplicity, development of nanosuspension is a commercially viable option for targeted delivery. Mucoadhesive nanosuspension was reported for targeting of Cryptosporidium parvum (Kayser; 2001). The surface properties of particles such as surface hydrophobicity, charge, presence and concentration of certain functional groups determine its organ distribution. Thus, Tween 80 coated nanocrystals can be used for brain targeting. Atovaquone nanocrystals coated with Tween 80 were used to treat toxoplasmosis; the parasites could be efficiently eradicated in brain (Shubar et al; 2009).

2.2 Nanoemulsion:

Oral route is the most preferred way for administration of most drugs for conventional formulations. However, growing number of drugs possessing inherent poor solubility and permeability characteristics results in low bioavailability. The utility of lipid based formulations for improving the gastrointestinal absorption of poorly water–soluble, hydrophobic drugs is well described in literature (Humberstone et al; 1997). The primary mechanism by which these systems enhance bioavailability is through solubilization of the drug. Other mechanisms for absorption enhancement were also reported and include reduction of P-glycoprotein mediated efflux, mitigation of hepatic first pass metabolism through enhanced lymphatic transport, prolongation of gastrointestinal transit time, or protection from degradation in GI tract (Gibson; 2007).

It has been estimated that anywhere from 40 to as much as 70 percent of all new chemical entities (NCE) entering drug development programs possess insufficient aqueous solubility [Gursoy et al; 2004]. This insufficient aqueous solubility leads to poor bioavailability in many cases. Poor bioavailability can be due to poor solubility, degradation in GI lumen, poor membrane permeation and presystemic elimination (Bruce; 1993). Recently, much attention has been focused on lipid based formulations to improve the oral bioavailability of poorly water soluble drugs. Lipid based formulations include surfactant dispersions, microemulsions, nanoemulsions, self-emulsifying formulations, self-microemulsifying formulations, emulsions and liposomes. One of the promising technologies is nanoemulsion drug delivery system, which is being applied to enhance the oral bioavailability of the poorly soluble drugs.

Nano-emulsions are emulsions (non-equilibrium systems) with a remarkably small droplet size (in the nanometer range, e.g. 20– 200 nm), regardless of the preparation method. There is a fundamental difference between microemulsions and nanoemulsions. Microemulsions are equilibrium systems (i.e. thermodynamically stable), while nanoemulsions are non-equilibrium systems with a spontaneous tendency to separate into the constituent phases. Another important difference between nanoemulsions and microemulsions is that the volume fraction, f, of droplets of the dispersed oil phase can be continuously controlled from zero to nearly unity through an applied osmotic pressure

without changing the droplet volumes, whereas the structure of the oil in microemulsions is typically subject to morphology changes (e.g., from spherical to a hexagonal or lamellar phase) when the volume fraction of oil is changed (Meleson et al; 2004). Nevertheless, nanoemulsions may possess a relatively high kinetic stability, even for several years (Solans et al; 2003). The long-term physical stability of nanoemulsions makes them unique and they are sometimes referred to as 'Approaching Thermodynamic Stability' (Tadros T. et al 2004). Nanoemulsions due to their characteristic size appear transparent or translucent to the naked eye (Fig. 2.6).

Fig.2.6. Picture of a nanoemulsion (left) and a macro-emulsion (right) with droplet diameters of 35 nm and 1 μm, respectively (Solons et al; 2005)

Advantages (Sarkar et al 2005; Tadros et al; 2004)

As compared to other colloidal systems, mass production favors nanoemulsions in terms of the ease of formation. Also, current methods of manufacture produce particles with high uniform size and stability, which have been found to lead to increased blood plasma concentrations (Seki et al; 2004). These beneficial attributes were facilitated by the

intrinsic properties of the particles and is a consequence of the tissue penetration facilitated by nanoemulsions over micron-sized regular emulsions. Nanoemulsions can lead to improved systemic distribution even in the case of passive delivery modes. The nanoemulsion also allows opportunities for sub-micron filter sterilization, screening-out microbes without the shear deformation that occurs with larger size droplets. The very small droplet size causes a large reduction in the gravity force and the Brownian motion may be sufficient for overcoming gravity. This means that no creaming or sedimentation occurs on storage. The small droplet size also prevents any flocculation of the droplets. Weak flocculation is prevented and this enables the system to remain dispersed with no separation. The small droplets also prevent their coalescence, since these droplets are non-deformable and hence surface fluctuations are prevented. In addition, the significant surfactant film thickness (relative to droplet radius) prevents any thinning or disruption of the liquid film between the droplets. Unlike microemulsions (which require a high surfactant concentration, usually in the region of 20% and higher), nanoemulsions can be prepared using reasonable surfactant concentration (5-10%). Nanoemulsion has translucent and fluidy properties which improve the patient compliance and safety in administration. These systems have been reported for targeted delivery of nobiletin (Yao et al; 2007) and for improving the bioavailability of colchicine (Shen Q et al; 2011).

Disadvantages (Tadros et al; 2004, Sarkar et al; 2005, Sharma et al; 2010)

Inspite of the above advantages, nanoemulsions have attracted interest in recent years for the following reasons: (i) There is a perception that nanoemulsions are expensive to produce. Expensive equipments and the use of high concentrations of emulsifiers are required. (iii) Lack of understanding of the mechanism of production of submicron droplets and the role of surfactants and cosurfactants. (iii) Preparation of nanoemulsions requires in many cases special application techniques, such as the use of high pressure homogenisers as well as ultrasonics. Such equipments (such as the Microfluidiser) became available only in recent years. (iv) Lack of understanding of the interfacial chemistry that is involved in production of nanoemulsions. (v) Lack of demonstration of the benefits that can be obtained from using nanoemulsions when compared with the classical macroemulsion systems. (vi) Stability of nanoemulsion is sometimes unacceptable and may create

problems in long term storage. Lack of knowledge on the mechanism of Ostwald ripening, which is perhaps the most serious instability problem with nanoemulsions. (vii) Selection of excipients in nanoemulsion is also major concern. For example, lack of knowledge of the ingredients that may be incorporated to overcome Ostwald ripening.

2.2.1 Theory (Tadros et al; 2004)

To prepare emulsion oil, water, surfactant and energy are needed. This can be understood from a consideration of the energy required to expand the interface, $\Delta A \gamma$ (where ΔA is the increase in interfacial area when the bulk oil with area $A1$ produces a large number of droplets with area $A2$; $A2 >> A1$, γ is the interfacial tension). Since γ is positive, the energy to expand the interface is large and positive. This energy term cannot be compensated by the small entropy of dispersion $T \Delta S$ (which is also positive) and the total free energy of formation of an emulsion, ΔG is positive.

$\Delta G = \Delta A \gamma - T \Delta S$

Thus, emulsion formation is non-spontaneous and energy is required to produce the droplets. The formation of large droplets (few micrometers) as is the case for macroemulsions is fairly easy and hence high speed stirrers such as the Ultraturrax or Silverson Mixer are sufficient to produce the emulsion. In contrast, the formation of small drops is difficult and this requires a large amount of surfactant and/or energy.

The high energy required for formation of nanoemulsions can be understood from a consideration of the Laplace pressure (the difference in pressure between inside and outside the droplet). To break up a drop into smaller ones, it must be strongly deformed and this deformation increases Laplace pressure. Consequently, the stress needed to deform the drop is higher for a smaller drop. Since the stress is generally transmitted by the surrounding liquid via agitation, higher stresses need more vigorous agitation, hence more energy is needed to produce smaller drops. Surfactants play major role in the formation of nanoemulsions: By lowering the interfacial tension, p is reduced and hence the stress needed to break up a drop is reduced. Surfactants prevent coalescence of newly formed drops.

Various processes occurring during emulsification namely break up of droplets, adsorption of surfactants and droplet collision (which may or may not lead to coalescence to occur). Each of these processes occurs numerous times during emulsification and the time scale of each process is very short, typically a microsecond. This shows that the emulsification process is a dynamic process and events that occur in a microsecond range could be very important.

2.2.2 Methods of preparation

With macroemulsions, several procedures may be applied for emulsion preparation, ranging from simple pipe flow (low agitation energy L), static mixers and general stirrers (low to medium energy, $L–M$), high speed mixers such as the UltraTurrax (M), colloid mills and high pressure homogenizers (high energy, H), ultrasound generators ($M–H$). With nanoemulsions, however, a higher power density is required and this restricts the preparation of nanoemulsions to the use of energy input. Being non-equilibrium systems, nanoemulsions cannot be formed spontaneously. Thus, energy input generally from mechanical devices or from the chemical potential of the components, is required. The methods using mechanical energy (high shear stirring, high-pressure homogenizers and ultrasound generators) are designed as dispersion or high energy emulsification methods, while those making use of chemical energy stored in the components are referred to as condensation or low-energy emulsification methods. The performance of the method of preparation is generally assessed by the size of the nanoemulsion droplet and stability of the system. The high energy methods have control over particle size distribution and ability to produce fine emulsion from large variety of materials. Low-energy emulsification methods are also reported for preparation of nanoemulsions which involve transitional inversion induced by changing factors that affects HLB of the system or by catastrophic inversion induced by increasing dispersed phase volume fraction (Jafari et al; 2007). These methods have several limitations such as requirement of large amount of surfactants and careful selection of surfactant–cosurfactant combination, and are not applicable to large scale industrial productions.

For the preparation of nanoemulsions (covering the droplet radius size range 50–200 nm) generally following three methods are used.

1) Use of high energy emulsification methods (high pressure homogenisers or ultrasonication)
2) Use of low energy emulsification method at constant temperature
3) Application of the phase inversion temperature (PIT) concept

2.2.2.1 Use of high energy emulsification methods

The production of small droplets (submicron) requires application of high energy. These emulsions can be produced using high pressure homogenizer, membrane or ultrasonic devices and microfludizers.

The ultimate size of a high energy nanoemulsion is determined by the balance between two opposing processes; droplet break-up and droplet re-coalescence. When the applied shear is greater than the Laplace pressure of the emulsion droplet break-up occurs. The surfactant plays a critical role in both droplet break-up and coalescence. The surfactant aids droplet break-up by lowering the interfacial tension and prevents the immediate re-coalescence of newly formed droplets by rapid adsorption to, and stabilization of, the newly formed interface. The efficiency of droplet break-up is controlled by the nature and intensity of the shear (Leong et al; 2009).

High-energy emulsification methods have several advantages that are applicable to industrial operations. These advantages include control of droplet size distributions and the ability to produce fine emulsions from a large variety of materials.

Studies comparing ultrasonic emulsification with rotor–stator dispersion have found ultrasound to be competitive or even superior in terms of droplet size and energy efficiency (Canselieret al; 2002). The same studies also have shown that microfluidization has been found to be more efficient than ultrasound, but less practicable with respect to production cost, equipment contamination. Comparing mechanical agitation to ultrasound at low frequency, Tadros et al found that for a given desired diameter, the surfactant amount

required was reduced, energy consumption (through heat loss) was lower and the ultrasonic emulsions were less polydisperse and more stable (Tadros et al; 2004).

HP-homogenisers of piston-gap type consist of one or two piston intensifier(s) able to generate high pressure, and high pressure valve (HP-valve) equipped with ceramic needles and seat of specially studied design. In such HP-homogenisers, the fluid under pressure is forced through a small orifice of some micrometers width, the HP-valve gap. The fluid accelerates on a very short distance to very high velocity and the resulting strong pressure gradient between the inlet and outlet of the HP-valve generates intense shear forces and extensional stress through the valve gap. Cavitation, turbulence and impact with solid surfaces take place at the outlet of the valve gap. Due to shear effects and conversion of kinetic energy into heat, the fluid travelling through the HP-valve is accompanied by short-life heating phenomena that can be controlled by efficient cooling devices. All these mechanical forces are expected to disrupt particles down to the submicron range. High pressure homogenisers are particularly suitable for continuous production of finely dispersed emulsions and are therefore of interest in pharmaceutical fields.

Both a batch and focused flow-through ultrasonic cell were utilized for emulsification with ultrasonic power. The key to efficient ultrasonic emulsification is to determine an optimum ultrasonic energy intensity input for these systems, as excess energy input may lead to an increase in droplet size. Ultrasonic emulsification is believed to occur through two mechanisms. Firstly, the application of an acoustic field produces interfacial waves which become unstable, eventually resulting in the eruption of the oil phase into the water medium in the form of droplets. Secondly, the application of low frequency ultrasound causes acoustic cavitation, that is, the formation and subsequent collapse of microbubbles by the pressure fluctuations of a simple sound wave. Each bubble collapse (an implosion on a microscopic scale) event causes extreme levels of highly localised turbulence. The turbulent micro-implosions act as a very effective method of breaking up primary droplets of dispersed oil into droplets of sub-micron size.

Microfluidizer devices comprise interaction chambers designed with a microchannel architecture that combines laminar extension flow at the inlet of the chamber to turbulent flow with cavitation and impact in and at the outlet of the chamber. The premix stream is

divided into two fluid jets at the inlet of the chamber and the fluid velocity is accelerated due to a sudden decrease in the pipe diameter. Laminar extension flow is considered responsible for droplet disruption at the inlet of the chamber. Inside the chamber, the fluid changes its flow direction leading to enhanced particle collision and impingement on the chamber walls. The fluid jets then collide (coming from two opposite microchannels) leading to enhanced particle disruption.

2.2.2.2 Low energy (Spontaneous emulsification) method

The procedure is based on the spontaneous emulsification process of an oil phase containing lipophilic surfactant, when an organic solution is mixed, under moderate mechanical agitation, with an excess aqueous phase containing surfactant. The organic solvent is removed by evaporation under reduced pressure (Yu et al; 1993). In this emulsification method, the addition of the solvent–oil solution results in the emulsification of the oily phase into nanodroplets, due to some kind of interface instability originating from rapid diffusion of the solvent across the interface and decrease of the interfacial tension (Vitale and Katz; 2003). This method is easy to perform in laboratory scale, does not require sophisticated equipment, no requirement of use of high temperature, and generally leads to the formation of small droplet size formulations (Kelmann et al; 2007). Droplet size and distribution are strongly affected by the nature of the solvent used during the process (Bouchemal et al; 2004). Considering its toxicity, solvents belonging to Class II or III should be preferred (European Pharmacopoeia). Spontaneous nanoemulsification method is receiving increased attention due to its large advantages and is interesting formulation approach due to its technological importance. Recently, improved oral bioavailability of amlodipine besilate was reported by nanoemulsion prepared by spontaneous emulsification method (Chhabra et al; 2011).

2.2.2.3 Phase inversion temperature (PIT) method

This low energy and solvent-free method uses the particular ability of emulsions stabilized by polyethoxylated nonionic surfactants to undergo a phase inversion following a variation of temperature (Shinoda and Saito; 1969). Emulsions stabilized with nonionic surfactants generally form o/w emulsions at lower temperature and w/o emulsions at higher temperature. There exists a phase inversion temperature (PIT) at which this inversion

occurs. The PIT is considered as a temperature at which hydrophilic-lipophilic property of a surfactant just balances. At a fixed composition, when the relative affinity of the surfactant for the different phases is changed and controlled by the temperature, *transitional* phase inversion occurs. As a result, oil-in-water (o/w) macro-emulsion undergoes a phase inversion to a water in-oil (w/o) one during increase in temperature, and *vice versa*. Within the transitional region between both macro-emulsions, for the temperatures at which the nonionic surfactants show very close affinities for the two unmiscible phases, the ternary system shows bicontinuous structure. The emulsion inversion temperature (PIT) is determined by the follow-up of the emulsion electrical conductivity. All nonionic polyethoxylated surfactant do not show emulsion phase inversion but it depends upon the polyethoxylated head groups and oil chain length. Some POE nonionic surfactants, for which the polyethoxylated head group is either too short or too long, or *vice versa* the oily chain is too long or too short, are not sensitive enough to the temperature, to induce a phase inversion. Only nonionic polyethoxylated surfactants will allow to perform the emulsion inversion, but the affinities of the surfactant for the aqueous and oily bulk phases have to be relatively balanced, right from the start (Anton et al; 2007). In the PIT method, emulsifier, oil and surfactant are mixed at the same time at slightly below the PIT. An emulsion is formed at this stage. Then sudden break-up of such a microemulsion network by performing rapid cooling and/or a sudden water dilution leads to formation of fine and uniform dispersion. This stage is considered as an irreversible process since it leads to the generation of the kinetically stable oil droplets, *i.e.* the o/w nanoemulsions. This great stability is due to the fact that the steric stabilization prevents the droplets flocculation and therefore coalescence.

2.2.3 Characterization

2.2.3.1 Droplet size and polydispersity

The most important parameter to exploit the advantages of nanoemulsions with respect to conventional emulsions (i.e. macroemulsion) is small size and low polydispersity. These properties of nanoemulsions depend not only on composition variables but preparation variables such as emulsifying path, agitation or emulsification time. These variables can

have a significant influence on the nanoemulsion properties such as droplet size and polydispersity. For emulsification by low-energy methods, composition variables will have a much higher influence than process variables. However, for shear emulsification, the influence of preparation variables will be determinant (Gutierrez et al; 2008).

The droplet size is the most important aspect of nanoemulsion structure. Although, there are a number of techniques that can be used for droplet size measurement, photon correlation spectroscopy (PCS), also known as dynamic light scattering (DLS) method, is widely used. Droplet size of the nanoemulsion is determined by photon correlation spectroscopy that analyzes the fluctuations in light scattering due to Brownian motion of the particles, using a Zetasizer (Malvern Instruments, UK). Generally, light scattering is monitored at 25 °C at a 90° angle. The droplet size of the nanoemulsion is the most representative parameter of emulsion stability.

2.2.3.2 Zeta Potential

Emulsifiers/surfactants can stabilize the emulsion droplet, not only by forming a mechanical barrier, but also by producing an electrical (electrostatic) barrier or surface charge. The electrical surface charge of the droplets is produced by the ionization of interfacial film-forming components. The surface potential and the resulting Zeta potential of emulsion droplets will depend on the extent of ionization of the emulsifying agents. The electrical charge on the emulsion droplets is measured using either a Zetasizer (Malvern Instruments, UK) or the moving boundary electrophoresis technique, which has been shown to yield accurate electrophoretic mobility data [Benita et al; 1986]. In addition to droplet size, zeta potential of the nanoemulsion is another representative parameter of emulsion stability. These parameters are evaluated during stability studies of the nanoemulsions.

2.2.3.3 Morphology

Transmission Electron Microscopy (TEM) analysis is carried out in order to observe the physical properties of the oil droplets in the nanoemulsions. TEM analysis is also important in order to study morphology of the oil droplets in the nanoemulsion formulations and to visualize any precipitation of the drug upon addition of the aqueous phase. TEM images are generally taken after negative staining and TEM studies are also useful to confirm the

particle size obtained by DLS methods. In addition to TEM, sometimes atomic force microscopy (AFM) is also used to observe morphology of the nanoemulsions.

2.2.3.4 pH and Drug content

It is important to note that the pH change result in no overall change in the measured mean diameter of nanoemulsion oil droplets and zeta potential. It is known that alteration is pH has significant effect on droplet size and zeta potential of the systems affecting the stability of the system. Nanoemulsions will be exposed to a varying degree of pH conditions in the gastrointestinal tract (GI) after oral administration. Thus, determination of pH of nanoemulsion is important in determining in vivo stability of the system. The pH adjustment should be done depending on route, when administered by different routes of administrations.

Drug content of the nanoemulsions is expressed as a percentage of drug found in the system to the theoretical quantity of the drug added. Drug content is determined by validated analytical method.

2.2.3.5 Viscosity

One of the characteristics of nanoemulsion formulations is low viscosity (Lawrence and Rees; 2000). The low viscosity ensures easy handling, packing, and hassle-free administration of these formulations. The continuous phase plays a fundamental role in the preparation, stabilization and characteristics of emulsions. This can be understood by taking in account destabilization of emulsion (e.g. increase in viscosity of continuous phase reduce creaming rate). Coalescence and flocculation are very much dependent on interfacial phenomena, but changes in the droplet collision rate (inversely proportional to the viscosity of the continuous phase) and in the interaction potentials (electrostatic, van der Waals) could be induced by varying the properties of the continuous phase (Rodriguez-Abreu and Lazzari; 2008). Viscosity measurements are generally performed by taking into consideration the route of administration. Viscosity measurements are not usually described for parenteral drug delivery emulsions, but this is a relevant characteristic as viscous emulsions are usually painful to the patient during i.v. administration. The viscosity of nanoemulsions is generally determined using a Brookfield viscometer. The viscometer is equipped with a Searle-type device having capacity to measure ultra low viscosity.

Additionally, capillary type viscometers, which measure time as function of flow, are also used to determine the viscosity of nanoemulsions.

2.2.3.6 In vitro release

Different methods are employed to determine the in vitro release from the nanoemulsion formulations, but dialysis bag technique is the most widely used. Maintenance of sink condition in release studies is the most important factor and if sink conditions are not achieved, erroneous results will obtained. A novel dialysis bag technique was designed to overcome this problem (Chidambaram and Burgess; 1999). In some cases, where the drug has poor solubility in release medium, use of surfactant or organic solvent is often permitted. In these studies, the nanoemulsion formulation is packed in dialysis bag and the bag is placed in release medium. Then at periodic time intervals samples are withdrawn and analyzed for the drug content. From the release profile, the release mechanism can be predicted by using different release kinetic models. The *in vitro* release studies are preliminary indicator of the *in vivo* performance of the formulations and also useful to identify parameters which affects its release. Thus, it is very important to perform in vitro release studies of nanoemulsions.

2.2.3.7 Stability

The inherent instability of nanoemulsions is a result of the system's tendency to reduce its free energy by progressively increasing the particle size and broadening the distribution until the dispersed particles separate out as free liquid. Thus, if this tendency could be drastically reduced, it could lead to acceptable kinetic stability in a pharmaceutical dosage form which does not require thermodynamic stability [Rieger; 1986]. The physical instability of the nanoemulsion is evidenced by flocculation and coalescence. In flocculation, the emulsion droplets form adherent masses, but retain their individual integrity, and in coalescence the interface between droplets is lost and they form single, larger droplets. An important distinction is that flocculation is often reversible while coalescence is not. Thus, detailed stability studies of the nanoemulsion formulation at different storage conditions are very important. Ostwald ripening is one of the main problems with nanoemulsions, which results from the difference in solubility between small and large droplets. Several methods are used to reduce Ostwald ripening which

include addition of second dispersed phase which is insoluble in continuous phase and modification of interfacial film at the interface. Reports on stability of nanoemulsion are well described in some articles (Washington; 1996). Generally nanoemulsions are stabilized by the addition of emulsifying agents which lower the interfacial tension and form a film at the oil–water interface, which acts as a mechanical barrier to droplet coalescence. Also, flocculation can be prevented by producing repulsive electrical forces between approaching droplets (Yang and Benita; 2000). In general, nanoemulsions are stabilized either by steric or electrostatic repulsion, depending on the nature of the surfactant. Lecithin-stabilized nanoemulsions are charge-stabilized, and steric forces do not play a significant role. Alternately, emulsions stabilized by block copolymers, such as poloxamers, are sterically stabilized, and charge is of minor importance. Mixed electrosteric systems have also been studied and found to possess sufficient physical stability.

Stability studies of nanoemulsion are generally performed as per ICH guidelines. The samples were kept at different conditions of temperature and relative humidity (%RH) e.g. 40 °C/75% RH, 30°C /65% RH, 25°C /60% RH and refrigeration condition. The stability is observed over specified period. The samples are usually evaluated for particle size, zeta potential, viscosity and drug content.

2.2.4 Applications

Applications of nanoemulsion in food technology, agrochemical, cosmetics and drug delivery are reported in last few decades. In last two decades, all original and review papers on nanoemulsions stress their great potential in drug delivery, as this field has tremendous possibilities in direct applications. Since then, growing interest in nanoemulsions was developed but direct applications of nanoemulsions are not as high as expected. Nanoemulsions possess major issues of stability and this stability issue has been addressed very carefully nowadays. This fact can be seen from the growing number of research papers and patents in this field.

Nanoemulsions are receiving increasing attention as colloidal drug carriers for various potential therapeutic applications, including drug targeting (Prakash and Thiagarajan; 2011). Nanoemulsion are reported for parenteral, oral, ocular, topical and targeted delivery

and their acceptance as drug delivery system by these routes is well known. They are well accepted as i.v. delivery systems for their ability to incorporate water insoluble drugs. Submicron emulsions, not administered intravenously, are also used to increase bioavailability and prolong pharmacological effects of drug with poor absorption or short biological half-life (Yang and Benita; 2000, Jain et al; 2009). Various research reports are available, which emphasized the advantages gained by nanoemulsions as a delivery system by these routes. The recent advances and applications of nanoemulsions by various routes are stated below.

2.2.4.1 Oral delivery: Increasing attention has been focused on nanoemulsion based oral drug delivery system due to their unique structure and properties, such as much smaller droplet size with larger surface area, fabrication of the delivery system with biocompatible materials, increasing dissolution rate and solubility, protection against enzymatic hydrolysis, improving diffusion across the unstirred aqueous layer and enhancing mucosal permeability (Gao et al; 2011, Tang et al; 2012). There have been numerous investigations of nanoemulsions as an alternative drug delivery strategy to increase bioavailability of water insoluble drugs and uniqueness of these systems is characterized by their increased drug solubility, rapid dissolution velocity, and enabling bioavailability after oral administration. Singh and Vinkar reported that nanoemulsion of primaquine exhibited improved oral bioavailability compared with the plain drug (Singh and Vinkar; 2008). Vyas et al reported improved oral bioavailability and brain transport of Saquinavir upon administration in novel nanoemulsion. Food and Drug Administration has also approved nanoemulsions of water insoluble drugs including Estrasorb®, Flexogan® and Restasis for clinical application [Chen H et al; 2011].

2.2.4.2 Parenteral delivery: Parenteral delivery of nanoemulsions is well studied for various purposes such as targeting, sustained release etc. Lipid-based nano-formulations are among the most attractive candidates for improving substance solubility and for site specific targeting following parenteral administration (Moghimi and Agrawal; 2005). For parenteral administration, the droplets size of the drug-carrier nanoemulsion must be be below 1 μm as with larger particle sizes, embolism may occur (Davis et al; 1985). Generally droplet size of nanoemulsion ranges from 100 to 500 nm and thus offers an attractive

system for delivery of drugs with solubility concern. These emulsion formulations offer an appealing alternative for the administration of poorly water soluble drugs due to their effectiveness for drug solubilization, potential for improved efficacy and anticipated patient acceptance and compliance due to the reduced side effects (Constantinides et al; 2004). In addition to effectiveness for drug solubilization, their compatibility and ability to protect drug from hydrolysis and enzymatic degradation makes nanoemulsions ideal vehicle for parenteral administration. Kakumanu et al reported increased efficacy of dacarbazine nanoemulsion by intramuscular injection on reducing tumor size in an epidermoid carcinoma xenograft mouse model as compared to dacarbazine suspension (Kakumanu et al; 2011). Araujo et al reported that pharmacokinetic simulation of low dose parenteral nanoemulsions containing thalidomide led to its therapeutic plasma concentrations (Araujo et al; 2011).

2.2.4.3 Ocular delivery: Nanoemulsions are useful drug delivery vehicles for ophthalmic use due to their numerous advantages such as sustained release of the drug applied to the cornea, high penetration in the deeper layers of the ocular structure, and aqueous humor as well as ease of sterilization. These systems are able to achieve therapeutic action with a smaller dose and a fewer systemic and ocular side effects. Nanoemulsions are reported to play important role in enhancing bioavailability of drug by ocular route and providing patient compliance by decreasing number of applications per day. Ammar et al showed formulation of dorzolamide hydrochloride in a nanoemulsion form offered more intensive treatment of glaucoma (Ammar et al; 2009). Shen et al showed enhanced ocular bioavailability of flurbiprofen axetil by prolonging drug corneal retention and reduction in irritation in case of nanoemulsions. Hagigit et al showed that nanoemulsion apparently enhanced the intraretinal penetration of the Antisense oligonucleotides (ODNs) up to the inner nuclear layer and yielded potential therapeutic levels of ODN in the retina over 72 h post injection from pharmacokinetic and ocular tissue distribution following intravitreal injection in rabbits (Hagigit et al; 2010).

2.2.4.4 Topical delivery: For effective delivery of drug by this route, it is necessary to overcome the barriers imposed by skin. Nanoemulsions are able to easily penetrate the pores of the skin and reach the systemic circulation and thus, effective in drug delivery by

this route. Nanoemulsions as the topical carrier offer several significant advantages such as low skin irritation, powerful permeation ability and high loading capacity for topical delivery. Puglia et al showed that nanoemulsion system significantly increased the transdermal permeability of glycyrrhetic acid in comparison to a control O/W emulsion containing the same amount of active compound (Puglia et al; 2010). Zhou et al demonstrated improved penetrability of Nile red (NR) into the dermis layer when an o/w cream incorporated with NR-loaded LNE applied on the abdominal skin of rat in vivo (Zhou et al; 2009).

2.2.4.5 Intranasal delivery: Nasal mucosa has emerged as a therapeutically viable channel for the administration of systemic drugs and also appears to be a favorable way to overcome the obstacles for the direct entry of drugs to the target site (Pires et al; 2009). This route is preferred when the drug is prone to gastrointestinal metabolism and is useful for targeting purpose. This route is non invasive, painless and favorably preferred. The olfactory region of the nasal mucosa provides a direct connection between the nose and brain and by the use of nanoemulsions loaded with drugs brain targeting can be achieved. Preparation of nanoemulsions containing risperidone for intranasal delivery to the brain has been reported (Kumar et al; 2008).

2.2.4.6Targeted delivery: Targeting the drug to site of action is main goal of a delivery system and it can be achieved with or without modification. Recently, nanoemulsions are reported for drug targeting. Madhusudhan et al developed carbamazepine nanoemulsions employing 1-o-alkylglycerols as a way to achieve selective brain delivery of this antiepileptic drug (Madhusudhan et al; 2007). Maranhao et al showed that cholesterol-rich nanoemulsion is taken up by the cells by the low-density lipoprotein (LDL) receptors. Because LDL receptors are upregulated in several neoplastic cells, after injection into the blood stream the nanoemulsion concentrates in the neoplastic tissues (Maranhao et al; 1994). Graziani SR et al showed that intravenous injection of the nanoemulsion may produce a concentration of the drug in the tumor as high as fivefold in breast cancer (Graziani SR et al; 2002). Mendes et al showed with intralesional injection of the lipidic nanoemulsion was promising approach for drug-targeting in neoadjuvant chemotherapy in breast cancer treatment (Mendes et al; 2009).

2.3 Drug profiles:

2.3.1 Simvastatin:

(Martindale, 2009; Merck Index, 2006; Drug bank, Rx Drug List, FDA Label)

Category: Anticholesteremic Agent, Antilipemic Agent, Hydroxymethylglutaryl-CoA Reductase Inhibitor

CAS Number: *79902–63–9*

Proprietary names: Zocor, Simlup, Simvotin, Simcard [India] Denan (Germany), Liponorm, Sivastin (Italy), Lipovas (Japan), Lodales (France), Zocord (Austria and Sweden)

Molecular formula: $C_{25}H_{38}O_5$

Molecular Weight: 418.56

Structural Formula and Chemical Name:
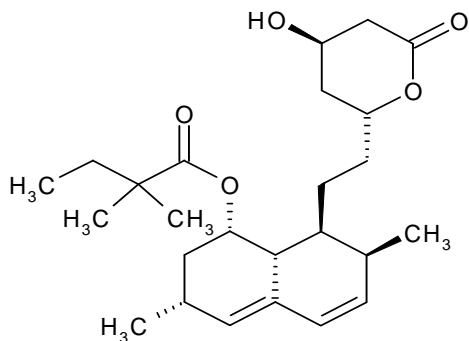
(1S,3R,7S,8S,8aR)-8-{2-[(4R)-4-hydroxy-6-oxooxan-2-yl]ethyl}-3,7-dimethyl-1,2,3,7,8,8a-hexahydronaphthalen-1-yl 2,2-dimethylbutanoate

Physicochemical Properties:

Appearance and colour: A white to off-white, nonhygroscopic, crystalline powder.

Solubility: It is practically insoluble in water, and freely soluble in chloroform, methanol and ethanol.

Partition Coefficient. Log *P* (octanol/water), 4.7.

Melting point: 135° to 138°.

Mechanism of action: The 6-membered lactone ring of Simvastatin is hydrolyzed *in vivo* to generate the beta, delta-dihydroxy acid, an active metabolite structurally similar to HMG-CoA (hydroxymethylglutaryl CoA). Once hydrolyzed, Simvastatin competes with HMG-CoA for HMG-CoA reductase, a hepatic microsomal enzyme. Interference with the activity of this enzyme reduces the quantity of mevalonic acid, a precursor of cholesterol.

Pharmacokinetics

Absorption:

Simvastatin, a lipophilic drug, can easily penetrate the plasma membrane in a nonspecific manner indicating high absorption from the intestine after an oral dose. After oral dosing, Simvastatin achieved substantially higher concentrations in the liver than in non-target tissues. Simvastatin undergoes extensive first-pass extraction in the liver, its primary site of action, with subsequent excretion of drug equivalents in the bile. As a consequence of extensive hepatic extraction of Simvastatin, the availability of drug to the general circulation is low. Bioavailability of Simvastatin was estimated to be less than 5% of an oral dose of Simvastatin.

Distribution:

Both Simvastatin and its (beta)-hydroxy acid metabolite are highly bound (approx. 95%) to human plasma proteins. The lipophilic nature allows Simvastatin to penetrate the CNS.

Metabolism:

The systemic availability of Simvastatin (< 5%) is caused by cytochrome P450 mediated enzymatic conversion in the gut and in the liver. The extensive oxidative metabolism of Simvastatin in human liver is primarily mediated by CYP 3A (CYP 3A4 and CYP 3A5), with the remaining metabolism being attributed to CYP 2C8, and CYP 2C9. Glucuronidation constitutes a common metabolic pathway for statins, in addition to the CYP P450-mediated oxidation and ß-oxidation processes. Simvastatin, administered as lactone, is metabolically activated to the open chain nonlactone Simvastatin acid. This reversible conversion to the active form occurs by nonspecific carboxyesterases in the intestinal wall, liver and to some extent in plasma or by nonenzymatic hydrolysis. (Tubic-Grozdanis et al; 2008)

Elimination:

The predominant route of elimination for Simvastatin is via the bile after metabolism by the liver. Following an oral dose of Simvastatin, 13% of the dose was excreted in urine and 60% in feces. The latter represents absorbed drug equivalents excreted in bile, as well as any unabsorbed drug. The elimination half life of Simvastatin is 1.9 hr.

Usage and Administration: Therapy with Simvastatin is indicated in those individuals at increased risk for atherosclerosis-related clinical events as a function of cholesterol level,

the presence of Coronary heart disease (CHD), or other risk factors. Lipid-altering agents should be used in addition to a diet restricted in saturated fat and cholesterol when the response to diet and other nonpharmacological measures alone has been inadequate. The dosage should be individualized according to the baseline LDL-C level, the recommended goal of therapy, and the patient's response. The dosage range is 5-80 mg/day. The recommended usual starting dose is 20 mg once a day in the evening. Patients who require a large reduction in LDL-C (more than 45%) may be started at 40 mg/day in the evening. Adjustments of dosage should be made at intervals of 4 weeks or more.

Contraindications:

Simvastatin is contraindicated in case of hypersensitivity to any component of this medication, active liver disease or unexplained persistent elevations of serum transaminases and pregnancy and lactation.

Adverse Effects:

The most common adverse effects of Simvastatin include gastrointestinal disorders, myalgia, arthralgia, upper respiratory infections, headache, abdominal pain, constipation and nausea.

Analytical Methods:

The reported analytical methods for estimation of Simvastatin are as follows:

UV-spectrophotometric method

1) A simple accurate and sensitive UV-spectrophotometric method for estimation of Simvastatin in methanol was developed by Arayne et al. (Arayne et al; 2007).

HPLC method

1) A simple HPLC method was reported for simvastain analysis in plasma by Carlucci et al 1992. The separation was performed on ODS Hypersil column (250 X 4.6 mm i.d, 10 μm). The mobile phase consist of mixture of 0.025M sodium dihydrogenphosphate (pH 4.5)-acetonitrile (35:65, v/v). Flow rate was maintained 1.5 ml/min and compound eluted were recorded by UV detector at 238nm. The retention time of Simvastatin was 7.2 min.

2) USP method is a gradient HPLC method and uses variable mixture of mobile phase solution A and solution B as mobile phase. [Solution A is mixture of acetonitrile and dilute phosphoric acid (50:50) while solution B is 0.1% solution of phosphoric acid in

acetonitrile. The liquid chromatograph is equipped with a 238 nm detector and a 4.4 X 33mm column that contain packing L1. The flow rate is 3 ml/min.

Formulations available:

Tablet (5, 10, 20, 40 and 80 mg) available for oral administration

2.3.2 Entacapone:

(Martindale, 2009; Merck Index, 2006; Drug bank, Rx Drug List)

Category: Catechol-O-methyltransferase (COMT) inhibitor

CAS Number: 130929–57–6

Proprietary names: Comtan, Comtess

Molecular formula: $C_{14}H_{15}N_3O_5$

Molecular Weight: 305.29

Structural Formula and Chemical Name:
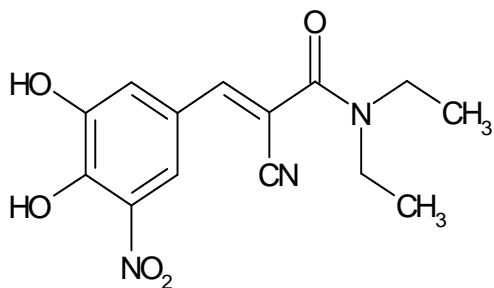
(E)-2-cyano-3-(3,4-dihydroxy-5-nitrophenyl)-N,N-diethyl-2-propenamide

Physicochemical Properties:

Appearance and colour: A yellow crystalline powder.

Solubility: Insoluble in water, soluble or sparingly soluble in acetone, and slightly soluble in anhydrous ethanol.
Partition Coefficient. Log P (octanol/water), 2.8.

Melting point: 162° to 163°.

Mechanism of action: Entacapone is a selective and reversible inhibitor of catechol-O-methyltransferase (COMT).

The mechanism of action of Entacapone is believed to be through its ability to inhibit COMT and alter the plasma pharmacokinetics of levodopa. When Entacapone is given in conjunction with levodopa and an aromatic amino acid decarboxylase inhibitor, plasma levels of levodopa are greater and more sustained than after administration of levodopa and an aromatic amino acid decarboxylase inhibitor alone. It is believed that at a given frequency of levodopa administration, these more sustained plasma levels of levodopa result in more constant dopaminergic stimulation in the brain, leading to greater effects on the signs and symptoms of Parkinson's disease.

Pharmacokinetics

Absorption: Entacapone is rapidly absorbed, with a t_{max} of approximately 1 hour. The absolute bioavailability following oral administration is 35%. Food does not affect the pharmacokinetics of Entacapone.

Distribution: The volume of distribution of Entacapone at steady state after i.v. Injection is small (20 L). Entacapone does not distribute widely into tissues due to its high plasma protein binding (98%). Entacapone binds mainly to serum albumin.

Metabolism and Elimination: Entacapone is almost completely metabolized prior to excretion, with only a very small amount (0.2 % of dose) found unchanged in urine. The main metabolic pathway is isomerization to the *cis*-isomer, followed by direct glucuronidation of the parent and *cis*-isomer; the glucuronide conjugate is inactive. As only about 10% of the Entacapone dose is excreted in urine as parent compound and conjugated glucuronide, biliary excretion appears to be the major route of excretion of this drug. The elimination half life is 0.4-0.7 hr.

Indications: Entacapone is indicated as an adjunct to levodopa/carbidopa to treat patients with idiopathic Parkinson's disease.

Contraindications: Entacapone is contraindicated in patients who have demonstrated Hypersensitivity to the drug or its ingredients.

Dosage and administration: The recommended dose of Entacapone is one 200 mg tablet administered concomitantly with each levodopa/carbidopa dose to a maximum of 8 times daily (200 mg x 8 = 1600 mg per day). Clinical experience with daily doses above 1600 mg is limited.

Adverse reactions: The most commonly observed adverse events associated with the use of Entacapone are dyskinesia/hyperkinesia, nausea, urine discoloration, diarrhea, and abdominal pain.

Analytical Methods:

UV method

1) A UV method was reported by Paim et al 2005 for determination of Entacapone using acetonitrile as solvent.

HPLC method

2) A simple HPLC method was reported by Ramkrishna et al 2005 for determination of Entacapone in plasma samples. In this method, the separation was performed on reverse phase C_{18} column (250 X 4.6 mm i.d, 5 µm). The mobile phase consist of mixture of 30 mM phosphate buffer (pH 2.75)-acetonitrile (62:38, v/v). Flow rate was maintained 1.0 ml/min and compound eluted were recorded by UV detector at 315nm. The method was validated for linearity, accuracy and precision.

3) Another reversed-phase HPLC method was developed and validated for the assay of Entacapone by Soukhova et al (Soukhova et al. 2011). The method employed a C18 column, a mobile phase of potassium phosphate buffer (pH 2.75, 30 mM)-methanol (50:50, v/v) at a flow rate of 1.0 mL/min, and ultraviolet (UV) detection at 310 nm.

Formulation Available:

Tablet (200 mg) available for oral administration.

2.4 References

- Ammar HO, Salama HA, Ghorab M, Mahmoud AA. Nanoemulsion as a Potential Ophthalmic Delivery System for Dorzolamide Hydrochloride. AAPS PharmSciTech. 10(3), 2009, 808–819.

- Anton N, Gayet P, Benoit J, Saulnier P. Nano-emulsions and nanocapsules by the PIT method: An investigation on the role of the temperature cycling on the emulsion phase inversion. Int J Pharm. 344, 2007, 44–52.

- Araujo FA, Kelmann RG, Araujo BV, Finatto RB, Teixeira HF, Koester LS. Development and characterization of parenteral nanoemulsions containing thalid132±9nmomide. Eur J Pharm Sci. 42(3), 2011, 238-245.

- Arayne MS, Sultana N, Hussain F, Ali SA. Validated spectrophotometric method for quantitative determination of Simvastatin in pharmaceutical formulations and human serum. J Analytical Chem. 62(6), 2007, 536-541.

- Badens E, Majerik V, Horvath H, Szokonya L, Bosc N, Teillaud E, Charbit G. Comparison of solid dispersions produced by supercritical antisolvent and spray-freezing technologies. Int J Pharm. 377, 2009, 25-34.

- Benita S, Friedman D, Weinstock M. Physostigmine emulsion: a new injectable controlled release delivery system. Int J Pharm. 30, 1986, 47–55.

- Bouchemal K, Briancon S, Perrier E, Fessi H. Nano-emulsion formulation using spontaneous emulsification: solvent, oil and surfactant optimization. Int J Pharm. 280, 2004, 241–251.

- Bruce JA. Novel formulation strategies for improving oral bioavailability of drugs with poor membrane permeation or presystemic metabolism. J Pharm Sci. 82, 1993, 979–987.

- Carlucci G, Mazzeo P, Biordi L, Bologna M. Simultaneous determination of simvastain and its hydroxyl acid form in human plasma by high performance liquid chromatography with UV detection. J Pharm Biomed Analysis. 10(9), 1992, 693-697.

- Chattopadhyay P, Gupta RB. Production of griseofulvin nanoparticles using supercritical CO2 antisolvent with enhanced mass transfer. Int J Pharm. 228, 2001, 19-31.

- Chen H, Khemtong C, Yang X, Chang X, Gao J. Nanonization strategies for poorly water-soluble drugs. Drug Discov Today 16(7-8), 2011, 354-360.

- Chen JF, Zhou MY, Shao L, Wang YY, Yun J, Chew N, Chan HK. Feasibility of preparing nanodrugs by high gravity reactive precipitation. Int J Pharm. 269, 2004, 267–274.

- Chhabra G, Chuttani K, Mishra AK, Pathak K. Design and development of nanoemulsion drug delivery system of amlodipine besilate for improvement of oral bioavailability. Drug Dev Ind Pharm. 37(8), 2011, 907-916.

- Chidambaram N, Burgess DJ. A Novel In Vitro Release Method for Submicron-Sized Dispersed Systems. AAPS Pharmsci. 1(3), 1999, 1-4

- Chingunpituk J. Nanosuspension Technology for Drug Delivery. Walailak J Sci & Tech. 4, 2007, 139-153.

- Constantinides PP, Tustian A, Kessler DR, Tocol emulsions for drug solubilization and parenteral delivery. Adv Drug Deliv Rev. 56, 2004, 1243–1255.

- Craig DQM. The mechanisms of drug release from solid dispersions in water-soluble polymers. Int J Pharm. 231, 2002, 131–144.

- Date AA, Patravale VB. Current strategies for engineering drug nanoparticles. Curr Opin Colloid Interface Sci. *9,* 2004, 222–235.

- Davis SS, Hadgraft J, Palin JK, Medical and Pharmaceutical application of emulsions. In: Becher, P. (Ed.), Encyclopedia of Emulsion Technology, vol. 2.Marcel Dekker, New York, 1985. pp. 160–225.

- Dhirendra K, Lewis S, Udupa N, Atin K. Solid dispersions: a review. Pak J Pharm Sci. 22(2), 2009, 234-246.

- Dhumal RS, Biradar SV, Yamamura S, Paradkar AR. Preparation of amorphous cefuroxime axetil nanoparticles by sonoprecipitation for enhancement of bioavailability. Eur J Pharm Biopharm. 70, 2008, 109-115.

- Fakes MG, Vakkalagadda B, Qian F, Desikan S, Gandhi RB, Lai C, Hsieh A, Franchini MK, Toale H, Brown J. Enhancement of oral bioavailability of an HIV-attachment inhibitor by nanosizing and amorphous formulation approaches. Int J Pharm. 370(1-2), 2009, 167-174.

- Gao F, Zhang Z, Bu H, Huang Y, Gao Z, Shen J, Zhao C, Li Y. Nanoemulsion improves the oral absorption of candesartan cilexetil in rats: Performance and mechanism. J Control Rel. 149, 2011, 168–174.

- Gibson L. Lipid based excipients for oral drug delivery. In Hauss DJ (Ed). Oral lipid based formulations, Informa Healthcare, volume 170, 2007, pp. 33-45.

- Gonzales-Caballero F, de Dios Garcia Lopez-Duran J. Suspension formulation. In: Nielloud F, Marti-Mestres G, Editors. Pharmaceutical Emulsions and Suspensions, Drugs and the Pharmaceutical Sciences. New York: Marcel Dekker Inc; 2000. pp. 127–190.

- Graziani SR, Igreja FAF, Hegg R, Meneghetti C, Brandizzi LI, Barboza R, Amancio R, Pinnoti J, Maranhao R. Uptake of a cholesterol-rich emulsion by breast cancer. Gynecol Oncol. 85, 2002, 493–497.

- Gursoy RN, Benita S. Self-emulsifying drug delivery systems (SEDDS) for improved oral delivery of lipophilic drugs. Biomed Pharmacother. 58(3), 2004, 173–182.

- Gutierrez JM, Gonzalez C, Maestro A, Sole I, Pey CM, Nolla J. Nano-emulsions: New applications and optimization of their preparation. Curr Opin Colloid Interface Sci. 13, 2008, 245–251.

- Hagigit T, Abdulrazik M, Orucov F, Valamanesh F, Hagedorn M, Lambert G, Behar-Cohen F, Benita S. Topical and intravenous administration of cationic nanoemulsions to deliver antisense oligonucleotides directed towards VEGF KDR receptors to the eye. J Control Rel. 145(3), 2010, 297-305.

- Hofstee BHJ. In: Methods of Protein Separation. Catsimpoolas N, editor. New York: Plenum Press; 1976, pp. 245-278.

- Humberstone AJ, Charman WN. Lipid based vesicles for oral delivery of poorly water-soluble drugs. Adv Drug Del Rev. 25(1), 1997, 103-128.

- Jafari SM, He Y, Bhandari B. Production of sub-micron emulsions by ultrasound and microfluidization techniques. J Food Engi. 82, 2007, 478–488.

- Jain V, Prasad V, Jadhav P, Mishra PR. Preparation and performance evaluation of saquinavir laden cationic submicron emulsions. Drug Deliv. 16(1), 2009, 37-40.

- Kakumanu S, Tagne JB, Wilson TA, Nicolosi RJ. A nanoemulsion formulation of dacarbazine reduces tumor size in a xenograft mouse epidermoid carcinoma model compared to dacarbazine suspension . Nanomedicine: Nanotech Biol Med. 7(3), 2011, 277-283.

- Kashchiev D. Nucleation: Basic Theory with Applications. Butterworth-Heinemann, Oxford, 2000, pp.30-33.

- Kassem MA. Abdel RA, Ghorab MM, Ahmed MB, Khalil RM. Nanosuspension as an ophthalmic delivery system for certain glucocorticoid drugs. Int J Pharm. 340(1-2), 2007, 126-133.

- Kayser O. A new approach for targeting to Cryptosporidium parvum using mucoadhesive nanosuspensions: research and applications. Int J Pharm. 214, 2001, 83-85.

- Keck CM. Particle size analysis of nanocrystals: Improved analysis method. Int J Pharm. 390, 2010, 3–12.

- Kelmann RG, Kuminek G, Teixeira HF, Koester LS. Carbamazepine parenteral nanoemulsions prepared by spontaneous emulsification process. Int J Pharm. 342, 2007, 231–239.

- Kesisoglou F, Panmai S, Wu Y. Nanosizing—oral formulation development and biopharmaceutical evaluation. Adv Drug Deliv Rev. 59, 2007, 631–644.

- Kipp JE. The role of solid nanoparticle technology in the parenteral delivery of poorly water-soluble drugs. Int J Pharm. 284, 2004, 109–122.

- Krishnaiah YSR. Pharmaceutical technologies for enhancing oral bioavailability of poorly soluble drugs, J. Bioequivalence Bioavailability 2, 2010, 28–36.

- Kumar M, Misra A, Babbar AK, Mishra AK. Intranasal nanoemulsion based brain targeting drug delivery system of risperidone. Int J Pharm. 358, 2008, 285-291.

- Lawrence MJ, Rees GD. Microemulsion based media as a novel drug delivery system. Adv Drug Del Rev. 45, 2000, 89–121.

- Leong TSH, Wooster TJ, Kentish SE, Ashokkumar M. Minimising oil droplet size using ultrasonic emulsification. Ultrasonics sonochemistry 16 (2009) 721–727.

- Louhi-Kultanen M, Karjalainen M, Rantanen J, Huhtanen M, Kallas J. Crystallization of glycine with ultrasound. Int J Pharm. 320, 2006, 23–29.

- Madhusudhan B, Rambhau D, Apte SS, Gopinath D. 1-O-alkylglycerol stabilized carbamazepine intravenous o/w nanoemulsions for drug targeting in mice. J Drug Target. 15(2), 2007, 154-161.

- Majumdar AK, Howard L, Goldberg MR, Hickey L, Constanzer M, Rothenberg PL, Crumley TM, Panebianco D, Bradstreet TE, Bergman AJ, Waldman SA, Greenberg HE, Butler K, Knops A, De Lepeleire I, Michiels N, Petty KJ. Pharmacokinetics of aprepitant after single and multiple oral doses in healthy volunteers. J Clin Pharmacol. 46(3), 2006, 291–300.

- Maranhao RC, Garicochea B, Silva EL, Dorlhiac-Llacer P, Cadena SMS, Coelho IJC, et al. Plasma kinetics and biodistribution of a lipid emulsion resembling low density lipoprotein in patients with acute leukemia. Cancer Res. 54, 1994, 4660–4666.

- Martindale Extra Pharmacopoeia, 36th Ed. Pharmaceutical Press, London, 2009, pp. 804 and 1390-1396.

- Meleson K, Graves S, Thomas G. Mason Formation of Concentrated Nanoemulsions by Extreme Shear. Soft Materials 2(2&3), 2004, 109–123.

- Mendes S, Graziani SR, Vitório TS, Padoveze AF, Hegg R, Bydlowski SP, Maranhao RC. Uptake by breast carcinoma of a lipidic nanoemulsion after intralesional injection into the patients: A new strategy for neoadjuvant chemotherapy. Gynecologic Oncol. 112(2), 2009, 400-404.

- Merisko-Liversidge E, Liversidge GG, Cooper ER. Nanosizing: a formulation approach for poorly water-soluble compounds. Eur J Pharm Sci. 18, 2003, 113–120.

- Merisko-Liversidge E, Liversidge GG. Nanosizing for oral and parenteral drug delivery: A perspective on formulating poorly-water soluble compounds using wet media milling technology. Adv Drug Deliv Rev. 63(6), 2011, 427-440.

- Mochalin VN, Sagar A, Gour S, Gogotsi Y. Manufacturing Nanosized Fenofibrate by Salt Assisted Milling. Pharm Res. 26, 2009, 1365-1370.

- Moghimi SM, Agrawal A. Lipid-based nanosystems and complexes in experimental and clinical therapeutics. Curr Drug Deliv. 2, 2005, 295-296.

- Molpeceres J, Aberturas MR, Guzman M. Biodegradable nanoparticles as a delivery system for cyclosporin: preparation and characterization. J Microencapsulation 17, 2000, 599-614.

- Mosqueira VCF, Legrand P, Gulik A, Bourdon O, Gref R, Labarre D, Barratt G. Relationship between complement activation, cellular uptake and surface physicochemical aspects of novel PEG-modified nanocapsules. Biomaterials. 22, 2001, 2967-2979.

- Muller RH, Benita S, Bohm B. Emulsions and nanosuspensions for the formulation of poorly water soluble drugs. Stuttgard, Med. Pharm. 1998, 15-28.

- Muller RH, Grau MJ. Increase in dissolution velocity and solubility of poorly water soluble drugs as nanosuspensions. Proceeding of World Meeting APGI APV; 2, 1998, 623-624.

- Muller RH, Jacobs C, Kayser O. Nanosuspension as particulate drug formulations in therapy rationale for development and what we can expect for the future. Adv Drug Del Rev. 47, 2001, 3-19.

- Muller RH, Jacobs C. Buparvaquone mucoadhesive nanosuspension: preparation, optimisation and long-term stability. Int J Pharm. 237, 2002, 151-161.

- Muller RH, Moschwitzer J, Bushrab FN. Manufacturing of nanoparticles by milling and homogenization techniques. In: Gupta RB, Kompella UB, Editors. Nanoparticle Technology for Drug Delivery, Drugs and the Pharmaceutical Sciences. New York: Taylor & Francis Group LLC; 2006. pp. 21–51.

- Muller RH, Peters K. Nanosuspension for formulation of poorly soluble drugs I: Preparation by size reduction technique. Int J Pharm. 160, 1998, 229-237.

- Muller RH. Particle size analysis of latex suspensions and microemulsions by photon correlation spectroscopy. J Pharm Sci. 73, 1984, 915-918.

- Nizri G, Magdassi S, Schimdt J, Cohen Y, Talmon Y. Microstructural characterization of micro- and nanoparticles formed by polymer-surfactant interaction. Langmuir 20, 2004, 4380-4438.

- Paim CS, Alves HG; Lange A, Miron D, Steppe M. Validation of UV spectrophotometric method for quantitative determination of Entacapone in tablets

using experimental design of Plackett-Burmam for robustness evaluation and comparison with HPLC. Analytical Lett. 41 (4), 2008, 571-581.

- Pecora R. Dynamic light scattering measurements of nanometre particles in liquids. J Nanopart Res. 2, 2000, 123-131.

- Piao H, Kamiya N, Hirata A, Fujii T, Goto M. A novel solid-in-oil nanosuspension for transdermal delivery of diclofenac sodium. Pharm Res. 25, 2008, 896–901.

- Prakash RU, Thiagarajan P. Nanoemulsions for drug delivery through different routes. Res Biotech. 2(3), 2011, 1-13.

- Puglia C, Rizza L, Drechsler M, Bonina F. Nanoemulsions as vehicles for topical administration of glycyrrhetic acid: characterization and in vitro and in vivo evaluation. Drug Deliv. 2010; 17(3):123-9.

- Ramakrishna NVS, Vishwottam KN, Wishu S, Koteshwara M, Chidambara J. High-performance liquid chromatography method for the quantification of Entacapone in human plasma. J Chromatography B. 823, 2005, 189–194.

- Rieger MM. Emulsions. In: Lachman L, Lieberman HA, Konig JL, editors. The theory and practice of industrial pharmacy. Philadelphia: Lea and Febiger. 1986. pp. 502–533.

- Rodriguez-Abreu C, Lazzari M. Emulsions with structured continuous phases. Curr Opin Colloid Interface Sci. 13, 2008, 198–205.

- Sarker DK. Engineering of Nanoemulsions for Drug Delivery. Current Drug Deliv. 2, 2005, 297-310.

- Scholer N, Krause K, Kayser O, Muller RH, Borner K, Hahn H, Liesenfeld O. Atovaquone nanosuspensions show excellent therapeutic effect in a new murine model of reactivated toxoplasmosis. Antimicrob Agents Chemother. 45, 2001, 1771–1779.

- Seki J, Sonoke S, Saheki A, Fukui H, Sasaki H, Mayumi T. A nanometer lipid emulsion, lipid nano-sphere (LNS), as a parenteral drug carrier for passive drug targeting. Int J Pharm. 273(1-2), 2004, 75-83.

- Shanthakumar TR, Prakash S, Basavraj RM, Ramesh M, Kant R, Venketesh P, Rao K, Singh S, Shrinivas NR. Comparative pharmacokinetic data of DRF 4367 using

nanosuspension and HP 8-CD formulation. Proceeding of the International symposium on Advances in Technology and Business Potential of New Drug Delivery systems. Mumbai 2004. B V Patel Education Trust and B V Patel PERD Centre, Abstract 55.

- Sharma N, Bansal M, Visht S, Sharma PK, Kulkarni GT. Nanoemulsion: A new concept of delivery system. Chronicles of Young Scientist. 1(2), 2010, 2-6.

- Sharma P, Garg S. Pure drug and polymer based nanotechnologies for the improved solubility, stability, bioavailability and targeting of anti-HIV drugs. Adv Drug Deliv Rev. 62, 2010, 491–502.

- Shen JQ, Gan Y, Gan L, Zhu CL, Zhu JB. Ion-sensitive nanoemulsion-in situ gel system for ophthalmic delivery of flurbiprofen axetil. Yao Xue Xue Bao. 45(1), 2010, 120-125.

- Shen Q, Wang Y, Zhang Y. Improvement of colchicine oral bioavailability by incorporating eugenol in the nanoemulsion as an oil excipient and enhancer. Int J Nanomedicine. 6, 2011, 1237-1243.

- Shinoda K, Saito H. The stability of o/w type of emulsion as a function of temperature and HLB of emulsifier: The emulsification by PIT method. J colloids Interface Sci. 30(2), 1969, 258-263.

- Shono Y, Jantratid E, Kesisoglou F, Reppas C, Dressman JB. Forecasting in vivo oral absorption and food effect of micronized and nanosized aprepitant formulations in humans. Eur J Pharm Biopharm. 76, 2010, 95–104.

- Shubar HM, Dunay IR, Lachenmaier S, Dathe M, Bushrab FN, Mauludin R, Muller RH, Fitzner R, Borner K, Liesenfeld O. The role of apolipoprotein E in uptake of atovaquone into the brain in murine acute and reactivated toxoplasmosis, J Drug Target. 17, 2009, 257–267.

- Singh KK, Vingkar SK. Formulation, antimalarial activity and biodistribution of oral lipid nanoemulsion of primaquine. Int J Pharm. 347, 2008, 136–143.

- Siostrom B, Kronberg B, Carlfors J. A method for the preparation of submicron particles of sparingly water soluble drugs by precipitation in oil-in-water emulsions.

1. Influence of emulsification and surfactant concentration. J Pharm Sci. 82, 1993, 579–583.

- Solans C, Esquena J, Forgiarini AM, Uson N, Morales D, Izquierdo P, Azemar N, Garcia-Celma MJ. Nano-emulsions: formation, properties and applications. Surfactant Science Series 109, 2003, 525–554.

- Soukhova N, Kassymbek Z, Bradby S, Martin-Esker A, White P, Wahab S. Development of characterization methods for Entacapone in a pharmaceutical bulk. J Pharm Biomed Anal. 54(4), 2011, 860-865.

- Stolnik S, Davies MC, Illum L, Davis SS, Boustta M, Vert M. The preparation of sub-200 nm biodegradable colloidal particles from poly (β-malic acid-co-benzyl malate) copolymers and their surface modification with Poloxamer and Poloxamine surfactants. J Control Rel. 30, 1994, 57-67.

- Tabibi SF, Rhodes CT. In: Baiker G. S. Modem Pharmaceutics. New York: Marcel Dekker 1996, 3rd edn.

- Tadros T, Izquierdo P, Esquena J, Solans C. Formation and stability of nanoemulsions. Adv Colloid Interface Sci. 108 –109, 2004, 303–318.

- Tang SY, Manickam S, Wei TK, Nashiru B. Formulation development and optimization of a novel Cremophore EL-based nanoemulsion using ultrasound cavitation. Ultrasonics Sonochem. 19(2), 2012, 330-345.

- The Merck Index, 14th Ed. US Pharm Merck & Company Publication, NJ, USA, 2006, p. 613 and 1471.

- Tozuka Y, Miyazaki Y, Takeuchi H. A combinational supercritical CO_2 system for nanoparticle preparation of indomethacin. Int J Pharm. 386, 2010, 243-248.

- Trotta M, Gallarate M, Carlotti ME, Morel S. Preparation of griseofulvin nanoparticles from water-dilutable microemulsions. Int J Pharm. 254, 2003, 235–242.

- Tubic-Grozdanis M, Hilfinger JM, Amidon GL, Kim JS, Kijek P, Staubach P, Langguth P. Pharmacokinetics of the CYP 3A Substrate Simvastatin following Administration of Delayed Versus Immediate Release Oral Dosage Forms. Pharm Res. 25(7), 2008, 1591-1600.

- Vanderhoff JW. In: Pharmaceutical Dosage Forms Disperse Systems. New York: Marcel Dekker; 1996, pp. 91-152.

- Vasconcelos T, Sarmento B, Costa P. Solid dispersions as strategy to improve oral bioavailability of poor water soluble drugs. Drug Discovery Today. 12(23, 24), 2007, 1068-1075.

- Vitale SA, Katz JL. Liquid droplet dispersions formed by homogeneous liquid–liquid nucleation: the Ouzo effect. Langmuir 19, 2003, 4105–4110.

- Vyas TK, Shahiwala A, Amiji MM. Improved oral bioavailability and brain transport of Saquinavir upon administration in novel nanoemulsion formulations. Int J Pharm. 347, 2008, 93–101.

- Washington C. Stability of lipid emulsions for drug delivery. Adv Drug Deliv Rev. 20, 1996, 131-145.

- Won D, Kim M, Lee S, Park J, Hwang S. Improved physicochemical characteristics of felodipine solid dispersion particles by supercritical anti-solvent precipitation process. Int J Pharm. 301, 2005, 199–208.

- Xiong R, Lu W, Li J, Wang P, Xu R, Chen T. Preparation and characterization of intravenously injectable nimodipine nanosuspension. Int J Pharm. 350, 2008, 338–343.

- Yang JZ, Young AL, Chiang PC, Thurston A, Pretzer DK. Fluticasone and budesonide nanosuspensions for pulmonary delivery: preparation, characterization, and pharmacokinetic studies. J Pharm Sci. 97(11), 2008; 4869-4878.

- Yang SC, Benita S. Enhanced Absorption and Drug Targeting by Positively Charged Submicron Emulsions. Drug Develop Res. 50, 2000, 476–486.

- Yang SC, Zhu JB. Preparation and characterization of camptothecin solid lipid nanoparticles. Drug Dev Ind Pharm. 28, 2002, 265-274.

- Yao J, Zhou JP, Ping QN. Characteristics of nobiletin-loaded nanoemulsion and its in vivo distribution in mice [Article in Chinese]. Yao Xue Xue Bao. 42(6), 2007, 663-8.

- York P. Strategies for particle design using supercritical fluid technologies. PSTT 2, 1999, 430-440.

- Yu W, Tabosa Do Egito ES, Barrat G, Fessi JP, Devissaguet JP, Puisieux F. A novel approach to the preparation of injectable emulsions by spontaneous emulsification process. Int J Pharm. 89, 1993, 139–146.

- Zhong J, Shen Z, Yang Y, Chen J. Preparation and characterization of uniform nanosized cephradine by combination of reactive precipitation and liquid anti-solvent precipitation under high gravity environment. Int J Pharm. 301, 2005, 286–293.

- Zhou H, Yue Y, Liu G, Li Y, Zhang J, Gong Q, Yan Z, Duan M. Preparation and characterization of a lecithin nanoemulsion as a topical delivery system. Nanoscale Res Lett. 5(1), 2009, 224-30.

- Ziller KH, Rupprecht HH. Control of crystal growth in drug suspension. Pharm Ind. 52 (8), 1990, 1017-1022.

3.1 Materials

Simvastatin (Ajanta Pharmaceuticals, Mumbai, India) and Entacapone (Alembic Limited, Vadodara, India) were received as gift samples. Potassium phosphate monobasic (KH_2PO_4), Sodium hydroxide, Methanol, Hydrochloric acid and Tween 80 were procured from SD Fine Chemicals, Mumbai, India. Double distilled water (DDW) was purified by passing through 0.45µ Millipore filters (Millipore, Bangalore, India).

3.2 Estimation of Simvastatin by Ultraviolet Spectroscopy (UV)

Stock solution

Standard stock solution (100 µg/ml) was prepared by dissolving 10 mg of Simvastatin in 100 ml of methanol.

3.2.1 Calibration Plot in methanol

Aryane et al reported the UV spectrophotometric method for estimation of Simvastatin in methanol (Aryane et al., 2007). The analysis was performed by first scanning solution of Simvastatin (10 µg/ml) in the ultraviolet range between 200 and 400 nm and determining its λmax. Suitable aliquots of the stock solution of Simvastatin were pipetted out into 10 ml volumetric flasks and the volume was made upto 10 ml with methanol to give final concentrations ranging from 2-20 µg/ml. The solutions were mixed using vortex mixer and their absorbances measured at λmax using methanol as blank on Shimadzu 1601 UV-Visible Spectrophotometer and calibration curve was plotted. The above procedure was repeated three times. Standard concentrations (1.0, 5.0, and 10.0 µg/ml) were prepared and subjected to interday and intraday analysis to estimate accuracy and precision. The interference of the formulation excipients was studied by analysis formulation sample without drug and absorbance at λmax of drug was noted.

3.2.2 Calibration Plot in pH 7.2 phosphate buffer

The UV-spectrophotometric method was developed for estimation of Simvastatin in pH 7.2 buffer by first scanning solution of Simvastatin (10 µg/ml) in the ultraviolet range between 200 and 400 nm and determining its λmax. Suitable aliquots of the stock solution of Simvastatin were pipetted out into 10 ml volumetric flasks and the volume was made upto 10ml with pH 7.2 phosphate buffer to give final concentrations ranging from 4-20 µg/ml.

The solutions were mixed using vortex mixer and their absorbances measured at λmax using pH 7.2 phosphate buffer as blank on Shimadzu 1601 UV-Visible Spectrophotometer and calibration curve was plotted). The above procedure was repeated three times. Standard concentration (1.0, 5.0, and 10.0 µg/ml) were prepared and subjected to interday and intraday analysis to estimate accuracy and precision.

3.2.3 Analytical method validation

The method was validated for accuracy, precision and linearity.

3.2.3.1 Linearity

The linearity of an analytical method is its ability within a definite range to obtain results directly proportional to the concentrations (quantities) of the analyte in the sample (Hubert et al., 1999; Hubert et al., 2003). Linearity of a light absorption determination should be examined to ensure that Beer's law operates over the range of interest.

For evaluation of the linearity of the UV method of Simvastatin, the standard solutions were prepared at 2, 4, 8, 12, 16 and 20 µg/ml concentrations (n = 3) and absorbance were taken at 238 nm. The method was said to be linear for estimation of Simvastatin if it R^2 was near to 1. Least square regression method was used to determine the regression coefficient, r and the equation for the best fitting line.

3.2.3.2 Accuracy

Accuracy refers to the closeness of an individual observation or mean of the observations to true value (Bolton, 1990). The "true" value is the result which would be observed in absence of error. Accuracy of the assay is defined as the percentage of the agreement between the measured value and the true value as follows (Merodia et al, 2000). The accuracy is calculated by using following formula:

$$\text{Accuracy} = \frac{\text{True value} - \text{Measured value}}{\text{True value}} \, 100 \qquad \text{......... 3.1}$$

3.2.3.3 Precision

It refers to the extent of variability of a group of measurements observed under similar conditions. Precision provides an indication of random errors and is generally subdivided

into two cases: repeatability and reproducibility, which were determined by calculating RSD (Relative standard deviation) or CV (Coefficient of variation) of inter-day and intra-day determinations. One of the common ways of expressing the variability, which takes into account its relative magnitude, is the ratio of the standard deviation (SD) to the mean, SD/Mean. This ratio, often expressed as a percentage, is called the **Coefficient of Variation** abbreviated as CV or RSD, the **relative standard deviation**. In biological data, the CV is often between 20 -50%, and one would not be surprised to see an occasional CV as high as 100% or more. The relatively large CV observed in biological experiments is due mostly to "biological variation", the lack of reproducibility in living material. On the other hand, the variability in chemical and instrumental analysis of drugs is usually relatively small (Bolton, 1990).

3.2.4 Results and Discussion

3.2.4.1 Calibration Plot in methanol

Simvastatin in methanol showed absorption maximum at 238 nm and this wavelength was chosen as the analytical wavelength. Beer's law was obeyed between 4 and 20 μg/ml (Table 3.1). Regression analysis was performed on the experimental data. Regression equation for standard curve was y = 0.0597x + 0.028 (Fig. 3.1). Correlation coefficient for developed method was found to be 0.9998 signifying that a linear relationship existed between absorbance and concentration of the drug. Parameters indicating linearity for the used UV spectrometric method of analysis for Simvastatin are shown in Table 3.2.

Table 3.3 and 3.4 show intraday and interday precision and accuracy for the Simvastatin assay by UV spectroscopy. The low % CV values indicate precision of the method. No significant difference between the amount of drug added (actual) and observed concentration was noticed indicating accuracy of the method (Guidance for industry, 2001; Boulangeret al., 2003). The interference studies with formulation excipients studies were carried out and no difference in absorbance was observed at 238 nm.

Table 3.1 Calibration data for Simvastain in methanol

Sr. No	Concentration (µg/ml)	Mean Absorbance ± SD
1	4	0.267±0.001
2	8	0.499±0.014
3	12	0.752±0.018
4	16	0.983±0.043
5	20	1.218±0.051

*Average of 3 determinations
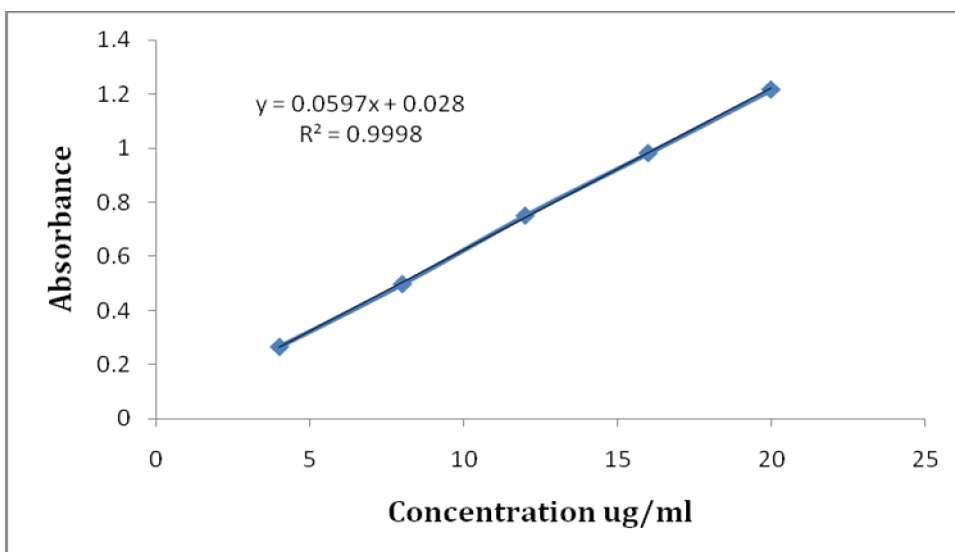
Fig. 3.1 Standard Curve of Simvastatin in methanol

Table 3.2 Parameters for UV spectrometric method of analysis for Simvastatin in Methanol

Parameters	Results
λmax	238 nm
Linearity range	2-20 µg/ml
Regression equation	y=0.0597x+0.028
Correlation coefficient	0.9998

3.2.4.2 Calibration Plot in pH 7.2 Phosphate buffer

A characteristic spectrum was obtained for Simvastatin in pH 7.2 Phosphate buffer when scanned in the ultraviolet range between 200 and 400 nm. The scan showed absorption

maximum at 238 nm and this wavelength was chosen as the analytical wavelength. Beer's law was obeyed between 4 and 20 µg/ml (Table 3.3). Regression analysis was performed on the experimental data. Regression equation for standard curve was y=0.0565x -0.0142 (Fig.3.2). Correlation coefficient for developed method was found to be 0.9992 signifying that a linear relationship existed between absorbance and concentration of the drug. Parameters indicating linearity for the method of analysis for Simvastatin are shown in Table 3.4.

Table 3.3 Calibration data for Simvastain in pH 7.2 phosphate buffer

Sr. No	Concentration (µg/ml)	Mean Absorbance ± SD
1	4	0.215±0.003
2	8	0.445±0.018
3	12	0.649±0.024
4	16	0.885±0.038
5	20	1.125±0.054

*Average of 3 determinations
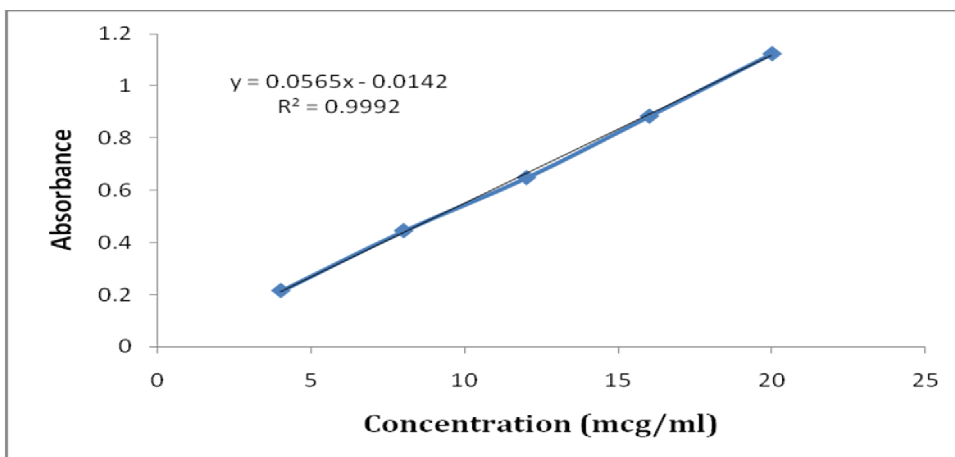
Fig. 3.2 Standard Curve of Simvastatin in pH 7.2 phosphate buffer

Table 3.5 and 3.6 show intraday and interday precision and accuracy for the Simvastatin assay in pH 7.2 phosphate buffer by UV spectroscopy. The low % CV values in Table 3.5 and 3.6 indicate precision of the method. No significant difference between the amount of drug added (actual) and observed concentration was noticed indicating accuracy of the method (Guidance for industry, 2001; Boulangeret al., 2003).

Table 3.4 Parameters for UV spectrometric method of analysis for Simvastatin in pH 7.2 phosphate buffer

Parameters	Results
λmax	238 nm
Linearity range	4-20 µg/ml
Regression equation	y=0.0565x-0.0142
Correlation coefficient	0.9992

Table 3.5 Intraday precision and accuracy for the Simvastatin assay in pH 7.2 phosphate buffer by UV spectroscopy.

Standard Concentration (µg/ml)		Precision[a] (%)	Accuracy[b] (%)
Actual	Observed		
1	1.02±0.005	0.4901	102.0
5	5.01±0.010	0.40	100.2
10	9.97±0.065	0.6519	99.7

[a] Expressed as relative standard deviation, RSD

RSD = (standard deviation/mean concentration) x 100

[b] Expressed as (mean observed concentration/actual concentration) × 100

Table 3.6 Interday precision and accuracy for the Simvastatin assay in pH 7.2 phosphate buffer by UV spectroscopy.

Standard Concentration (µg/ml)		Precision (%)	Accuracy (%)
Actual	Observed		
1	1.01±0.010	0.9901	101.0
5	5.02±0.020	0.40	100.4
10	9.96±0.015	0.1506	99.6

a Expressed as relative standard deviation, RSD

RSD = (standard deviation/mean concentration) x 100

b Expressed as (mean observed concentration/actual concentration) × 100

3.3 Estimation of Entacapone by Ultraviolet Spectroscopy (UV)

3.3.1 Calibration Plot in methanol

Standard stock solution (100 µg/ml) was prepared by dissolving 10 mg of Entacapone in 100 ml of methanol. Then UV spectrophotometric method of analysis was developed by first scanning solution of Entacapone (10 µg/ml) in the ultraviolet range between 200 and 600 nm and determining its λmax. Suitable aliquots of the stock solution of Entacapone were pipetted out into 10 ml volumetric flasks and the volume was made upto 10 ml with methanol to give final concentrations ranging from 4-20 µg/ml. The solutions were mixed using vortex mixer and their absorbances measured at λmax using methanol as blank on Shimadzu 1700 UV-Visible Spectrophotometer and calibration curve was plotted. The above procedure was repeated three times. Standard concentration (1.0, 5.0, and 10.0 µg/ml) were prepared and subjected to interday and intraday analysis to estimate accuracy and precision.

3.3.2 Calibration Plot in methanol and water and (8:2)

Standard stock solution (100 µg/ml) was prepared by dissolving 10 mg of Entacapone in 100 ml of methanol and water (8:2). The UV-spectrophotometric method of analysis was developed by first scanning solution of Entacapone (10 µg/ml) in the ultraviolet range between 200 and 600 nm and determining its λmax. Suitable aliquots of the stock solution of Entacapone were pipetted out into 10 ml volumetric flasks and the volume was made upto 10ml to give final concentrations ranging from 4-20 µg/ml. The solutions were mixed using vortex mixer and their absorbances measured at λmax using respective blank on Shimadzu 1700 UV-Visible Spectrophotometer and calibration curve was plotted. The above procedure was repeated three times. Standard concentration (1.0, 5.0, and 10.0 µg/ml) were prepared and subjected to interday and intraday analysis to estimate accuracy and precision.

3.3.3 Calibration Plot in 0.1N HCl and methanol (9:1)

Standard stock solution (100 µg/ml) was prepared by dissolving 10 mg of Entacapone in 100 ml of 0.1N HCl and methanol (9:1). The UV-spectrophotometric method of analysis was developed by first scanning solution of Entacapone (10 µg/ml) in the ultraviolet range between 200 and 600 nm and determining its λmax. Suitable aliquots of the stock solution

of Entacapone were pipetted out into 10 ml volumetric flasks and the volume was made upto 10ml to give final concentrations ranging from 4-20 μg/ml. The solutions were mixed using vortex mixer and their absorbances measured at λmax using respective blank on Shimadzu 1700 UV-Visible Spectrophotometer and calibration curve was plotted. The above procedure was repeated three times. Standard concentration (1.0, 5.0, and 10.0 μg/ml) were prepared and subjected to interday and intraday analysis to estimate accuracy and precision.

3.3.4 Calibration Plot in pH 7.2 phosphate buffer

Standard stock solution (100 μg/ml) was prepared by dissolving 10 mg of Entacapone in 100 ml of pH 7.2 phosphate buffer. Then UV-spectrophotometric method of analysis was developed by first scanning solution of Entacapone (10 μg/ml) in the ultraviolet range between 200 and 600 nm and determining its λmax. Suitable aliquots of the stock solution of Entacapone were pipetted out into 10 ml volumetric flasks and the volume was made upto 10ml with pH 7.2 phosphate buffer to give final concentrations ranging from 2-16 μg/ml. The solutions were mixed using vortex mixer and their absorbances measured at λmax using pH 7.2 phosphate buffer as blank on Shimadzu 1700 UV-Visible Spectrophotometer and calibration curve was plotted. The above procedure was repeated three times. Standard concentration (1.0, 5.0, and 10.0 μg/ml) were prepared and subjected to interday and intraday analysis to estimate accuracy and precision.

3.3.5 Results and Discussion

3.3.5.1 Calibration Plot in methanol

Entacapone in methanol showed a characteristic spectrum when scanned in the ultraviolet range between 200 and 600 nm. The scan showed absorption maximum 384 nm and this wavelength was chosen as the analytical wavelength. Beer's law was obeyed between 4 and 20 μg/ml (Table 3.7). Regression analysis was performed on the experimental data. Regression equation for standard curve was y = 0.0597x - 0.0013 (Fig. 3.3). Correlation coefficient for developed method was found to be 0.9999 signifying that a linear relationship existed between absorbance and concentration of the drug. Parameters

indicating linearity for the developed UV spectrometric method of analysis for Entacapone are shown in Table 3.8.

Table 3.7 Calibration data for Entacapone in methanol

Sr. No	Concentration (µg/ml)	Mean Absorbance ± SD
1	4	0.240±0.013
2	8	0.477±0.014
3	12	0.708±0.021
4	16	0.954±0.032
5	20	1.195±0.044

*Average of 3 determinations

Table 3.8 Parameters for UV spectrometric method of analysis for Entacapone in Methanol

Parameters	Results
λmax	384 nm
Linearity range	4-20 µg/ml
Regression equation	y=0.0597x-0.0013
Correlation coefficient	0.9999
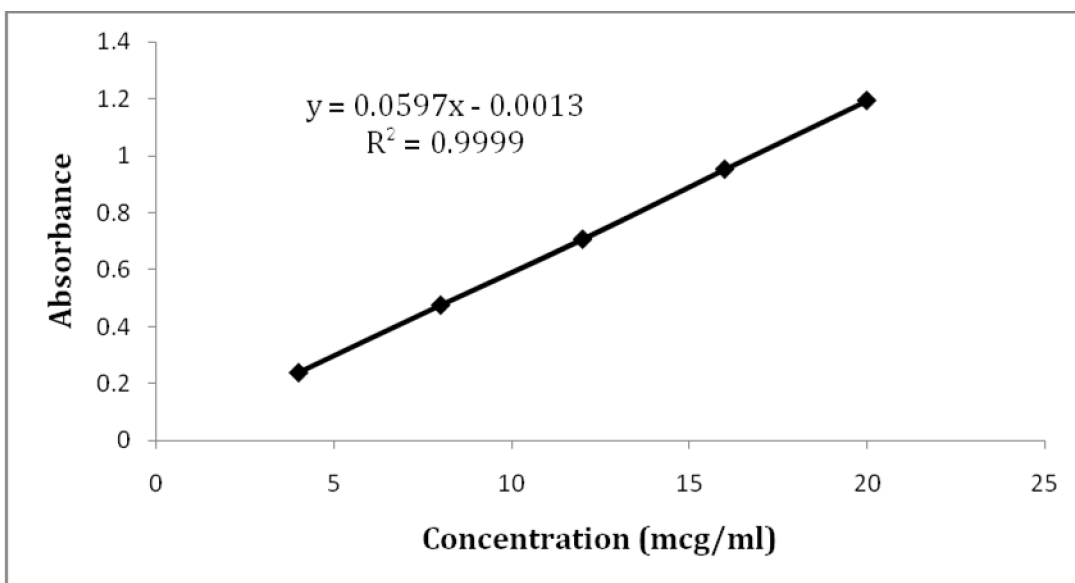
Fig. 3.3 Standard Curve of Entacapone in methanol

Table 3.9 and 3.10 show intraday and interday precision and accuracy for the Entacapone assay by UV spectroscopy. The low % CV in Table 3.9 and 3.10 values indicate precision of the method. No significant difference between the amount of drug added (actual) and observed concentration was noticed indicating accuracy of the method. The interference studies with blank formulation showed no difference in absorbance was observed at 384 nm.

Table 3.9 Intraday precision and accuracy for Entacapone assay in methanol by UV spectroscopy.

Standard Concentration (µg/ml)		Precision (%)[a]	Accuracy (%)[b]
Actual	**Observed**		
1	1.00±0.005	0.5	100.0
5	5.02±0.030	0.5976	100.4
10	10.02±0.015	0.1502	100.2

[a] Expressed as relative standard deviation, RSD

RSD = (standard deviation/mean concentration) x 100

[b] Expressed as (mean observed concentration/actual concentration) × 100

Table 3.10 Interday precision and accuracy for Entacapone assay in methanol by UV spectroscopy**.**

Standard Concentration (µg/ml)		Precision (%)	Accuracy (%)
Actual	**Observed**		
1	1.02±0.015	1.47	102.0
5	5.01±0.010	0.1996	100.2
10	9.98±0.015	0.1503	99.8

a Expressed as relative standard deviation, RSD

RSD = (standard deviation/mean concentration) x 100

b Expressed as (mean observed concentration/actual concentration) × 100

3.3.5.2 Calibration Plot in methanol: water (8:2)

Entacapone in methanol: water (8:2) showed a characteristic spectrum when scanned in the ultraviolet range between 200 and 600 nm. The scan showed absorption maximum 384 nm and this wavelength was chosen as the analytical wavelength. Beer's law was obeyed between 4 and 20 μg/ml (Table 3.11). Regression analysis was performed on the experimental data. Regression equation for standard curve was y=0.0597x+0.1435 (Fig. 3.4). Correlation coefficient for developed method was found to be 0.9977 signifying that a linear relationship existed between absorbance and concentration of the drug. Parameters indicating linearity for the developed UV spectrometric method of analysis for Entacapone are shown in Table 3.12.

Table 3.11 Calibration data for Entacapone in methanol: water (8:2)

Sr. No	Concentration (μg/ml)	Mean Absorbance ± SD
1	4	0.361±0.011
2	8	0.635±0.016
3	12	0.879±0.028
4	16	1.102±0.032
5	20	1.321±0.042

*Average of 3 determinations

Table 3.12 Parameters for UV spectrometric method of analysis for Entacapone methanol: water (8:2)

Parameters	Results
λmax	384 nm
Linearity range	4-20 μg/ml
Regression equation	y=0.0597x+0.1435
Correlation coefficient	0.9977
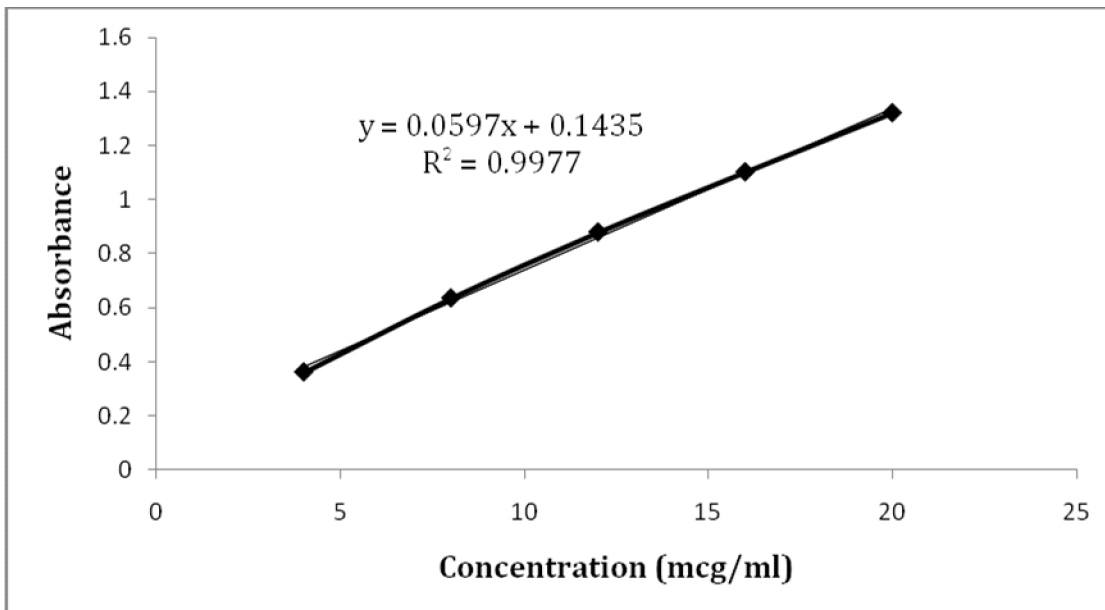
Fig. 3.4 Standard Curve of Entacapone in methanol: water (8:2)

Table 3.13 and 3.14 show intraday and interday precision and accuracy for the Entacapone assay in methanol: water (8:2) by UV spectroscopy. The low % CV in Table 3.13 and 3.14 values indicate precision of the method. No significant difference between the amount of drug added (actual) and observed concentration was noticed indicating accuracy of the method. The interference studies with blank formulation showed no difference in absorbance was observed at 384 nm.

Table 3.13 Intraday precision and accuracy for Entacapone assay in methanol: water (8:2) by UV spectroscopy.

Standard Concentration (µg/ml)		Precision (%)[a]	Accuracy (%)[b]
Actual	**Observed**		
1	1.01±0.015	1.485	101.0
5	5.02±0.025	0.498	100.4
10	9.98±0.015	0.1503	99.8

[a] Expressed as relative standard deviation, RSD

RSD = (standard deviation/mean concentration) x 100

[b] Expressed as (mean observed concentration/actual concentration) × 100

Table 3.14 Interday precision and accuracy for Entacapone assay in methanol: water (8:2) by UV spectroscopy.

Standard Concentration (µg/ml)		Precision (%)	Accuracy (%)
Actual	**Observed**		
1	1.01±0.015	1.485	101.0
5	5.02±0.025	0.498	100.2
10	10.02±0.015	0.1502	100.2

a Expressed as relative standard deviation, RSD

RSD = (standard deviation/mean concentration) x 100

b Expressed as (mean observed concentration/actual concentration) × 100

3.3.5.3 Calibration Plot in 0.1 N HCl and methanol (9:1)

Entacapone in 0.1 N HCl and methanol (9:1) showed a characteristic spectrum when scanned in the ultraviolet range between 200 and 600 nm. The scan showed absorption maximum 315 nm and this wavelength was chosen as the analytical wavelength. Beer's law was obeyed between 4 and 20 µg/ml (Table 3.15). Regression analysis was performed on the experimental data. Regression equation for standard curve was y = 0.0629x - 0.0081 (Fig. 3.5). Correlation coefficient for developed method was found to be 0.9959 signifying that a linear relationship existed between absorbance and concentration of the drug. Parameters for the developed UV spectrometric method of analysis for Entacapone are shown in Table 3.16.

Table 3.15 Calibration data for Entacapone in 0.1 N HCl: Methanol (9:1)

Sr. No	Concentration (µg/ml)	Mean Absorbance ± SD
1	4	0.267±0.010
2	8	0.476±0.011
3	12	0.742±0.023
4	16	0.969±0.022
5	20	1.278±0.038

*Average of 3 determinations
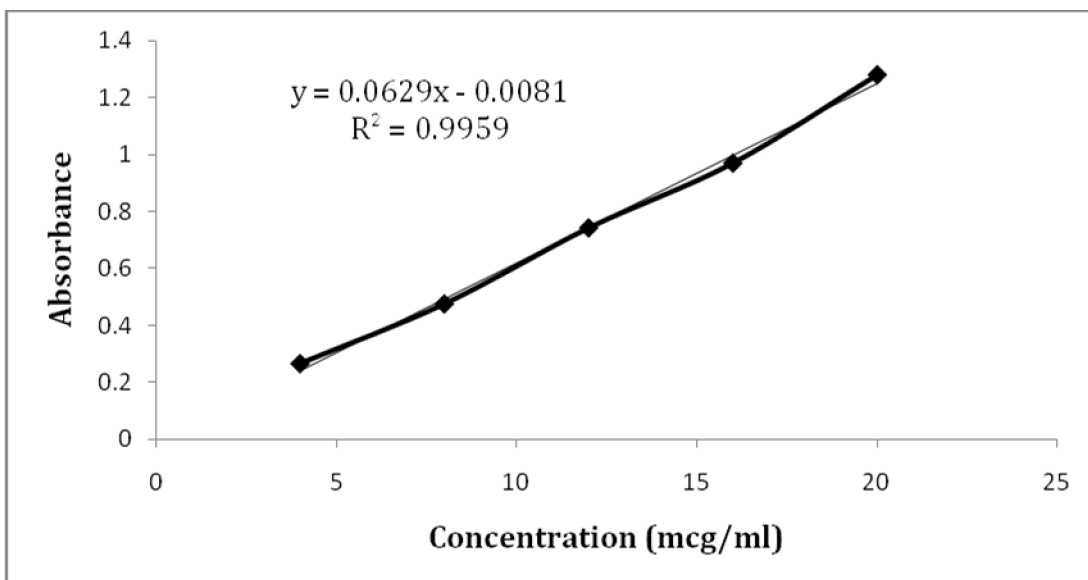
Fig. 3.5 Standard Curve of Entacapone in 0.1 N HCl: Methanol (9:1)

Table 3.16 Parameters for UV spectrometric method of analysis for Entacapone in 0.1 N HCl: Methanol (9:1)

Parameters	Results
λmax	315 nm
Linearity range	4-20 µg/ml
Regression equation	y=0.0629x-0.0081
Correlation coefficient	0.9959

Table 3.17 and 3.18 show intraday and interday precision and accuracy for the Entacapone assay by UV spectroscopy. The low % CV values indicate precision of the method. No significant difference between the amount of drug added (actual) and observed concentration was noticed indicating accuracy of the method.

Table 3.17 Intraday precision and accuracy for Entacapone assay in 0.1 N HCl: Methanol (9:1) by UV spectroscopy.

Standard Concentration (µg/ml)		Precision (%)[a]	Accuracy (%)[b]
Actual	**Observed**		
1	1.01±0.015	1.485	101.0
5	5.02±0.025	0.498	100.4
10	9.99±0.015	0.1501	99.9

[a] Expressed as relative standard deviation, RSD

RSD = (standard deviation/mean concentration) x 100

[b] Expressed as (mean observed concentration/actual concentration) × 100

Table 3.18 Interday precision and accuracy for Entacapone assay in 0.1 N HCl: Methanol (9:1) by UV spectroscopy.

Standard Concentration (µg/ml)		Precision (%)	Accuracy (%)
Actual	**Observed**		
1	1.00±0.015	1.50	100.0
5	5.00±0.020	0.40	100.0
10	9.98±0.015	0.1502	99.8

a Expressed as relative standard deviation, RSD

RSD = (standard deviation/mean concentration) x 100

b Expressed as (mean observed concentration/actual concentration) × 100

3.3.5.4 Calibration Plot in pH 7.2 phosphate buffer

Entacapone in pH 7.2 phosphate buffer showed a characteristic spectrum when scanned in the ultraviolet range between 200 and 600 nm. The scan showed absorption maximum 384 nm and this wavelength was chosen as the analytical wavelength. Beer's law was obeyed between 2 and 16 µg/ml (Table 3.19). Regression analysis was performed on the experimental data. Regression equation for standard curve was y = 0.0629x - 0.0081 (Fig. 3.6). Correlation coefficient for developed method was found to be 0.9995 signifying that a linear relationship existed between absorbance and concentration of the drug. Parameters for the developed UV spectrometric method of analysis for Entacapone are shown in Table 3.20.

Table 3.19 Calibration data for Entacapone in pH 7.2 phosphate buffer

Sr. No	Concentration (µg/ml)	Mean Absorbance ± SD
1	2	0.175±0.010
2	4	0.302±0.011
3	6	0.459±0.023
4	8	0.608±0.022
5	10	0.755±0.038
6	12	0.920±0.022
7	16	1.211±0.038

*Average of 3 determinations
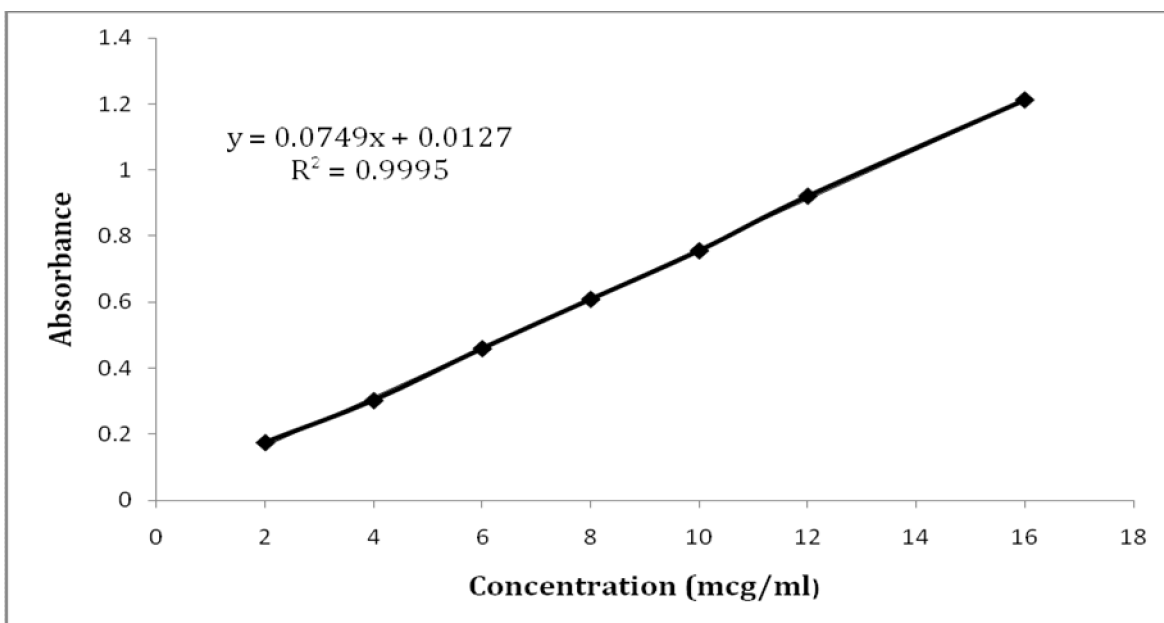
Fig. 3.6 Standard Curve of Entacapone in pH 7.2 phosphate buffer

Table 3.20 Parameters for UV spectrometric method of analysis for Entacapone in pH 7.2 phosphate buffer

Parameters	Results
λmax	384 nm
Linearity range	2-16 µg/ml
Regression equation	y=0.0749x+0.0127
Correlation coefficient	0.9995

Table 3.21 and 3.22 show intraday and interday precision and accuracy for the Entacapone assay by UV spectroscopy. The low % CV values indicate precision of the method. No significant difference between the amount of drug added (actual) and observed concentration was noticed indicating accuracy of the method.

Table 3.21 Intraday precision and accuracy for Entacapone assay in pH 7.2 phosphate buffer by UV spectroscopy.

Standard Concentration (µg/ml)		Precision (%)[a]	Accuracy (%)[b]
Actual	**Observed**		
1	1.01±0.010	0.9901	101.0
5	5.03±0.020	0.3976	100.6
10	9.99±0.015	0.1502	99.9

Table 3.22 Interday precision and accuracy for Entacapone assay in pH 7.2 phosphate buffer by UV spectroscopy

Standard Concentration (µg/ml)		Precision (%)[a]	Accuracy (%)[b]
Actual	**Observed**		
1	1.00±0.010	1.10	100.0
5	5.02±0.020	0.40	100.4
10	9.98±0.015	0.1502	99.8

a Expressed as relative standard deviation, RSD

RSD = (standard deviation/mean concentration) x 100

b Expressed as (mean observed concentration/actual concentration) × 100

3.4 High Performance Liquid Chromatography (HPLC) method for estimation of Simvastatin in plasma

3.4.1 Method:

Estimation of Simvastatin in plasma sample was carried out as per reported method with some modification (Carlucci et al 1992). The method validated by Carlucci et al for determination of Simvastatin and Simvastatin acid (SVA) concentration simultaneously was used. The column of particle size 10 μm was used instead of 5 μm (Thermo Hypersil) and flow rate of 1.0 ml/min. This method involves liquid-liquid extraction using mixture of acetonitrile-water (60:40). Shimadzu isocratic HPLC with a UV-visible detector was used for HPLC analysis. The separation was done on analytical column (250 X 4.6 mm, i.d), packed with reverse phase material 10 μm (Thermo Hypersil) and connected to 2 cm precolumn. The mobile phase was a mixture of 0.025 M sodium dihydrogen phosphate (pH 4.5)-acetonitrile (35:65 v/v). After preparation the mobile phase was degassed and filtered through 0.45 μ inorganic filter. The required parameters were programmed using software. Human Plasma was obtained from Indu Blood Bank, Vadodara, India. Calibration plot of Simvastatin in plasma was prepared in concentration in the range (50 -2000 ng/ml). The blank plasma samples were spiked with stock solution prepared in acetonitrile (1mg/ml) to get concentration in above range. The protein precipitation was carried out by addition of acetonitrile. For 0.2 ml of plasma sample, 170 μl of acetonitrile was used. The separation of precipitate from organic phase was achieved by centrifugation (4000 rpm X 10min). The obtained organic phase (acetonitrile solution) was evaporated to dryness and used for analysis after reconstitution with acetonitrile: water (1:1). Calibration curves were drawn by plotting peak area of curve vs. drug concentration. Program parameters were: Flow rate-1.0 ml/min, Detection wavelength- 238nm, Run time- 15 min. The column was equilibrated by passing at least 150-200 ml of mobile phase. 20μl of sample was loaded using syringe through rheodyne injector.

3.4.2 Validation

Analytical method was validated for linearity, precision, and accuracy as described in section 3.1. The recovery studies were performed to know the extraction efficiency. Aqueous and plasma samples of known concentration were used. The aqueous sample of known concentration was prepared in same way as that of plasma sample except addition of plasma. The recovery in case of plasma sample compared to aqueous sample was recorded.

3.4.3 Results and Discussions

The retention time for simvastain was found to be 6.3 min. The standard plot for Simvastatin is shown in Fig. 3.7 and Table 3.23.

3.4.3.1 Linearity**:**

The data for calibration plot of Simvastatin in plasma by HPLC (Table 3.24) was fitted into a linear equation (y=0.014x-0.001) with correlation coefficient of R^2=0.9976, which indicated the linearity of the plot.

3.4.3.2 Precision:

Precision of the method was assessed by analyzing the plasma samples spiked with Simvastatin at different concentrations (100, 500 and 2000ng/ml). Three replicate of each concentration were analyzed and results are given in Table 3.25 and 3.26. To evaluate precision, the mean values and the % RSD values were calculated for each concentration. The % RSD values for intraday and interday assay precision are presented in Table 3.25 and 3.26. The low % CV values indicate precision of the method.

3.4.3.3 Accuracy:

The accuracy is expressed as % bias or % relative error (difference from added concentration) and it takes into account the total error, i.e. systematic and random errors, related to the test result (Hubert et al, 2003). The tolerance limits for intraday assay and interday assay samples are presented in Table 3.25 and 3.26 as a function of the introduced concentrations. No significant difference between the amount of drug added (actual) and observed concentration at all the concentration levels tested was noticed indicating accuracy of the method (Boulanger et al, 2003; Guidance for industry, 2001).

Table 3.23 Calibration data for Simvastatin in plasma

Sr. No.	Concentration (ng/ml)	Area under curve (mAU)
1	50	0.981±0.404
2	200	3.075±0.113
3	400	5.409±0.235
4	1000	13.512±0.210
5	1600	21.695±0.385
6	2000	28.772±0.488

*Average of 3 determinations
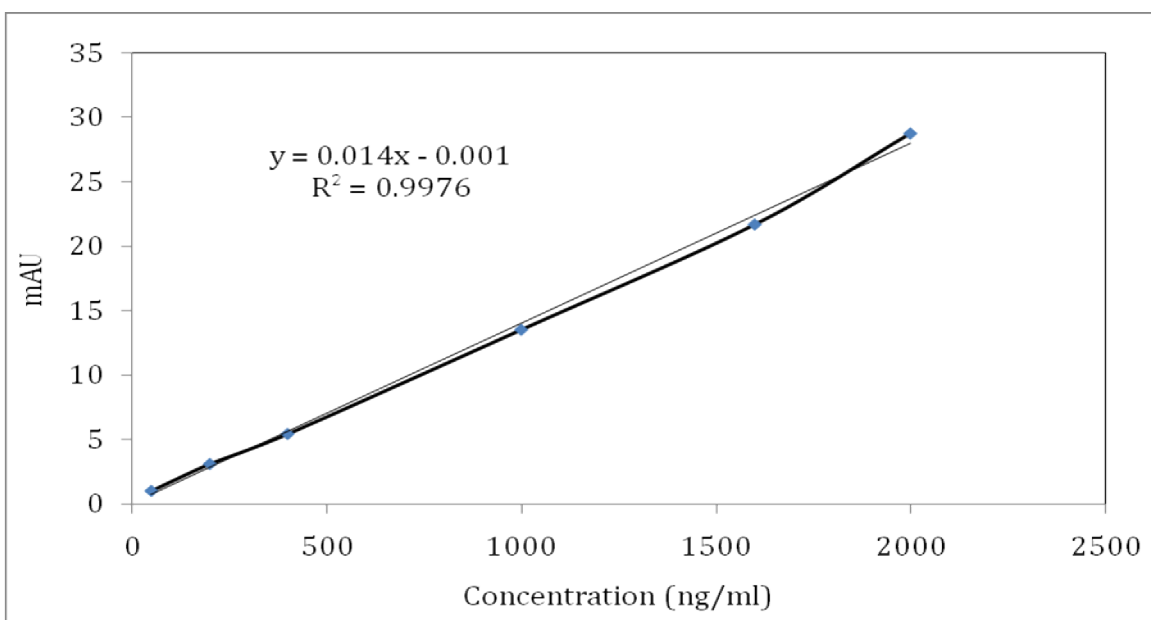
Fig. 3.7 Standard Curve of Simvastatin in plasma by HPLC

Table 3.24 Parameters for HPLV method for estimation of Simvastatin in plasma

Parameters	Results
Λmax	238 nm
Linearity range	50-2000 ng/ml
Regression equation	y=0.014x-0.001
Correlation coefficient	0.9976
Retention time	6.3 min

Table 3.25 Intraday precision and accuracy for Simvastatin in plasma by HPLC

Standard Concentration (ng/ml)		Precision (%)[a]	Accuracy (%)[b]
Actual	**Observed**		
100	92.0±4.1	4.4562	92.0
500	514.4±16.2	3.1493	102.8
2000	1968.5±32.5	1.6510	98.4

Table 3.26 Interday precision and accuracy Simvastatin in plasma by HPLC

Standard Concentration (ng/ml)		Precision (%)[a]	Accuracy (%)[b]
Actual	**Observed**		
100	91.6±5.4	5.8951	91.6
500	528.4±14.8	1.8009	105.6
2000	1932.5±48.5	2.5097	96.62

a Expressed as relative standard deviation (RSD)

RSD = (standard deviation/mean concentration) x 100

b Expressed as (mean observed concentration/actual concentration) × 100

3.4.3.4 Absolute recovery:

The absolute recovery of Simvastatin at three concentration levels was determined by comparing the peak areas measured after analysis of spiked plasma samples (containing FU= 200, 500 and 2000 ng/ml) according to the procedure discussed in 3.5.1 with those found after direct injection into the chromatographic system of non-biological samples at the same concentration levels. As shown in Table 3.27, the analyte recoveries were close to 100% and the extraction efficiency satisfactorily ranged from 96.3% to 98.8% for plasma samples.

Table 3.27 Extraction efficiency of Simvastatin at various concentrations

Concentration (ng/ml)	Extraction efficiency (±SD)
200	96.44±3.2
500	98.8±2.8
2000	96.3±5.4

3.5 High Performance Liquid Chromatography (HPLC) method for estimation of Entacapone in plasma

3.5.1 Method:

Estimation of Entacapone in plasma sample was carried out as per reported method (Ramakrishna et al; 2005). This method involves liquid-liquid extraction using mixture of ethyl acetate-n-hexane (30:70, v/v). Shimadzu isocratic HPLC with a UV-visible detector was used for HPLC analysis. The separation was done on analytical column (250 X 4.6 mm, i.d), packed with reverse phase material 5 µm (Thermo Hypersil) and connected to 2 cm precolumn. The mobile phase was a mixture of 30mM phosphate buffer (20mM potassium dihydrogen phosphate buffer and 10mMdi-potassium hydrogen phosphate buffer; pH adjusted to 2.75 with ortho-phosphoric acid)/acetonitrile (62/38, v/v) pumped at a flow-rate of 1.0 ml/min. Detection was set at a wavelength of 315 nm. The mobile phase was prepared using distilled deionized water (DDW), degassed and filtered through a 0.45 µ inorganic filter before use. The required parameters were programmed using software.

Standard solutions:

Standard stock solutions of Entacapone (1 mg/ml) and I.S. (1 mg/ml) were prepared in acetonitrile. The Internal Standard (I.S.) of Rofecoxib working solution (100 µg/ml) was prepared by diluting stock solution with water/acetonitrile (50/50, v/v).

The plasma sample (0.2 ml) was transferred to a 5 ml glass test tube and 25 µl of I.S. working solution was spiked. Then 10 µl of 10% ortho phosphoric acid was added to the mixture and vortex mixed for 10 s. Next a 1 ml aliquot of extraction solvent, ethyl acetate/n-hexane (3/7) was added using micropipette. The sample was vortex mixed for 4 min using vortexer. The sample was then centrifuged for 10 min at 4000 rpm. The organic layer (0.8 ml) was quantitatively transferred to a 5 m1 glass tube and evaporated to dryness at 40 °C under a stream of nitrogen. Then, the dried extract was reconstituted in 50 µl of water/acetonitrile (50/50, v/v; diluent) and 20 µl aliquot was injected into chromatographic system.

3.5.2 Results and discussion

Table 3.28 and Fig. 3.8 show calibration curve of Entacapone in plasma. Table 3.29 shows parameters for HPLC method for the estimation of Entacapone in plasma.

Table 3.28 Calibration data for Entacapone in plasma

Sr. No.	Concentration (ng/ml)	Area under curve (mAU)
1	100	6.254±0.141
2	400	21.107±1.234
3	800	34.333±1.354
4	1600	56.137±5.211
5	2400	87.823±4.357
6	3200	122.00±3.820
7	4000	159.697±9.885

*Average of 3 determinations
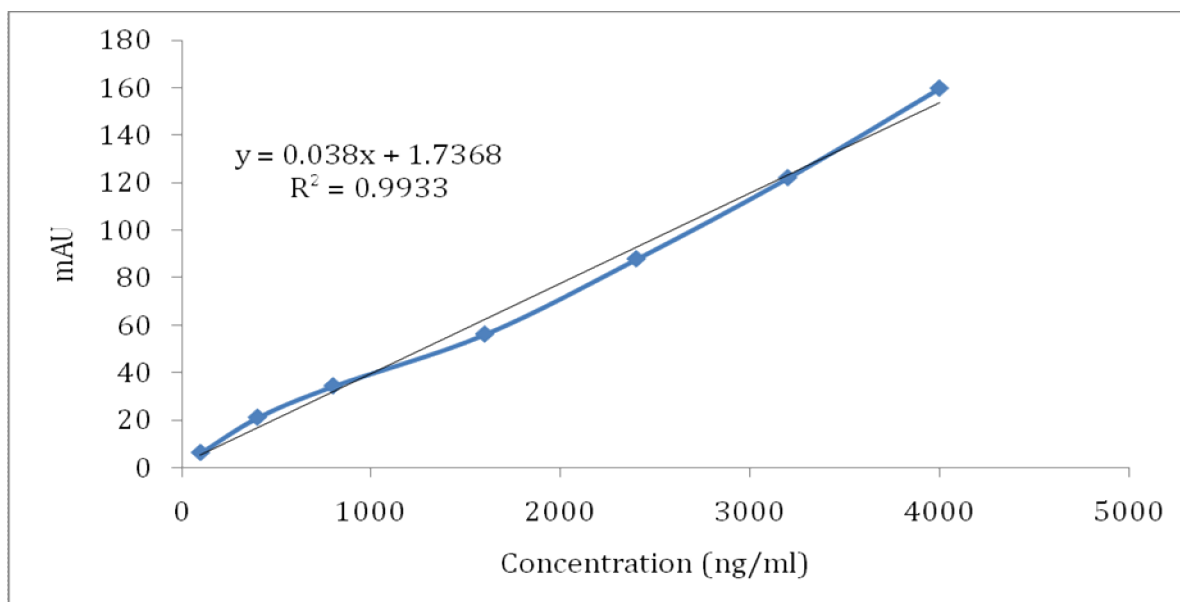
Fig. 3.8 Standard Curve of Entacapone in plasma by HPLC

Table 3.29 Parameters for HPLC method for estimation of Entacapone in plasma

Parameters	Results
Λmax	315 nm
Linearity range	100-4000 ng/ml
Regression equation	y=0.038x+1.7368
Correlation coefficient	0.9933
Retention time	8.3 min

From these parameters, it can be concluded that the HPLV method was linear in the above range and was suitable for determination of Entacapone concentration in plasma samples.

3.5 References

- Arayne MS, Sultana N, Hussain F, Ali SA. Validated spectrophotometric method for quantitative determination of Simvastatin in pharmaceutical formulations and human serum. J Analytical Chem. 62(6), 2007, 536-541.

- Merodia M, Mirshahi T, Mirshahi M. Development of a sensitive method for the determination of ganciclovir by reversed phase high-performance liquid chromatography. J Chromatogr. 870, 2000, 159-167

- Hubert PH, Chiap P, Crommen J, Boulanger B, Chapuzet E, Mercier N, Bervoas MS, Chevalier P, Grandjean D, Lagorce P, Lallier M, Laparra MC, Laurentie M, Nivet JC. Validation of the quantitative analytical procedures. Harmonization of the steps. STP Pharma practice 13, 2003, 101-138.

- Bolton S, Swarbrick J. Basic definitions and concepts In: Pharmaceutical statistics: Practical and clinical applications. 3rd Ed., Marcel Dekker, New York, 1990, pp 24.

- Boulanger B, Dewe W, Chiap P, Crommen J, Hubert PH. An analysis of the SFSTP guide on validation of bioanalytical methods: progress and limitations. J Pharm Biomed Anal. 32, 2003, 753-765.

- Guidance for industry: Bioanalytical Method Validation, U.S. Department of Health and Human Services, Food and Drug Administration, Center for Drug Evaluation and Research (CDER), Center for Biologics Evaluation and Research (CBER), May 2001.

- Carlucci G, Mazzeo P, Biordi L, Bologna M. Simultaneous determination of Simvastatin and its hydroxyl acid form in human plasma by high –performance liquid chromatography with UV detection. J Pharm Biomed Ana. 10(9), 1992, 693-697.

- Ramakrishna NVS, Vishwottam KN, Wishu S, Koteshwara M, Chidambara J. High-performance liquid chromatography method for the quantification of Entacapone in human plasma. J Chromatography B 823, 2005, 189–194.

4.0 MATERIALS AND METHODS

4.1 Materials

Simvastatin was obtained as gift sample from Ajanta Pharmaceuticals Ltd, Mumbai, India. Zirconium oxide beads were obtained as gift sample from Lupin Pharmaceuticals Ltd, Pune, India. Pluronic F88 (Poloxamer 188) was procured from Sigma Chemicals, Mumbai, India. Tween 80 (Polysorbate 80), disodium hydrogen phosphate and sodium hydroxide were purchased from S.D. Finechem., Mumbai, India. PVP was obtained from BASF, Mumbai, India. Cellulose dialysis tubing (Molecular weight cut of 14000; pore size 0.4nm) and membrane filter of pore size 0.2 μm were purchased from Himedia Lab, Mumbai, India. Distilled water used in the study was filtered using 0.22-lm nylon filter (Nylon N66 membrane filters 47 mm, Rankem, India). All other chemicals and reagents used in this study were of analytical grade.

4.2 Equipments:

1. High speed magnetic stirrer (Remi, MS500, Remi equipments, Mumbai, India)

2. High speed Centrifuge (Sigma 3K30, Germany)

3. Particle size Analyzer (Zeta sizer Nano series, Malvern Instruments, UK)

4. UV-VIS Spectrophotometer (Shimadzu, Japan)

5. Lyophilizer (Heto, Vaccubrand, Denmark)

6. Differential Scanning Calorimeter. (Mettler Toledo DSC 822e, Japan)

7. Laser diffraction particle size analyzer (Malvern Mastersizer, 2000, UK)

8. Supercritical Particle former (SAS) (Thar Instruments, PA, USA)

9. Transmission Electron Microscope (Philips, Tecnai 20, Holland)

4.3 Preparation of nanosuspension by media milling

Media milling was carried out in a sealed glass vial containing starting suspension and milling beads (Eerdenbrugh et al. 2007). The starting suspensions contained drug (0.5w/v) and the surfactant (1%w/v) and distilled water as medium (5ml) in glass vial. Then magnetic bead and zirconium oxide beads (100%w/v) as milling media were incorporated

and comminution was carried out on magnetic stirrer at 500rpm for 14 hrs (Sigfridsson et al, 2007). This milling led to nanonization of Simvastatin, producing Simvastatin nanosuspension (SNS). This obtained suspension was freeze dried using trehalose as cryoprotectant (Heto Dry Winner, Denmark) at 1:3 ratio of total solid. Plain drug suspension used for comparison was prepared by dispersing the plain drug powder and Tween 80 in water with same concentration of drug and surfactant as that of nanosuspension.

4.3.1 Optimization of parameters:

In preliminary optimization, the possible parameters influencing the formation of nanosuspension and size of nanosuspension were identified and optimized. The parameters studied were milling time, ratio of beads, drug concentration and surfactant selection.

Milling time:

Milling was carried out for 16 hrs to study the effect of milling time on nanosuspension formation. Samples were taken at different intervals (0.5, 1, 2, 4, 8, 10, 12, 14 and 16 h) and particle size and PDI were determined. The surfactant used for the study was Tween 80 at 2 %w/v concentration.

Composition of batch:

Simvastatin	1 % w/v
Tween 80	2.0 % v/v
Volume of beads	80% w/v
Distilled water	10 ml

Type and Ratio of beads:

Firstly, Zirconium oxide beads and glass beads were tried to evaluate their effectiveness in particle size reduction. Then zirconium oxide beads of two different size ranges (i.e. small and large) were used for preparation of nanosuspension. Beads of small size range were in between 0.4 mm to 0.7 mm while large size beads were between 1.2 mm to 1.5 mm. Ratio of bead was varied from 0:100 to 100:0 for small : large size range beads. Tween 80 at 2%

concentration was used in this study. Volume of beads was maintained at 80 % w/v while milling time was kept at 12 hrs.

Selection of surfactant:

Batches were prepared with different surfactants [Tween 80, Pluronic-F68, polyvinyl pyrrolidone (PVP K30) and Pluronic F68: Tween 80 (1:1)]. Zirconium oxide beads at 80% volume were used in this study and milling was carried out for 12 hr. Concentration of surfactant was kept at 1%.

Selection of drug concentration:

Batches were prepared with different drug concentration (0.5%, 1% and 2.0%) to achieve most efficient nanosizing of Simvastatin. Surfactant used in this study was Tween 80 at 2% w/v concentration. Zirconium oxide small beads at 80% w/v were used in this study and milling time was done for 12 hr. The obtained nanosuspension was studied for particle size and PDI.

4.3.2 Optimization by Factorial design:

For the preparation of SNS, process parameters were set as per preliminary optimization studies as described above. The optimization of parameters like volume of milling media and concentration of surfactant was carried out by factorial design. Effect of these parameters on mean particle diameter was studied. A 3^2 randomized full factorial design was used in the study (Joshi et al; 2010). In this design, two factors were evaluated, each at 3 levels, and experimental trials were performed at all 9 possible combinations with two replicates. The replicate experimental runs were carried out in complete randomized manner. The volume of milling media (X_1) and concentration of surfactant (X_2) were selected as independent variables. Mean particle diameter - (Y) was chosen as dependent variable. A statistical model incorporating interactive and polynomial terms was used to evaluate the responses. The response surface curves and contour plots were prepared to study the effects of independent variables. All the statistical operations were carried out using DESIGN EXPERT 8.0.5.2. Table 4.1 and Table 4.2 summarize experimental runs studied, their factor combinations, and the translation of the coded levels to the experimental units employed during the study.

Table 4.1. Factorial design parameters and experimental conditions for optimization of nanosuspension formulation.

Factors	Levels used, Actual (coded)		
	Low (-1)	Medium (0)	High (+1)
X_1-Volume of Milling Media (% w/v)	60	80	100
X_2-Concentration of surfactant (%w/v)	1	2	3

Table 4.2. Formulation of the nanosuspension utilizing 3^2 factorial design (Coded values)

Batch No.	X_1	X_2
F1	-1	-1
F2	-1	0
F3	-1	+1
F4	0	-1
F5	0	0
F6	0	+1
F7	+1	-1
F8	+1	0
F9	+1	+1

Optimization Data Analysis

Various RSM (Response Surface Methodology) computations for the current optimization study were performed employing Design Expert® software (version 8.0.5.2, Stat-Ease Inc, Minneapolis, MN). Polynomial models including interaction and quadratic terms were generated for the response variable using multiple regression analysis (MLRA) approach. The general form of MLRA model is represented as equation 4.1.

$$Y=B_0+B_1X_1+B_2X_2+B_3X_1{}^2+B_4X_2{}^2+B_5X_1X_2+B_6\ X_1{}^2X_2+B_7\ X_1\ X_2{}^2\ ...\ (4.1)$$

Where B_0 is the intercept representing the arithmetic average of all quantitative outcomes of 9 runs; B_1 to B_7 are the coefficients computed from the observed experimental values of

Y; and X_1 and X_2 are the coded levels of the independent variable(s). The terms X_1X_2 and X_i^2 (i=1to2) represents the interaction and quadratic terms, respectively. The main effects (X_1 and X_2) represent the average result of changing one factor at a time from its low to high value. The interaction terms (X_1X_2) show how the response changes when two factors are simultaneously changed. The polynomial terms (X_1^2 and X_2^2) are included to investigate nonlinearity. The polynomial equation was used to draw conclusions after considering the magnitude of coefficients and the mathematical sign it carries, i.e., positive or negative. A positive sign signifies a synergistic effect, whereas a negative sign stands for an antagonistic effect (Haung et al; 2005).

Statistical validity of the polynomials was established on the basis of ANOVA provision in the Design Expert ®software. Level of significance was considered at $P<0.05$. The best fitting mathematical model was selected based on the comparisons of several statistical parameters including the coefficient of variation (CV), the multiple correlation coefficient (R^2), adjusted multiple correlation coefficient (adjusted R^2), and the predicted residual sum of squares (PRESS), provided by the software. Among them, PRESS indicates how well the model fits the data, and for the chosen model it should be small relative to the other models under consideration (Huang et al., 2005). Also, the 3-D response surface graphs and the 2-D contour plots were generated by the Design Expert® software.

4.3.4. Lyophilization of Nanosuspension

The optimized Nanosuspension formulation was lyophilized using lyophilizer (Drywinner Hetodryer). Different cryoprotectants (Trehalose dehydrate, Mannitol and Sucrose) at different ratio (1:1w/w, 1:3w/w, 1:5w/w) were tried to select the cryoprotectant which showed minimum increment in particle size. Ten milliliters of each sample with respective concentration of cryoprotectant was rapidly frozen to -80°C using liquid nitrogen, and lyophilized for 24hrs.

4.4 Preparation of nanosuspension by Supercritical Antisolvent (SAS) method

First, required quantity of Simvastatin was dissolved in dichloromethane to obtain a 40mg/ml drug solution. Then, CO_2 from a storage tank was delivered into the top of the particle precipitation vessel at a constant rate until the desired pressure [Automated back pressure regulator (ABPR) 80 bar] was obtained. Once the pressure and temperature (40°C) had equilibrated, the drug solution was co-introduced into the particle precipitation vessel by a HPLC liquid pump (Model 307, Gilson Inc., USA) with SC-CO_2 through the spray nozzle. The residual solvent (SC-CO_2 and dichloromethane) was drained out of the particle precipitation vessel by the backpressure regulator (Tescom, model 26-1723-24-194). In washing step, an additional SC-CO2 continued to flow into the precipitation vessel for further 30 min to wash out the residual dichloromethane solubilized in the supercritical antisolvent. The precipitation vessel was slowly depressurized down to the atmospheric pressure and finally the particles were collected from the internal basket of the precipitation vessel (retained by a 0.1 lm metal frit and paper filter).

4.4.1 Optimization of process parameters:

Determination of drug solubility in supercritical CO_2 and selection of solvent

Determination of the drug solubility in supercritical CO2 is the most important parameter in case of SAS process as it determines product formation. To determine the solubility of SIM in supercritical CO_2, fixed quantity (100mg) of Simvastatin bulk drug was placed in the precipitation chamber of the supercritical particle former (Thar Instruments, USA). Then, supercritical conditions were maintained for 30 min (i.e. ABPR 80 bar and precipitation chamber temperature 45°C) and the residual product in the container was collected and weighed. Solubility of the drug in CO_2 was indirectly determined from weight of the product obtained.

Optimization of process parameters

Stepwise batches were prepared for selection of process parameters such as Automated back pressure (ABPR), product temperature, CO_2 flow, solution spraying rate and drying time. Different solvents such as DCM, chloroform, acetone and mixture of DCM and ethanol were tried to find out the solvent which could provide maximum supersaturation,

identified based on product yield. The concentration of drug in the solvent was kept (80 mg/ml) and other processing parameters as follows;

ABPR	80 Bar
Solution spray rate	0.2 ml/min
CO_2 flow rate	20g/min
Product temperature	40 °C
Drying time	30 min

After selection of the solvent, other process parameters such as pressure, temperature, drug concentration and molar fraction of CO_2 were optimized.

Effect of pressure

The automated back pressure determines the possible precipitation of the compound in the SAS process. The effect of ABPR at three different levels (80, 100 and 120 bar) was studied to find out optimum ABPR required for size reduction of the bulk drug. Other process parameters such as temperature, CO_2 flow rate, spraying rate, drying time were kept constant.

Effect of temperature

The product chamber temperature also determines the possible precipitation of the compound in the SAS process. The effect of temperature at three different levels (40°C, 45°C and 50°C) was studied to find out optimum temperature required for size reduction of the bulk drug. Other process parameters such as ABPR, CO_2 flow rate, spraying rate, drying time were kept constant.

Effect of drug concentration

The drug concentration of the solution also has important influence on particle size of the drug in the SAS process. The effect of drug concentration at three different levels (40mg/ml, 80mg/ml, and 120mg/ml) was studied to find out optimum concentration required for reducing particle size of the bulk drug. Other process parameters such as temperature, ABPR, CO_2 flow rate, spraying rate, drying time were kept constant.

Effect of feed rate ratio

The feed rate ratio is another important parameter which has major influence on size reduction of the drug in the SAS process. The effect of feed rate ratio on size reduction of the drug at different levels (60, 100, 120 and 180) was studied to find out optimum feed rate ratio required for size reduction of the bulk Simvastatin. Other process parameters such as temperature, ABPR, spraying rate, drying time were kept constant.

From above studies, the process parameters required to obtain minimum particle size of the drug were identified. The formulation with minimum particle size was selected as optimum formulation.

4.5 Characterization of Nanosuspension and SCF formulation

Particle Size

For the measurement of the particle size of the nanosuspensions, Dynamic Light Scattering (DLS) was used. DLS was performed using Zetasizer Nano ZS (Malvern Instruments, UK). The particle size of the plain drug and particles prepared by SAS method was determined by Malvern Mastersizer 2000. The plain drug and SAS powder obtained were dispersed in water containing surfactant and after 3 min sonication the particle size of both samples was determined. Prior to measurement, samples were diluted with distilled water to avoid multiple scattering. The dilution was adjusted to achieve the count rate of 200-400 kbps. Detection was carried out at a scattering angle of 90°; sample temperature was set at 25℃ and 9-15 runs of 30 s were performed on each sample. The average mean particle size and standard deviation were recorded. The measurements were performed in triplicate.

Zeta Potential

Electrophoretic mobility measurements were performed with Zetasizer Nano-ZS (Malvern Instruments, Worcestershire, UK) at 25.0 °C. Approx. 1 mL of wet-milled nanosuspension diluted by filtered water to obtain count rate in the 200-400. The zeta potentials were calculated by the instrument according to the Helmholts–Smoluchowski's equation. The measurements were performed in triplicate.

Morphology

Morphology of the nanosuspension was studied by Transmission Electron Microscopy (TEM). A drop of nanosuspension was placed on a coated carbon grid and air dried. The grid was then examined immediately under Transmission Electron microscope (Philips, Tecnai 20, Japan). The electron micrographs were obtained after magnifications. The physical characteristics of the particles observed by TEM were determined using selected area diffraction (SAD) technique. The measurement conditions were $\lambda = 0.0251$ A$^\circ$ radiation generated at 200 kV as X-ray source with camera length of 100 cm. The morphology of the bulk Simvastatin particles and SAS powder was observed under a Scanning Electron Microscope 205 (SEM, JSM-6060, JEOL Ltd. Tokyo, Japan). The samples were mounted directly onto the SEM sample holder using double-sided sticking tape and images were recorded at the required magnification at the acceleration voltage of 10 kV.

Crystallinity

The freeze dried nanosuspension was used for crystallinity analysis of the drug. Thermal properties of the freeze-dried nanosuspension powder, SAS powder and plain drug were investigated with a Differential Scanning Calorimeter (DSC-41, Shimadzu, Japan). Accurately weighed samples (4-7 mg) were placed in hermetically closed aluminum pans and empty aluminum pan was used as a reference. Heating scans by heat runs for each sample was set from 30 °C to 500 °C at 10 °C min-1 in a nitrogen atmosphere. The X-RD patterns were recorded using an X-ray diffractometer (Bruker AXS D8 Advance, with X-ray source of Cu, Wavelength 1.5406A° and Si (Li) PSD detector). The samples were mounted on a sample holder and X-RD patterns were recorded in the range of 5–50° at the speed of 5°per min.

Saturation solubility

The saturation solubility of Simvastatin bulk drug, SNS and SCF powder was determined by adding an excess of the material in distilled water and mechanical shaking at 25 °C for 24 h. After equilibrium was reached, the dispersion was centrifuged at 20000 rpm for 10 min (Sigma centrifuge, Osterode, Germany) to sediment the undissolved drug. Then, 1 ml of

supernatant was withdrawn and filtered (cut-off 0.22 μm, PVDF, Millipore, Ireland). The content of dissolved Simvastatin was analyzed by UV spectrophotometer (UV 1700, Shimadzu, Japan) at 238 nm after suitable dilution with methanol.

Drug content

Drug content in the SNS and SCF powder was determined by dissolving 5mg of obtained lyophilized powder and SCF powder in methanol. The samples were analyzed by UV spectrophotometer at 238 nm after suitable dilution with methanol.

In vitro Release

The in vitro release was carried out by dialysis bag technique (Calvo et al; 1996). A dialysis membrane (Himedia Laboratories, Mumbai, India) having pore size 2.4nm (molecular weight cut-off between 12,000 Da) was used for in vitro release studies. 1 ml of formulation (SNS, SCF and plain drug) equivalent to 400 μg of Simvastatin was placed in dialysis bag and then the bag sealed at both ends was placed in a beaker containing 40 ml of receptor medium (pH 7.2 buffer) maintained at 37 °C. Samples were collected at predetermined time intervals and an equal volume of medium was added each time after sampling to maintain constant volume in the recipient compartment. The amount of drug in the samples was measured at 238 nm spectrophotometrically (UV, Shimadzu 1700).

Stability study

The stability SNS in a glass vial was studied at 4°C and room temperature for up to 3 months. Periodically, samples were withdrawn and the particle size as well as Simvastatin content was determined. Nanonization was not observed in case of SAS method hence stability of this formulation was not carried out.

4.6 Results and Discussion

4.6.1 Nanosuspensions: Results and Discussion

Optimization of Parameters

Milling time :

The mean particle diameter of bulk Simvastatin was 51.84±3.18 μm with a broad particle size distribution (PI, 0.922) (Fig. 4.1). But after media milling for 14h, mean particle diameter of 0.375 ± 0.016 μm and PI of 0.286 were obtained, indicating suitability of the media milling method for nanosizing the Simvastatin (Fig. 4.2). Further milling beyond 14 h did not result in significant reduction as mean particle diameter after 16 hrs was found to be 0.368 ± 0.018 μm (PI – 0.293). The results are tabulated in Table. 4.3.
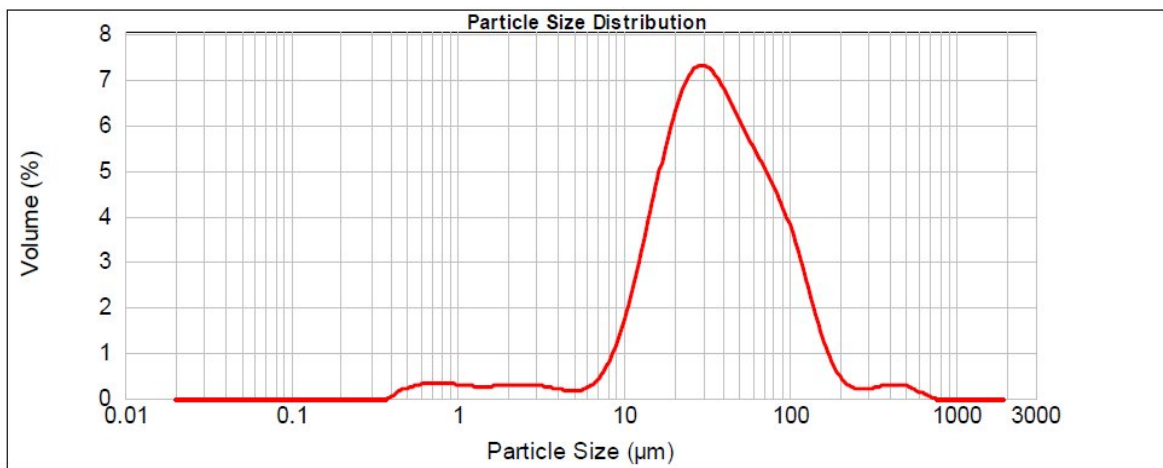
Fig 4.1 Particle size distribution of Bulk Simvastatin by Malvern Mastersizer
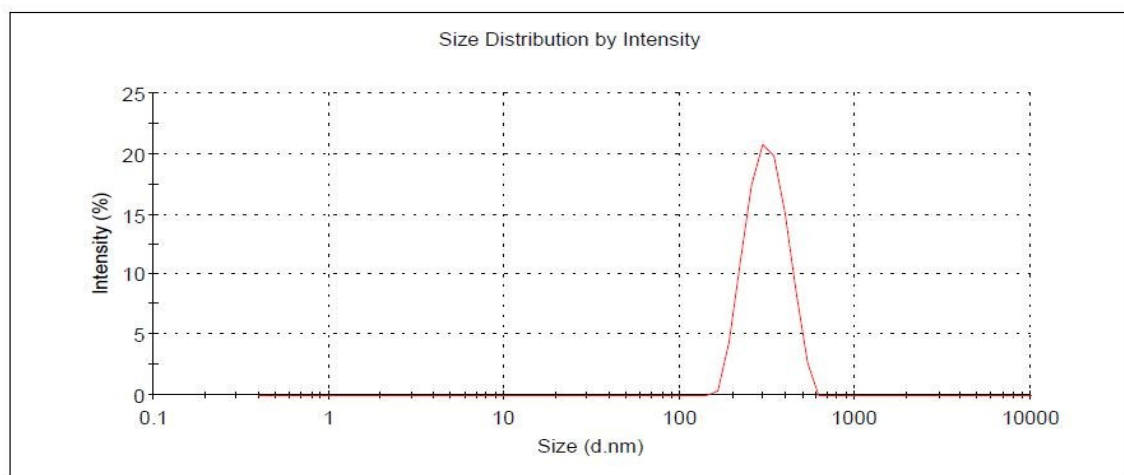
Fig 4.2 Particle size distribution of Simvastatin nanosuspension after 14 hr media milling

Table 4.3. Effect of milling time on Mean particle diameter and PI

Sample No.*	Milling time (hours)	d (4,3) / Mean particle diameter ± S.D. (µm)	Polydispersity Index. (PI)
1	Initial	51.845 ± 3.18	0.922
2	0.5	2.771 ± 0.29	0.616
3	1	2.452 ± 0.079	0.532
4	2	1.343 ± 0.069	0.514
5	4	0.917 ± 0.048	0.394
6	8	0.686 ± 0.023	0.323
7	10	0.623 ± 0.010	0.336
8	12	0.428 ± 0.013	0.313
9	14	0.377± 0.016	0.286
10	16	0.368± 0.018	0.293

(* Sample No. 1 to 4 were measured by Malvern Mastersizer 2000 while sample 6 to 10 were measured by Malvern Zeta Sizer Nano ZS 90)

Type and Ratio of beads

Initially, glass and Zirconium oxide beads were tried to study effect of bead type on size reduction of drug by media milling. With zirconuim oxide beads, higher particle size reduction of Simvastatin was observed as compared to glass beads. Particle size of 428 ± 23 nm (PI – 0.313) was obtained for zirconuim oxide beads while glass beads showed particle size of 570 ± 58 nm (PI – 0.456). Hence, zirconuim oxide beads were used for further studies.

Zirconium oxide beads of two sizes were tried. The use of small size range beads (0.4 mm - 0.7 mm) resulted in significant decrease in mean particle diameter of nanosuspension. When only large size beads were used, higher particle size (570 ± 58 nm) was observed while increase in ratio of small:large bead resulted in decrease in particle diameter. Hence,

different combination of small : large beads were tried (25:75, 50:50 and 75:25). When only small size beads were used, minimun particle diameter (428 ± 23) was obtained. Hence, only small beads were selected as milling media.The results are given in Table 4.4.

Table 4.4. Effect of ratio of beads on Particle diameter and Polydispersity Index

Ratio of beads (small : large)	Mean Particle diameter ± S.D. (nm)	Polydispersity Index (PI)
0:100	570 ± 32	0.386
25:75	496 ± 37	0.411
50:50	464 ± 26	0.309
75:25	437 ± 29	0.296
100:0	428 ± 23	0.284

Selection of surfactant:

During the course of optimization, the type of surfactant was chosen between Pluronic F68, Tween 80, PVP K30 and Pluronic F68: Tween 80. Here, drug concentration and concentration of surfactant was kept at 1 %. Formulation prepared with Tween 80 showed smallest particle diameter (432 ± 18 nm) compared to other surfactants (Table 4.5). Hence, Tween 80 was used as a surfactant for further studies. It could be concluded that the main reason for efficient formation of droplets and stabilization of the nanosuspension appeared to be the type of surfactant.

Table 4.5. Effect of surfactants on Particle diameter

Sr.No	Surfactant	Zavg In nm ± SD	PI
01	Tween 80	432 ± 18	0.314
02	Pluronic-F68	498 ± 27	0.386
03	Polyvinyl pyrrolidone (PVPK 30)	583 ± 24	0.451
04	Pluronic F68: Tween 80 (1:2)	494 ± 16	0.385
05	Pluronic F68: Tween 80 (1:4)	475 ± 19	0.367

The effectiveness of Tween 80 in terms of particle size was significantly high than polymeric materials such as PVP and Pluronic F68 due to its high adsorption potential. Nonionic nonpolymeric surfactants (e.g. Tween 80) offer an advantage over polymers in that they have a higher adsorption potential than an equal-chain-length polymer (Palla and Shah, 2002).

Selection of drug concentration:

With all other parameters kept constant, batches with different drug concentration (0.5%, 1% and 2.0%) were prepared. Results showed that particle size was dependent on drug concentration (Table 4.6). Higher particle size was obtained with higher drug concentration. Hence, we concluded that optimum concentration of drug was required to get desired particle size in milling method. With 0.5% drug concentration, minimum particle size was obtained in 12 hr milling.

Table 4.6. Effect of drug concentration on Particle diameter

Sr.No	Drug concentration (w/v)	Zavg in nm ± SD	PI
01	0.5 %	388 ± 24	0.271
02	1.0 %	448 ± 57	0.364
03	2 %	683 ± 78	0.428

From these preliminary investigations, various process parameters (type of milling media, surfactant and milling time) required for nanonization of Simvastatin were finalized and then other parameters such as milling media volume and surfactant concentration were optimized by factorial design.

Following parameters were kept constant in factorial design studies

Surfactant: Tween 80

Milling Media: Small zirconium oxide beads

Milling time: 14 hrs

After preliminary experiments, above parameters were kept constant to study the effect of volume of milling media and surfactant concentration on particle size to avoid design complexity. Other important parameters such as volume of milling media (X_1) and surfactant concentration (X_2) were optimized based on 3^2 factorial design.

Optimization by Factorial design:

Nine formulations were prepared as per 3^2 Factorial Design. Table 4.7 enlists the response parameters of all the nine formulations.

Effect of formulation variables on the response parameters:

On analyzing the data of all the 9 formulations prepared as per 3^2 Factorial design using Design Expert® 8.0 software, various polynomial equations, response surface and contour plots were generated. The information obtained from the software is discussed in the following sections, depicting the effects of variables on the respective response parameters (Y).

Table 4.7. Response parameters for formulation of Simvastatin nanosuspension prepared as per 3^2 factorial design.

Formulation code (coded values)	Factors		Particle Mean Diameter – (nm) [Y]
	Volume of milling media – X_1 (%w/v)	Concentration of surfactant - X_2 (%w/v)	
SN1 (-1,-1)	60	1	450±17
SN2 (-1,0)	60	2	413±16
SN3 (-1,1)	60	3	384±08
SN4 (0, -1)	80	1	361±15
SN5 (0, 0)	80	2	336±16
SN6 (0,1)	80	3	320±12
SN7 (1,-1)	100	1	250±09
SN8 (1, 0)	100	2	263±12
SN9 (1, 1)	100	3	258±11

The responses obtained were fitted in either simple linear equation (Eq. 4.2), interactive equation (Eq. 4.3) or quadratic model equation (Eq. 4.4) by carrying out multiple regression analysis and F-statistic to identify statistically significant terms.

$$Y = b_0 + b_1X_1 + b_2X_2 \tag{4.2}$$

$$Y = b_0 + b_1X_1 + b_2X_2 + b_{12}X_1X_2 \tag{4.3}$$

$$Y = b_0 + b_1X_1 + b_2X_2 + b_1{}^2X_{11} + b_2{}^2X_{22} + b_{12}X_1X_2 \tag{4.4}$$

From the multiple regressions, it was observed that factors X_1, X_2 and X_1X_2 had significant effect on the dependent variable. The model suggested was polynomial model (Eq. 4.5).

Table 4.8. Observed and Predicted values of response parameters

Batch	Response parameters		
	Y1		
	Observed	Predicted	%RE
SQ1	450	450.38	0.086
SQ2	413	415.88	0.695
SQ3	384	380.72	0.861
SQ4	361	354.88	1.440
SQ5	336	338.88	0.852
SQ6	320	322.22	0.690
SQ7	250	254.72	1.854
SQ8	263	257.22	2.246
SQ9	258	259.05	0.407

% RE= % Relative Error

% RE = Observed (Actual) – Predicted / Predicted * 100

The polynomial equation and regression coefficient for Y (Mean particle diameter) are as follows:

$$Y= 337.11 -79.33\ X_1 – 16.33\ X_2+18.5\ X_1X_2 \tag{4.5}$$

$R^2 = 0.9969$

The model (Eq 4.5) was found to be significant with an F value of 536.42 ($p< 0.0001$). The value of correlation coefficient (R^2) was found to be 0.9969. The R^2 value is a measure of total variability explained by the model. The R^2 value of 0.9969 for the model indicated that the model was significant. Value of probability very much less than 0.05 indicated that the model terms were highly significant. The value of Predicted Residual Sum of Squares (PRESS) for the polynomial model was 616.47. The PRESS value indicates how well the model fits the data, and for the chosen model it should be small relative to the other models under consideration (Huang et al., 2005). The polynomial model with the lower PRESS value was selected.

Negative values of X_1 and X_2 in Eq.4.5 indicate antagonistic effect on Y of Simvastatin nanosuspension i.e. any increase in X_1 and X_2 reduces the value of Y. Effect of X_1 was found to be higher than the effect of X_2 on Y. The combined effect of these parameters (X_1X_2) was also significant. The combined effect of factors X_1 and X_2 can further be elucidated with the help of response surface and contour plots (Fig. 4.3a and 4.3b respectively) which demonstrated that Y varies in a reverse fashion with X_1. The effect of X_2 was comparatively less as compared to X_1.

The effects of X_1 and X_2 on Y by contour plots and response surface are shown in Fig. 4.3(a) and Fig. 4.3(b). Increase in value of X_1 from low (-1) to high (+1) level while keeping value of X_2 constant at low level (-1) did result in significant decrease in mean particle size while increase in value of X_2 from low (-1) to high (+1) level while keeping value of X_1 constant at low level (-1) resulted in slight decrease in value of mean particle size. In comparion, at low level X_1, high level of X_2 was better for obtaining minimum particle size.

High level of X_1 gave minimum value of mean particle size at all the 3 levels of X_2 which indicated that X_1 had significantly synergistic effect on Y. Contour plot [Fig 4.3(a)] reveals that Y varies in nearly linear fashion with X_1 and X_2. However, the effect of X_1 seems to be more pronounced as compared with that of X_1.

The predicted and observed values of response parameters are shown in Table 4.8. Low values of the relative error showed that there was a reasonable agreement between predicted values and experimental values indicating suitability of the model. ANOVA results of PS for full model are given in Table 4.9.
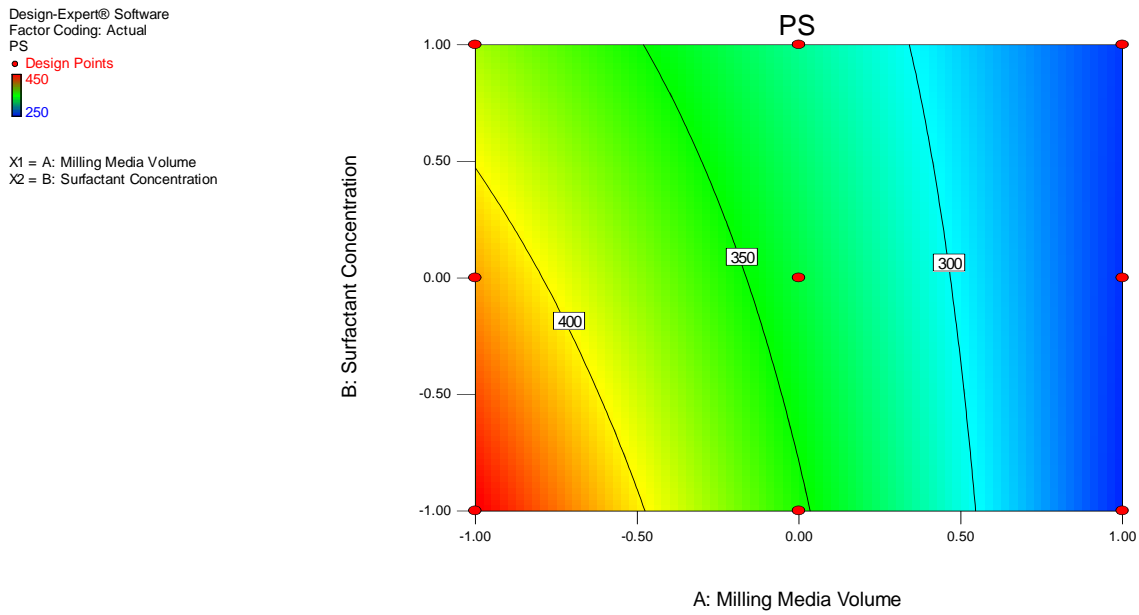
Design-Expert® Software
Factor Coding: Actual
PS
● Design Points
450
250

X1 = A: Milling Media Volume
X2 = B: Surfactant Concentration

Fig 4.3 (a): Contour plot showing the effect of independent factors on Mean Particle size (PS)

Design-Expert® Software
Factor Coding: Actual
PS
● Design points above predicted value
○ Design points below predicted value
450
250

X1 = A: Milling Media Volume
X2 = B: Surfactant Concentration
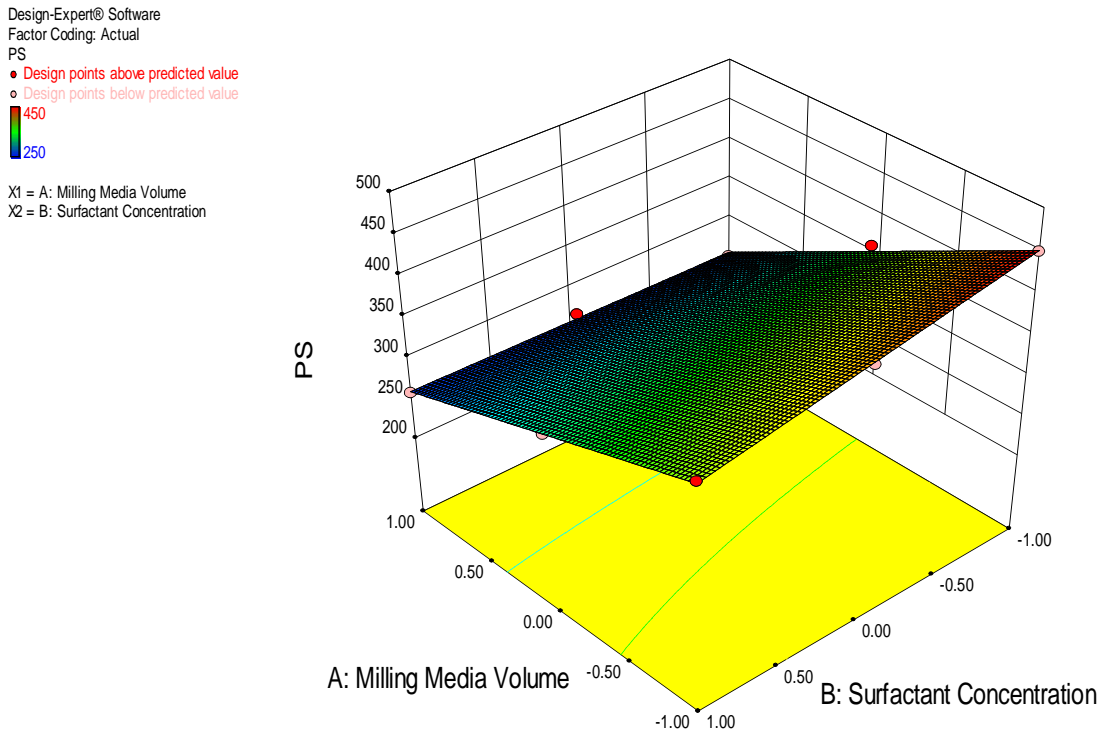
Fig 4.3 (b): Response surface plot showing the effect of independent factors on Mean Particle size (PS)

Table 4.9. Analysis of variance (ANOVA) of PS for full models of NS

	DF	SS	MS	F	R^2	Adj R^2
FM	5	40732.33	13577.44	536.42	0.9969	0.9950
Residual	3	126.56	25.31			
Total	8	40858.89	---			

Optimum Formulation:

A numerical optimization technique by the desirability approach was used to generate the optimum settings for the formulation. The process was optimized for the dependent (response) variable Y and the optimized formula was arrived by keeping the mean particle diameter in range of 200 to 300 nm. Formulation SN7 (containing high (+1) level of variable, X_1 and low level of variable X_2) fulfilled all the criteria set from desirability search (Narendra et al, 2005). To gainsay the reliability of the response surface model, new optimized formulation (as per formula SN7) was prepared according to the predicted model and evaluated for the response (Y). The result in Table 4.11 illustrates a good relationship between the experimental and predicted values, which confirms the practicability and validity of the model. The predicted error of the response variable was below 5 % indicating that the Response Surface Methodology (RSM) optimization technique was appropriate for optimizing Simvastatin Nanosuspension. The optimized formulation of SNS is shown in Table 4.10.

Table 4.10. Optimized Simvastatin Nanosuspension

Parameters	Value
Milling time	14 hours
Ratio of Beads (Small : Large)	100:00
Drug concentration	0.5 % w/v
Surfactant	Tween 80
Volume of milling media	100 % w/v
Concentration of surfactant	1 % w/w

Table 4.11. The predicted and observed response variables of the optimized Simvastatin Nanosuspension

	Y (nm)
Predicted	254.74
Observed	250.60 ± 09
Predicted Error (%)	1.854

Predicted Error (%) = (Observed value – Predicted value)/ Predicted value x 100%

Lyophilization of Nanosuspension

The optimized Nanosuspension formulations were lyophilized using lyophilizer (Heto Drywinner, Vaccubrand, Denmark). Different cryoprotectants (Trehalose dehydrate, Mannitol and Sucrose) were used at different ratios to find out optimum concentration of cryoprotectant which showed minimum increment in particle size. The initial particle size of the formulation was 250.60 ± 09. The results are shown in Table 4. 12. At 1:1 ratio (solid contents: cryoprotectant) sticky material was obtained which may be due to presence of Tween 80 in the formulation. At 1:3 and 1:5 ratios, dry powder was obtained. It was observed that trehalose dihydrate showed minimum particle size at 1:3 ratios indicating its suitability in maintaining particle size of Simvastatin nanosuspension after lyophilization. Thus, this formulation was considered for further studies.

Table 4.12. Optimization of cryoprotectant concentration in Nanosuspension

Cryoprotectant	Particle size after lyophilization
Trehalose dehydrate (1:3)	283.4 ± 12.8
Trehalose dehydrate (1:5)	296.7 ± 21.6
Sucrose (1:3)	448.6 ± 42.8
Sucrose (1:5)	496.3 ± 76.2
Mannitol (1:3)	314.5 ± 52.8
Mannitol (1:5)	485.2 ± 42.2

4.6.2 Results and discussion- Supercritical process:

Determination of Simvastatin solubility in supercritical CO_2 (Sc-CO2)

The prerequisites for successful micro/nanonization using SAS process are the complete miscibility between the liquid solvent and the antisolvent and the insolubility of the solute in the antisolvent. Hence, the solubility of Simvastatin in Sc-CO2 was determined. After maintaining the supercritical condition for 30min, the drug remained in the product chamber was collected and nearly 85% of the drug was obtained as such indicating insolubility of Simvastatin in Sc-CO2. Thus, SAS method could be a useful approach for nanosizing Simvastatin.

From the literature available, it was observed that micronization using SAS was performed using CO_2 in pressures ranging from 75 to 120 bars. Different organic solvents were used for micro/nanonization of the poorly water soluble drugs using SAS include ethanol, methanol, DCM, DMSO, ethyl acetate, acetone and chloroform. The temperature condition used in SAS method varies from 35 to 60 °C. Thus, selection of these parameters to successfully micro/nanosize the drug is very important. Hence, stepwise optimization of these parameters was performed.

Selection of solvent

Different solvents such as DCM, chloroform, and acetone were tried to find out the solvent which gave maximum precipitation yield. The results obtained by using different solvents were reported in Table No. 4.13. The ABPR (80bar), product chamber temperature (40 °C), solution spray rate (0.3 ml/min), CO2 flow rate (30g/min), the drying time (30 min), drug concentration of the solution used (80mg/ml) were fixed.

Table 4.13. Selection of solvent in SAS process

Sr. No.	Solvent	Yield	Particle size (μm)
1	Dichloromethane (DCM)	12-20%	16.54±0.38
2	Chloroform	6-10%	22.64±0.94
4	Acetone	6-10%	28.35±0.83

From the results, it can be observed that DCM showed lesser particle size and higher yield as compared to acetone and chloroform. This may be attributed to higher mixing with

$ScCO_2$ and high supersaturation, resulting in better precipitation. DCM is a common choice for SAS experiments because of its ability to dissolve wide number of compounds or materials and good miscibility with Sc-CO_2 at low temperatures and pressures. Thus, DCM was used as solvent for Simvastatin for micro/nanosizing using SAS method. The phase behaviour of Simvastatin in DCM was reported to be suitable for supercritical method (Dong-Joon Oh and Byung-Chul Lee. 2007).

Effect of pressure and temperature

The density of CO_2 is influenced by temperature and pressure at supercritical conditions and it plays important role in mass transfer between two phases and thus, determines particle size and morphology. The changes in automated back pressure (ABPR) and temperature affect the particle size and size distribution of the product due to change in critical mixing point of the binary system. The effect of ABPR at three different levels (80, 100 and 120 bar) on precipitation (particle size) of Simvastatin is given in Table No. 6.14. In this study solution spray rate (0.3 ml/min), CO_2 flow rate (30g/min), drug concentration (80mg/ml) and drying time (30 min) were fixed.

Table 4.14. Effect of temperature and pressure on particle size of Simvastatin by SAS

Sr. No.	Temperature (°C)	Pressure (bar)	Particle size (μm)
1	40	80	16.54±0.38 (yield high)
2	40	100	28.18±0.42 (low yield)
3	40	120	No precipitation
4	45	80	17.18±2.94
5	50	80	17.88±3.12

From the results, it was observed that, at constant temperature the precipitation of Simvastatin was decreased with increase in ABPR. At 100bar, the mass transfer between DCM and SCF-CO_2 could be slow, resulting in increase in particle size. Further increase in pressure might have resulted in decreased miscibility between solvent and antisolvent. The effect of temperature at three different levels (40°C, 45°C and 50°C) on size reduction of the bulk Simvastatin at constant pressure was also studied. From the results, it was observed that temperature had negligible effect on mean particle size of Simvastatin.

Effect of drug concentration

The effect of drug concentration at three different levels (80mg/ml, 120mg/ml, and 150mg/ml) was reported in Table No. 4.15. There was reduction is particle size with decrease in drug concentration was observed. The reduction in drug concentration below 40mg/ ml resulted in very low yield and further reduction led to no precipitation. As the solution concentration is increased, fast reduction of solvent power by the antisolvent CO_2 allows homogeneous particles to nucleate. Beyond a certain point, as the solution concentration is increased, particle growth dominates the nucleation process, which results in larger particles (Reverchon et al; 1998).

Table 4.15. Effect of drug concentration on Particle size of Simvastatin

Sr. No.	Drug concentration (mg/ml)	Particle size (µm)
1	80	16.54±0.38
2	120	22.64±0.63
3	150	32.17±1.82

Effect of feed flow ratio

The feed flow ratio determines the particle size of the drug in the SAS process. The effect on particle size at different feed flow ratio was studied and results are reported in Table 4.16.

Table 4.16. Summary of experiments performed

Experiments	Pressure (bar)	Temperature (°C)	Drug solution Flow (ml/min)	CO_2 flow rate (g/min)	Feed flow ratio*	Particle size obtained (µm)
1	80	40	0.5	20	40	27.66±2.82
2	80	40	0.3	20	66.6	30.89±1.62
3	80	40	0.3	30	100	16.54±0.38
4	80	40	0.3	40	133.3	17.58±0.54
5	80	40	0.2	30	150	25.18±1.10
6	80	40	0.2	40	200	26.13±1.28

*Feed flow ratio= CO_2 flow rate/drug solution flow rate

Optimum feed flow ratio required for size reduction of the bulk Simvastatin was identified from the results obtained in Table 4.16. The drug concentration used in this process was 80mg/ml. Experiments were performed at values of the feed rate ratios ranging between 40 and 200 on a weight basis of CO_2 and drug solution. From the results, it was observed that feed flow rate had significant influence on particle size of the Simvastatin obtained by SAS process. At low feed flow rate, such as 40 and 66.6, there was increase in particle size obtained, but it was decreased with further increase in feed flow rate to 100. But this trend was not followed throughout the studies, as with high feed flow rate (such as 150 and 200) there is further increase in the particle size. This indicates that the CO_2 flow rate and drug flow rate must be kept such that there will be maximum supersaturation.

Thus, from these studies it can be concluded that drug concentration and feed flow ratio are the two important parameters which determine the particle size of the product obtained in the SAS process. Further trials with decrease in drug concentration from 80 mg/ml were tried but no significant decrease in particle size was observed.

Table 4.17: Optimized formula for SAS process

Parameter	Value
Drug Concentration	80mg/ml
ABPR	80 bar
Temperature	40 °C
CO_2 flow rate	30g/min
Solvent flow rate	0.3 ml/min
Drying time	30 min

The aim of this SAS process was to nanosize Simvastatin plain drug, but the minimum particle size obtained was 16.54±0.38 µm. However, as the powder obtained had different physical properties such as bulk density and also there was also reduction in particle size of the plain drug, the SCF product obtained was evaluated for further studies.

4.6.3 Characterization of optimized nanosuspension and SCF formulation

Particle size and zeta potential

In the wet milling process, the high energy, shear forces and turbulent environment generated as a result of the impaction of the grinding media with the drug particles provides sufficient energy to break the drug microparticles into nanoparticles [E. Merisko-Liversidge et al 2003]. Simvastatin nanosuspension was successfully prepared by milling the slurry of drug and stabilizers, reaching a particle size of 250 ± 09 nm (PI 0.238) after 14hrs. The polydispersity index (PI) measures the width of distribution. The PDI value of Simvastatin nanosuspension was below 0.25 indicating a narrow size distribution of the milled suspension. PI value of 0.1-0.3 indicates a narrow size distribution whereas a PDI value greater than 0.3 indicates a very broad size distribution [H. S. Ali et al 2009]. There was no significant difference in particle size before and after lyophilization indicating suitability of the lyophilization method. Zeta potential analysis was performed to get information about the surface properties of the nanocrystal. The zeta potential of the prepared Simvastatin nanosuspension was -27.1 ± 3.5 mV. It is generally acknowledged that a zeta potential of approximately ± 30 mV is required as minimum (Zetasizer manual). The particle size of optimized SCF formulation was determined by Malvern Masterizer 2000 and it was found to be 16.54±0.38 (PI 0.546). Thus, there was reduction in particle size of Simvastatin by SAS processing and the particles obtained were very fluffy in nature.

Saturation solubility

Saturation solubility is a compound-specific constant, which is temperature dependent. However, the saturation solubility increases below a particle size of approximately 1 μm [Muller et al 2001]. The saturation solubility of plain drug was compared with lyophilized nanosuspension. The Simvastatin nanosuspension showed 1.835± 0.125 mg/ml as compared to plain drug 0.548± 0.062 mg/ml indicating enhancement in solubility due to nanosizing. The saturation solubility of SCF formulations was found to be 0.614 ± 0.078 mg/ml. The saturation solubility of Simvastatin increased significantly after formulating as nanosuspension but the improvement in solubility of SCF formulation was negligible. The increase in solubility in case of SNS was almost 3.5 folds higher than the bulk Simvastatin and this could be attributed to nanosizing of the drug which lead to improvement in

dissolution pressure, enhanced surface area, creation of high energy surface and increased concentration gradient.

Morphology

The appearance of the SNS was compared to suspension of plain drug and SCF powder. The visual appearance of SNS was bluish and transparent relative to the coarse suspension, indicating the nanosized state of Simvastatin particles [S. Kamiya et al 2009]. The size and shape of raw and nanosized Simvastatin particles were confirmed by SEM and TEM microscopy. Particles of raw Simvastatin exhibited large aggregates of needle shaped crystals Fig. 4.4 (a) while Fig. 4.4 (b) shows nanoparticles of Simvastatin produced by media milling method. The TEM micrographs confirmed that the milling process is effective in converting the bulk Simvastatin particles into the submicron range. The particle size observed in TEM image is in accordance with particle size obtained by DLS method. The nanosized particles with irregular shape and without any tendency of aggregation were observed. Fig. 4.4 (c) shows particles produced by SCF method by SEM. It can be confirmed that morphology of bulk drug was changed by SCF method but the reduction in particle size was not very high. Particles of bulk drug were much larger particles and lacked size uniformity.
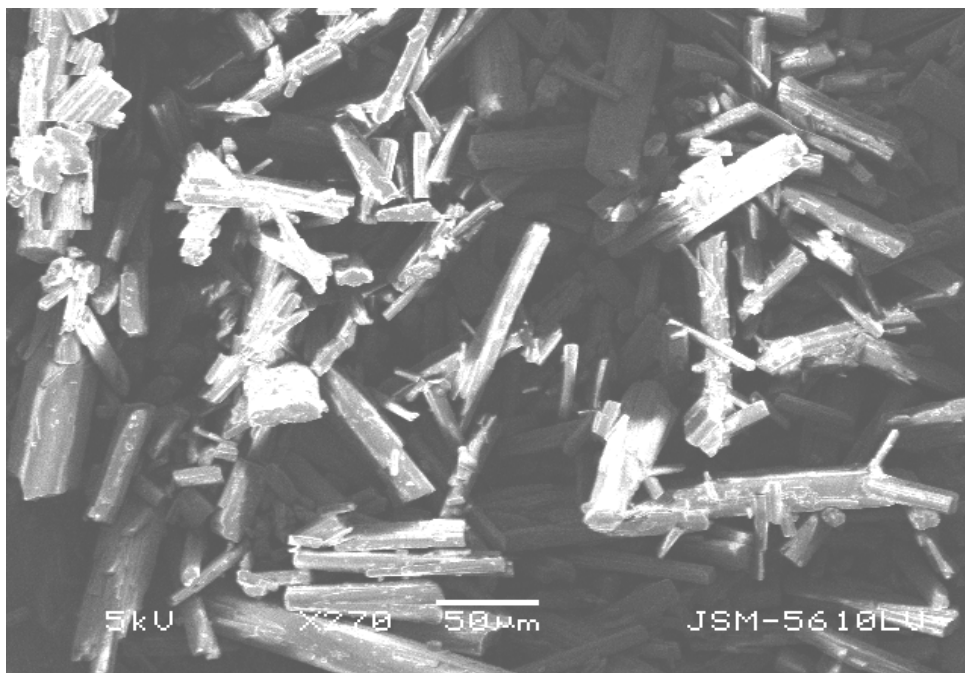
Fig 4.4 (a): SEM image Simvastatin plain drug
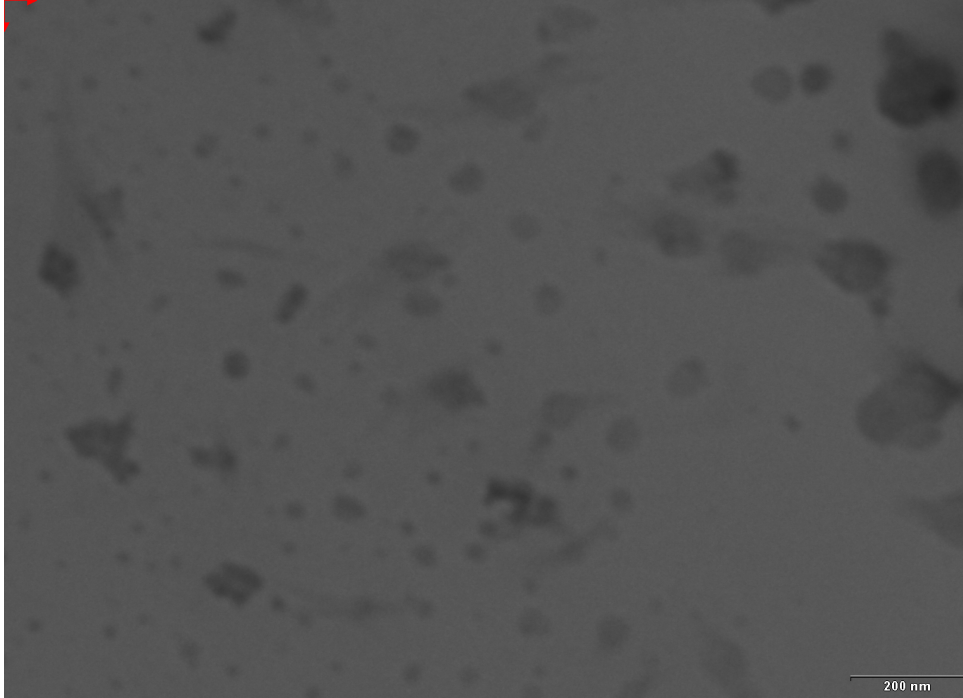
Fig. 4(b) TEM image Simvastatin Nanosuspension
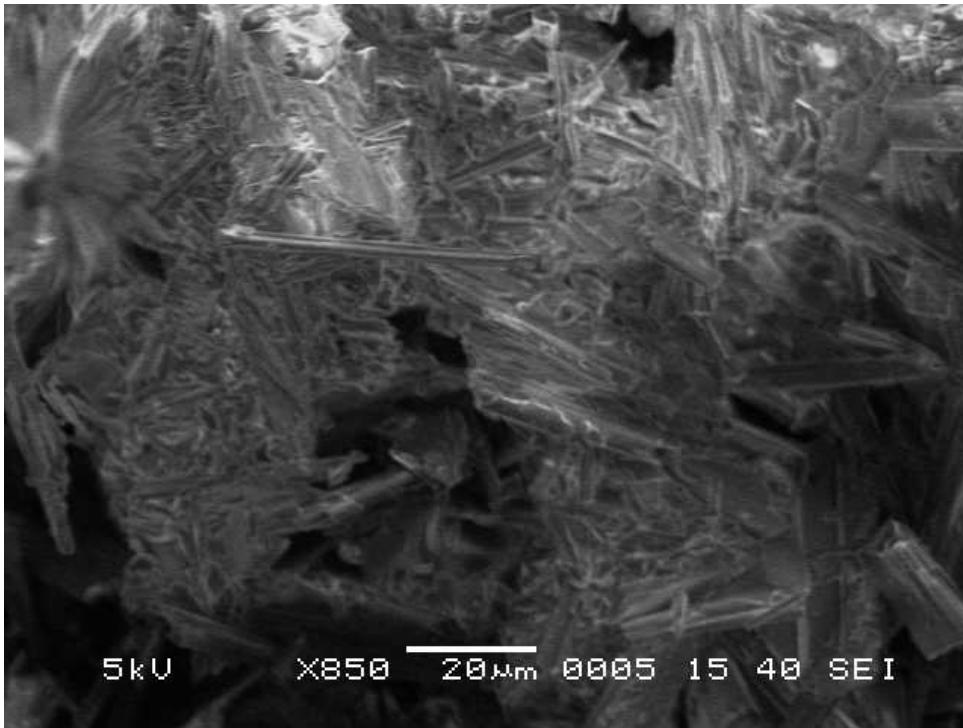
Fig 4 (c): SEM image Simvastatin SCF formulation

Crystallinity

Crystalline state is another factor influencing the dissolution and stability behavior of a compound. The crystalline state of the samples was evaluated to prove the effect of milling

on the physical state of Simvastatin. The X-Ray Diffraction (XRD) patterns for bulk Simvastatin, SCF formulation and SNS are displayed in Fig. 4.5. Upon X-ray examinations, it was observed that the specific peaks for Simvastatin at specified 2Ө value were not observed for SNS. This suggested that the crystallinity of Simvastatin was not preserved in the SNS formulation, indicating that the crystalline state of Simvastatin was altered following milling. The absence of major peaks of Simvastatin in case of SNS confirmed formation of amorphous product which might leads to enhanced solubility of the drug in case of SNS. But in case of SCF formulation all the peaks of Simvastatin were retained indicating no change in crystallinity of Simvastatin after SCF processing.
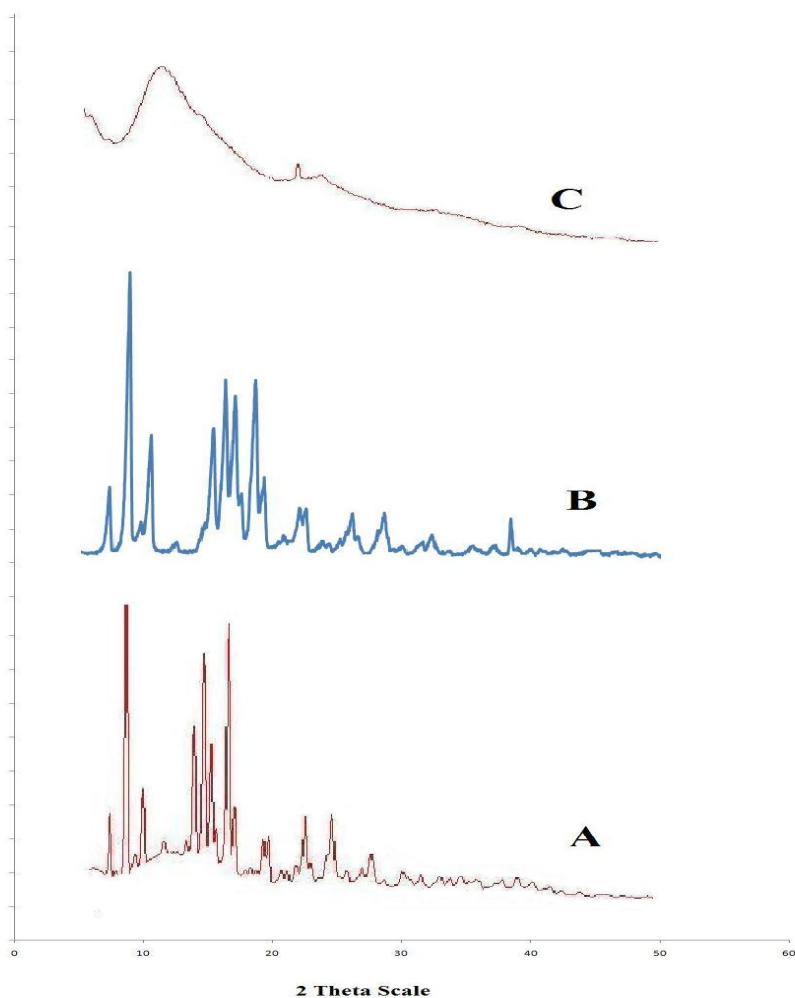
Fig.4.5. XRD pattern of Simvastatin un-milled drug (A), Supercritical formulation (B) and lyophilized Simvastatin nanosuspension (C)

DSC was also performed for Simvastatin, SNS and SCF formulation in order to further confirm the physical state. In this case, DSC scan of bulk Simvastatin sample showed a single sharp endothermic peak at 140 °C (Fig. 4.6) ascribed to the melting of the drug. In case of SNS the crystalline structure had been reduced substantially or lost after nanosizing as reflected by disappearance of melting endothermic peak. Ali et al confirmed loss in crystallinity of hydrocortisone nanosuspension from DSC studies (Ali et al; 2010). But in case of SCF formulation the peak at 140 °C of Simvastatin was retained indicating no change in crystallinity of Simvastatin after SCF processing. Thus, a combined XRD and DSC study proved that crystallanity of Simvastatin was significantly reduced due to the size reduction in the crystals.
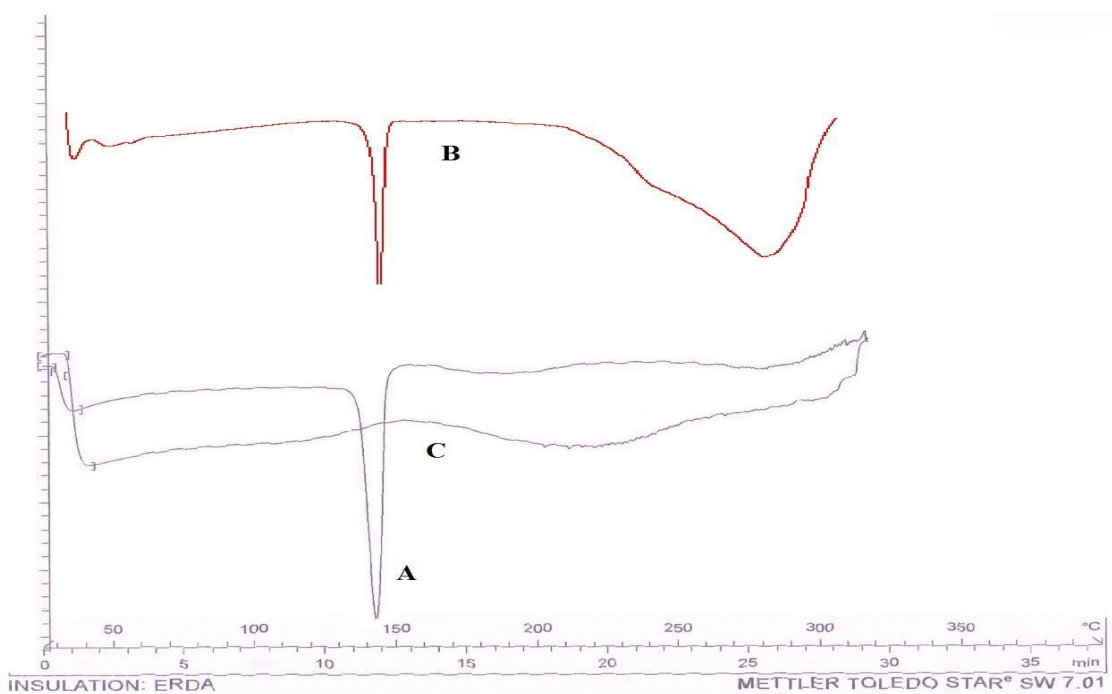
Fig. 4.6. DSC spectra of Simvastatin un-milled drug (A), Supercritical formulation (B) and lyophilized Simvastatin nanosuspension (C)

Drug content

Drug content of SNS and SCF formulation was found to be 98.53±1.65 %, 97.94±1.65 % respectively indicating suitability of these methods for particle size reduction. Thus, both methods could be useful for particle size engineering of Simvastain as chemical stability was not affected by processing.

In vitro release studies:

The release profiles of SNS and SCF powder in comparison to plain drug are given in Fig 4.7. The drug release of 12.35±0.44 % and 15.8±0.94% was observed in case of plain drug and SCF formulation at 2 hr respectively while the drug release in case of nanosuspension formulation was 39.96±0.34 %. At the end of 8 hr, 16.69±0.98 and 18.71±0.95% of drug was released in case of plain drug and SCF formulation respectively while the drug release in case of nanosuspension formulation at the same time point was 52.4±0.84 %. The release profiles clearly indicated the faster release rate of Simvastatin in case of nanosuspension formulation. This increase in release rate can be attributed to increase in the surface area after nanosizing the crystals. Thus, it can be said that nanosizing approach could play important role in improving solubility of Simvastatin which will ultimately lead to enhancement in its bioavailability.
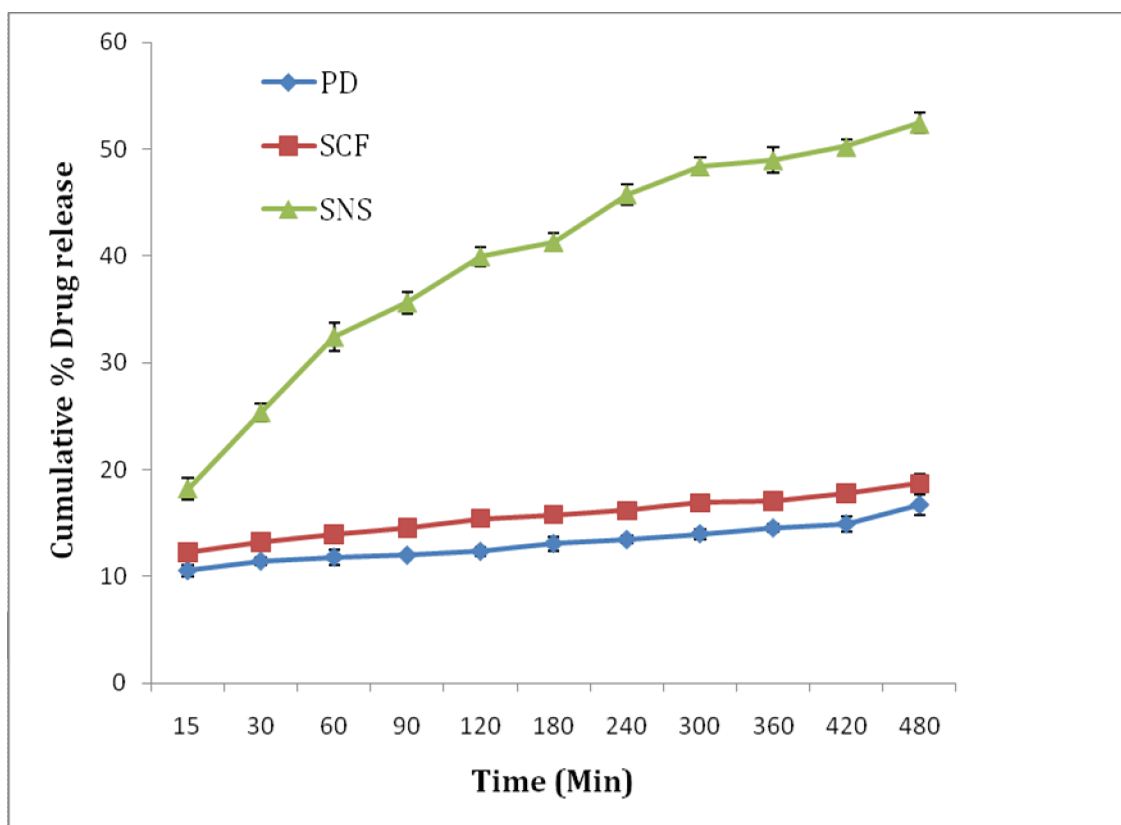
Fig 4.7 I*n vitro* release of plain drug, SCF formulation and SNS in pH 7.2 phosphate buffer

The release profiles were then fitted into different exponential equations such as zero order, first order, Higuchi, Hixson-Crowell, and Korsmeyer-Peppas to characterize the

release. It was found that drug release from SNS followed Korsmeyer- Peppas (r^2=0.9711) more than Higuchi (r^2=0.9388), Zero order (r^2=0.8392), Hixson-Crowell (r^2=0.8578) and First order (r^2=0.8964). Release from Plain drug was found to followed Korsmeyer- Peppas (r^2=0.9579) more than First order (r^2=0.9453), Zero order (r^2=0.9142), Hixson-Crowell (r^2=0.9158) and Higuchi (r^2=0.9540) model. Release from SCF formulation was found to followed Korsmeyer- Peppas (r^2=0.9854) more than Zero order (r^2=0.9149), First order (r^2=0.9809), Hixson-Crowell (r^2=0.9167) and Higuchi (r^2=0.9747) model. Value of 'n' indicates that SNS, PD and SCF formulation followed fickian diffusion as the release component values were below 0.5 (Costa P et al .2001).

Stability

The stability of SNS in terms of drug content and particle size distribution was monitored for 3 months at 2-8 °C and RT (25-30 °C). The formulation showed physical stability for the period of 3 months at both conditions. The particle size and drug content of the SNS at different time interval is given in Table 4.18. It was found that no significant difference was observed in the particle size of SNS after 3 months at both conditions indicating its suitability for storage at both conditions.

Table 4.18: Stability of SNS at RT and cold conditions (2-8°C)

Sr. No	Time	Drug content (%) (2-8 °C)	Drug content (%) (RT)	Particle size (nm) (2-8 °C)	Particle size (nm) (RT)
1	Initial	99.8±1.1	99.8±1.4	283.4±12.6	283.4±12.6
2	1 month	99.6±1.3	99.5±1.0	283.3±10.2	286.3±12.5
3	2 months	99.6±1.0	99.4±1.5	285.1±15.3	292.6±11.2
4	3 months	98.9±1.6	98.8±1.3	288.6±13.9	298.1±10.9

4.9 References:

- Ali HS, York P, Blagden N. Preparation of hydrocortisone nanosuspension through a bottom-up nanoprecipitation technique using microfluidic reactors. Int J Pharm. 375, 2009, 107-113.

- Calvo P, Vila-Jato JL, Alonso MJ. Comparative in vitro evaluation of several colloidal systems, nanoparticles, nanocapsules and nanoemulsions as ocular drug carrier. J Pharm Sci. 85, 1996, 530–536.

- Costa P, Sousa Lobo JM. Modeling and comparison of dissolution profiles. Eur J Pharm Sci. 13, 2001, 123–33.

- Eerdenbrugh BV, Froyen L, Martens JA, Blaton N, Augustijns P, Brewster M. Characterization of physico-chemical properties and pharmaceutical performance of sucrose co-freeze–dried solid nanoparticulate powders of the anti-HIV agent loviride prepared by media milling. Int J Pharm. 338, 2007, 198-206.

- Huang YB, Tsai YH, Lee SH, Chang JS, Wu PC. Optimization of pH-independent release of nicardipine hydrochloride extended-release matrix tablets using response surface methodology. Int J Pharm. 289, 2005, 87-95.

- Joshi SA, Chavhan SS, Sawant KK. Rivastigmine-loaded PLGA and PBCA nanoparticles: Preparation, optimization, characterization, in vitro and pharmacodynamic studies. Eur J Pharm Biopharm. 76, 2010, 189–199.

- Kamiya S, Kurita T, Miyagishima A, Arakawa M. Preparation of griseofulvin nanoparticle suspension by high-pressure homogenization and preservation of the suspension with saccharides and sugar alcohols. Drug Dev Ind Pharm. 35(8), 2009, 1022–1028.

- Merisko-Liversidge E, Liversidge GG, Cooper ER. Nanosizing: a formulation approach for poorly-water-soluble compounds. Eur J Pharm Sci. 18, 2003, 113–120.

- Muller RH, Jacobs C, Kayser O. Nanosuspensions as particulate drug formulations in therapy: Rationale for development and what we can expect for the future. Adv Drug Delivery Rev. 47, 2001, 3-19.

- Oh DJ, & Lee BC. Solubility of Simvastatin and Lovastatin in Mixtures of Dichloromethane and Supercritical Carbon Dioxide. J Chem Eng Data 52, 2007, 1273-1279.

- Palla BJ, Shah DO. Stabilization of high ionic strength slurries using surfactant mixtures: molecular factors that determine optimal stability. J Colloid Interface Sci. 256, 2002, 143–152.

- Reverchon G, Della P, Di T, Pace S. Supercritical antisolvent precipitation of nanoparticles of superconductor precursors. Ind Engg Chem Res. 37, 1998, 952–958.

- Sigfridsson K, Forssen S, Hollander P, Skantze U, Verdier J. A formulation comparison, using a solution and different nanosuspensions of a poorly soluble compound. Eur J Pharm Biopharm. 67, 2007, 540-547.

- Zetasizer Manual

5.0 MATERIALS AND METHODS

5.1 Materials

Simvastain of pharmaceutical grade was obtained as kind gift from Lupin Pharmaceuticals Ltd, Pune, India. Capryol 90 was obtained as generous gift sample from Gattefosse Ltd (Mumbai, India). Soya PC (Phospholipon 90G) and Egg PC was obtained as kind gift from Lipoid GMBH (Ludwigshafen, Germany). Methanol was purchased from Merck Chemicals, Mumbai, India. Pluronic F68 (Poloxamer 188) was a gift sample from BASF, India. Double distilled water was used for the preparation of the nanoemulsions and other aqueous solutions.

5.2 Equipments:

1. High speed magnetic stirrer (Remi, MS500, Remi equipments, Mumbai)

2. High Speed Centrifuge (Sigma 3K30, Germany)

3. Particle Size Analyzer (Zetasizer Nano series, Malvern Instruments, UK)

4. UV-VIS spectrophotometer (Shimadzu, Japan)

5. Ultra-turrax (IKA Werke, Germany)

6. High Pressure Homogenizer (Emulsiflex C5, Avestin, Canada).

7. Probe Sonicator (LABSONIC®M, Sartorius Ltd, Mumbai, India)

8. Digital pH meter (Lab India, Ltd, Mumbai, India)

9. Analytical weighing balance (Shimadzu, Switzerland)

10. Isothermal shaker (VORCO, York Scientific Industries, Delhi, India)

5.3 Methods

5.3.1 Determination of solubility of Simvastatin in different oils

Simvastatin was added into the selected oils and vortexing was done for 2 min, and then the mixture was shaken for 48 hrs on mechanical stirrer to achieve equilibrium. The mixture was then centrifuged at 25000 rpm for 10 min to separate the undissolved Simvastatin drug and the supernatant of the oil solution was withdrawn and after appropriate dilution with methanol, the absorbance was measured against respective blank by UV visible spectrophotometer (UV Shimadzu 1700) at 238nm. The concentration of Simvastatin was calculated from the calibration curve.

5.3.2 Preparation of nanoemulsion by ultrasonication

The nanoemulsion formulation of Simvastatin was prepared as per reported method (Kentish et al, 2008) with slight modification (Both phases were heated to 70°C in this method). For preparation of oil phase, the required quantity (2 %w/v) of lipophilic surfactant (Phospholipon 90) and Simvastatin (0.8% w/v) were dissolved in selected oil i.e. Capryol 90 (15% v/v) with stirring. The aqueous phase contained hydrophilic surfactant (Pluronic F68 1%) in required quantity of distilled water (85%). Both phases were heated to 70°C and then oil phase was added to aqueous phase drop wise while premixing using Ultra-turrax at 9500 rpm. Premixing was done for 10 min (2 cycles of 5 min). The pre-emulsion obtained was then ultra-sonicated for 9 min (3 cycles of 3 min) at 80% amplitude and 0.6 duty cycles. The obtained nanoemulsion was transferred to clean glass vial, packed and used for further evaluation. The process and formulation parameters were optimized by factorial design.

5.3.2.1 Optimization of process parameters

High speed mixing and sonication time

All batches were prepared using oil (Capryol 90), which showed maximum solubility of the drug. Unless otherwise stated, the emulsion composition for preliminary optimization was 20% v/v oil (Capryol 90), 1% w/v Pluronic F68, 1% w/v soya PC (phospholipon 90G) and water 80% v/v which were selected based on available literature on nanoemulsion preparation.

Firstly, the effect of high speed mixing (by Ultra-turrax) on globule size of the pre-emulsion was studied. In this experiment, the globule size obtained with different speed (9500 and 11500) and time (1, 3, 5, 10 and 15 min) was recorded. The readings were recorded in triplicate.

Thereafter, the effect of sonication time on globule size was recorded. Emulsification was performed using probe sonicator (LABSONIC®M). Probe tip was immersed 2/3rd into pre-emulsion. Sonication was done at 100W, (i.e. 80 amplitude, 0.6 cycle/second). Pre-emulsion (20 ml) was subjected to sonication for total of 18 minutes, with each sonication

cycle lasting for 3 minutes and gap of 3 minutes between 2 sonication cycles. At each cycle, the globule size and PDI were determined. The readings were recorded in triplicate.

Selection of surfactants

After selection of mixing speed, time and sonication time, formulation parameters were optimized. Selection of non-ionic surfactant was carried out based on stability of emulsion observed over period of 15 days. Two nonionic surfactants commonly used for preparation of nanoemulsion i.e. Tween 80 and Pluronic F68 were tried at different at 3-7% and 1-3% concentration respectively.

After selection of hydrophilic surfactant, lipophilic surfactant was selected. In this study, two commonly used lipophilic surfactants i.e. soya PC (Phospholipin90) and Egg PC were tried at different concentrations. Visual observations were made to identify change in appearance/phase separation and lipophilic surfactant which provided most stable nanoemulsion was selected for further studies.

5.3.2.2 Factorial Design and Optimization

Based on preliminary experiments, percentages of oil phase (X_1) and ratio of Phospholipin90: Pluronic F68 (X_2), were found to be the major factors affecting the particle size, polydispersity Index (PI). Hence, 3^2 factorial design was applied to obtain minimum particle size, minimum PI and maximum stability. The formulation parameters for factorial design are given in Table 1. In developing the regression equations, the test factors were coded according to

$$X_i = \left(X_i - X_i^{X} \right) / \Delta X_i \quad \text{...................................... (5.1)}$$

Where, X_i is the coded value of the ith independent variable, X_i is the natural value of the ith independent variable, X_i^x is the natural value of the ith independent variable at the center point and ΔX_i is the step change value. According to quadratic model, multiple regressions was carried out using

$$Y = b_0 + \sum_i b_i X_i + \sum_i \sum_y b_{ij} X_i X_j + \sum b_{ii} X_i^2 \quad \text{............................... (5.2)}$$

Where, Y is the measured response, b_0 is the intercept, b_i, b_{ij}, and b_{ii} are the measures of the variables X_i, X_iX_j, and X_i^2 respectively. The variable X_iX_j represents the first-order interactions between X_i and X_j ($i<j$) (Huang et al. 2005). The multiple regression was applied using Microsoft excel in order to deduce the factors having significant effect on the formulation properties, and the best fitting mathematical model was selected (Akhnazarova and Kafarov 1982). Three-dimensional response surface plots and two-dimensional contour plots resulting from equations were obtained by the NCSS software.

Table 5.1: Coded Values of the formulation parameters of Simvastatin Nanoemulsions

Coded Values	Actual values	
	X1	X2
-1	10 % v/v	1:1
0	15 % v/v	1:2
1	20 % v/v	2:1
	X_1—Oil concentration	
	X_2—Ratio of Phospholipon90G: Pluronic F68	

5.4 Characterization of Simvastatin nanoemulsion

Particle size:

Particle size analysis was performed by photon correlation spectroscopy (PCS) with Zetasizer (NanoZS, Malvern Instruments, UK). Photon correlation spectroscopy yields mean particle size and polydispersity Index (PI). PDI represents the width and particle size distribution of the sample. The particle size analysis was determined using after dilution. Approximately 100µl of sample was diluted to 10 ml with deionized water. The particle size and PDI values obtained by averaging results 10-20 measurement cycles at an angle of 90° at 25° C in 10 mm diameter disposable cell. During the measurement, average particle count rate was maintained between 50 and 500 kcps (Meyer et al., 2006).All the samples

were diluted with double distilled water before measurement to obtain sufficient light scattering.

Measurement of surface charge

Surface charge (Zeta potential) was measured using Zetasizer (NanoZS, Malvern Instruments, UK). The measurements were performed after above described dilution with deionized water. The Zeta potential values were determined from the electrophoretic mobility of the oil globules using the Helmholtz–Smoluchowsky equation. The measurements were repeated three times at 25 °C with field strength of 20 V/cm.

Morphological examination by Transmission Electron Microscope (TEM)

By using TEM, the morphology of the oil globules in nanoemulsion was visualized. A drop of the nanoemulsion was placed on a piece of parafilm after 10-fold dilution in distilled water. A carbon coated grid was placed on top of the drop and left for 1 min. With filter paper excess fluid was removed. If necessary, negative staining was then performed by placing the grid on a drop of 2% phosphotungsten acid (PTA) for 1 min. The grid was examined under a transmission electron microscope (model JEM-100S, Joel, Tokyo, Japan) at an accelerated voltage of 20 kV.

Drug content, pH

Encapsulation efficiency was expressed as a percentage of Simvastatin found in nanoemulsion to the theoretical quantity of the drug added. Drug content was determined after suitable dilution with methanol by UV spectrophotometer at 234 nm. The pH of the nanoemulsions was measured using a pH meter (PICO +, Lab India).

Viscosity Measurement

The rheological measurements were performed using Ostwald Viscometer. Approximately, 15-20ml of nanoemulsion was poured into the filling tube and transferred to capillary tube by gentle suction. The time required for the nanoemulsion to flow from upper mark to lower mark of the capillary tube was recorded. The values for reference liquid i.e. water was also recorded and then from the densities and time reading, the viscosity of the nanoemulsion was calculated.

In vitro Release

A dialysis membrane having pore size 2.4nm (molecular weight cut-off between 12,000 Da) was used for in vitro release studies. The membrane was activated as per reported procedure and soaked in distilled water overnight before using for in vitro release studies. 1 ml of nanoemulsion was placed in dialysis bag and then the bag packed at both end was placed in beaker containing 40 ml of receptor medium (pH 7.2 phosphate buffer) maintained at 37 °C. Samples were collected at predetermined time intervals and an equal volume of media was added each time after sampling to maintain constant volume in the recipient compartment. The amount of drug in the samples was measured at absorption maximum of 238 nm using UV spectrophotometer (UV, Shimadzu 1700).

Stability

The stability of nanoemulsion was monitored in terms of drug content and particle size over 3 months at 2-8 and 25 °C. The nanoemulsion was diluted with distilled water to avoid multiple scattering and evaluated for particle size distribution using the Zetasizer, (NanoZS, Malvern Instruments, UK) after 1h. Also visual observations for creaming, cracking or phase separation were noted. The stability at high speed centrifugation at various speeds starting from 2000 up to 10,000 rpm for 10 min was carried out.

5.5 Results and discussion:

5.5.1 Solubility of Simvastatin in oils

The solubility of Simvastatin in different was oils was determined using UV method and using following calibration curve, y= 0.0577x+ 0.0028 (r^2 = 0.9994). Fig. 5.1 represents solubility of Simvastatin in different oils. Capryol 90 exhibited highest solubility of Simvastatin as compared to other oils and hence it was selected for preparation of nanoemulsion.
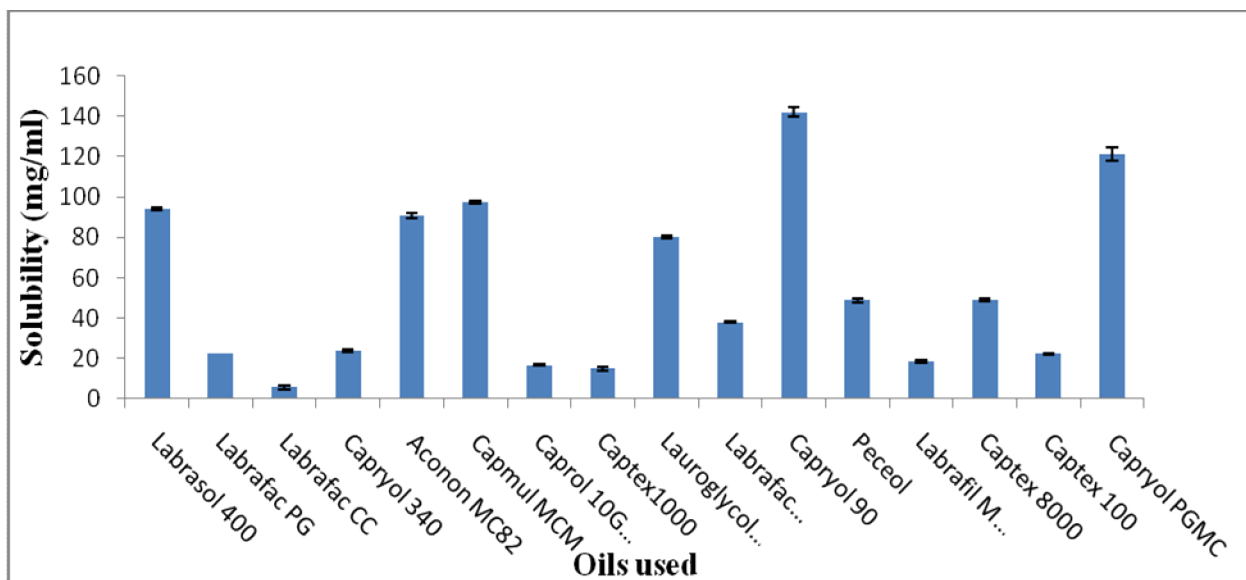
Fig. 5.1: Solubility of Simvastatin in different oils.

5.5.2 Optimization of Parameters

High speed mixing and sonication time:

The effect of high speed mixing at two different speeds (9500 rpm and 11500 rpm) on globule size of the pre-emulsion was studied and results are recorded in Table 5.2. After 1 min of high speed mixing, nanoemulsion with globule size about 700 nm was obtained. The polydispersity index (PI) was also very high after high speed mixing indicating non-uniform distribution in both cases. There was no significant difference in globule size at these two speeds at 1 and 3min of high speed mixing. Thus, further processing time was increased. After 10 min of high speed mixing globule size of 364.5±12.0 and PDI of 0.482 was obtained. Further increase in mixing time did not result in significant reduction in globule size. Thus, 10 min high speed mixing at 9500 rpm was considered suitable for obtaining pre-emulsion with globule size in nanometer range. The pre-emulsion samples were stored at room temperature to study its stability. But after 1 week, slight phase separation occurred, which indicated that high speed mixing was not sufficient to obtain nanoemulsion with sufficient stability. Hence combination of high speed mixing and sonication were tried.

After finalizing the high speed mixing speed and time, the effect of sonication was studied and the results are recorded in Table 5.3. Firstly, sonication was carried out at different

amplitude (sonication power) and the globule size and PDI were recorded. The globule size of nanoemulsion passed through a minimum size at an intermediate power application and then increased at higher power levels. This effect is described as "over-processing" which is caused by increase in emulsion globule coalescence at higher shear rates. The minimum globule size and PDI was obtained at 80% amplitude. Hence, it was considered suitable to obtain nanoemulsion with suitable globule size.

Table 5.2 Effect of high speed mixing on globule size of pre-emulsion

Sr. No.	Parameter	Globule size	PDI
1	1 min (9500 rpm)	751.4±34.2	0.678
2	1 min (11500 rpm)	721.0±40.6	0.718
3	3 min (9500 rpm)	536.0±24.2	0.593
4	3 min (11500 rpm)	528.0±28.8	0.599
5	5 min (9500 rpm)	521.8±16.6	0.532
6	10 min (9500 rpm)	364.5±12.0	0.482
7	15 min(9500 rpm)	351.4±14.2	0.508

Table 5.3 Effect of sonication on globule size of nanoemulsion

Sr. No.	Parameter*#	Globule size	PDI
1	3 min (40 % amp)	176.4±1.2	0.213
2	3 min (60 % amp)	184.1±1.6	0.248
3	3 min (80 % amp)	168.8±2.2	0.143
4	3 min (100 % amp)	172.6±4.9	0.155
5	6 min (80 % amp)	152.8±1.6	0.139
6	9 min (80 % amp)	153.8±1.0	0.126
7	12 min (80 % amp)	155.9±4.2	0.108
8	15 min (80 % amp)	157.4±3.7	0.138
9	18 min (80 % amp)	219.4±15.8	0.251

* High speed mixing was done at 9500 rpm for 10 min before sonication

duty cycle 0.6 sec

Further, the effect of increase in sonication time at 80% amplitude was studied and it was observed that the globule size of the nanoemulsion decreased with sonication time upto 9 min and thereafter negligible reduction in globule size was obtained. At 9 min sonication time, minimum globule size (153.8±1.0) with low PDI (0.126) was obtained and hence, it was considered as optimum condition to obtain nanoemulsion with uniform distribution.

Selection of surfactants

After selection of mixing speed and sonication parameters, formulation parameters were optimized. Selection of surfactant was carried out based on stability of emulsion observed over period of 10 days. Two nonionic surfactants commonly used for preparation of nanoemulsion i.e. Tween 80 and Pluronic F68 were tried at 1 to 3% and 3 to 7% concentration respectively. The results obtained from these studies are recorded in the Table 5.4.

Table 5.4 Selection of non-ionic surfactant for Simvastatin nanoemulsion

Surfactant	Concentration (%w/v)	Day 1	Day 5	Day 10
Pluronic F68	1%	Milky & stable	Milky & stable	Milky & stable
	2%	Milky & stable	Milky & stable	Milky & stable
	3%	Milky & stable	Milky & stable	Milky & stable
Tween 80	3%	Milky & stable	Phase Separation	–
	5%	Milky & stable	Milky & stable	Phase Separation
	7%	Milky & stable	Milky & stable	Phase Separation

From these results, it was clear that Tween 80 as a nonionic surfactant could not produce stable nanoemulsion. However, with Pluronic F68 at all the concentration stable nanoemulsion was obtained. Hence, Pluronic F68 was selected as hydrophilic surfactant for further studies.

Two lipophilic surfactants commonly used for preparation of nanoemulsion i.e. Soya PC and Egg PC were tried at 1 to 2% concentration. The results obtained from these studies are recorded in the Table 5.5.

Table 5.5 Selection of lipophilic surfactants for Simvastatin nanoemulsion

Surfactant	Concentration (%w/v)	Day 1	Day 5	Day 10
Soya PC	1%	Milky & stable	Milky & stable	Milky & stable
	2%	Milky & stable	Milky & stable	Milky & stable
Egg PC	1%	Milky & stable	Phase Separation	–
	2%	Milky & stable	Phase Separation	-

Phase separation was observed in case of egg PC at day 5 at both concentrations and the nanoemulsion obtained with soya PC was stable at the end of 10 days. Hence, soya PC was used as lipophilic surfactant for further studies.

5.5.3 Optimization by Factorial design:

Nine formulations were prepared as per 3^2 Factorial Design. Table 5.6 enlists the response parameters of all the nine formulations.

Effect of formulation variables on the response parameters:

On analyzing the data of the formulations prepared as per 3^2 Factorial design using Design Expert® 8.0.5.2 software, various polynomial equations, response surface and contour plots were generated. The information obtained from the software is discussed in the following sections, depicting the effects of variables on the respective response parameters [Initial globule size-Day 0 (Y_1) and globule size at 15 days (Y_2)].

Table 5.6 Response parameters for Simvastatin nanoemulsion prepared as per 3^2 factorial design.

Formulation code	Factors		Globule Size – Day 0 (nm) [Y_1]	Globule Size – Day 15 (nm) [Y_2]
	Oil percentage – X_1 (% v/v)	Ratio of PL90G: P188 - X_2		
NE1 (-1,-1)	10	1:1	131	88.1
NE2 (-1,0)	10	1:2	124.6	80.8
NE3 (-1,1)	10	2:1	117.5	93.2
NE4 (0, -1)	15	1:1	142	127.4
NE5 (0, 0)	15	1:2	117.3	112.2
NE6 (0,1)	15	2:1	132	128.7
NE7 (1,-1)	20	1:1	164.5	194.2
NE8 (1, 0)	20	1:2	154.4	187.6
NE9 (1, 1)	20	2:1	143.5	211.2

Table 5.7   Observed and Predicted values of response parameters for Simvastatin nanoemulsion

| Batch | Response parameters | | | | | |
| | Y_1 | | | Y_2 | | |
	Observed	Predicted	%RE	Observed	Predicted	%RE
NE1	131.0	132.0	0.75	88.1	90.98	3.16
NE2	124.6	120.2	3.66	80.8	78.3	3.19
NE3	117.5	120.9	2.81	93.2	92.8	0.43
NE4	142.0	140.0	1.42	127.4	123.4	3.24
NE5	117.3	126.2	7.05	112.2	113.7	1.32
NE6	132.0	125.1	5.51	128.7	131.2	1.90
NE7	164.5	165.5	0.60	194.2	195.3	0.56
NE8	154.4	149.9	3.00	187.6	188.6	0.53
NE9	143.5	146.9	2.31	211.2	209.1	1.00

% RE= % Relative Error

CALCULATED % RE = OBSERVED (ACTUAL) – PREDICTED / PREDICTED * 100

Globule size - Day 0:

The polynomial equation and regression coefficient for Y_1 (Globule size - Day 0) are as follows:

$Y1 = 136.31 + 14.88 X_1 - 7.41 X_2$ 5.3

R-Squared =   0.7881

The linear model (Eq 5.3) was found to be significant with an F value of 11.16 (p< 0.05). The value of correlation coefficient (R^2) was found to be 0.7881 which indicates that the model was significant. Value of probability was less than 0.05 which indicated that model term X_1 is significant. Positive values of X_1 and negative values of X_2 in Eq.5.3 indicate

synergetic effect of X_1 on Y_1 of Simvastatin Nanoemulsion i.e. any increase in X_1 resulted in increase in value of Y_1. Negative values of X_2 in Eq.5.1 indicate antagonistic effect of X_2 on Y_1 of Simvastatin Nanoemulsion i.e. any increase in X_2 resulted in reduction in value of Y_1. Effect of X_1 was found to be higher than the effect of X_2 on Y_1.

The combined effect of factors X_1 and X_2 can further be elucidated with the help of response surface and contour plots [Fig. 5.2(a) and 5.2(b) respectively] which demonstrated that Y_1 varies in reverse fashion with X_2 while it increases with X_1. Increase in X_1 resulted in corresponding increase in globule size of nanoemulsion. Thus, oil percentage plays a major role in determining globule size of the nanoemulsion. At low (-1) level of X_1 (oil percentage), decrease in globule size with increase in X_2 (ratio of PL90:P188) was observed, indicating suitability of 2:1 ratio of PL90:P188 for obtaining minimum particle size. At low (-1) level of X_2 higher globule size was observed at all three level of X_1 while at high (1) level of X_2 the particle size was comparatively low. The effect of X_1 seemed to be more pronounced than that of X_2. The predicted and observed values of response parameters are shown in Table 5.7. Low values of the relative error showed that there was a reasonable agreement of predicted values and experimental values.
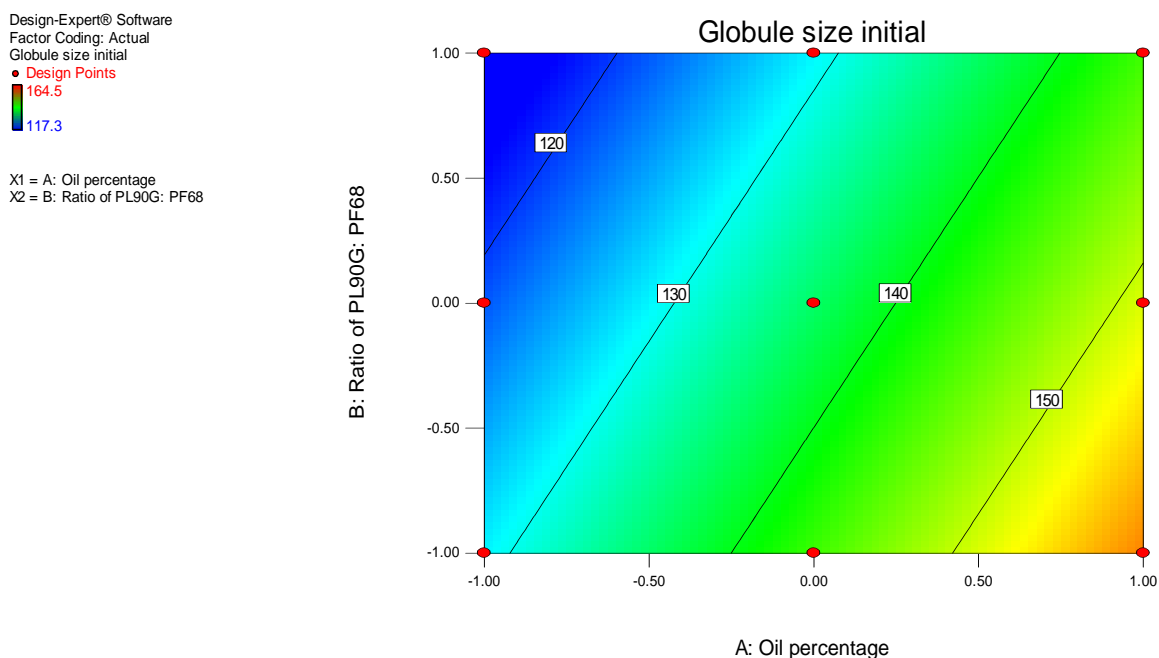
Fig. 5.2(a). Contour plot showing the effect of oil concentration and ratio of surfactants on Globule size of Simvastatin nanoemulsion - Day 0.
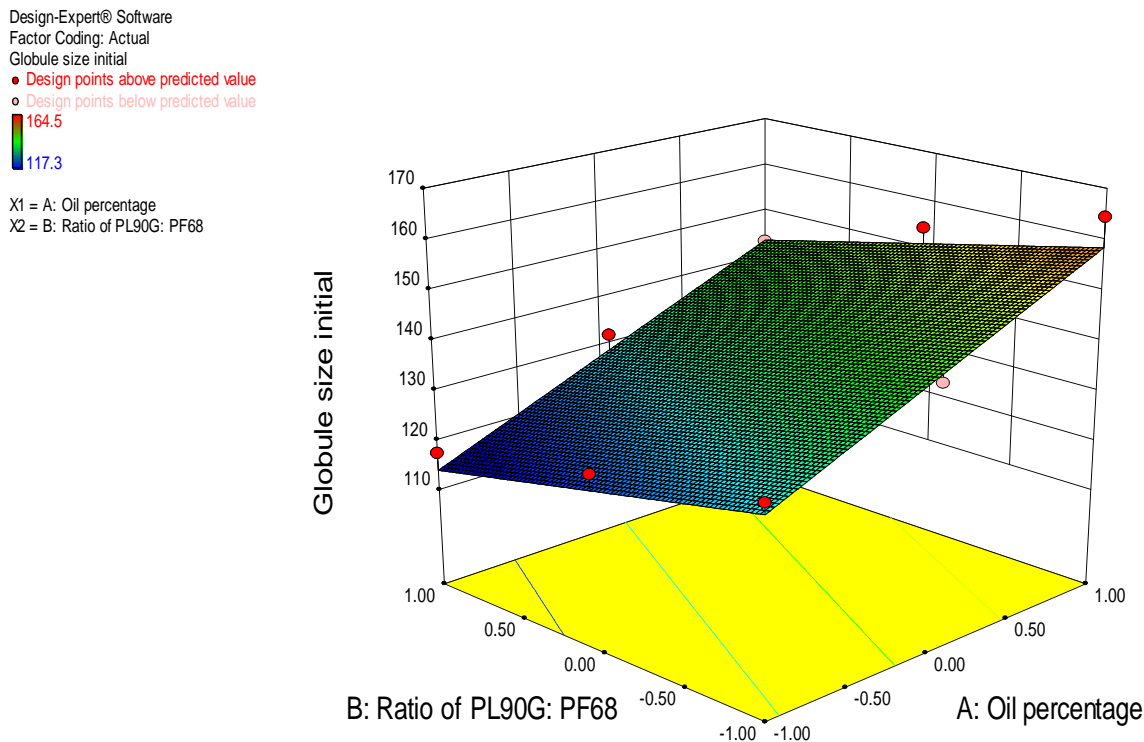
Fig. 5.2 (b). Response surface plot showing the effect of oil concentration and ratio of surfactants on globule size of Simvastatin nanoemulsion on Day 0

Globule size - Day 15 (Y$_2$):

The quadratic model for Y$_2$ was found to be significant (p=0.0075) with an F value of 37.55. Thus, model becomes:

Y$_2$ = 113.70 +55.15 X$_1$ + 3.90 X$_2$ +2.97 X$_1$ X$_2$ + 19.75 X$_1{}^2$ + 13.60 X$_2{}^2$ .... (5.4)

R^2 =0.9977

The value of correlation coefficient (R^2) was found to be 0.9977 which indicates that the model was significant (Table 5.8). Values of probability below 0.05 were obatined for X$_1$, X$_1{}^2$, and X^{22} which indicates that these model terms are significant. Value of probability less than 0.05 indicate model terms are significant.

The values of Predicted Residual Sum of Squares (PRESS) for the quadratic model was 535.98 and indicated suitability of the model. The PRESS value indicates how well the model fits the data, and for the chosen model it should be small relative to the other models under consideration.

Positive values of X_1 and X_2 in Eq.5.4 indicated synergetic effect on globule size – Day 15 (Y_2). According to Eq. 5.4, there is significant difference in value of X_1 (55.15) and X_2 (3.90) which indicated that effect of concentration of oil (X_1) on globule size - Day 15 was more pronounced than ratio of surfactants.

Response surface and contour plots for effect of X_1 and X_2 on Y_2 are shown in Fig. 5.3(a) and Fig. 5.3(b). At low level of X_1, slight difference in globule size was observed with change in X_2 (surfactant ratio). However, at all the levels of X_2, there was significant increase in globule size observed with increase in X_1. Thus, the effect of X_1 was more pronounced than that of X_2. At high level of X_1, higher globule size was observed with all levels of X_2.
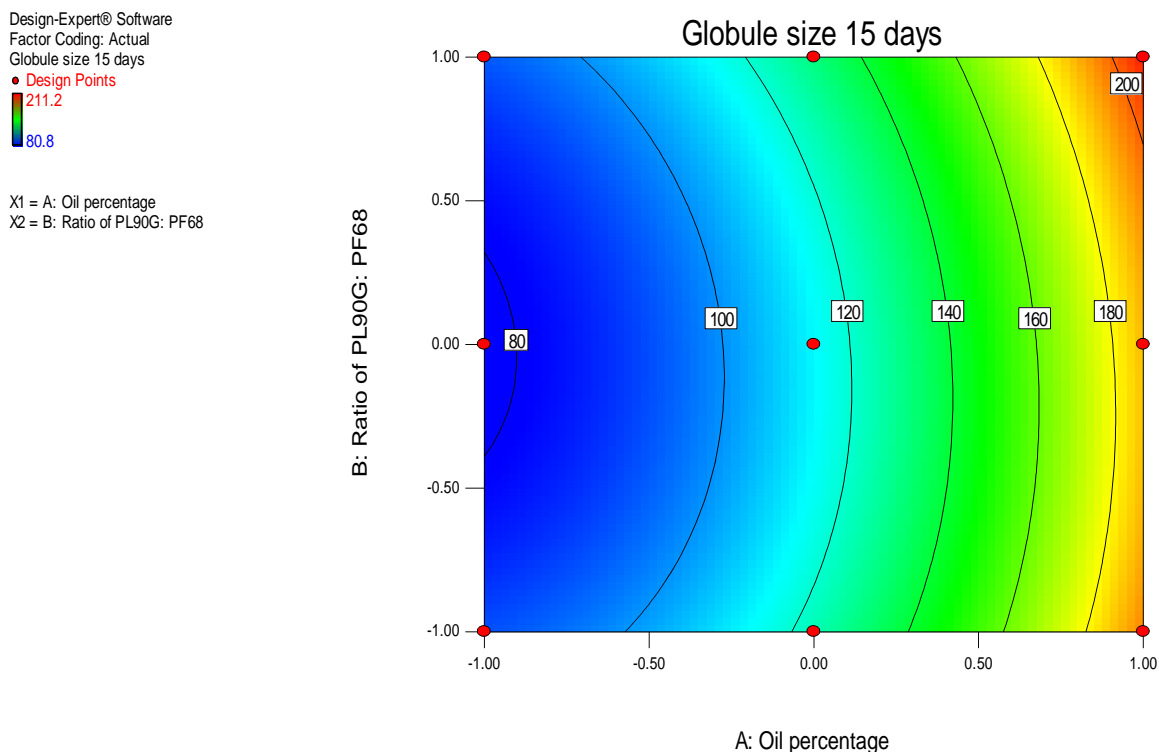
Fig. 5.3(a). Contour plot showing the effect of oil concentration and ratio of surfactants on Globule size of Simvastatin nanoemulsion - Day 15.

Design-Expert® Software
Factor Coding: Actual
Globule size 15 days
● Design points above predicted value
○ Design points below predicted value
211.2

80.8

X1 = A: Oil percentage
X2 = B: Ratio of PL90G: PF68
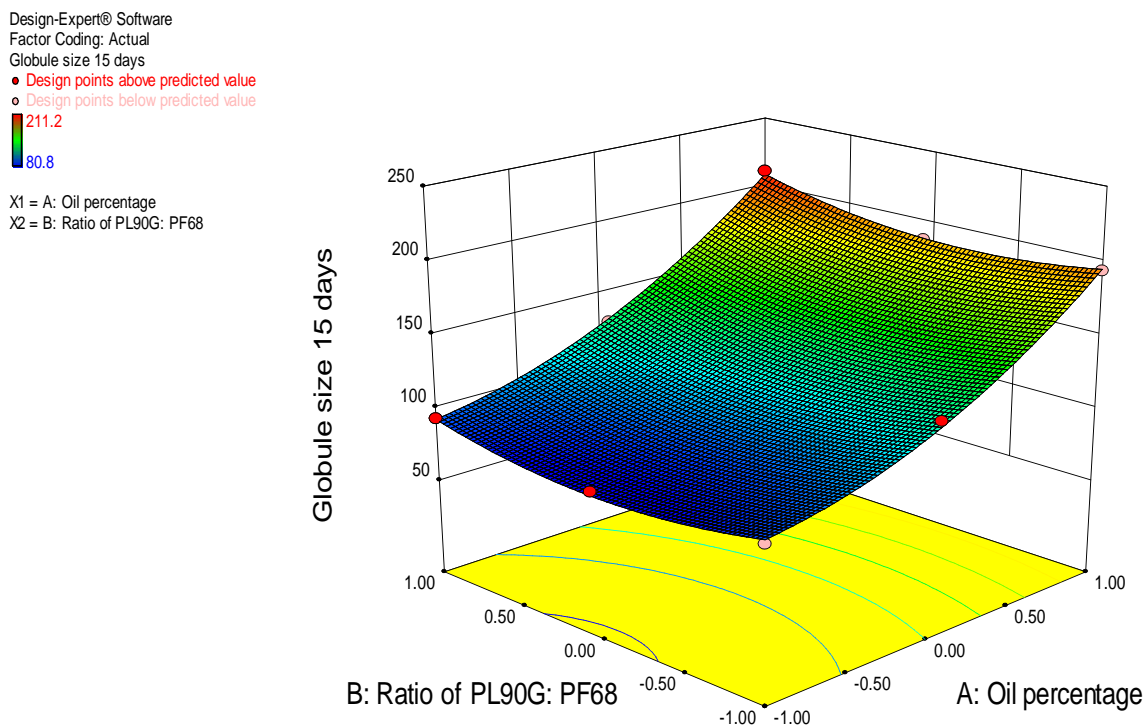
Fig. 5.3(b). Response surface plot showing the influence of oil concentration and ratio of surfactants on globule size of Simvastatin nanoemulsion on Day 15

Table 5.8.   Multiple Regression Output for Dependent Variables for Simvastatin nanoemulsion

	Coefficient of regression parameters							
Parameters	b_0	b_1	b_2	b_3	b_4	b_5	r^2	P
Globule size - Day 0	136.31	14.88	-7.42	--	--	--	0.7881	0.0095
Globule size - Day 15	113.7	55.15	3.9	2.9	19.75	13.6	0.9977	0.0004

Table 5.9.   Results of Analysis of Variance (ANOVA) for measured responses for Simvastatin nanoemulsion

Parameters	df	SS	MS	F	Significance F
Globule size – Day 0 (Y_1)					
Model	2	1659.12	829.56	11.16	0.0095
Residual	6	445.97	74.33	--	--
Total	8	2105.09	--	--	--
Globule size – Day 15 (Y_2)					
Model	5	19525.84	3905.17	255.03	0.0004
Residual	3	45.94	15.31	--	--
Total	8	19571.78	--	--	--

Optimum Formulation:

A numerical optimization technique by the desirability approach was used to generate the optimum settings for the formulation. The process was optimized for the dependent (response) variables Y_1–Y_2 and the optimized formula was arrived by keeping the globule size – Day 0 in range of 100 to 150 nm. Another dependant variable globule size – Day 15 was kept at minimum level. Formulation (NE6) fulfilled all the criteria set from desirability search indicated by desirability obtained from design expert software (Narendra et al, 2005).

New optimized formulation (Table 5.10) was prepared according to the predicted model and evaluated for the responses (Y_1, and Y_2) to evaluate reliability of the response surface model. The result in Table 5.11 illustrates a good relationship between the experimental and predicted values, which confirms the practicability and validity of the model. The predicted error of all the response variables was below 6 % indicating that the Response Surface Methodology (RSM) optimization technique was appropriate for optimizing Simvastatin nanoemulsion.

Table 5.10: Optimized Simvastatin Nanoemulsion

Parameters	Value
Capryol 90 (oil)	15 % v/v
Phospholipon 90 (Lipophilic surfactant)	2 % w/v
Pluronic F68 (Hydrophilic surfactant)	1 % w/v
Drug concentration	1.8 % w/v
Distilled water	85 % v/v

Table 5.11.   The predicted and observed response variables of the optimal Simvastatin Nanoemulsion

	Y_1 (nm)	Y_2 (nm)
Predicted	132.0	128.7
Observed	125.1 ± 1.6	131.2 ±11
Predicted Error (%)	5.22	1.94

Predicted Error (%) = (Observed value – Predicted value)/ Predicted value x 100%

5.5.4 Characterization of optimized formulation:

Particle size and surface charge: The results of globule size and zeta potential measurements of nanoemulsions are shown in Fig. 5.4. There was no significant difference in globule size in drug loaded (132±9nm) and blank nanoemulsion (130±8nm). The polydispersity index (PI) of both formulations was very low (below 0.2) and this unimodal distribution indicates uniformity in globule size. Zeta potential is an important parameter to which determine the stability of the nanoemulsion. Emulsifiers can stabilize oil globules due to not only the formation of a mechanical barrier but also the production of an electrical barrier on the emulsion surface. This surface charge is zeta potential. Higher zeta potential value means more resistance to coalescence of the globules. Nanoemulsion can either be stabilized by steric, electrostatic mechanism or by combination of these two. Nanoformulations with zeta potential of 30 mV are considered stable if stabilized by single mechanism and zeta potential of 20 mV for combination of these two mechanisms (Muller and Jacobs; 2002).
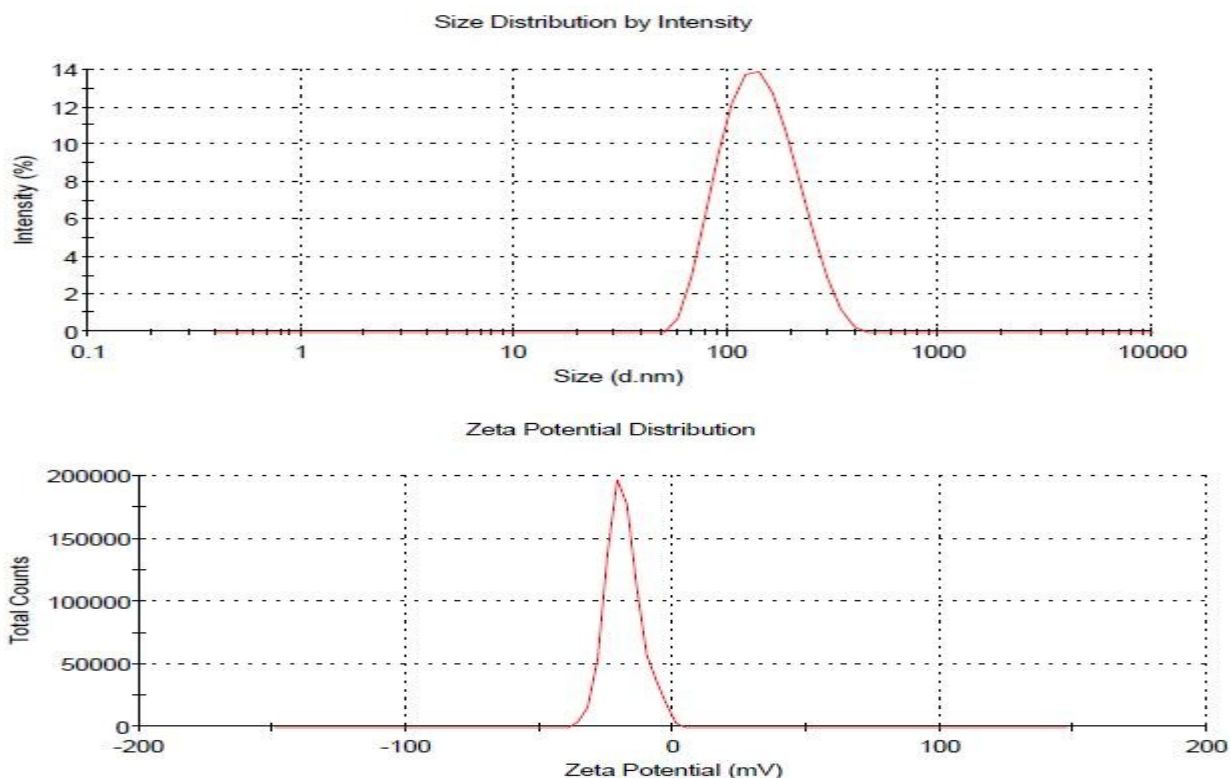
Fig. 5.4. Globule Size and zeta potential of nanoemulsion

Lecithin-stabilized nanoemulsions are charge-stabilized while nanoemulsions stabilized by block copolymers, such as poloxamers, are sterically stabilized. As the zeta potential of the prepared formulation was found to be -19±1.2 mV, it could impart stability to prepared nanoemulsion by combination of electrostatic and steric mechanism.

Morphological examination by Transmission Electron Microscope (TEM)

TEM analysis is important in order to study morphology of the oil globules in the nanoemulsion formulations and to visualize any precipitation of the drug upon addition of the aqueous phase. Morphology and globule size of the prepared nanoemulsion was evaluated by TEM. As observed in the TEM image, the globules were spherical, possessed diameter ranging from 120-180 nm and had smooth surface (Fig.5.5). The globules were segregated and globule size observed in the TEM image was in accordance with result obtained by DLS.
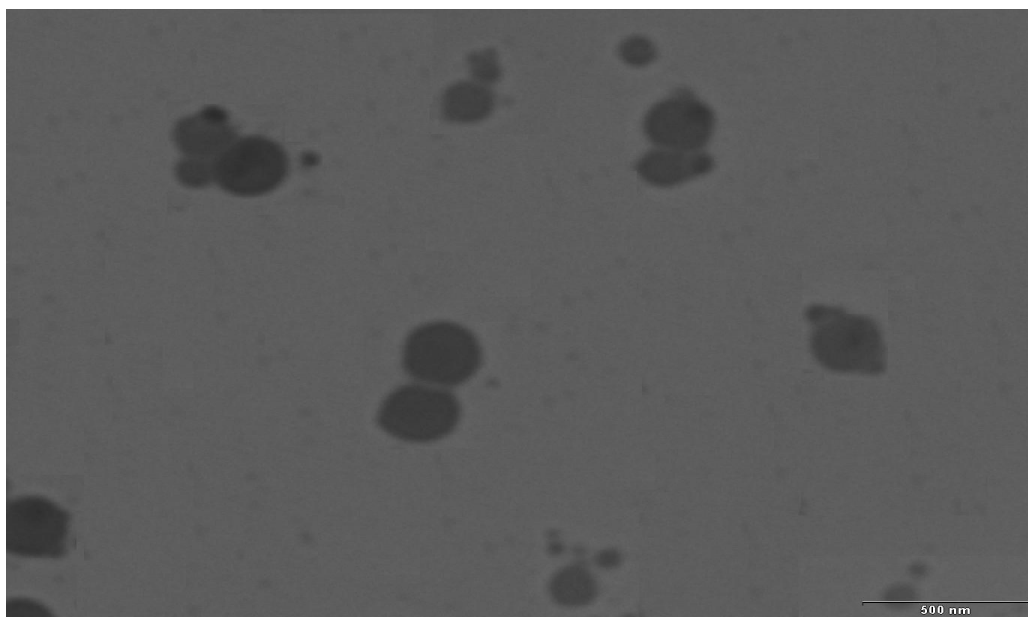
Fig. 5.5: Transmission electron microscope (TEM) image of nanoemulsion

Drug content, pH and Viscosity

Important properties of nanoemulsion such as drug content, pH and viscosity were studied as per reported methods to evaluate physicochemical properties of the system. The drug content was found to be 98±1.2 %. The pH of the nanoemulsions was found to be 4.8±0.2 which was suitable for oral administration. One of the characteristics of nanoemulsion

formulations is low viscosity (Lawrence & Rees, 2000). The viscosity of the nanoemulsion was found to be low (2.020±0.01 cp), indicating suitability for oral administration.

In vitro Release

The in vitro release profiles of Simvastatin nanoemulsion and plain drug suspension are given in Fig. 5.6. The in vitro release studies showed significant increase in drug release as compared to plain drug suspension. Plain drug suspension (PD) showed only 12.35±0.44% drug release in 2 hr while nanoemulsion (NE) showed 22.37±0.92% drug release which was approximately double. At the end of 8 hr, plain drug suspension showed only 16.69±0.95% drug release while nanoemulsion formulation showed 33.81±0.98% drug release. This could be attributed to enhanced solubility and dissolution rate of Simvastatin which in turn can be due to low globule size and surface properties of the nanoemulsion. The potential of nanoemulsion in enhancing in vitro release thereby improving bioavailability was reported in some studies (Qhattal et al 2011; Chang et al 2011).
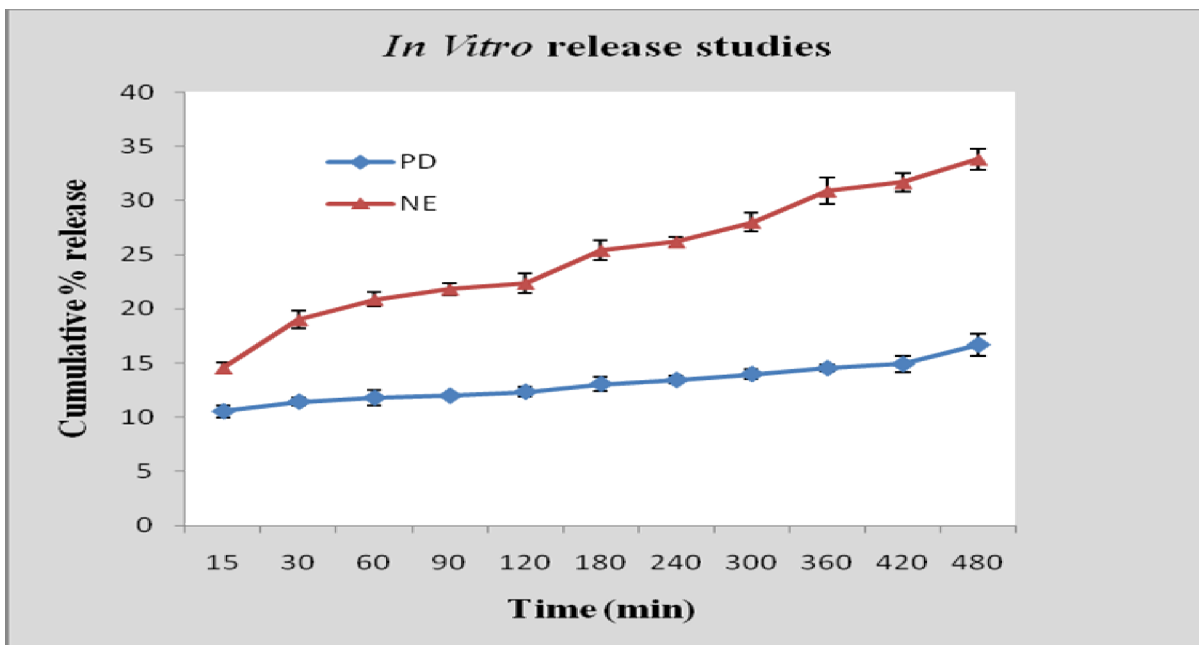
Fig. 5.6: In vitro release studies of nanoemulsion (NE) and plain drug suspension (PD)

The release profiles were then fitted into different exponential equations such as Zero order, First order, Higuchi, and Korsmeyer- Peppas to characterize the release. It was found that drug release from SNE follows Korsmeyer- Peppas (r^2=0.9387) more than Higuchi (r^2=0.9155), Hixson-Crowell (0.8535), Zero order (r^2=0.8434) and First order (r^2=0.8698). Release from Plain drug was found to follow Korsmeyer-Peppas (r^2=0.9579) more than

First order (r^2=0.9453), Zero order (r^2=0.9142), Hixson-Crowell (0.9158) and Higuchi (r^2=0.9540) model. Value of 'n' indicates that PD, SNE formulation followed fickian diffusion as the release component values were below 0.5 (Costa P et al .2001).

Stability

The stability of nanoemulsions in terms of drug content and particle size distribution was monitored for 3 months at 2-8 °C and RT (25-30 °C). The nanoemulsion formulation showed physical stability for the period of 3 months at both conditions in terms of drug content and globule size. The particle size and drug content of the nanoemulsion at different time intervals is given in Table 5.12. It was found that no significant difference was observed in the globule size of nanoemulsion after 3 months at both conditions indicating its suitability for storage at both conditions.

Table 5.12: Stability of nanoemulsion at RT and cold conditions (2-8°C)

Sr. No	Time	Drug content (%) (2-8 °C)	Drug content (%) (RT)	Globule size (nm) (2-8 °C)	Globule size (nm) (RT)
1	Initial	99.8±1.2	99.8±1.2	132±9	132±9
2	1 month	99.6±1.8	99.6±1.8	143±11	147±12
3	2 months	99.2±1.0	99.2±1.0	144±14	152±9
4	3 months	98.8±1.4	98.8±1.4	146±13	153±14

Another parameter which determines the stability of the nanoemulsion is its viscosity. It was established that increasing the viscosity of the emulsions leads to an increase in droplet diameter (Fang et al; 2009). There was no change in viscosity of the prepared Simvastatin nanoemulsion for 3 months, showing its stability. The emulsion was found to be stable without any incidence of creaming, cracking or phase separation upon undisturbed standing and could withstand high speed centrifugation from 2000 rpm to 10000 rpm. Thus, nanoemulsion formulation possessed good physicochemical stability and was suitable for storage at RT.

5.6 References:

- Akhnazarova A, Kafarov V. Experiment Optimization in Chemistry and Chemical Engineering, Mir publications, Moscow, 1982. pp. 18–94.

- Chang LC, Wu CL, Liu CW, Chuo WH, Li PC, Tsai TR. Preparation, characterization and cytotoxicity evaluation of tanshinone IIA nanoemulsions. J Biomed Nanotechnol. 7, 2011, 558-67.

- Costa P, Sousa Lobo JM. Modeling and comparison of dissolution profiles. Eur J Pharm Sci. 13, 2001, 123–33.

- Fang J, Hung C, Hua S, Hwang T. Acoustically active perfluorocarbon nanoemulsions as drug delivery carriers for camptothecin: Drug release and cytotoxicity against cancer cells. Ultrasonics 49, 2009, 39–46.

- Huang YB, Tsai YH, Lee SH, Chang JS, Wu PC. Optimization of pH independent release of nicardipine hydrochloride extended-release matrix tablets using response surface methodology. Int J Pharm. 289, 2005, 87–95.

- Kentish S, Wooster TJ, Ashokkumar M, Balachandran S, Mawson R, Simons L. The use of ultrasonics for nanoemulsion preparation. Inno Food Sci Emer Tech. 9, 2008, 170–175.

- Lawrence MJ, Rees GD. Microemulsion based media as a novel drug delivery system. Adv Drug Del Rev. 45, 2000, 89–121.

- Meyer S, Berrut S, Goodenough TIJ, Rajendram VS, Pinfield VJ, Povey MJW. A comparative study of ultrasound and laser light diffraction techniques for particle size determination in dairy beverages. Meas Sci Technol. 17, 2006, 289–297.

- Muller RH, Jacobs C. Buparvaquone mucoadhesive nanosuspension: preparation, optimization and long-term stability. Int J Pharm. 2002, 237, 151–161.

- Narendra C, Srinath MS, Prakash Rao B. Development of three layered buccal compact containing metoprolol tartarate by statistical optimization technique. Int J Pharm. 304, 2005, 102-114.

- Qhattal HSS, Wang S, Salihima T, Srivastava KS, Liu X. Nanoemulsions of cancer chemopreventive agent benzyl isothiocyanate display enhanced solubility, dissolution and permeability. J Agric Food Chem. In Press, DOI: 10.1021/jf202612b.

6.0 MATERIALS AND METHODS

6.1 Materials

Entacapone was obtained as gift sample from Alembic Pharmaceuticals Ltd, Vadodara, India. Zirconium oxide beads were obtained as gift sample from Lupin Pharmaceuticals Ltd, Pune, India. Pluronic F127 and Pluronic F68 were procured from Sigma Chemicals, Mumbai, India. Tween 80 (Polysorbate 80), disodium hydrogen phosphate and sodium hydroxide were purchased from S.D. Finechem., Mumbai, India. Polyvinyl pyrrolidone (PVP K30) was obtained from BASF, Mumbai, India. Hydroxypropyl methyl cellulose (HPMC K15 M) was obtained from Colorcon Ltd, Mumbai, India. Methanol, Dichloromethane, chloroform and acetone were purchased from Merck Ltd, Mumbai, India. Cellulose dialysis tubing (Molecular weight cut of 12000; pore size 0.4nm) and membrane filter of pore size 0.2 μm were purchased from Pall Corporation, Mumbai, India. Distilled water used in the study was filtered using 0.22-μm nylon filter (Nylon N66 membrane filters 47 mm, Rankem, India). All other chemicals and reagents used in this study were of analytical grade.

6.2 Equipments:

1. High speed magnetic stirrer (Remi, MS500, Remi equipments, Mumbai)

2. High Speed Centrifuge (Sigma 3K30, Germany)

3. Particle size Analyzer (Zetasizer Nano series, Malvern Instruments, UK)

4. UV-VIS spectrophotometer (Shimadzu, Japan)

5. Lyophilizer (Heto, Dry Winner, Denmark)

6. Differential Scanning Calorimeter. (Mettler Toledo DSC 822e, Japan)

7. Laser diffraction particle size analyzer (Malvern Mastersizer, 2000, UK)

8. Supercritical Particle former (SAS) (Thar Instruments, PA, USA)

9. Transmission Electron Microscope (Philips, Tecnai 20, Holland)

6.3 Preparation of nanosuspension by media milling

Media milling was carried out in a sealed glass vial containing starting suspension and milling beads (Eerdenbrugh et al. 2007). The starting suspension contained Entacapone (2.0% w/v) and the surfactant (Pluronic F127 -1%w/v) in distilled water as medium. Then magnetic bead and zirconium oxide beads (100%w/v) as milling media were incorporated

in glass vial and comminution was carried out on magnetic stirrer [Remi Equipment Pvt Ltd, India] at 500rpm for 12 hrs (Sigfridsson et al, 2007). This milling resulted in nanonization of Entacapone, producing Entacapone nanosuspension (ENS). This obtained nanosuspension was freeze dried for 24 hr using trehalose as cryoprotectant (at 1:3 ratio of total solid) using lyophilizer (Heto, Dry Winner, Denmark). Plain drug suspension was prepared by dispersing the plain drug powder and surfactant in water with respective concentration of drug and surfactant as that of nanosuspension.

6.3.1 Optimization of parameters:

Prior to the formulation step, the possible parameters influencing the formation of nanosuspension and size of nanosuspension were identified and optimized. The parameters studied were milling time, type of beads, drug concentration and suitable surfactant.

Milling time:

To study the effect of milling time on nanosuspension formation, milling was continued for 24 hrs. Samples were taken at different intervals and studied for particle size and PDI. The surfactant used for the study was Pluronic F127 at 1 %w/v concentration.

Composition of batch:

Entacapone	1 % w/v
Pluronic F 127	1.0 % v/v
Volume of beads	100% w/v
Distilled water	10 ml

Type of beads:

Zirconium oxide beads and glass beads were tried to evaluate effectiveness in particle size reduction. Then zirconium oxide beads of two different size ranges (i.e. small and large) were used for preparation of nanosuspension. Beads of small size range were in between 0.4 mm to 0.7 mm while large size ranges were between 1.2 mm to 1.5 mm. Pluronic F127 at 1% concentration was used in this study. Volume of beads was maintained at 100 % w/v while milling time was kept at 8 hrs.

Selection of surfactant:

The choice of a surfactant i.e. stabilizer is specific to each drug candidate and each formulation procedure. In order to stabilize the nanosuspensions, the stabilizer (or mixture of stabilizers) should exhibit sufficient affinity for the particle surface (Kocbek et al., 2006). Batches were prepared with different surfactants (Tween 80, Pluronic F127, polyvinyl pyrrolidone (PVP K30) and Pluronic F127: Tween 80). Zirconium oxide beads at 100% volume were used in this study and milling was carried out for 12 hr. Concentration of surfactant was kept at 1% w/v.

Selection of drug concentration:

Batches were prepared with different drug concentration (1%, 2% and 4%) to obtain desired particle size. Surfactant used in this study was Pluronic F127 at 2% concentration and zirconium oxide beads at 100% volume. Milling was continued for 12 hr and samples were taken and studied for particle size and PDI.

Optimization by Factorial designs:

For the preparation of ENS, process parameters were set as per preliminary optimization studies as described above. The optimization of parameters like volume of milling media and concentration of surfactant was carried out by factorial design. Effect of these parameters on mean particle diameter after milling was studied. A 3^2 randomized full factorial design was used in the study. In this design, two factors were evaluated, each at 3 levels, and experimental trials were performed at all 9 possible combinations with three replicates. The replicate experimental runs were carried out in complete randomized manner. The volume of milling media (X_1) and concentration of surfactant (X_2) were selected as independent variables. Mean particle diameter (Y) was chosen as dependent variable. A statistical model incorporating interactive and polynomial terms was used to evaluate the responses. The results of statistical analysis were tabulated. The response surface curves and contour plots were prepared to study the effects of independent variables. All the statistical operations were carried out using DESIGN EXPERT 8.0.5.2. Table 6.1 and Table 6.2 summarize experimental runs studied, their factor combinations, and the translation of the coded levels to the experimental units employed during the study.

Table 6.1. Factorial design parameters for Entacapone nanosuspension.

Factors	Levels used, Actual (coded)		
	Low (-1)	Medium (0)	High (+1)
X_1-Volume of Milling Media (%w/v)	60	80	100
X_2-Concentration of surfactant (%w/v)	0.5	1	2

Table 6.2. Formulation of the Entacapone nanosuspension utilizing 3^2 factorial design (Coded values)

Batch No.	X_1	X_2
F1	-1	-1
F2	-1	0
F3	-1	+1
F4	0	-1
F5	0	0
F6	0	+1
F7	+1	-1
F8	+1	0
F9	+1	+1

Optimization Data Analysis

Various RSM (Response Surface Methodology) computations for the current optimization study were performed employing Design Expert® software (version 8.0.5.2, Stat-Ease Inc, Minneapolis, MN). Polynomial models including interaction and quadratic terms were generated for the response variable using multiple regression analysis (MLRA) approach. The general form of MLRA model is represented as equation 6.1.

$$Y=B_0+B_1X_1+B_2X_2+B_3X_1^2+B_4X_2^2+B_5X_1X_2+B_6 X_1^2X_2+B_7 X_1 X_2^2 \dots (6.1)$$

Where B_0 is the intercept representing the arithmetic average of all quantitative outcomes of 9 runs; B_1 to B_7 are the coefficients computed from the observed experimental values of

Y; and X_1 and X_2 are the coded levels of the independent variable(s). The terms X_1X_2 and X_i^2 (i=1to2) represents the interaction and quadratic terms, respectively. The main effects (X_1 and X_2) represent the average result of changing one factor at a time from its low to high value. The interaction terms (X_1X_2) show how the response changes when two factors are simultaneously changed. The polynomial terms (X_1^2 and X_2^2) are included to investigate nonlinearity. The polynomial equation was used to draw conclusions after considering the magnitude of coefficients and the mathematical sign it carries, i.e., positive or negative. A positive sign signifies a synergistic effect, whereas a negative sign stands for an antagonistic effect.

Statistical validity of the polynomials was established on the basis of ANOVA provision in the Design Expert ®software. Level of significance was considered at $P<0.05$. The best fitting mathematical model was selected based on the comparisons of several statistical parameters including the coefficient of variation (CV), the multiple correlation coefficient (R^2), adjusted multiple correlation coefficient (adjusted R^2), and the predicted residual sum of squares (PRESS), provided by software. Among them, PRESS indicates how well the model fits the data, and for the chosen model it should be small relative to the other models under consideration (Patil and Sawant, 2009). Also, the 3-D response surface graphs and the 2-D contour plots were generated by the Design Expert® software.

Lyophilization of Nanosuspension

The optimized Nanosuspension formulation was lyophilized using lyophilizer (Drywinner Hetodryer, Denmark). Different cryoprotectants (Trehalose dehydrate, Mannitol and Sucrose) at different ratio (1:1, 1:3, 1:5) were used to select cryoprotectant which showed minimum increment in particle size. Ten milliliters of each sample with respective concentration of cryoprotectant was rapidly frozen to -80°C using liquid nitrogen, and lyophilized for 24hrs.

6.4 Entacapone nanosizing by supercritical antisolvent method

Preparation of Entacapone nanoparticles by supercritical antisolvent method

Firstly, plain drug nanoparticles of Entacapone were prepared by supercritical antisolvent (SAS) method. Required quantity of Entacapone was dissolved in DCM to get the drug solution of 20 mg/ml. Then, CO_2 from a storage tank was delivered into the top of the particle precipitation vessel at a constant rate (30g/min) until the desired pressure [Automated back pressure regulator (ABPR) 80 bar] was obtained. Once the pressure and temperature (40°C) had equilibrated, the drug solution was co-introduced into the particle precipitation vessel at 0.3 ml/min by a HPLC liquid pump (Model 307, Gilson Inc., USA) with $SC\text{-}CO_2$ through the spray nozzle. The residual solvent ($SC\text{-}CO_2$ and DCM) was drained out of the particle precipitation vessel by the backpressure regulator (Tescom, model 26-1723-24-194). At washing step, an additional $SC\text{-}CO_2$ continued to flow into the precipitation vessel for further 30 min to wash out the residual content of DCM solubilized in the supercritical antisolvent. The precipitation vessel was slowly depressurized down to the atmospheric pressure and finally the particles were collected from the internal basket of the precipitation vessel (retained by a 0.1 μm metal frit and paper filter).

Preparation of Entacapone solid dispersion (E-SDP) particles

Solid dispersion particles of Entacapone (E-SDP) were prepared as per reported method (Wong et al 2005). In this method, Entacapone (50mg), HPMC K15 M (150mg) and Pluronic F68 (20mg) were dissolved in 20 ml DCM: methanol (1:1) to get the drug solution of concentration 0f 2.5 mg/ml. Then, CO_2 from a storage tank was delivered into the top of the particle precipitation vessel at a constant rate (30g/min) until the desired pressure [Automated back pressure regulator (ABPR) 120 bar] was obtained. Once the pressure and temperature (45°C) had equilibrated, the drug solution was co-introduced into the particle precipitation vessel at 0.5 ml/min by a HPLC liquid pump (Model 307, Gilson Inc., USA) with $SC\text{-}CO_2$ through the spray nozzle. The residual solvent (methanol and DCM) was drained out of the particle precipitation vessel by the backpressure regulator (Tescom, model 26-1723-24-194). At washing step, an additional $SC\text{-}CO_2$ continued to flow into the precipitation vessel for further 30 min to wash out the residual content of DCM and

methanol solubilized in the supercritical antisolvent. The precipitation vessel was slowly depressurized down to the atmospheric pressure and finally the particles were collected from the internal basket of the precipitation vessel (retained by a 0.1 μm metal frit and paper filter).

6.4.1 Optimization of process parameters:

Determination of Entacapone solubility in supercritical CO_2 and selection of solvent

Determination of the drug solubility in supercritical CO_2 is the most important parameter in case of SAS process as it determines product formation. To determine the solubility of Entacapone in supercritical CO_2, fixed quantity (100mg) of Entacapone bulk drug was placed in the precipitation chamber of the supercritical particle former (Thar Instruments, USA). Then, supercritical conditions were maintained for 30 min (i.e. ABPR 80 bar and precipitation chamber temperature 45°C) and the residual product in the container was collected and weighed. Solubility of the drug was determined from the difference in weight which indicates drug solubility in supercritical CO_2.

Optimization of process parameters for Entacapone nanoparticles

Stepwise batches were prepared for selection of process parameters such as ABPR, product temperature, CO_2 flow, solution spraying rate, drying time. Different solvents such as DCM, chloroform and methanol were tried to find out the solvent which gave maximum supersaturation, identified based on the precipitation yield. The concentration of drug in the solvent was kept 20 mg/ml and other processing parameters as follows;

ABPR   80 Bar

Solution spray rate   0.5 ml/min

CO2 flow rate   20g/min

Product temperature   40 °C

Drying time   30 min

After selection of the solvent, other process parameters such as effect of pressure, effect of temperature, effect of drug concentration and effect of molar fraction of CO2 was studied.

The effect of ABPR at three different levels (80, 100 and 120 bar) was studied to find out optimum ABPR required for size reduction of the bulk drug. The product chamber temperature also determines the possible precipitation of the compound in the SAS process. The effect of temperature at three different levels (40°C, 45°C and 50°C) was studied to find out optimum temperature required for size reduction of the bulk drug. The feed rate ratio is another important parameter which has major influence on size reduction of the drug in the SAS process. The effect of feed rate ratio on size reduction of the drug at different levels (60, 100, 120 and 180) was studied to find out optimum feed rate ratio required for size reduction of the bulk Entacapone.

From above studies the process parameters to obtain minimum particle size of the drug were identified.

Second formulation (solid dispersion particles) was prepared for Entacapone using SAS method. Solid dispersions are widely used for improving solubility of drugs. Recently, solid dispersion particles with nanometer size were prepared by SAS method and were reported to improve dissolution rate of felodipine, a drug with poor solubility (Won D et al; 2005). Hence, an attempt was made here to prepare solid dispersion particles of Entacapone. For preparation of solid dispersion particles, the process and formulation parameters were optimized.

Optimization of process parameters for Entacapone solid dispersion particles (E-SDP)

Solid dispersion particles of Entacapone were prepared by SAS method. The effects of process parameters such as pressure (80, 100, 120 bar) and temperature (40, 45 and 50 °C) were studied and effect on precipitation and particle size was determined. The solvents (DCM, methanol, chloroform and their mixture) were selected based on solubility of the hydrophilic polymer and drug. The effect of addition of Pluronic F68 (surfactant) on particle size of particles was also studied by preparing batches with and without surfactant. Solid dispersion particles of Entacapone were prepared by using different drug to HPMC ratios (1:2, 1:3 and 1:4) and the effect of these ratios on yield and particle size was

determined. The formulation with minimum particle size and maximum yield was selected as optimum formulation.

6.5 Characterization of nanosuspension and SCF formulations

The particle size, Zeta potential, morphology and crystallinity of the prepared formulations was determined as per procedure given in Section 4.5.

Saturation solubility

The saturation solubility of Entacapone bulk drug, ENS was determined by adding an excess of the product in distilled water and mechanical shaking at 25 °C for 24 h. After the equilibrium reached, the dispersion was centrifuged at 20000 rpm for 10 min in a centrifuge (Sigma, Osterode, Germany) to sediment the undissolved drug. Then, 1 ml of supernatant was withdrawn and filtered (cut-off 0.22 μm, PVDF, Millipore, Ireland). The content of dissolved Entacapone was analyzed by UV spectrophotometer (UV 1700, Shimadzu, Japan) at 384 nm after suitable dilution with methanol.

Drug content and incorporation efficiency: Drug content in the ENS was determined by dissolving 5 mg of obtained lyophilized powder and solid dispersion particles in methanol. The incorporation efficiency of solid dispersion particles was calculated by dissolving obtained product in methanol: water (8:2) mixture. The samples were analyzed by UV spectrophotometer at 384 nm after suitable dilution with respective solvents.

$$\text{Incorporation efficiency} = \frac{\text{Amount obtained in formulation}}{\text{Theorotical amount in the formulation}} \times 100$$

In vitro Release

A dialysis membrane having pore size 2.4nm (molecular weight cut-off between 12,000 Da) was used for in vitro release studies. The release studies were performed at two pH conditions [0.1 N HCl (pH 1.2) and pH 7.2 phosphate buffer] as Entacapone has pH dependent solubility. For pH 1.2 condition, 1 ml of formulation (ENS, E-SDPs and plain drug) equivalent to 0.5 mg of Entacapone was placed in dialysis bag and then the bag sealed at both ends was placed in beaker containing 60 ml of receptor medium (0.1N HCl, pH 1.2) maintained at 37°C. Samples were collected at predetermined time intervals and an equal volume of media was added each time after sampling to maintain constant volume in

the recipient compartment. The amount of drug in the samples was measured at 315 nm using UV spectrophotometer (UV, Shimadzu 1700).

For pH 7.2 condition, 1 ml of formulation (ENS, E-SDPs and plain drug) equivalent to 3 mg of Entacapone was placed in dialysis bag and then the bag sealed at both ends was placed in beaker containing 60 ml of receptor medium (pH 7.2 phosphate buffer, prepared as per USP) maintained at 37°C. Samples were collected at predetermined time intervals and an equal volume of media was added each time after sampling to maintain constant volume in the recipient compartment. The amount of drug in the samples was measured at absorption maximum of 384 nm using UV spectrophotometer (UV, Shimadzu 1700).

Stability studies

The stability studies of ENS, E-SDP in glass vial were performed at 2-8°C and room temperature (RT) for 3 months. Periodically, samples were withdrawn and the particle size as well as Entacapone content was measured.

6.6 Results and Discussion

6.6.1 Optimization of Parameters for Entacapone nanosuspension

Milling time :

The mean particle diameter of bulk Entacapone was 45.32±2.18 μm with a broad particle size distribution (PI – 2.21) (Fig. 6.1). But after media milling of 12h, mean particle diameter of 0.218 ± 0.016 μm (PI – 0.211) was obtained, indicating suitability of media milling method for nanosizing Entacapone (Fig. 6.2). Further milling beyond 12 h did not result in significant reduction as mean particle diameter after 14 hrs was found to be 0.213± 0.014 μm (PI – 0.220) and it was 0.194 ± 0.015 μm (PI – 0.237) at 24 hr. The results are tabulated in Table. 6.3.
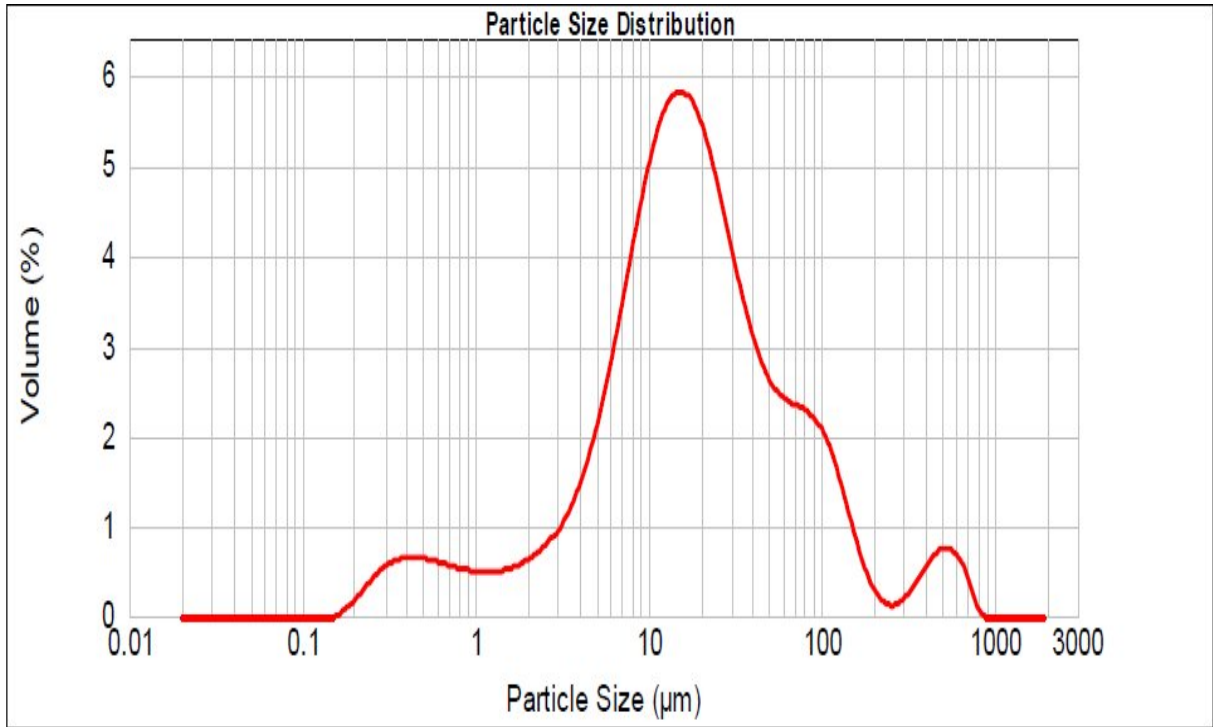
Fig 6.1 Particle size distribution of Bulk Entacapone by Malvern Mastersizer
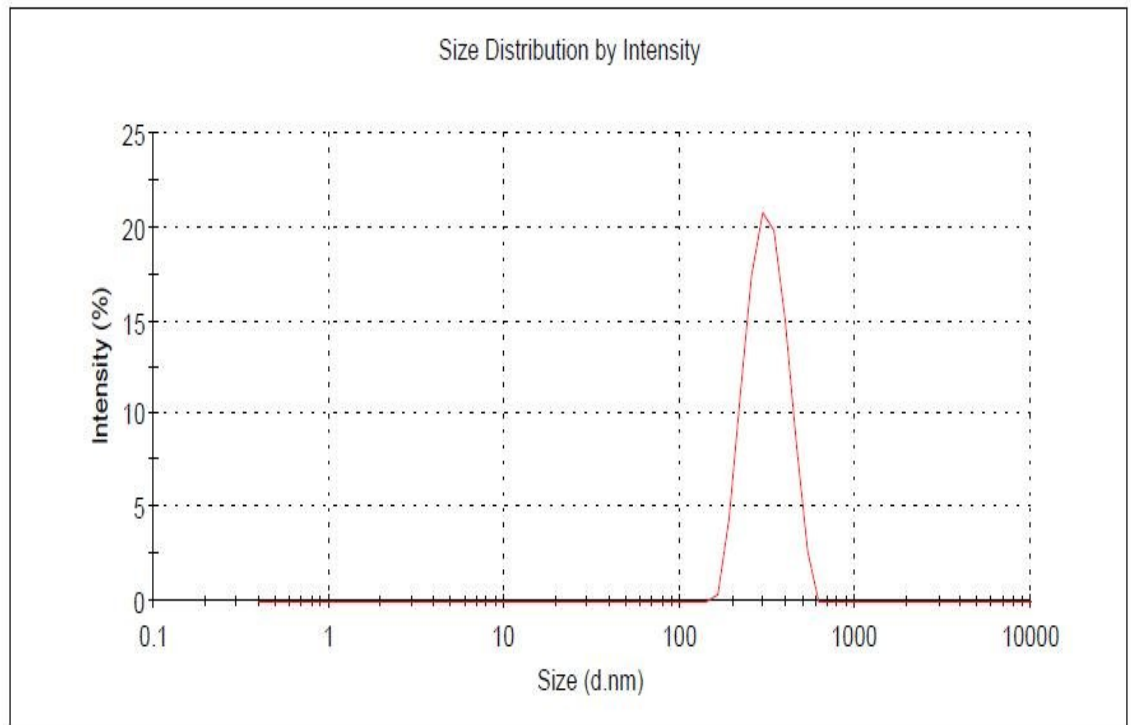
Fig 6.2 Particle size distribution of Entacapone nanosuspension after 12 hr milling

Table 6.3 Effect of milling time on Entacapone mean particle diameter and PI

Sample No.*	Milling time (hours)	d (4,3) / Mean particle diameter ± S.D. (µm)	Polydispersity Index. (PI)
1	Initial	45.32±2.182	2.221
2	1	1.243±0.214	0.753
3	2	0.843 ± 0.056	0.414
4	4	0.458 ± 0.028	0.361
5	6	0.310± 0.031	0.198
6	8	0.275 ± 0.018	0.189
7	12	0.218 ± 0.011	0.234
8	14	0.213 ± 0.014	0.220
9	24	0.194± 0.015	0.237

(* Sample No. 1 to 2 were measured by Malvern Mastersizer 2000 while sample number 3 to 9 were measured by Malvern Zeta Sizer Nano ZS 90)

Type of beads

Initially glass and zirconium oxide beads were tried to study effect of bead type on size reduction of drug by media milling. With zirconuim oxide beads, higher particle size reduction of Entacapone was observed as compared to glass beads. When small zirconuim oxide beads were used, particle size of 275.6 ± 18.3nm (PI – 0.189) was obtained after 8 hr milling while glass beads showed particle size of 465.6± 38.2 (PI- 0.171). When only large zirconuim oxide beads were used, particle size of 759.3 ± 45.8 nm (PI – 0.449) was obtained after 8 hr milling. Hence, small zirconuim oxide beads were used for further studies. The results are given in Table 6.4.

Table 6.4 Effect of type of beads on mean particle diameter and PI of Entacapone nanosuspension

Type of beads	Mean Particle diameter ± S.D. (nm)	Polydispersity Index (PI)
Small Glass beads	465.6 ± 38.2	0.171
Small Zirconium oxide beads	275.6 ± 18.3	0.189
Large Zirconium oxide beads	759.3 ± 45.8	0.449

Selection of surfactant:

During the course of optimization, the type of surfactant was chosen between Pluronic F127, Tween 80, PVP K30 and Pluronic F68. Here, drug concentration and concentration of surfactant was kept at 1 % and milling was carried out for 24 hr. Formulation prepared with Pluronic F127 showed smallest particle diameter (179.5 ± 1.8 nm) compared to other surfactants (Table 6.5). Combination of Tween 80 and Pluronic F127 produced nanosuspensions particle size of 248.0±3.8, but it was higher than nanosuspension prepared with Pluronic F127 alone which indicate that single surfactant was suitable for nanosizing. Hence, Pluronic F127 was used as a surfactant for further studies.

Table 6.5 Effect of surfactants on Particle diameter

Sr.No	Surfactant	Zavg (nm ± SD)	PI
01	Tween 80	270.2 ± 5.6	0.243
02	Pluronic F127	194.9 ± 2.8	0.237
03	Pluronic F68	198.4 ± 3.9	0.258
04	Polyvinyl pyrrolidone (PVPK 30)	351.8 ± 4.8	0.422
05	Tween 80: Pluronic F127	248.0 ± 3.8	0.230

Selection of drug concentration:

With all other parameters kept constant, batches with different drug concentration(1%, 2% and 4.0%) were prepared by 12 hr milling and results showed that particle size reduction was drug concentration dependent (Table 6.6). Higher particle size was obtained with higher drug concentration which may be attributed to insufficient milling with increased drug concentration. With 2 % drug concentration, 231.8 ± 1.4 particle size was obtained in 12 hr milling while it was 218.6 ± 3.6 at 1%. Thus, 2% concentration of drug can be used to achieve particle size below 250nm.

Table 6.6 Effect of drug concentration on Particle diameter

Sr.No.	Drug concentration (%w/v)	Zavg in nm ± SD	PI
01	1.0 %	218.6 ± 3.6	0.234
02	2.0 %	231.8 ± 1.4	0.211
03	4.0 %	318.0 ± 1.4	0.288

From these preliminary investigations, various process parameters (type of milling media, surfactant and milling time) required for nanonization of Entacapone were identified and kept constant to avoid factorial design complexity.

After the preliminary experiments, above parameters were kept constant. Other important parameters such as volume of milling media volume (X_1) and surfactant concentration (X_2) were optimized based on 3^2 factorial design.

Surfactant: Pluronic F127

Milling Media: Small zirconium oxide beads -100%

Milling time: 12 hrs

Optimization by Factorial design:

Nine formulations were prepared as per 3^2 Factorial Design. Table 6.7 enlists the response parameters of all the nine formulations.

Effect of formulation variables on the response parameter:

On analyzing the data of all the 9 formulations prepared as per 3^2 Factorial design using Design Expert® 8.0.5.2 software, various polynomial equations, response surface and contour plots were generated. The information obtained from the software is discussed in the following sections, depicting the effects of variables on the respective response parameter (Y).

The responses obtained were fitted in either simple linear equation (Eq. 6.2), interactive equation (Eq. 6.3) or quadratic model equation (Eq. 6.4) by carrying out multiple regression analysis and F-statistic to identify statistically significant terms.

$$Y = b_0 + b_1X_1 + b_2X_2 \tag{6.2}$$

$$Y = b_0 + b_1X_1 + b_2X_2 + b_{12}X_1X_2 \tag{6.3}$$

$$Y = b_0 + b_1X_1 + b_2X_2 + b_1{}^2X_{11} + b_2{}^2X_{22} + b_{12}X_1X_2 \tag{6.4}$$

From the multiple regressions, it was observed that factor X_1, X_2 and X_1X_2 have significant effect on the dependent variable (Y). The model suggested was interactive model.

Table 6.7 Response parameter for formulations of Entacapone nanosuspension prepared as per 3^2 factorial design.

| Formulation code | Factors | | Particle Mean Diameter – (nm) [Y] |
	Volume of milling media – X_1 (%w/v)	Concentration of surfactant - X_2 (%w/v)	
EN1 (-1,-1)	60	0.5	386±7.2
EN2 (-1,0)	60	1	361±6.1
EN3 (-1,1)	60	2	304±4.4
EN4 (0, -1)	80	0.5	306±5.8
EN5 (0, 0)	80	1	284±3.6
EN6 (0,1)	80	2	280±3.1
EN7 (1,-1)	100	0.5	236±2.9
EN8 (1, 0)	100	1	231±1.2
EN9 (1, 1)	100	2	254±3.1

The polynomial equation and regression coefficient for Y (Mean particle diameter) are as follows:

$$Y= 293.44 -54.83\ X_1 – 15.0\ X_2 + 25.0\ X_1X_2 \qquad\qquad (6.5)$$

R square = 0.9821

The model (Eq 6.5) was found to be significant with an F value of 91.20 ($p< 0.0001$). The value of correlation coefficient (R^2) was found to be 0.9821. The R^2 value is a measure of total variability explained by the model. The R^2 value of 0.9821 for model indicates that the model was significant. Value of probability less than 0.05 indicated model terms were significant. The value of Predicted Residual Sum of Squares (PRESS) for the polynomial model was 1650.85. The PRESS value indicates how well the model fits the data, and for the

chosen model it should be small relative to the other models under consideration (Haung et al, 2004). The interactive model with the lower PRESS value was selected.

Negative values of X_1 and X_2 in Eq.6.5 indicate antagonistic effect on Y of Entacapone nanosuspension i.e. any increase in X_1 and X_2 reduces value of Y. Effect of X_1 is found to be higher than the effect of X_2 on Y. The combined effect of these parameters was also significant and agonistic. The combined effect of factors X_1 and X_2 can further be elucidated with the help of response surface and contour plots (Fig. 6.3a and 6.3b respectively) which demonstrated that Y varies linearly with X_1, while the effect of X2 was not significant as it did not show large variations.

Table 6.8   Observed and Predicted values of response parameter

Batch	Response parameters		
	Y1		
	Observed	Predicted	%RE
EN 1	386±7.2	391.1	1.30
EN 2	361±6.1	348.7	3.53
EN 3	304±4.4	311.1	2.28
EN 4	306±5.8	305.7	0.09
EN 5	284±3.6	288.4	1.53
EN 6	280±3.1	275.7	1.56
EN 7	236±2.9	231.1	2.12
EN 8	231±1.2	238.7	3.23
EN 9	254±3.1	251.1	1.15

% RE= % Relative Error

Calculated % RE = Observed (Actual) – Predicted / Predicted * 100

Response surface and contour plots for effect of X_1 and X_2 on Y are shown in Fig. 6.3a and Fig. 6.3b. Increase in value of X_1 from low (-1) to high (+1) level while keeping value of X_2 constant at low level (-1) did result in significant decrease in mean particle size while increase in value of X_2 from low (-1) to high (+1) level while keeping value of X_1 constant at low level (-1) resulted in only slight decrease in value of mean particle size. However, at low level X_1, high level of X_2 was required in obtaining minimum particle size. High level of X_1 gave minimum value of mean particle size at all the 3 levels of X_2 which indicates that X_1 has major effect on Y. Contour plot (Fig 6.3a) revealed that Y varied in somewhat reverse fashion with X_1 i.e. with high concentration of X_1 minimum particle size obtained. However, the effect of X_1 seemed to be more pronounced as compared with that of X_2.

The predicted and observed values of response parameters are shown in Table 6.8. Low values of the relative error showed that there was a reasonable agreement of predicted values and experimental values.

Table 6.9 Analysis of variance (ANOVA) of PS for full models of Entacapone Nanosuspension

	DF	SS	MS	F	R^2	Adj R^2
FM	3	21890.17	7296.72	91.20	0.9821	0.9713
Residual	5	400.06	80.01			
Total	8	22290.22	---			
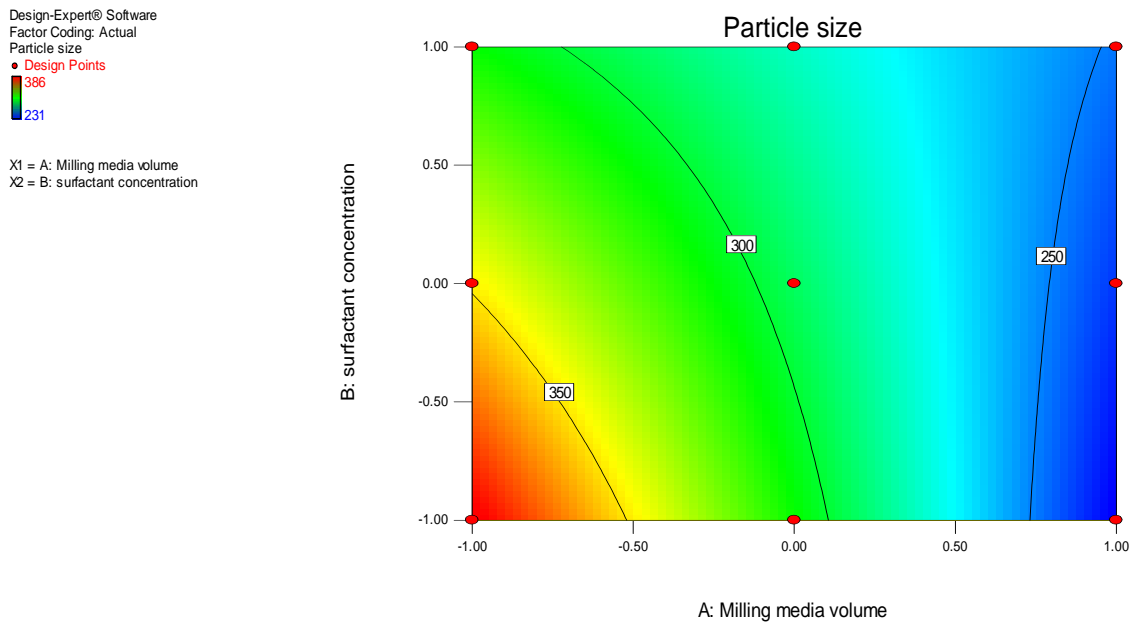
Fig 6.3 (a): Contour plot showing the effect of factors on Mean Particle size (PS) of Entacapone nanosuspension
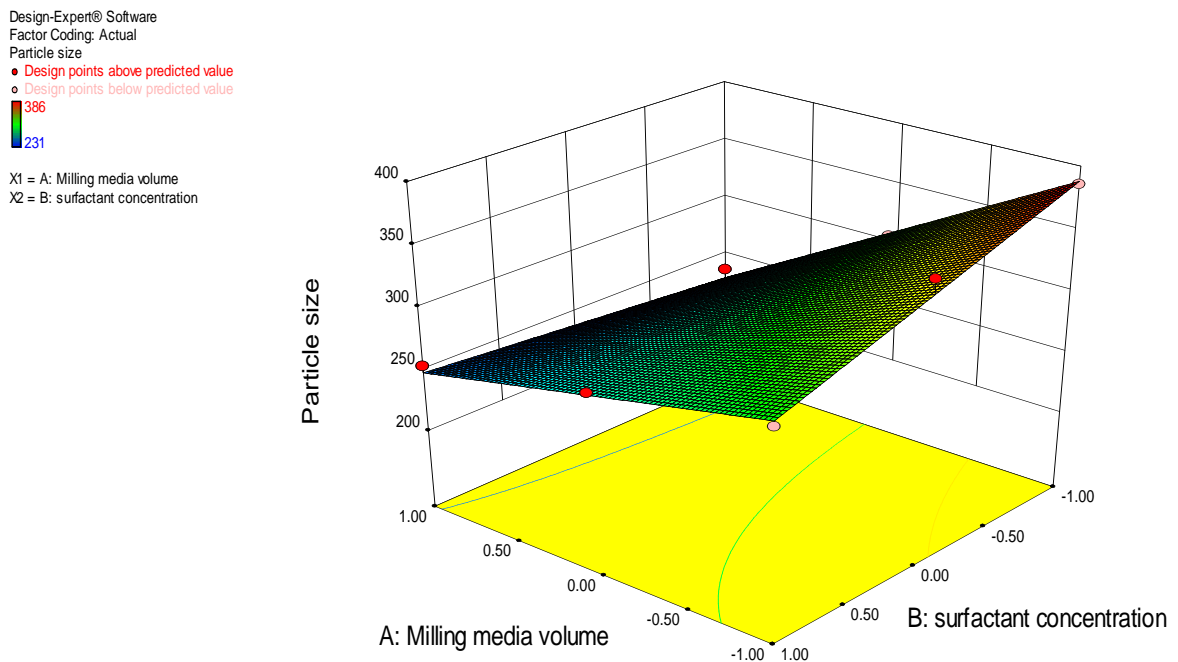
Fig 6.3 (b): Surface plot showing the effect of factors on Mean Particle size (PS) of Entacapone nanosuspension

Optimum Formulation:

A numerical optimization technique by the desirability approach was used to generate the optimum settings for the formulation. The process was optimized for the dependent (response) variables Y and the optimized formula was arrived by keeping the Mean particle diameter in range of 200 to 250 nm. Formulation EN8 (containing high (+1) levels of variable, X_1 and medium (0) level of variable X_2) fulfilled all the criteria set from desirability search (Narendra et al, 2005). To gainsay the reliability of the response surface model, new optimized formulation (as per formula EN8) was prepared according to the predicted model and evaluated for the responses (Y). The result in Table 6.11 illustrates a good relationship between the experimental and predicted values, which confirms the practicability and validity of the model. The predicted error of all the response variables was below 5 % indicating that the Response Surface Methodology (RSM) optimization technique was appropriate for optimizing Entacapone Nanosuspension. The optimized formulation of ENS is shown in Table 6.10.

Table No. 6.10 Optimized Entacapone Nanosuspension

Parameters	Value
Milling time	12 hours
Drug concentration	2.0 % w/v
Volume of milling media	100 % w/v (ZrO small beads)
Concentration of surfactant	1 % w/w

Table 6.11. The predicted and observed response variables of the optimal Entacapone Nanosuspension

	Y (nm)
Predicted	238.7
Observed	231.6 ± 3.2
Predicted Error (%)	2.974

Predicted Error (%) = (Observed value – Predicted value)/ Predicted value x 100%

Lyophilization of Nanosuspension

The optimized Nanosuspension formulations were lyophilized using lyophilizer (Drywinner Hetodryer). Different cryoprotectants (Trehalose dehydrate, Mannitol and Sucrose) were used at different ratio to find out optimum concentration of cryoprotectant which showed minimum increment in particle size. Initial particle size of the formulation used was 231.6 ± 3.2. The results are shown in Table 6. 12. At all ratios, dry powder was obtained after lyophilization. It was observed that trehalose dihydate was found to be more effective in maintaining particle size of Entacapone nanosuspension at 1:3 ratio. Thus, this formulation was considered for further studies.

Table 6.12 Optimization of cryoprotectant concentration in Nanosuspension

Croprotectant	Particle size after lyophilization
Trehalose dehydrate (1:1)	250.7 ± 6.6
Trehalose dehydrate (1:3)	243.4 ± 4.8
Trehalose dehydrate (1:5)	256.7 ± 9.6
Mannitol (1:1)	324.5 ± 5.8
Mannitol (1:3)	314.5 ± 8.0
Mannitol (1:5)	305.2 ± 4.2
Sucrose (1:1)	404.5 ± 11.8
Sucrose (1:3)	348.6 ± 4.8
Sucrose (1:5)	406.3 ± 6.2

6.6.2 Optimization by Supercritical Process:

Determination of Entacapone solubility in supercritical CO_2 (Sc-CO2)

The prerequisites for successful micro/nanonization using SAS process are the complete miscibility between the liquid solvent and the antisolvent and the insolubility of the solute in the antisolvent. Hence, the solubility of the Entacapone in Sc-CO2 was determined. About 80% of the drug added in the product chamber was observed as such, indicating insolubility of the Entacapone in Sc-CO2. Thus, it can be concluded that SAS method could be a useful approach for nanosizing Entacapone.

Selection of solvent

Different solvents such as DCM, chloroform, and methanol were tried to find out the solvent which gives maximum precipitation yield. The results obtained by using different solvents are reported in Table 6.13.

Table 6.13 Selection of solvent in SAS process

Sr. No.	Solvent	Yield	Particle size (μm)
1	Dichloromethane (DCM)	25-30 %	0.758±0.18
2	Chloroform	15-20 %	1.153±0.38
4	Methanol	20-25 %	1.355±0.53

From the results, it can be observed that minimum particle size and high yield was obtained with DCM as compared to methanol and chloroform which could be attributed to high mixing with Sc-CO2. DCM is a common choice for SAS experiments because of its dissolution of a wide number of compounds or materials and good miscibility with Sc-CO2 at low temperatures and pressures. The particle size obtained with methanol and chloroform was also above 1μm and these results indicate that, these solvents could be used for SAS processing of Entacapone. DCM was used for further studies of Entacapone by SAS method as in addition to particle size, better yield was also obtained.

Effect of process parameters

Process parameters play an important role in product formation in SAS process. Hence, the effect of various process parameters on precipitation and particle size of Entacapone were studied and results are shown in Table 6.14.

Table 6.14 Effect of process parameters on particle size of Entacapone plain drug

Sr. No.	Temperature (°C)	Pressure (bar)	Concentra-tion (mg/ml)	Feed rate Ratio "R"	Particle size (µm)
1	40	80	10	100 (30/0.3)	1.158±0.180
2	40	100	10	100 (30/0.3)	0.920±0.124
3	40	120	10	100 (30/0.3)	Poor yield
4	45	80	10	100 (30/0.3)	1.098±0.147
5	40	80	10	75 (30/0.4)	1.118±0.164
6	40	80	10	60 (30/0.5)	1.365±0.276
7	40	80	5	100 (30/0.3)	0.648±0.143 (low yield)
8	40	80	5	60 (30/0.5)	1.708±0.273
9	40	80	5	40 (20/0.5)	Poor yield

R-CO_2 flow rate/drug solution flow rate

The effect of pressure at three different levels (80, 100 and 120 bar) on particle size of Entacapone at constant temperature showed slight change in particle size with increase in pressure from 80 to 100 bar but the yield decreased with increase in pressure. At 120 bar, the yield was negligible. With increase in temperature, there was only slight reduction in particle size at constant pressure (1.098±0.147 compared to 1.158±0.180) indicating non significant effect of temperature on particle size. The effect of concentration of drug solution on particle size was studied and it was observed that at 5 mg/ml drug solution concentration, reduction in particle size was observed (1.158±0.180 to 0.648±0.143) at constant feed flow rate but the yield also reduced.

There was significant change in precipitation of the drug particles with change in feed flow rate. At low feed flow rate (40) negligible precipitation occurred. The minimum particle size obtained at feed flow rate of 100 at drug solution concentration of 5 mg/ml, but the yield was low.

From all these results, it was observed that the particle size of Entacapone could be reduced by SAS method upto 700nm, but these results showed high variations and broad particle size distribution, indicating partial nanonization. Hence, alternative approach to

obtain nanoparticles by SAS was tried (D.H. Won et al; 2005). This approach of solid dispersion particles by SAS method demonstrated improved dissolution kinetics of felodipine (D.H. Won et al 2005) and oxeglitazar (Badens et al 2009).

Effect of process parameters in preparation of solid dispersion particles

Solid dispersion particles of Entacapone (E-SDPs) were prepared by SAS method. The solid dispersion of Entacapone was prepared with hydrophilic polymer (HPMC K15) at different ratios (1:2 1:3 and 1:4). To dissolve the polymer and drug, mixture of DCM and methanol at 1:1 ratio was used. The effects of all other process parameters were studied and given in Table 6.15. Batches with and without additions of surfactant (Pluronic F68) were prepared and minimum particle size was obtained with formulation containing surfactant (635.6±23.4 and 1035.4±56.6 μm respectively). Thus, all batches were prepared with Pluronic F68 concentration of 0.1% w/v. The concentration of drug in all batches was kept 0.25 %w/v and the ratios of HPMC K15 were varied accordingly. Precipitation yield was in the range of 50-80%.

Table 6.15 Effect of process parameters on particle size of Entacapone solid dispersion particles (E-SDPs)

Sr. No.	Temperature (°C)	Pressure (bar)	Drug:polymer ratio	Feed rate Ratio "R"	Particle size (nm)
1	40	80	1:3	60 (30/0.5)	No precipitation
2	45	80	1:3	60 (30/0.5)	No precipitation
3	40	100	1:3	60 (30/0.5)	654 (0.519)
4	45	100	1:2	60 (30/0.5)	714±24 (0.377)
5	45	100	1:3	60 (30/0.5)	635.8±19 (0.401)
6	45	100	1:3	90 (45/0.5)	785±28 (0.527)
7	45	100	1:3	100 (30/0.3)	1095±58 (0.655)
8	45	100	1:4	60 (30/0.5)	606±33 (0.567)
9	45	120	1:3	60 (30/0.5)	560±14 (0.492)
10	50	100	1:3	60 (30/0.5)	1106±64 (0.559)

The effect of pressure was studied at temperatures 40 and 45°C, there was no precipitation observed at 80 bars. With pressure of 100 bar, good precipitation was observed at temperatures 45 and 50°C. With further increase in pressure to 120 bars at 45 °C minimum particle size (560±14) was observed. This could be attributed to single phase precipitation. The effect of temperature on particle size was studied at pressure 100 bar and it was observed that temperature has important effect on particle size. With increase in temperature higher particle size was observed (1106±64 and 635.8±19 nm at 50°C and 45°C respectively) which could be due to its effect on critical point of the mixture.

Solid dispersion particles of Entacapone were prepared by using different concentration of HPMC K 15 (batches 4, 6 and 8). The effect of concentration of HPMC K15 on precipitation and particle size was determined and it was observed that at 1:2 ratio of drug: polymer, higher particle size (714±24 nm) was obtained while with ratio 1:3 and 1:4, the particle size of 635.8±19 and 606±33 nm was obtained respectively. This means that the increased potential of particle growth was effectively inhibited by higher concentration of HPMC. The precipitation yield was higher in both cases.

When the feed flow rate was compared (batches 5, 6 and 7), it was observed that minimum particle size was obtained at feed flow rate of 60 while increase in feed flow rate led to increase in particle size. This indicates that at feed flow rate of 60, supersaturation occurred effectively and optimal mole fraction value was obtained. In SAS process, firstly, premixing is created between a fresh drug solution and SC-CO_2, at high supersaturation and predominantly occurs during co-introduction of drug solution and SC-CO2 into precipitation vessel. This high supersaturation was very important and optimal mole fraction value was observed in terms of product yield and minimum particle size [Bristow et al 2001]. The particle size of 635.8±19 nm (PI 0.401) was obtained at feed flow rate of 60 while increase of feed flow rate to 100 led to particle size of 1095±58 nm (PI 0.655). Therefore, mean particle size and particle size distribution was mainly dependent upon feed rate ratio of CO_2 and drug solution.

From all these experiments, it was observed that at higher pressure (120 bar) minimum particle size was obtained at optimum temperature (45 °C). Minimum particle size with

narrow particle distribution was obtained at 1:3 drug: polymer ratio. Thus, batch 9 was considered as optimum batch (Table 6.16) and was used for further studies.

Table 6.16: Optimized formula of Entacapone solid dispersion particles (E-SDP)

Parameter	Value
Drug Concentration	50 mg (0.25% w/v)
Surfactant concentration	20 mg (0.1% w/v)
HPMC concentration	150 mg (0.75% w/v)
ABPR	120 bar
Temperature	45 °C
CO_2 flow rate	30g/min
Solvent flow rate	0.5 ml/min
Drying time	30 min

6.6.3 Characterization of optimized formulations

Particle size and zeta potential

Wet media milling is process in which micron sized particles are shear fractured into nanometer size particles. In Wet media milling method, generally smaller particle size and a tighter monodisperse of particle size profiles without need of pre-process was obtained [Pu et al; 2009], hence it was used for preparation of Entacapone nanosuspension. Entacapone nanosuspension was successfully prepared by milling slurry of drug and stabilizer, reaching a particle size of 231 ± 1.2 nm (PI 0.211) after 12hrs. The PDI value of Entacapone nanosuspension was below 0.25 indicating a narrow size distribution of the milled suspension. PI value of 0.1-0.3 indicates a narrow size distribution whereas a PDI value greater than 0.3 indicate a very broad size distribution [H. S. Ali et al 2009]. There was no significant difference in particle size before (231 ± 1.2 nm) and after (234 ± 5.8 nm) lyophilization indicating suitability of the lyophilization method. Zeta potential analysis was performed to get information about the surface properties of the nanocrystal. The zeta potential of the prepared Entacapone nanosuspension was -22.8 ± 3.5 mV, indicating reasonable stability of formulation.
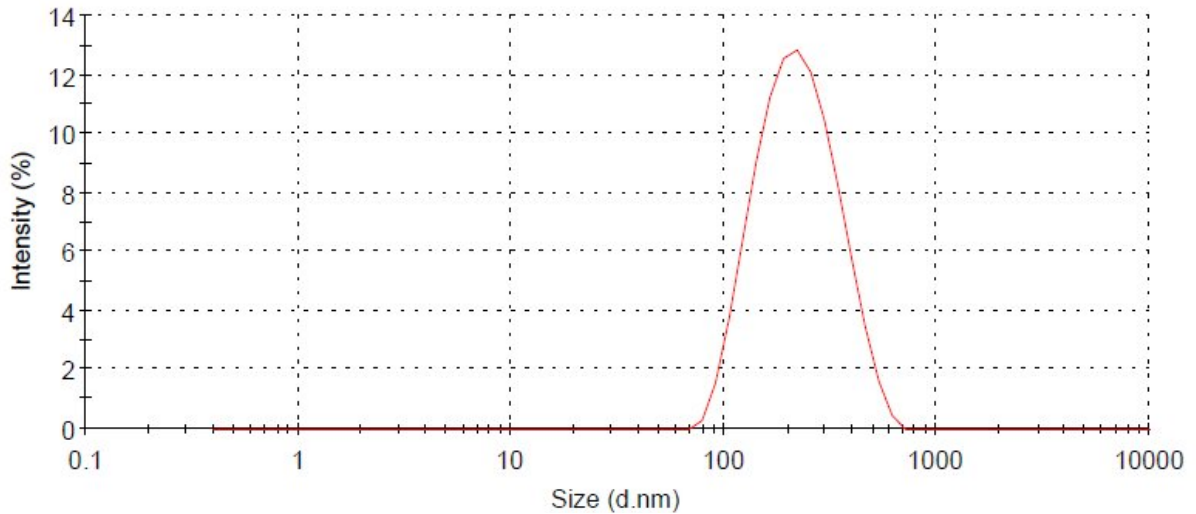
Fig. 6.4 (a). Particle size distribution of Entacapone nanosuspension
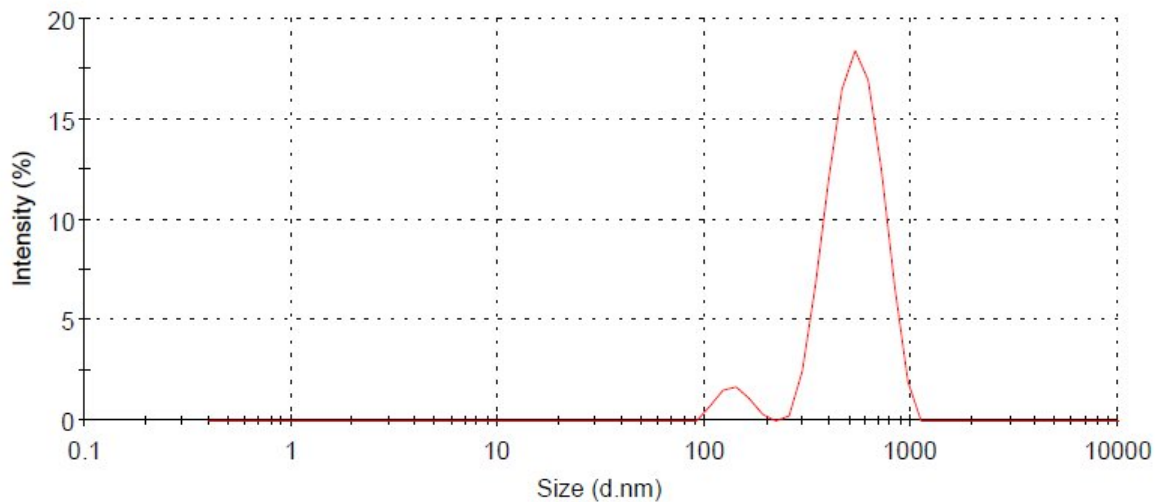
Fig. 6.4 (b). Particle size distribution of Entacapone solid dispersion particles (E-SDPs).

Solid dispersion particles of Entacapone (E-SDPs) were successfully prepared by SAS process with high yield (about 60 %). The particle size of optimized solid dispersion particles was found to be 560±14 nm (PI 0.492). The results showed the solid dispersion particles of Entacapone obtained by supercritical antisolvent method had particle size in nanometer range. The particle size distribution of optimized Entacapone nanosuspension and solid dispersion particles are shown in Fig. 6.4. The zeta potential of solid dispersion particles was found to be -12.3 mV which may be due to presence of high amount of HPMC. The zeta potential of nanosuspension prepared using HPMC was reported to be -10mV

(http://abstracts.aapspharmaceutica.com/ExpoAAPS08/CC/forms/attendee/index.aspx?content=sessionInfo&sessionId=1911).

Saturation solubility:

Saturation solubility is a compound-specific constant, which is temperature dependent. However, the saturation solubility increases below a particle size of approximately 1 µm [Muller et al 2001]. The saturation solubility of plain drug was compared with Entacapone nanosuspension. The Entacapone nanosuspension had solubility of 2.208± 0.125 mg/ml as compared to Entacapone plain drug 0.315± 0.036 mg/ml, indicating significant enhancement in solubility. The increase in solubility in case of ENS was almost 7.0 folds higher than the bulk Entacapone. Thus, the saturation solubility of Entacapone increased significantly after formulating as nanosuspension using media milling method.

Drug content and incorporation efficiency: Drug content of ENS was found to be 99.03±0.305 %. The incorporation efficiency of solid dispersion particles of Entacapone (E-SDPs) was found to be 20.88±2.35 % indicating the SC CO_2-solvent system does not always dissolve the two ingredients to the same extent.

Morphology

The appearance of Entacapone nanosuspension and solid dispersion particles was compared with plain drug suspension. The size and shape of Entacapone nanosuspension(ENS) and solid dispersion particles (E-SDPs) by TEM while plain drug size and shape was confirmed by SEM. Entacapone plain drug exhibited large aggregates of needle shaped crystals (Fig. 6.5a). Fig. 6.5b shows solid dispersion particles produced by SAS method while Fig. 6.5c shows nanoparticles of Entacapone produced by media milling method. The image of E-SDP shows quite regular and nearly spherical agglomerates of solid dispersion particles of drug and HPMC. The surrounding matrix around the particles indicates the eroded HPMC matrix. It can be confirmed that morphology of bulk drug was changed by SAS method and the reduction in particle size to nanometer size was observed. The TEM image of ENS shows that the particles obtained were slightly elliptical shaped had smooth surface and non-aggregated in case of ENS. In addition to particle size analysis, the

TEM micrographs further confirmed that the milling process was effective in converting the Entacapone plain drug particles into the submicron range.
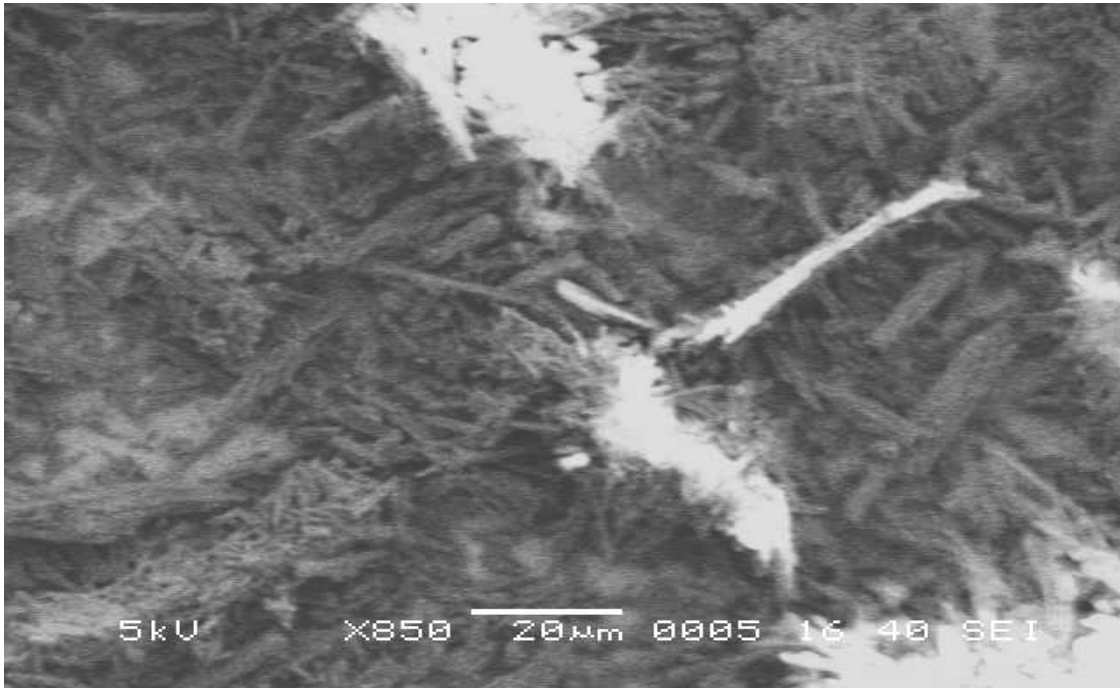
Fig 6.5 (a): SEM image Entacapone plain drug
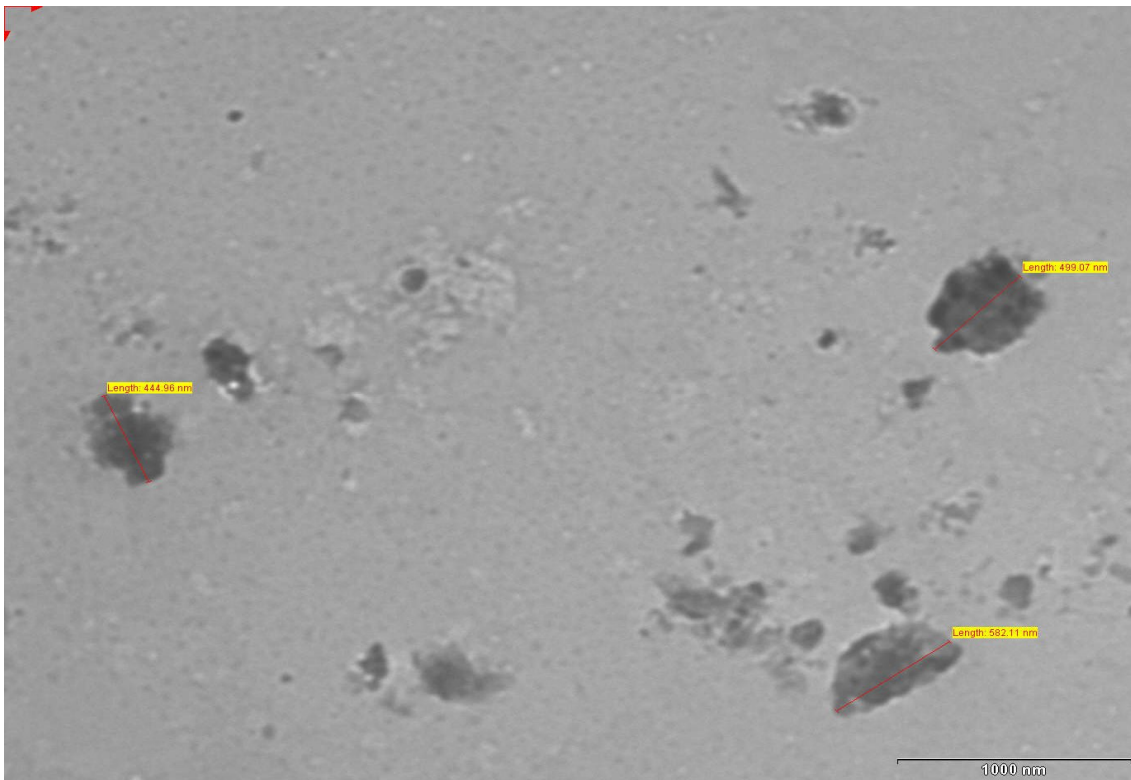
Fig 6.5 (b): SEM image Entacapone solid dispersion particles (E-SDP)
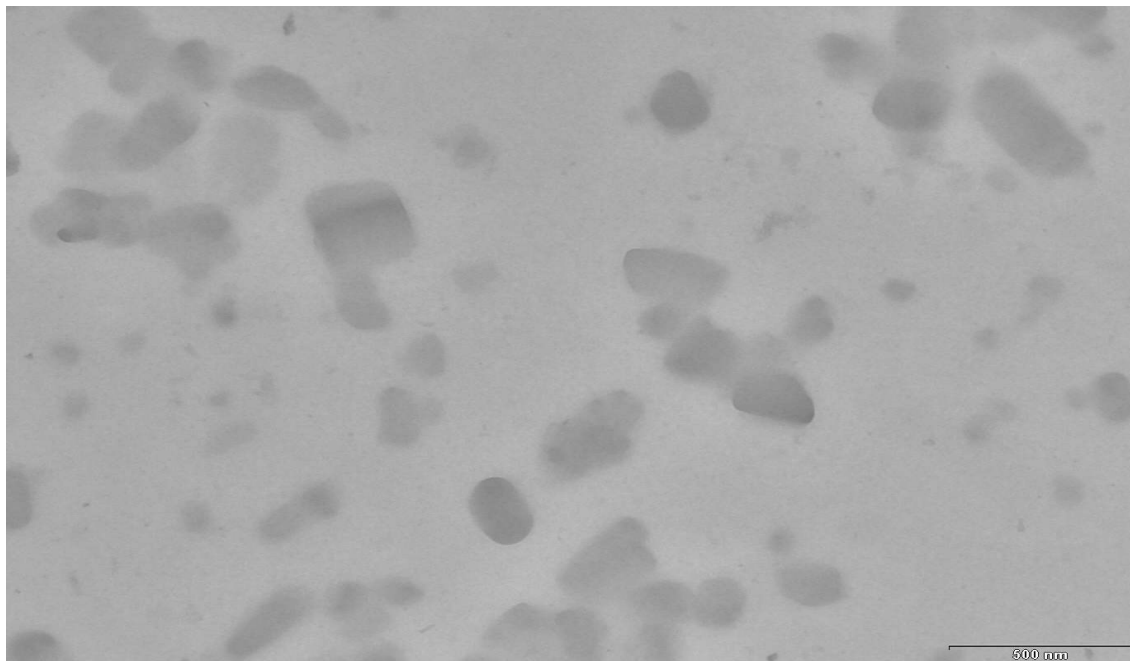
Fig. 6.5 (c): TEM image Entacapone Nanosuspension (ENS)

The plain drug exhibited larger particles and had no size uniformity. The particle size obtained with SEM and TEM studies was in accordance with particle obtained by Malvern Zatasizer.

Crystallinity

Crystalline state is another factor influencing the dissolution and stability of a compound. The crystalline state of the samples was evaluated to prove the effect of milling on the physical state of Entacapone. X-ray diffraction has been used to analyze potential changes in the inner structure of Entacapone crystals. The XRD patterns for bulk Entacapone, Entacapone nanosuspension and solid dispersion particles are displayed in Fig. 6.6.

The results indicated that significant reduction in crystallinity of Entacapone was observed in case of ENS as compared to plain drug. All major peaks which are associated with PD were disappeared in case of ENS except the peak at 6.9 2θ, but the intensity of it was reduced significantly, indicating reduction in crystallinity. In case of E-SPD, all the major peaks (6.9, 11.8, 13.5, 15.6, 24.6 2θ) associated with plain drug were disappeared indicating complete reduction in crystallinity due to molecular dispersion of the drug in HPMC.
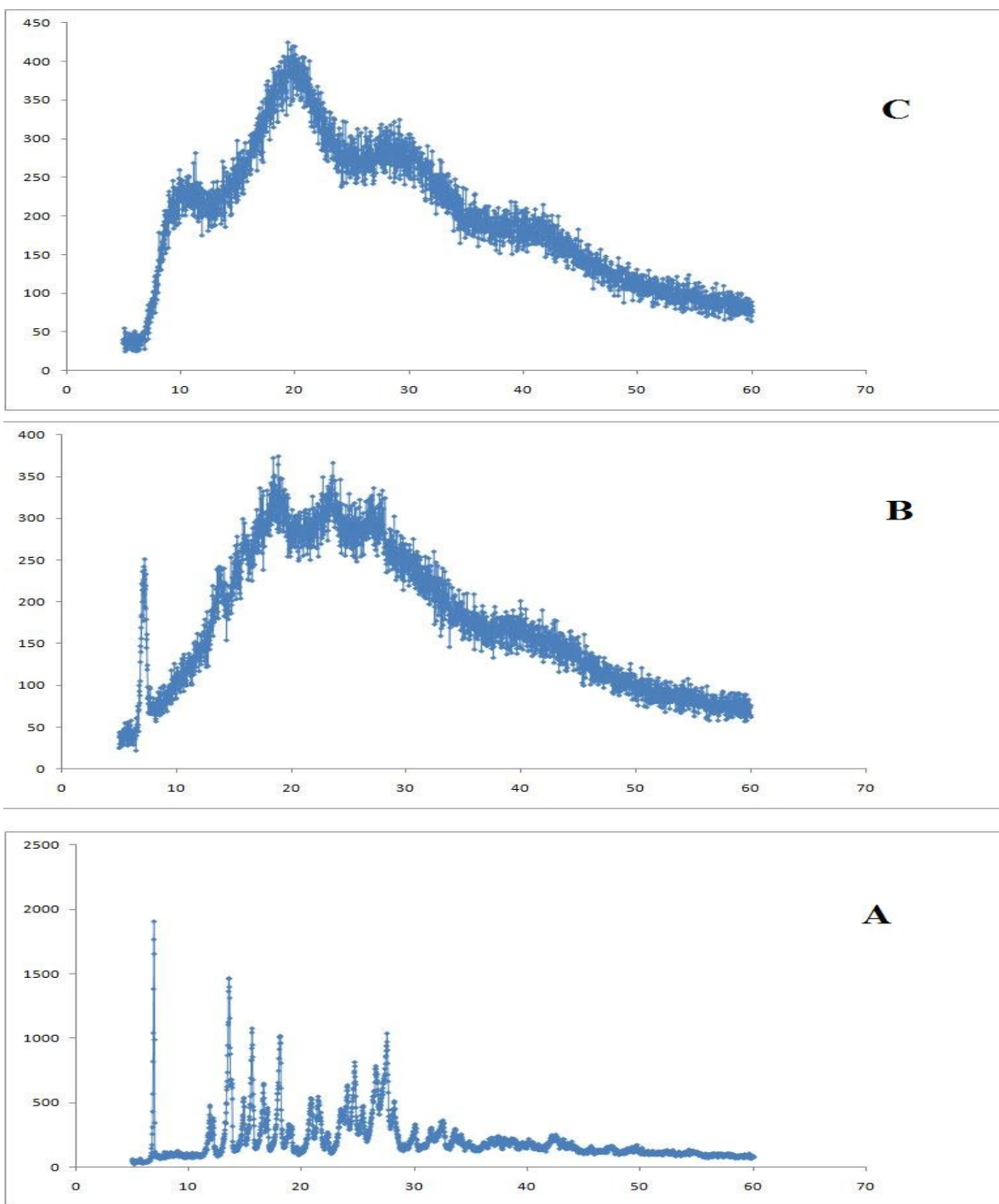
Fig.6.6. XRD pattern of Entacapone un-milled drug (A), ENS (B) and E-SDPs (C)

DSC
mW

13.36 min
159.48 C
-0.79 mW

13.96 min
165.29 C
-0.95 mW

A

B

C

100.00   200.00   300.00

Temp [C]
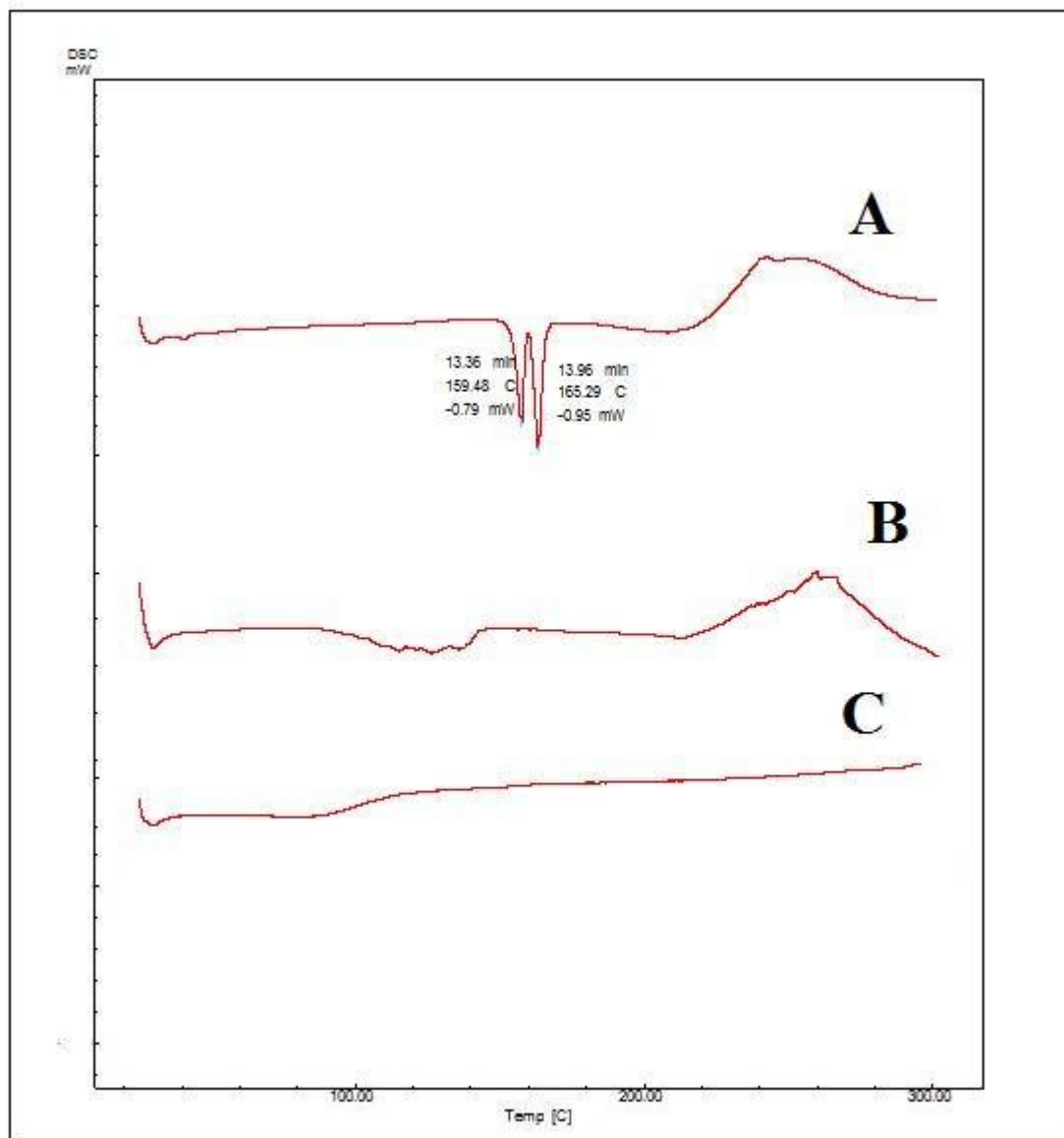
Fig. 6.7. DSC spectra of Entacapone un-milled drug (A) and ENS (B), E-SDPs (C)

In order to further confirm the physical state, DSC was also performed for Entacapone plain drug, solid dispersion particles and ENS. In this case, DSC scan of bulk Entacapone sample showed sharp endothermic peaks at 155 and 159 °C (Fig. 6.7) related to the melting of the drug. These peaks were not observed in case of ENS, which also indicated that significant reduction in crystallinity of the drug. Also the characteristics peaks of Entacapone were not observed for solid dispersion particles indicating formation of amorphous product. In case

of physical mixture the peaks corresponding to drug were observed but intensity was slightly reduced. Thus, combined XRD and DSC study proved that crystallinity of Entacapone was changed by these nanosizing approaches and this could be attributed to nanonization.

In vitro release studies:

As Entacapone possesses pH dependent solubility, the drug release profiles were studied in two media [0.1 N HCl (pH 1.2) and pH 7.2 phosphate buffer]. The release profiles of ENS and solid dispersion particles (E-SDPs) in comparison to plain drug suspension (PD) in 0.1N HCl are given in Fig 6.8.
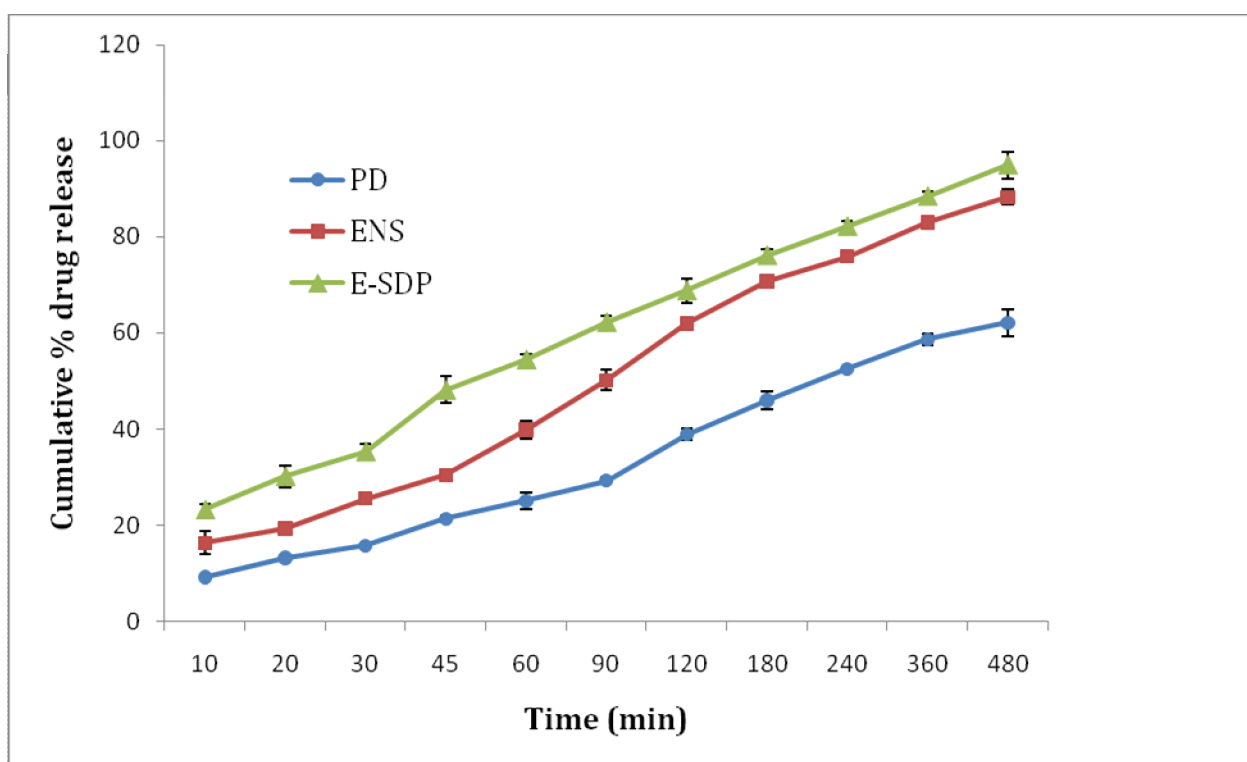
Fig 6.8 In vitro release of plain drug, E-SDP and ENS in 0.1N HCl

From Fig 6.8, it can be observed that the drug release of Entacapone was significantly improved in case of ENS and solid dispersion particles in 0.1 N HCl. The increase in drug release in case of ENS can be attributed to the increased saturation solubility and surface area due to nanosizing. Within initial 10 min, 23.27 % of drug was released in case of SDP while the corresponding release for ENS and plain drug was 16.33 and 9.17%. At the end of 8 hr, 94.93% of drug was released from SDP while the corresponding release for ENS and plain drug was 88.23 and 62.12%. The release was higher for solid dispersion particles

compared to ENS; this could be attributed to nanosize of the particles and enhanced solubility due to presence of hydrophilic polymer (i.e. HPMC) in the solid dispersion formulation. In addition, this enhanced release could also be attributed to change from crystalline to amorphous form.
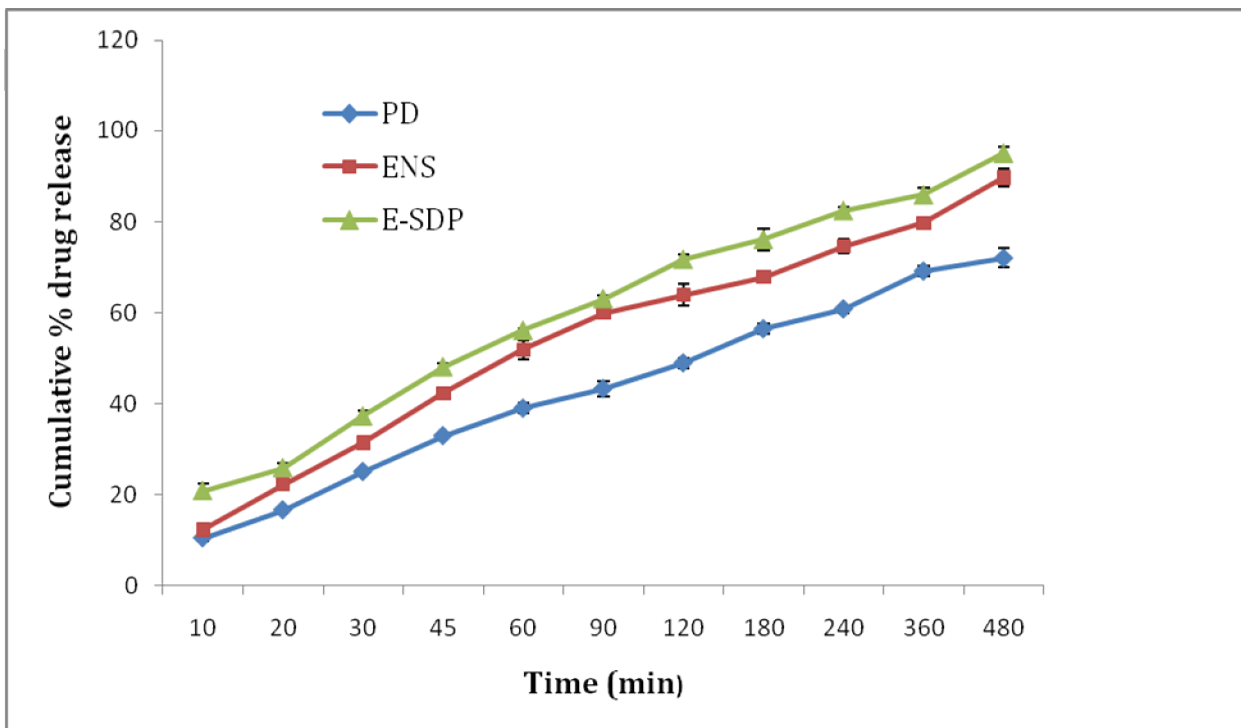
Fig 6.9 In vitro release of plain drug, E-SDP and ENS in pH 7.2 phosphate buffer

From Fig 6.9, it can be observed that higher drug release of Entacapone was observed for ENS and solid dispersion particles in pH 7.2 phosphate buffer as compared to PD. At 10 min, 20.91 % of drug was released in case of E-SDP while the corresponding release for ENS and plain drug was 12.27 and 10.47% respectively. At 8 hr, 95.04 % of drug was released in case of E-SDP while the corresponding release for ENS and plain drug was 89.64 and 71.96% respectively. The drug release was higher in case of ENS and E-SDP than PD which could be attributed due enhanced solubility due to nanosizing of the drug. E-SDP showed slightly higher release than ENS which could be due to enhanced hydrophilicity due to presence of HPMC. When drug release at pH 1.2 and pH 7.2 was compared higher release was observed in case of pH 7.2 which was attributed to pH dependent solubility of Entacapone. Thus, as observed from Fig. 6.8 and Fig. 6.9, conclusively it can be observed that, both nanosizing approaches (ENS and E-SDP) were useful in improving the drug

release at pH 1.2 HCl and pH 7.4 phosphate buffer. From these results, it can be concluded that pH dependency of Entacapone can be minimized with these approaches.

Table 6.17. Coefficient of correlation for various models for PD, ENS and E-SDPs

Formulation	First order	Zero order	Higuchi Model	Hixon model	Korsmeyer-Peppas model*
PD pH 1.2	0.9791	0.9613	0.9917	0.9688	0.9941 (0.5454)
ENS pH 1.2	0.9962	0.9912	0.9738	0.9925	0.9652 (0.5276)
E-SDP pH 1.2	0.9815	0.9507	0.9832	0.9706	0.9845 (0.4724)
PD pH 7.2	0.9393	0.9098	0.9709	0.9285	0.9769 (0.6822)
ENS pH 7.2	0.9427	0.9406	0.9880	0.9678	0.9853 (0.7417)
E-SDP pH 7.2	0.9696	0.9312	0.9746	0.9574	0.9737 (0.5466)

*Values in bracket indicate release component

The release profiles were then fitted into different exponential equations such as Zero order, First order, Higuchi, Hixon-Crowell, and Korsmeyer-Peppas to characterize the release (Table 6.17). The models followed by various formulations were identified from the correlation coefficient. The release mechanism by these formulations was identified from release exponent value obtained from Korsmeyer-Peppas model. Value of 'n' indicates that SPD formulations followed fickian diffusion as the release component values are below 0.5 at pH 1.2 conditions (Costa P et al .2001). All other formulations showed value of 'n' between 0.5-10 indicating anomalous transport mechanisms at both pH conditions.

Stability

The stability of ENS and E-SDP in terms of drug content and particle size distribution was monitored for 3 months at 2-8 °C and RT (25-30 °C). The formulation showed physical stability for the period of 3 months at both conditions. The particle size and drug content of the ENS at different time interval are given in Table 6.18 and Table 6.19. It was found that no significant difference was observed in the particle size of ENS after 3 months at both

conditions indicating its suitability for storage at both conditions. Also, the drug content was also not changed significantly.

Table 4.18: Stability of ENS at RT and cold conditions (2-8°C)

Sr. No	Time	Drug content (%) (2-8 °C)	Drug content (%) (RT)	Particle size (nm) (2-8 °C)	Particle size (nm) (RT)
1	Initial	99.6±1.1	99.3±1.4	250.4±7.6	250.4±7.6
2	1 month	99.6±1.3	99.2±1.0	254.3±6.5	258.3±8.2
3	2 months	99.6±1.0	99.2±1.5	255.6±10.2	265.1±5.3
4	3 months	98.9±1.6	98.8±1.3	258.1±6.9	268.6±3.9

In case of E-SDP also no significant difference was observed in the particle size after 3 months indicating its suitability for storage. The drug content compared to initial amount was also not affected much indicating suitability of the formulation.

Table 4.19: Stability of E-SDP at RT and cold conditions (2-8°C)

Sr. No	Time	Drug content (%) (RT)	Particle size (nm) (RT)	Drug content (%) (2-8 °C)	Particle size (nm) (2-8 °C)
1	Initial	99.8±1.1	283.4±12.6	99.8±1.1	283.4±12.6
2	1 month	98.5±1.3	283.3±10.2	98.5±1.3	283.3±10.2
3	2 months	98.6±1.0	285.1±15.3	98.6±1.0	285.1±15.3
4	3 months	96.9±1.6	288.6±13.9	96.9±1.6	288.6±13.9

Thus, these formulations could be stored at RT and cold conditions without any change in their particle size and chemical stability.

6.7 References:

1. Ali HS, York P, Blagden N. Preparation of hydrocortisone nanosuspension through a bottom-up nanoprecipitation technique using microfluidic reactors. Int J Pharm. 375, 2009, 107-113.

2. Badens E, Majerik V, Horvath H, Szokonya L, Bosc N, Teillaud E, Charbit G. Comparison of solid dispersions produced by supercritical antisolvent and spray-freezing technologies. Int J Pharm. 377, 2009, 25-34.

3. Bristow T, Shekunov BY, Shekunov P. Analysis of the supersaturation and precipitation process with supercritical CO_2. J Supercrit Fluids. 21, 2001, 257–271.

4. Costa P, Sousa Lobo JM. Modeling and comparison of dissolution profiles. Eur J Pharm Sci. 13, 2001, 123–33.

5. Eerdenbrugh BV, Froyen L, Martens JA, Blaton N, Augustijns P, Brewster M. Characterization of physico-chemical properties and pharmaceutical performance of sucrose co-freeze–dried solid nanoparticulate powders of the anti-HIV agent loviride prepared by media milling. Int J Pharm. 338(1-2), 2007, 198-206.

6. Huang YB, Tsai YH, Yang WC, Chang JS, Wu PC. Optimization of sustained-release propranolol dosage form using factorial design and response surface methodology. Biol Pharm Bull. 27, 2004, 1626-1629.

7. Kocbek P, Baumgartner S, Kristl J. Preparation and evaluation of nanosuspensions for enhancing the dissolution of poorly soluble drugs. Int J Pharm. 312, 2006, 179–186.

8. Muller RH, Jacobs C, Kayser O. Nanosuspensions as particulate drug formulations in therapy: Rationale for development and what we except from the future. Adv Drug Deliv Rev. 47, 2001, 3-19

9. Pu X, Sun J, Li M, He Z. Formulation of nanosuspension as a new approach for the delivery of poorly soluble drugs. Curr Nanosci. 5, 2009, 417-427.

10. Sigfridsson K, Forssen S, Hollander P, Skantze U, Verdier J. A formulation comparison, using a solution and different nanosuspensions of a poorly soluble compound. Eur J Pharm Biopharm. 67(2), 2007, 540-547.

11. Won D, Kim M, Lee S, Park J, Hwang S. Improved physicochemical characteristics of felodipine solid dispersion particles by supercritical anti-solvent precipitation process. Int J Pharm. 301, 2005, 199–208.

12. Zetasizer Manual

7.0 MATERIALS AND METHODS

7.1 Materials

Entacapone of pharmaceutical grade was obtained as kind gift from Alembic Pharmaceuticals Ltd, Vadodara, India. Capmul MCM was obtained as generous gift sample from Gattefosse Ltd (Mumbai, India). Soya PC (Phospholipon 90G) and Egg PC were obtained as kind gift from Lipoid GMBH (Ludwigshafen, Germany). Methanol was purchased from Merck Chemicals, Mumbai, India. Pluronic F 127(Poloxamer 407) was a gift sample from BASF, India. Double distilled water was used for the preparation of the nanoemulsions and other aqueous solutions.

7.2 Equipments:

1. High speed magnetic stirrer (Remi, MS500, Remi equipments, Mumbai)

2. High speed Centrifuge (Sigma 3K30, Germany)

3. Particle size Analyzer (Zeta sizer Nano series, Malvern Instruments, UK)

4. UV-VIS spectrophotometer (Shimadzu, Japan)

5. Ultra turrax (IKA werke, Germany)

6. High Pressure Homogenizer (Emulsiflex C5, Avestin, Canada).

7. Probe Sonicator (LABSONIC®M, Sartorius Ltd, Mumbai, India)

8. Digital pH meter (Lab India, Ltd, Mumbai, India)

9. Analytical weighing balance (Shimadzu, Switzerland)

10. Isothermal shaker (VORCO, York Scientific Industries, Delhi, India)

7.3 Methods

7.3.1 Determination solubility of Entacapone in different oils

Entacapone was added into the selected oils and vortexing was done for 2 min, and then the mixture was shaken for 48 hrs on mechanical stirrer to achieve equilibrium. The mixture was then centrifuged at 25000 rpm for 10 min to separate the undissoved drug and the supernatant of the oil solution was withdrawn and after appropriate dilution with methanol, the absorbance was measured against respective blank by UV visible

spectrophotometer (UV Shimadzu 1700) at 384 nm. The concentration of Entacapone was calculated from the calibration curve in methanol.

7.3.2 Preparation of nanoemulsion by ultrasonication

The nanoemulsion formulation of Entacapone was prepared as per reported method (Kentish et al, 2008). For preparation of oil phase, the required quantity (0.5% w/v) of lipophilic surfactant (Phospholipin90) and Entacapone (0.12% w/v) were dissolved in selected oil i.e. Capmul MCM (15% v/v) with stirring. The aqueous phase contained hydrophilic surfactant (0.5% w/v Pluronic F127) in required quantity of distilled water (85%). Both phases were heated to 70°C and then oil phase was added to aqueous phase drop wise while premixing using Ultra-turrax at 9500 rpm. Premixing was done for 10 min (2 cycles of 5 min). The pre-emulsion obtained was then ultra-sonicated for 9 min (3 cycles of 3 min) at 80% amplitude and 0.6 duty cycles. The obtained nanoemulsion was transferred to clean glass vial, packed and used for further evaluation.

Optimization of process parameters

High speed mixing and sonication time

All batches were prepared using oil (Capmul MCM), which showed maximum solubility of the drug. Unless otherwise stated, the emulsion formulation for preliminary optimization was 15% v/v oil (Capmul MCM), 1% w/v Pluronic F127, 1% w/v soya PC (phospholipon 90G) and water 85% v/v which was selected based on available literature on nanoemulsion preparation.

Firstly, the effects of high speed mixing (by Ultra-Turrax) on globule/droplet size of the pre-emulsion was studied. In this experiment, the droplet size obtained with different speed (9500 and 11500) and time (1, 3, 5, 10 and 15 min) was recorded.

Thereafter, the effect of sonication time on globule size was recorded. Emulsification was performed using 100W, 30kHz probe sonicator (LABSONIC®M). Probe tip was immersed 2/3rd into pre-emulsion. Sonication was done at 100W, (i.e. 80 amplitude, 0.6 cycle/second). Pre-emulsion (20 ml) was subjected to sonication for total of 18 minutes, with each sonication cycle lasting for 3 minutes and gap of 3 minutes between 2 sonication

cycles. After each cycle, the globule size and PDI were determined. The readings were recorded in triplicate.

Selection of surfactants

After selection of mixing speed and sonication parameters, formulation parameters were optimized. Selection of non-ionic surfactant was carried out based on stability of emulsion observed over period of 15 days. Two nonionic surfactants commonly used for preparation of nanoemulsion i.e. Tween 80 and Pluronic F127 were tried at different concentration. After selection of hydrophilic surfactant, lipophilic surfactant was selected. In this study, two commonly used lipophilic surfactants i.e. soya PC and Egg PC were tried at different concentrations. The appearance/phase separation was observed and lipophilic surfactant was selected for further studies.

Factorial Design and Optimization

Based on the preliminary experiments, percentages of oil phase (X_1) and ratio of Phospholipin90: Pluronic F127 (X_2), were found to be the major factors affecting the particle size, polydispersity Index (PDI) and stability of the nanoemulsion. Hence, 3^2 factorial design was applied to obtain the minimum particle size, minimum PDI and maximum stability. The formulation parameters for factorial design are given in Table 7.1. In developing the regression equations, the test factors were coded according to

$$X_i = \left(X_i - X_i^x\right)/\Delta X_i \quad \text{.. (1)}$$

Where, X_i is the coded value of the ith independent variable, X_i is the natural value of the ith independent variable, X_i^x is the natural value of the ith independent variable at the center point and ΔX_i is the step change value. According to quadratic model, multiple regressions was carried out using

$$Y = b_0 + \sum_i b_i X_i + \sum_i \sum_{j} b_{ij} X_i X_j + \sum b_{ii} X_i^2 \quad \text{.............................. (2)}$$

Where, Y is the measured response, b_0 is the intercept, b_i, b_{ij}, and b_{ii} are the measures of the variables X_i, $X_i X_j$, and X_i^2 respectively. The variable $X_i X_j$ represents the first-order interactions between X_i and X_j (i<j). The multiple regression was applied using Microsoft

excel in order to deduce the factors having significant effect on the formulation properties, and the best fitting mathematical model was selected (Akhnazarova and Kafarov 1982). Three-dimensional response surface plots and two-dimensional contour plots resulting from equations were obtained by the NCSS software.

Table 7.1: Coded Values of the formulation parameters of Entacapone Nanoemulsions

Coded Values	Actual values	
	X_1	X_2
-1	10 % v/v	1:1
0	15 % v/v	1:2
1	20 % v/v	2:1
	X_1—Oil concentration	
	X_2—Ratio of Phospholipon90G: Pluronic F127	

7.4 Characterization of Entacapone nanoemulsion

The Particle size, zeta potential, morphology, pH, viscosity and stability of Entacapone nanoemulsion were determined as per procedure given in section 5.3.5.

Drug content

Drug content was expressed as percentage of Entacapone obtained in nanoemulsion to the theoretical quantity of the drug added. Drug content was determined after dilution with methanol by UV spectrophotometer at 384 nm by using calibration curve plotted in methanol.

In vitro Release

The in vitro release studies of Entacapone nanoemulsion and plain drug suspension was performed in 0.1 N HCl (pH 1.2). A dialysis membrane having pore size 2.4nm (molecular weight cut-off between 12,000 Da) was used for in vitro release studies. 1 ml of nanoemulsion (containing quantity equivalent to 0.5 mg of drug) was placed in dialysis bag and then the bag sealed at both end was placed in beaker containing 40 ml of receptor medium (pH 1.2 buffer) maintained at 37 °C. Samples were collected at predetermined

time intervals and an equal volume of media was added each time after sampling to maintain constant volume in the recipient compartment. The amount of drug in the samples was measured at absorption maximum of 315 nm using UV spectrophotometer (UV, Shimadzu 1700).

7.5 Results and discussion:

7.5.1 Solubility of Entacapone in oils

The solubility of Entacapone in different oils was determined using calibration curve in methanol [y= 0.0576x- 0.0415 (r^2 = 0.9993)]. Fig. 7.1 represents solubility of Entacapone in different oils. Captex 500 exhibited highest solubility of Entacapone as compared to other oils but the nanoemulsion prepared using Captex 500 showed phase separation within 2 days. Hence, Capmul MCM having better solubility compared to other remaining oils was selected for preparation of nanoemulsion.
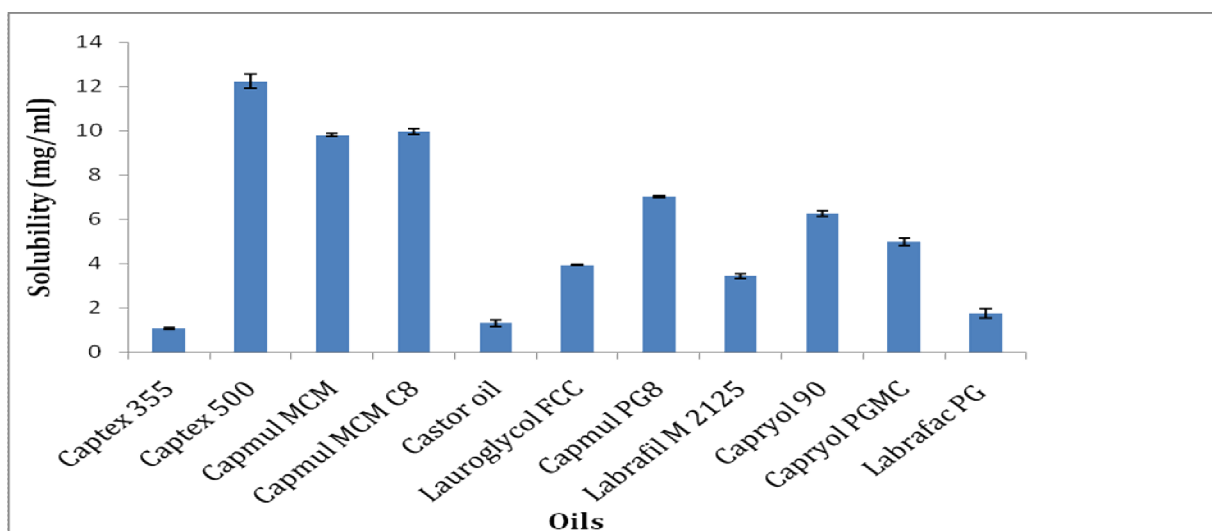
Fig. 7.1: Solubility of Entacapone in different oils.

7.5.2 Optimization of process parameters

High speed mixing and sonication time

The effect of high speed mixing (at 9500 rpm and 11500 rpm) on globule size of the pre-emulsion was studied and results are recorded in Table 7.1. After 5 min of high speed mixing, globule size of the nanoemulsion about 205±4.2 nm was obtained at 9500 rpm while it was 202.0±5.8 at 11500 rpm. In both cases, polydispersity index (PDI) was more

than 0.250 indicating non-uniform distribution. After 10 min of high speed mixing, globule size of 200.5±2.0 and PDI of 0.270 was obtained at 9500 rpm. Further increase in high speed mixing to 15 min did not result in significant reduction in globule size. Thus, 10 min high speed mixing was considered suitable for obtaining pre-emulsion with globule size in nanometer range. The pre-emulsion samples were stored at room temperature to study stability. But after 1 week, slight phase separation occurred, which indicated that only high speed mixing was not sufficient to obtain stable nanoemulsion. Hence, ultrasonication was also tried.

Table 7.2 (a) Effect of high speed mixing on globule size of pre-emulsion

Sr. No.	High speed mixing	Globule size	PDI
1	5 min (9500 rpm)	205.0±4.2	0.394
2	5 min (11500 rpm)	202.0±5.8	0.399
3	10 min (9500 rpm)	200.5±2.0	0.270
4	15 min(9500 rpm)	197.4±4.2	0.264

After finalizing the high speed mixing speed and time, the effect of sonication time was studied and the results are recorded in Table 7.2(a) and Table 7.2 (b). Sonication was carried out at intermediate power application (80% amplitude) based on our previous experiences. It was observed that the globule size of the nanoemulsion decreased with sonication time upto 9 min and thereafter negligible reduction in globule size was obtained.

Table 7.2 (b) Effect of sonication time on globule size of nanoemulsion

Sr. No.	Sonication time *#	Globule size	PDI
3	3 min	169.4±6.7	0.247
5	6 min	163.4±3.0	0.225
6	9 min	127.4±0.8	0.060
7	12 min	132.4±1.2	0.048
8	15 min	203.0±11.4	0.202

* High speed mixing at 9500 rpm for 10 min, # duty cycle 0.6 sec, 80% amplitude

At higher sonication time (15 min) particle size was increased above 200 which might be due to over-processing which is caused by an increase in emulsion droplet coalescence at higher shear rate (Jafari et al; 2006). At 9 min sonication time, minimum globule size (127.4±0.8) with low PDI (0.060) was obtained and hence, it was considered as optimum condition to obtain nanoemulsion with uniform distribution.

Selection of surfactants

After selection of mixing speed and sonication parameters, formulation parameters were optimized. Selection of surfactant was carried out based on stability of emulsion observed over period of 10 days. Two nonionic surfactants commonly used for preparation of nanoemulsion i.e. Tween 80 and Pluronic F127 were tried at 1-3% and 3-7% concentration respectively. These concentrations were selected based on literature. The results obtained from these studies are recorded in the Table 7.3.

Table 7.3 Selection of non-ionic surfactant for nanoemulsion

Surfactant	Concentration	Day 1	Day 5	Day 10
Pluronic F127	1%	Milky & stable	Milky & stable	Milky & stable
	2%	Milky & stable	Milky & stable	Milky & stable
	3%	Milky & stable	Milky & stable	Milky & stable
Tween 80	3%	Milky & stable	Phase Separation	–
	5%	Milky & stable	Phase separation	Phase Separation
	7%	Milky & stable	Milky & stable	Phase Separation

From these results, it was clear that Tween 80 could not produce stable nanoemulsion. However, with Pluronic F127, stable nanoemulsion was obtained at all the concentrations. Hence, Pluronic F127 was selected as hydrophilic surfactant for further studies.

Two lipophilic surfactants commonly used for preparation of nanoemulsion i.e. Soya PC and Egg PC were tried at 1-2% concentration. The results obtained from these studies are recorded in the Table 7.4.

Table 7.4 Selection of lipophilic surfactants for nanoemulsion

Surfactant	Concentration	Day 1	Day 5	Day 10
Soya PC	1%	Milky & stable	Milky & stable	Milky & stable
	2%	Milky & stable	Milky & stable	Milky & stable
Egg PC	1%	Milky & stable	Phase Separation	–
	2%	Milky & stable	Phase Separation	-

Phase separation was observed in case of egg PC at day 5 at both concentrations and the nanoemulsion obtained with soya PC was stable upto 10 days. Hence, soya PC was used as lipophilic surfactant for further studies.

7.5.3 Optimization by Factorial design:

Nine formulations were prepared as per 3^2 Factorial Design. Table 7.5 enlists the response parameters of all the nine formulations.

Effect of formulation variables on the response parameters:

On analyzing the data of all the 9 formulations prepared as per 3^2 Factorial design using Design Expert® 8.0.5.2 software, various polynomial equations, response surface and contour plots were generated. The information obtained from the software is discussed in the following sections, depicting the effects of variables on the respective response parameters (Y_1 and Y_2).

Table 7.5 Response parameters for formulations of nanoemulsion prepared as per 3^2 factorial design.

Formulation code	Factors		Globule Size – Day 0 (nm) [Y_1]	Globule Size – Day 15 (nm) [Y_2]
	Oil percentage – X_1 (% v/v)	Ratio of PL90G: PF127 - X_2		
NE1 (-1,-1)	10	1:1	110	112
NE2 (-1,0)	10	1:2	87	82
NE3 (-1,1)	10	2:1	114	108
NE4 (0, -1)	15	1:1	124	132
NE5 (0, 0)	15	1:2	119	124
NE6 (0,1)	15	2:1	138	154
NE7 (1,-1)	20	1:1	168	256
NE8 (1, 0)	20	1:2	128	182
NE9 (1, 1)	20	2:1	156	312

Globule size - Day 0:

The polynomial equation and regression coefficient for Y_1 (Globule size - Day 0) are as follows:

Y1 = 127.11 +23.50 X_1+ 1.00 X_2 .... 7.1

R-Squared =   0.6952

The linear model (Eq 5.1) was found to be significant with an F value of 6.84 ($p < 0.05$). The value of correlation coefficient (R^2) was found to be 0.6952. The R^2 value is a measure of total variability explained by the model. The R^2 value of 0.6952 for model indicates that the model was significant. Value of probability was less than 0.05 which indicated that model terms X_1 were significant. Positive values of X_1 and X_2 in Eq.7.1 indicated synergetic effect of X1 and X2 on Y_1 of Entacapone nanoemulsion i.e. any increase in X_1 and X_2 increased the value of Y_1. Effect of X_1 was found to be much higher than the effect of X_2 on Y_1. The effect of

X_1 was significant ($p<0.05$) while the effect of X2 was not significant. The combined effects of factors X_1 and X_2 were further elucidated with the help of contour and response surface plots (Fig. 7.2a and 7.2b respectively) which demonstrated that Y_1 increased with increase in X_1 but the effect of X_2 was minimum. Increase in X_1 resulted in increase in globule size of nanoemulsion. This showed that oil percentage plays a major role in determining globule size of the nanoemulsion. At low all levels of X_1 (oil percentage), non linear change in globule size with increase in X_2 was observed, indicating minimum effect of X_2 (ratio of PL90:PF127). However, increase in globule size was observed with increase in X_1 at all levels of X_2, indicating significant effect of X1 on droplet size of nanoemulsion. The effect of X_1 seemed to be highly pronounced than that of X_2. The predicted and observed values of response parameters are shown in Table 7.6. Low values of the relative error showed that there was a reasonable agreement of predicted values and experimental values.

Table 7.6   Observed and Predicted values of response parameters

Batch	Response parameters					
	Y_1			Y_2		
	Observed	Predicted	%RE	Observed	Predicted	%RE
NE1	110	106.5	3.28	112	111.6	0.36
NE2	87	87.8	0.9	76	78	2.56
NE3	114	116.5	2.1	108	106.3	1.60
NE4	124	133.8	7.3	132	128	3.12
NE5	119	111.2	7.0	104	109.3	4.85
NE6	138	135.8	1.6	154	152.6	0.92
NE7	168	161.5	4.0	256	260.3	1.65
NE8	128	134.8	5.0	264	256.6	2.88
NE9	156	155.5	0.3	312	315	0.95

% RE= % Relative Error

Calculated % RE = Observed (Actual) – Predicted / Predicted * 100
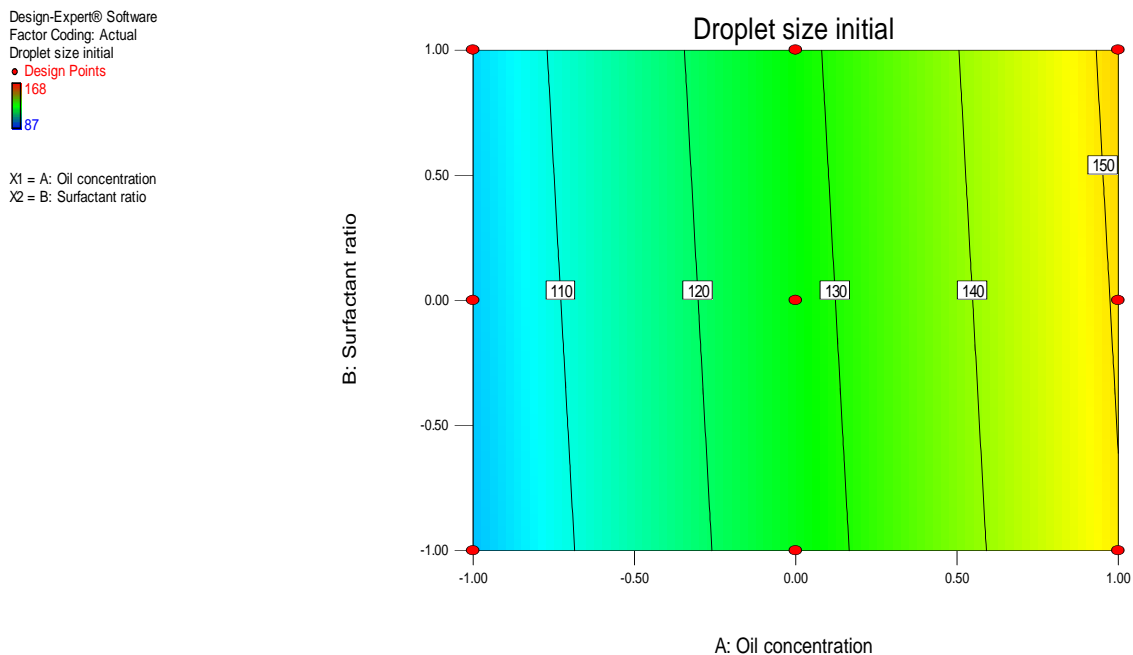
Fig.7.2 (a). Contour plot showing the effect of oil concentration and ratio of surfactants on Globule size - Day 0.

Fig. 7.2 (b). Response surface plot showing the effect of oil concentration and ratio of surfactants on globule size on Day 0

Globule size - Day 15 (Y_2):

The quadratic model for Y_2 was found to be significant (p=0.0004) with an F value of 259.95. Thus, model becomes:

$$Y_2 = 109.33 + 89.33\ X_1 + 12.33\ X_2 + 15.00\ X_1\ X_2 + 58.00\ X_1^2 + 31.00X_2^2 \ldots\ldots\ldots\ldots\ (7.2)$$

$$R^2 = 0.9977$$

The value of correlation coefficient (R^2) was found to be 0.9977. The R^2 value of 0.9977 indicated that the model was significant. Value of probability indicated that model term X_1, X_2, X_1X_2, X_1^2 and X_2^2 has significant effect on Y_2. Value of probability less than 0.05 indicated that model terms were significant.

The value of Predicted Residual Sum of Squares (PRESS) for the linear model was 1337.60, indicating best model suitability. Positive values of X_1, X_2, X_1X_2, X_1^2 and X_2^2 in Eq.7.2 indicated synergistic effect on globule size – Day 15 (Y_2). According to Eq. 7.2, there was significant difference in value of X_1 (89.33) and X_2 (12.33) which indicates that effect of concentration of oil (X_1) on globule size - Day 15 was more pronounced than ratio of surfactants.

Table 7.7. Multiple Regression Output for Dependent Variables*

Parameters	b_0	b_1	b_2	b_3	b_4	b_5	b_6	r^2	P
Globule size - Day 0	127.11	23.50	1.00	-	-	-	-	0.6952	0.028
Globule size - Day 15	109.33	89.33	12.33	15.0	58.0	31.0	0.9977	0.9977	0.0004

Response surface and contour plots for effect of X_1 and X_2 on Y_2 are shown in Fig. 7.3 (a) and Fig. 7.3(b). At low level of X_1 there was negligible difference in globule size observed with change in X_2 (surfactant ratio). However, at all the levels of X_2 there was very high increase in globule size with increase in X_1. Thus, the effect of X_1 is more pronounced than that of X_2. At high level of X_1, higher globule size was observed with all levels of X_2.
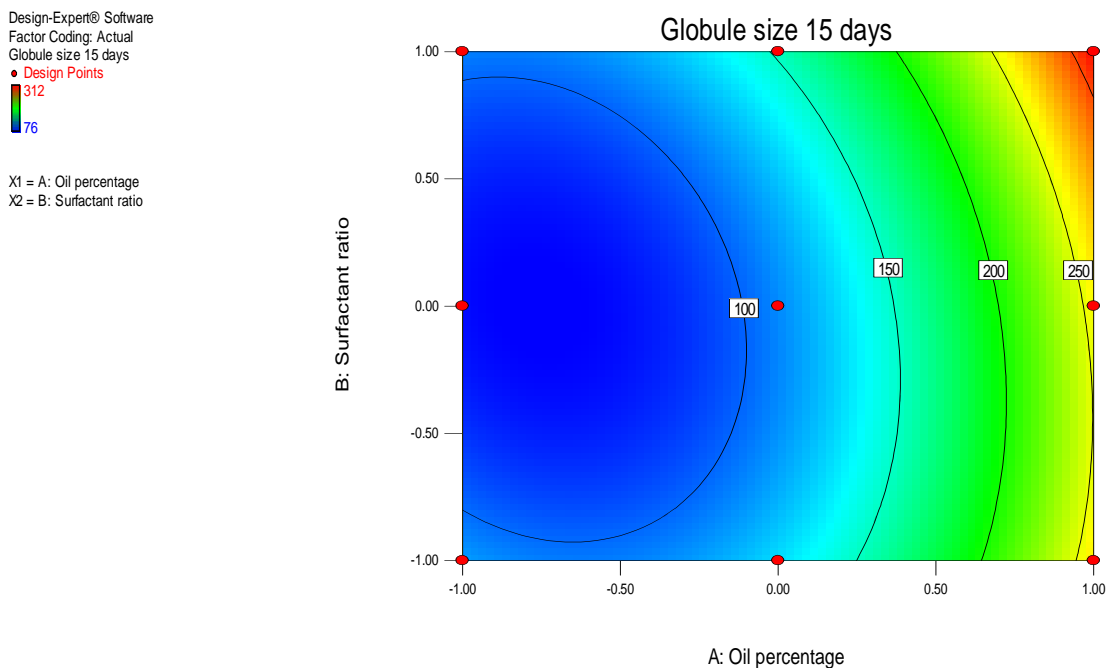
Fig. 7.3 (a) Corresponding contour plot showing the effect of factors on Globule size - Day 15.

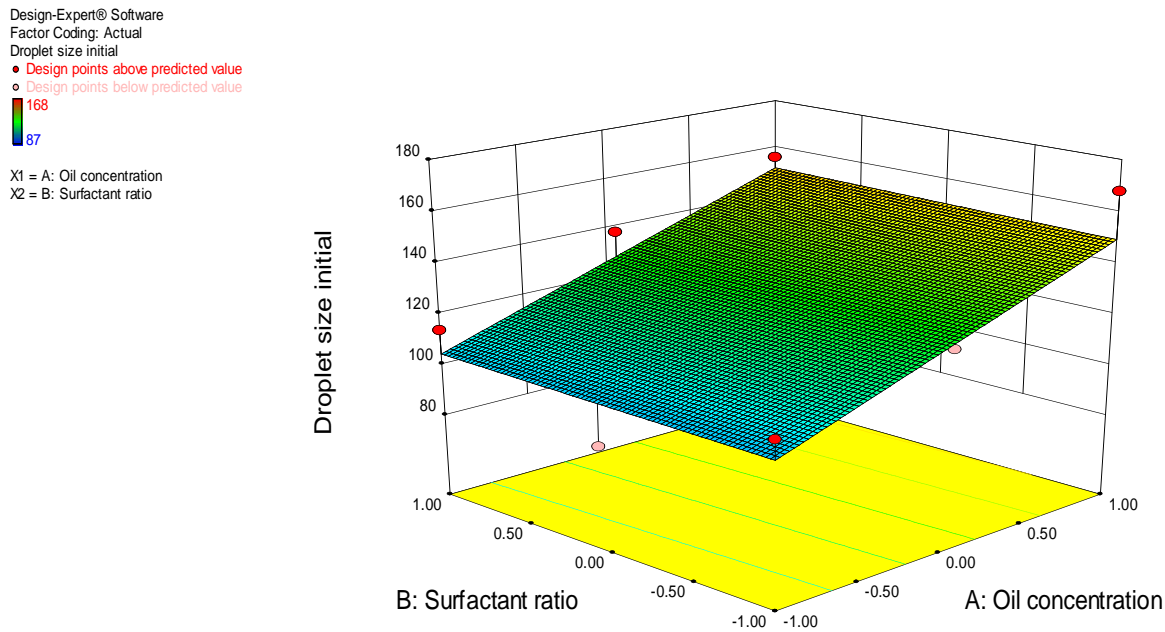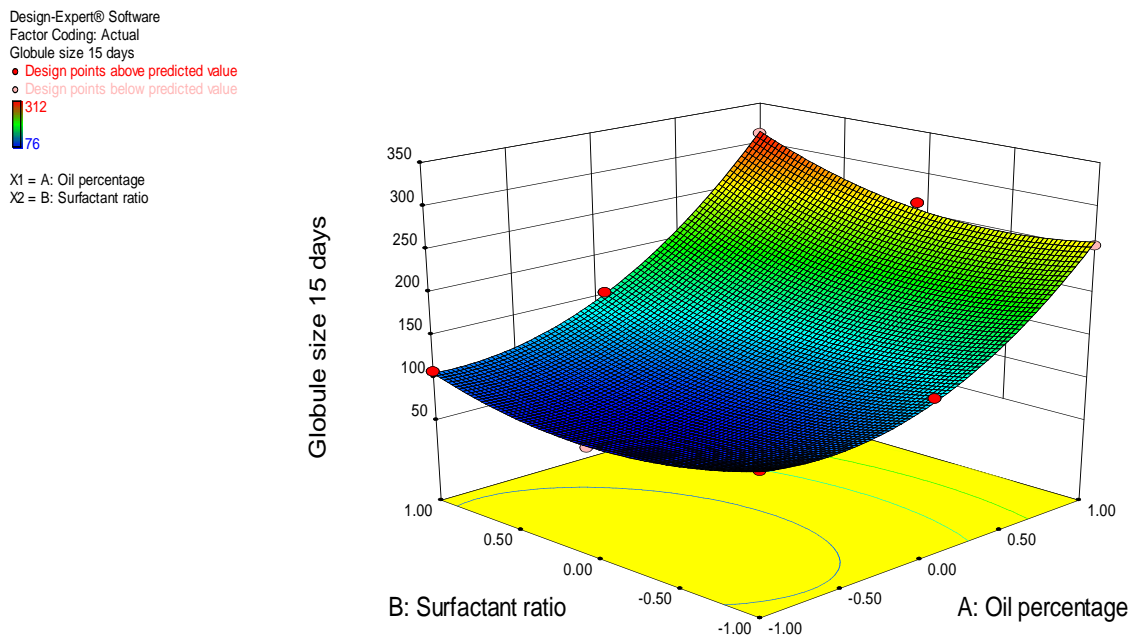Fig. 7.3 (b) Response surface plot showing the influence of oil concentration and ratio of surfactants on globule size on Day 15

Table 7.8.   Results of Analysis of Variance (ANOVA) for measured responses of nanoemulsion

Parameters	df	SS	MS	F	Significance F
Globule size – Day 0 (Y_1)					
Model	2	3319.50	1659.75	6.84	0.028
Residual	6	1445.39	242.56	--	--
Total	8	4774.89	--	--	--
Globule size – Day 15 (Y_2)					
Model	5	58345.33	11669.07	259.95	0.0004
Residual	3	134.67	44.89	--	--
Total	8	58480.00	--	--	--

Optimum Formulation:

A numerical optimization technique by the desirability approach was used to generate the optimum settings for the formulation. The process was optimized for the dependent (response) variables Y_1–Y_2 and the optimized formula was arrived by keeping the Mean particle diameter – Day 0 and day 15 in range of 100 to 150 nm. Formulation (NE4) fulfilled all the criteria set from desirability search (Narendra et al, 2005), so it was considered as optimum formulation.

New optimized formulation (as per formula NE4) was prepared according to the predicted model and evaluated for the responses (Y_1, and Y_2) to evaluate reliability of the response surface model. The result in Table 7.10 illustrates a good relationship between the experimental and predicted values, which confirmed the practicability and validity of the model. The predicted error of Y_1 and Y_2 variables was below 8 % indicating that the Response Surface Methodology (RSM) optimization technique was appropriate for optimizing Entacapone nanoemulsion.

Table 7.9 Optimized Entacapone Nanoemulsion

Parameters	Value
Capmul MCM (oil)	15 % v/v
Phospholipon 90 (Lipophilic surfactant)	0.5 % w/v
Pluronic F127 (Hydrophilic surfactant)	0.5 % w/v
Drug concentration	0.12 % w/v
Distilled water	85 % v/v

Table 7.10.   The predicted and observed response variables of the optimal Entacapone Nanoemulsion

	Y_1 (nm)	Y_2 (nm)
Predicted	133.8	140.8
Observed	124.0 ± 1.6	132.0 ±11
Predicted Error (%)	7.3	6.25

Predicted Error (%) = (Observed value – Predicted value)/ Predicted value x 100%

7.5.4 Characterization:

Particle size and surface charge: The results of droplet size and zeta potential measurements of nanoemulsions are shown in Fig. 7.4. The average particle size diameter of the Entacapone loaded nanoemulsions was found to be 120.8±1.9nm. There was no significant difference in droplet size in drug loaded and blank nanoemulsion. The polydispersity index (PI) of both formulations was 0.144 (below 0.2) and this unimodal distribution indicates uniformity in globule size.

Size Distribution by Intensity

Zeta Potential Distribution
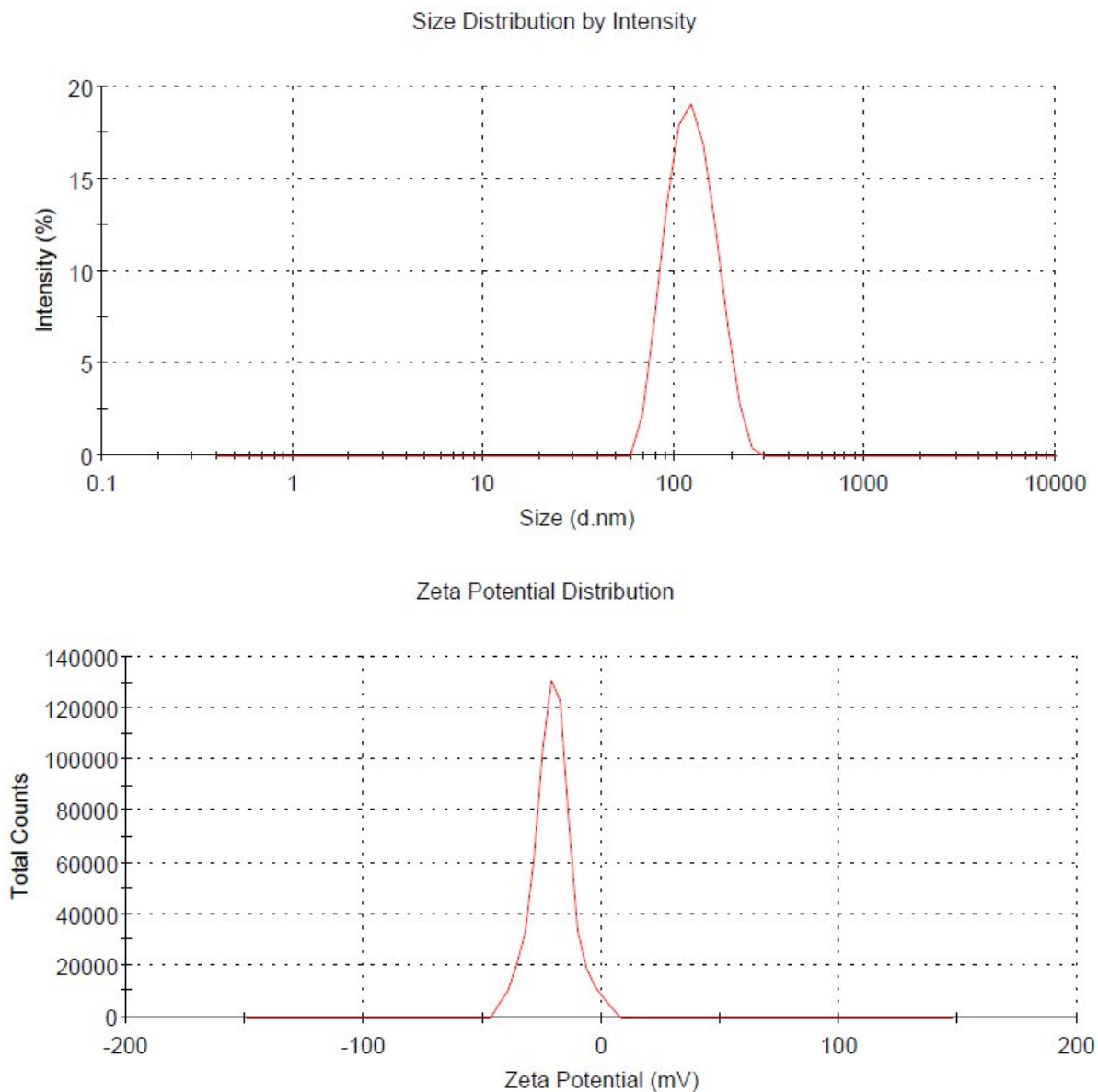
Fig. 7.4. Globule Size and zeta potential of Entacapone nanoemulsion

The zeta potential of the prepared formulation was found to be -20.6±0.8 mV. Nanoformulations with zeta potential of 30 mV are considered stable if stabilized by single mechanism and zeta potential of 20 mV for combination of these two mechanisms (Muller and Jacobs; 2002). The prepared nanoemulsion was stabilized by combined mechanism and hence, zeta potential value of about 20 mV could provide sufficient stability. The stability study supports the fact that zeta potential of -20.6±0.8 mV imparts stability to prepared nanoemulsion.

Morphological examination by Transmission Electron Microscope (TEM)

TEM analysis is important in order to study morphology of the oil droplets in the nanoemulsion formulations and to visualize any precipitation of the drug upon addition of the aqueous phase. Morphology and droplet size of the prepared nanoemulsion was evaluated by TEM. As observed in the TEM image, the globules were almost spherical, and had diameter ranging from 120-150 nm (Fig.7.5). The globules were segregated and showed no tendency of aggregation. The globule size observed in the TEM image was in accordance with result obtained by DLS.
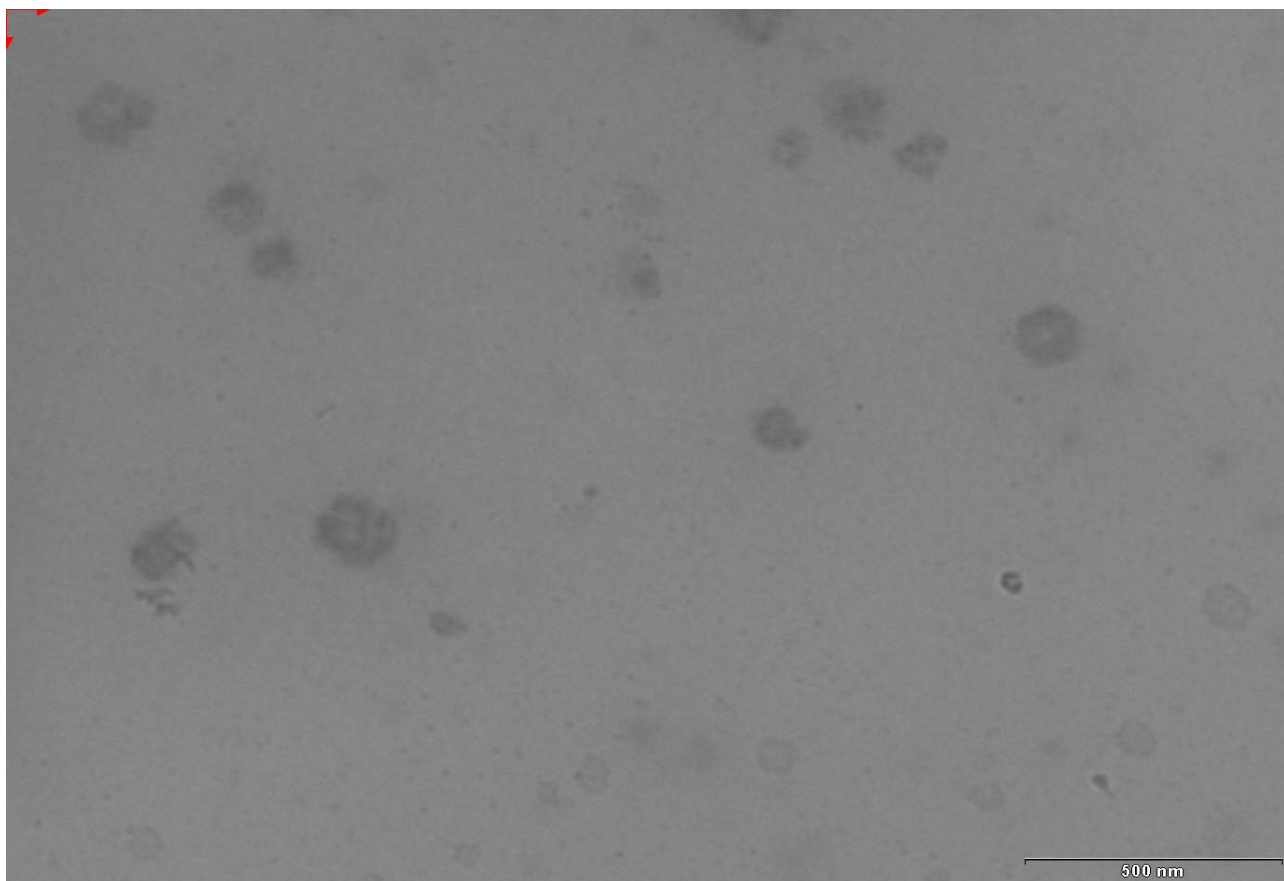
Fig. 7.5: Transmission electron microscope (TEM) image of Entacapone nanoemulsion

Drug content, pH and Viscosity

Important properties of nanoemulsion such as drug content, pH and viscosity were studied as per reported methods to evaluate physicochemical properties of the system. The drug content was found to be 99.4±0.8 %. The pH of the nanoemulsions was found to be 5.5±0.2 indicating suitability for oral administration.

One of the characteristics of nanoemulsion formulations is low viscosity (Lawrence & Rees, 2000). The viscosity of the nanoemulsion was found to be low (1.63 ±0.02 cp) indicating suitability for oral administration.

In vitro Release

The in vitro release profiles of nanoemulsion and plain drug suspension at pH 1.2 is given in Fig. 7.6. The in vitro release studies showed increase in drug release as compared to plain drug suspension at pH 1.2. Plain drug suspension showed only 25.05±0.44% drug release in 60 min while nanoemulsion formulation showed 31.77±0.92% drug release. At 8 hr, Plain drug suspension showed 62.12% drug release while nanoemulsion formulation showed 80.33±0.92% drug release indicating improved drug release which could be attributed to enhanced solubility of Entacapone and dissolution rate which in turn can be due to low droplet size and surface properties of the nanoemulsion. The overall increased release was observed in drug release with time for NE than PD.
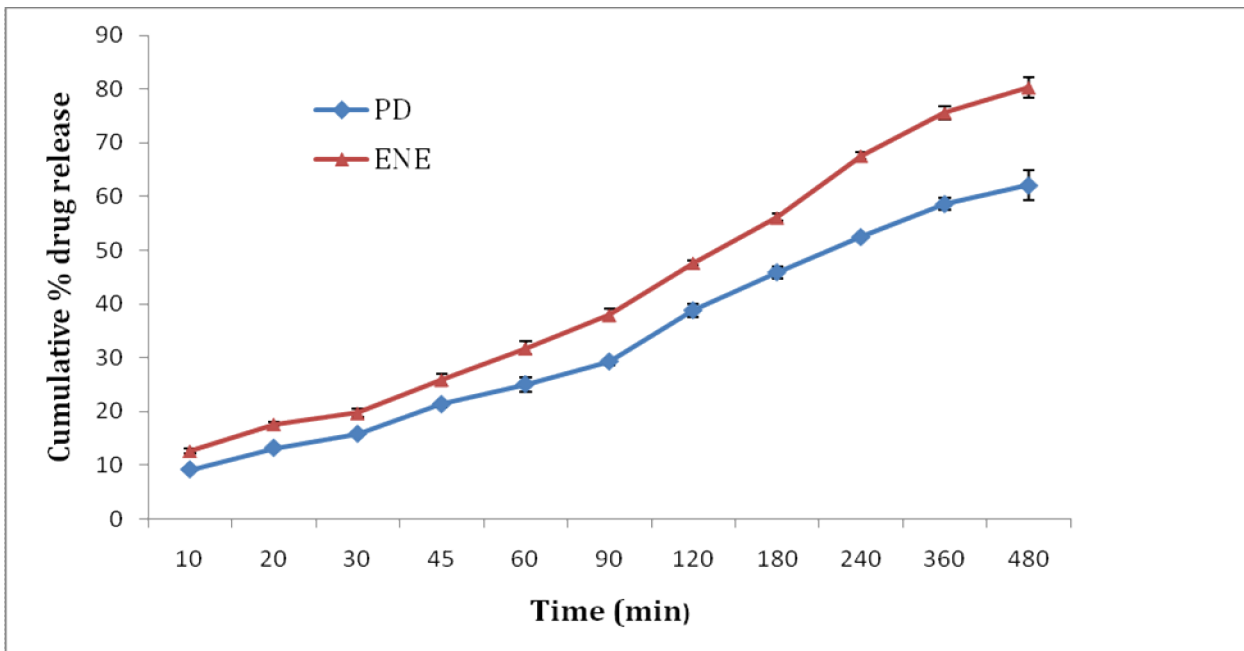
Fig. 7.6: In vitro release studies of NE in compariosn to plain drug at pH 1.2 HCl buffer

The release profiles were then fitted into different exponential equations such as Zero order, First order, Higuchi, Hixson-Crowell, and Korsmeyer-Peppas to characterize the release (Table 7.11). The model followed by prepared formulation was identified from the correlation coefficient. The release mechanism by these formulations was identified from release exponent value obtained from Korsmeyer-Peppas model. ENE showed value of 'n'

between 0.5-1.0 indicating anomalous transport mechanisms at pH 1.2 (Costa P et al; 2001).

Table 7.11. Coefficient of correlation for various models

Formulation	First order	Zero order	Higuchi Model	Hixson model	Korsmeyer-Peppas model*
PD pH 1.2	0.9791	0.9613	0.9917	0.9588	0.9941 (0.5454)
ENE pH 1.2	0.9882	0.9806	0.9889	0.9867	0.9875 (0.5054)

*Values in bracket indicate release component

Stability

The stability of nanoemulsions in terms of drug content and particle size distribution was monitored for 3 months at 2-8 °C and RT (25-30 °C). The nanoemulsion formulation showed physical stability for the period of 3 months at both conditions. The particle size and drug content of the nanoemulsion at different time interval is given in Table 7.12. It was found that no significant difference was observed in the droplet size of nanoemulsion after 3 months at both conditions indicating its suitability for storage at both conditions.

Table 7.12: Stability of nanoemulsion at RT and cold conditions (2-8°C)

Sr. No	Time	Drug content (%) (2-8 °C)	Drug content (%) (RT)	Globule size (nm) (RT)	Globule size (nm) (2-8 °C)
1	Initial	99.7±1.3	99.9±1.2	120±4	120±4
2	1 month	99.5±1.1	99.5±1.1	123±2	131±8
3	2 months	99.5±1.0	99.5±1.5	126±6	136±5
4	3 months	98.9±1.6	98.8±1.6	128±4	138±4

Another parameter which determined the stability of the nanoemulsion is its viscosity. No change in the viscosity and drug content was observed within 3 months. The emulsion was found to be stable without any incidence of creaming, cracking or phase separation upon undisturbed standing and could withstand high speed centrifugation from 2000 rpm to 10000 rpm. Thus, nanoemulsion formulation possessed good stability and was suitable for storage at RT.

7.6 References:

➢ Akhnazarova S, Kafarov V. Experiment Optimization in Chemistry and Chemical Engineering. Mir publications, Moscow, 1982. pp. 18–94.

➢ Huang YB, Tsai YH, Lee SH, Chang JS, Wu PC. Optimization of pH independent release of nicardipine hydrochloride extended-release matrix tablets using response surface methodology. Int J Pharm. 289, 2005, 87–95.

➢ Jafari SM, He Y, Bhandari B. Nano-emulsion production by sonication and microfluidization — a comparison. Int J Food Prop. 9, 2006, 475–485.

➢ Kentish S, Wooster TJ, Ashokkumar M, Balachandran S, Mawson R, Simons L. The use of ultrasonics for nanoemulsion preparation. Innovative Food Science and Emerging Technologies. 9, 2008, 170–175

➢ Lawrence, M. J., & Rees, G. D. Microemulsion based media as a novel drug delivery system. Adv Drug Del Rev. 45, 2000, 89–121.

➢ Muller RH, Jacobs C. Buparvaquone mucoadhesive nanosuspension: preparation, optimization and long-term stability. Int J Pharm. 237, 2002, 151–61.

➢ Narendra C, Srinath MS, Prakash Rao B. Development of three layered buccal compact containing metoprolol tartarate by statistical optimization technique. Int. J. Pharm. 304, 2005, 102-114.

8.0 Introduction:

Oral administration is regarded as the preferred route of drug administration, offering numerous advantages including, convenience, ease of compliance, availability to large population, and cost effectiveness. Thus, oral bioavailability plays an important role for successful therapy by this route. Oral bioavailability depends on number of factors like aqueous solubility, dissolution rate, drug permeability, presystemic metabolism, first pass metabolism and susceptibility to efflux mechanisms. Thus, only in vitro evaluation will not be able to predict exact role of nanosizing approach in improving bioavailability. Hence, to find exact improvement in bioavailability, pharmacokinetic studies must be performed which can be supported by pharmacodynamic studies. In these investigations, pharmacodynamic and pharmacokinetic studies of the prepared nanosized drug formulations were performed to know the effect of nanosizing on oral bioavailability of Simvastatin and Entacapone.

This chapter is divided in three parts:

 I.   Pharmacodynamic studies of Simvastatin formulations
 II.   Pharmacokinetic studies of Simvastatin formulations
 III. Pharmacokinetic studies of Entacapone formulations

8.1 Pharmacodynamic studies of Simvastatin formulations

Simvastatin, a HMG Co-A reductase enzyme inhibitor is known to reduce the elevated total cholesterol and TG levels in blood. At the same time, it causes an elevation of the HDL cholesterol level, which promote the removal of cholesterol from the peripheral cells and facilities its delivery back to the liver (Vogel 1997). The clinical effects of Simvastatin would be evident by lowering of total cholesterol (TC) level and increment in levels of high-density lipoprotein (HDL). This pharmacodynamic effect is reported to be dose dependent (ZOCOR literature, DFA Label) and hence, was used as a basis for the comparison of in vivo performance of the prepared formulations and the plain drug suspension.

8.1.1 Materials:

Cholesterol was purchased from National Chemicals, Vadodara, India. Coconut oil was purchased from Shanta Oil Mills, Vadodara, India. Diagnostic kit for estimation of cholesterol was purchased from Accurex diagnostics Pvt. Ltd., Mumbai, India.

8.1.2 Animals:

The hypolipidemic activity was evaluated in male Sprague-Dawley rats (250–350 g). The animals were maintained on a standard diet with free access to water and housed into groups of four. General and environmental conditions were strictly monitored. Animal handling routines were performed according to Good Laboratory Practice. The research protocol of the animal experimentation was approved by the Institutional Animal Ethics Committee of Pharmacy Department, The M.S. University of Baroda, Vadodara, India.

8.1.3 Method:

Animals were fasted overnight before starting the experiment, anesthetized by ether inhalation, and bled by retro-orbital puncture to obtain baseline values of total cholesterol (TC) in blood so that each animal served as its own control. Rats were divided into five groups namely control group receiving plain water, standard group receiving plain drug suspension (PD), and three test groups 1) Simvastatin nanosuspension (SNS) 2) Simvastatin nanoemulsion (SNE) 3) Simvastatin SCF powder (SCF). Hyperlipidemia was induced by feeding high fat diet (Ambike et al., 2005). The rats were fed with high fat diet consisting of 200 mg of cholesterol suspended in 2 ml of coconut oil daily for 14 days. Two hours following high fat diet, animals were administered with formulations at a dose of 20mg/kg of Simvastatin by oral gavage. The blood samples were withdrawn after 4, 7, and 14 days of the study. The serum was separated by centrifugation at 4000 rpm and stored at -20 C until analysis. The samples were analyzed for total cholesterol (TC), high density lipoproteins (HDL) and triglycerides (TG) by in vitro diagnostic kit (Accurex diagnostics Pvt. Ltd., Mumbai, India). The statistical analysis for the determination of the difference in the lipid levels of control and treatment groups was performed by unpaired t-test and results with P<0.05 were considered significant. The percent protection in terms of reduction in TC level was calculated as follows

$$\% \ protection = \frac{(Mean \ \% \ increase \ in \ TC \ value \ of \ control \ group - Mean \ \% \ increase \ in \ TC \ value \ of \ drug \ treated \ group) \ X \ 100}{Mean \ \% \ increase \ in \ TC \ value \ of \ drug \ treated \ group}$$

8.1.4 Results and discussion:

Administration of excess coconut oil, which is a rich source of saturated fatty acids, promotes biosynthesis of cholesterol in liver and leads to hypercholesterolemia (Elson, 1992). Hence, high fat diet i.e. coconut oil with cholesterol was used to induce hyperlipidemia (Dixit and Nagarsenkar, 2008). The serum lipid profiles of all the experimental groups at different time intervals are given in Fig. 8.1 to Fig. 8.3. Induction of hyperlipidemia was confirmed from the increase TC level and TG levels of control sample. At 4 days, 14.6 % increase in TC level was observed, which was further increased to 21.3 and 22.4 % after 7 and 14 days respectively while 29.7 % increase in TG level was observed, which was further increased to 47.3 and 43.7 % after 7 and 14 days respectively. The results indicate significant increase in TC and TG levels after administration of the high fat diet at 4, 7 and 14 days of the treatment (P<0.05). However, decrease in TC level was observed at all time intervals after administration of all formulations. But, the reduction in TC level after administration of SNS, SNE and SCF was higher as compared to PD at all time points (Fig 8.1). The change in TC levels and percent protection in term of TC reduction offered by these formulations is shown in Table 8.1 and Table 8.2.
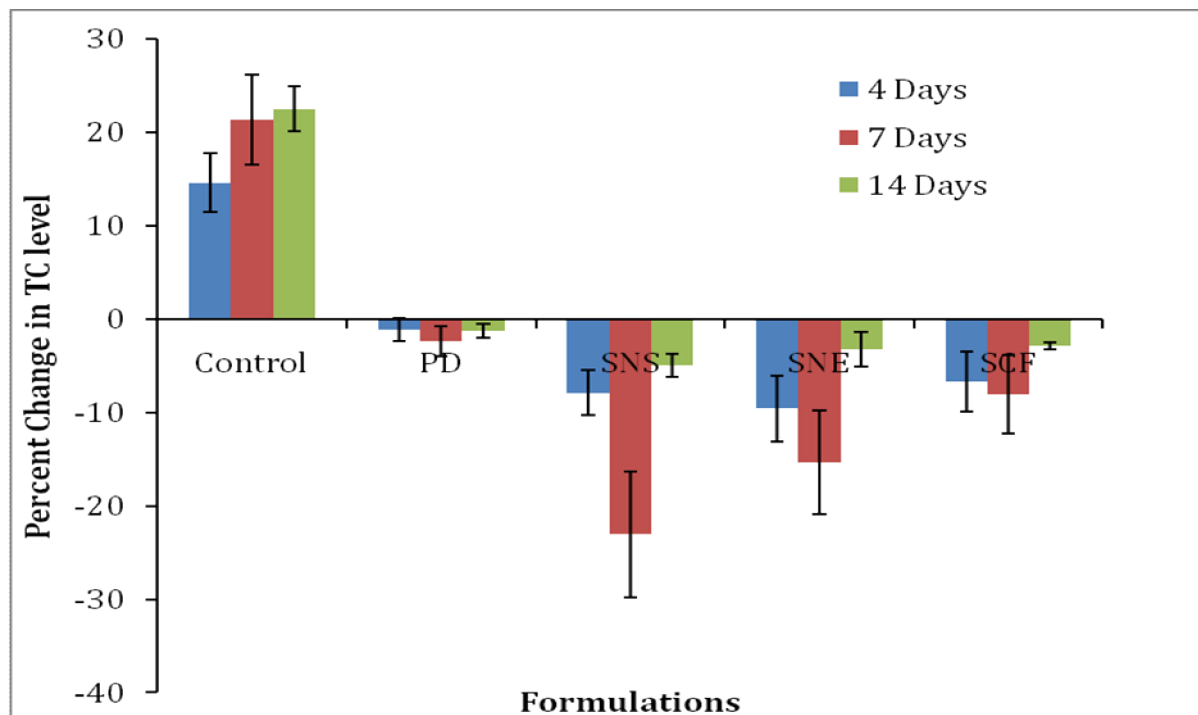
Fig. 8.1: Percent changes in serum total cholesterol level of experimental groups at different time intervals (n=4)

Table 8.1 Percent change TC level by formulations in comparison with control group

Formulations	4 days	7 days	14 days
	% changes in TC levels		
PD	-1.14±1.24	-2.39±1.66	-1.26±1.81
SNS	-7.88±2.43	-23.05±6.73	-4.97±1.24
SNE	-9.59±3.55	-15.34±5.63	-3.23±1.8
SCF	-6.74±3.26	-8.11±4.20	-2.85±0.40
Control	14.62±3.21	21.37±4.81	22.48±2.41

There was reduction in TC level for SNS (7.88±2.43), SNE (9.59±3.55) and SCF (6.74±3.26) formulation as compared to PD at 4 days. At 7 days of administration, SNS showed significant reduction in TC level (23.05±6.73 %) as compared to plain drug suspension (2.39±1.66 %) ($P<0.05$). SNE also showed significant reduction in TC level (15.34±5.63%) as compared to PD at 7 days of administration ($P<0.05$) while for SCF formulations reduction in TC level was 8.11±4.20 % at 7 days of administration. At 7 days the percent protection in term of TC reduction offered by SNS (207.8%), SNE (171.8%) was much higher than that of PD (111.3%) and SCF formulation (137.9%). At 14 days also, higher reduction in TC level was observed for SNS, SNE as compared to PD. Higher reduction in TC level was observed for SNE at 4 and 14 days as compared to PD. In all these cases, the reductions in TC levels were higher at 7 days. These results indicate that the prepared formulations (SNS, SNE and SCF) were efficient in controlling TC level as compared to PD and this can be attributed to enhanced dissolution rate of the formulations leading to improved bioavailability. Among all these formulations, SNS showed highest reduction followed by SNE and then SCF formulation.

Table 8.2 Percent protection offered by Simvastatin formulations and PD

Time in days	PD (%)	SNS	SNE	SCF
4	109.4	156.3	168.1	148.3
7	111.3	207.9	171.8	137.9
14	105.6	122.1	114.4	112.7
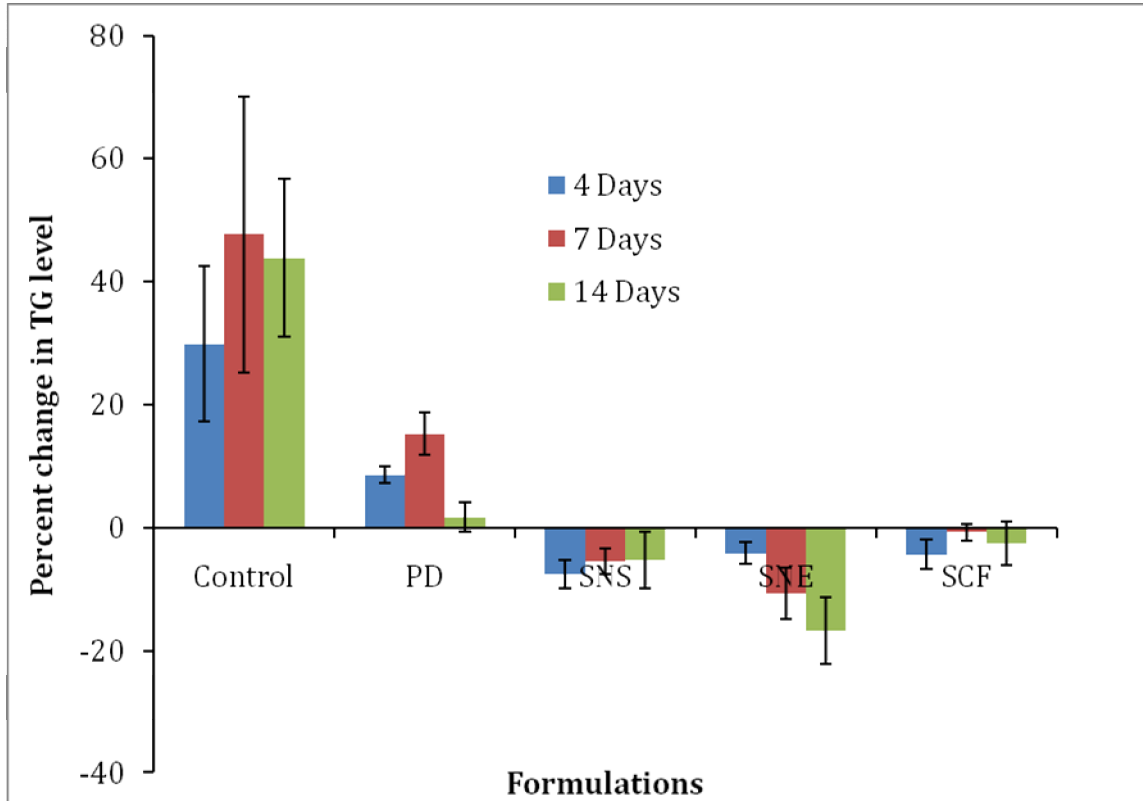
Fig. 8.2. Percent changes in serum TG level of experimental groups at different time intervals (n=4)

Similarly, the reduction in TG level in case of all formulations was higher at all intervals as compared to plain drug suspension. As compared to control, reduction in TG level was observed for plain drug suspension but it was less than other formulations. SNS showed significant reduction in TG level (7.54%) as compared to plain drug suspension at 4 days of administration (p<0.05). SNE showed significant reduction in TG level (16.70%) as compared to plain drug suspension at 14 days of administration (p<0.05). The reduction in TG levels was higher at 14 days for SNE while it was higher at 4 days for SNS and SCF formulation. These results indicate that the prepared formulations (SNS, SNE and SCF formulation) were effective in controlling lipid levels as compared to plain drug suspension which could be attributed to improved bioavailability of Simvastatin as a result of reduction in particle size and improved dissolution rate. The order of these formulation in reducing TG level was SNE>SNS>SCF>PD.
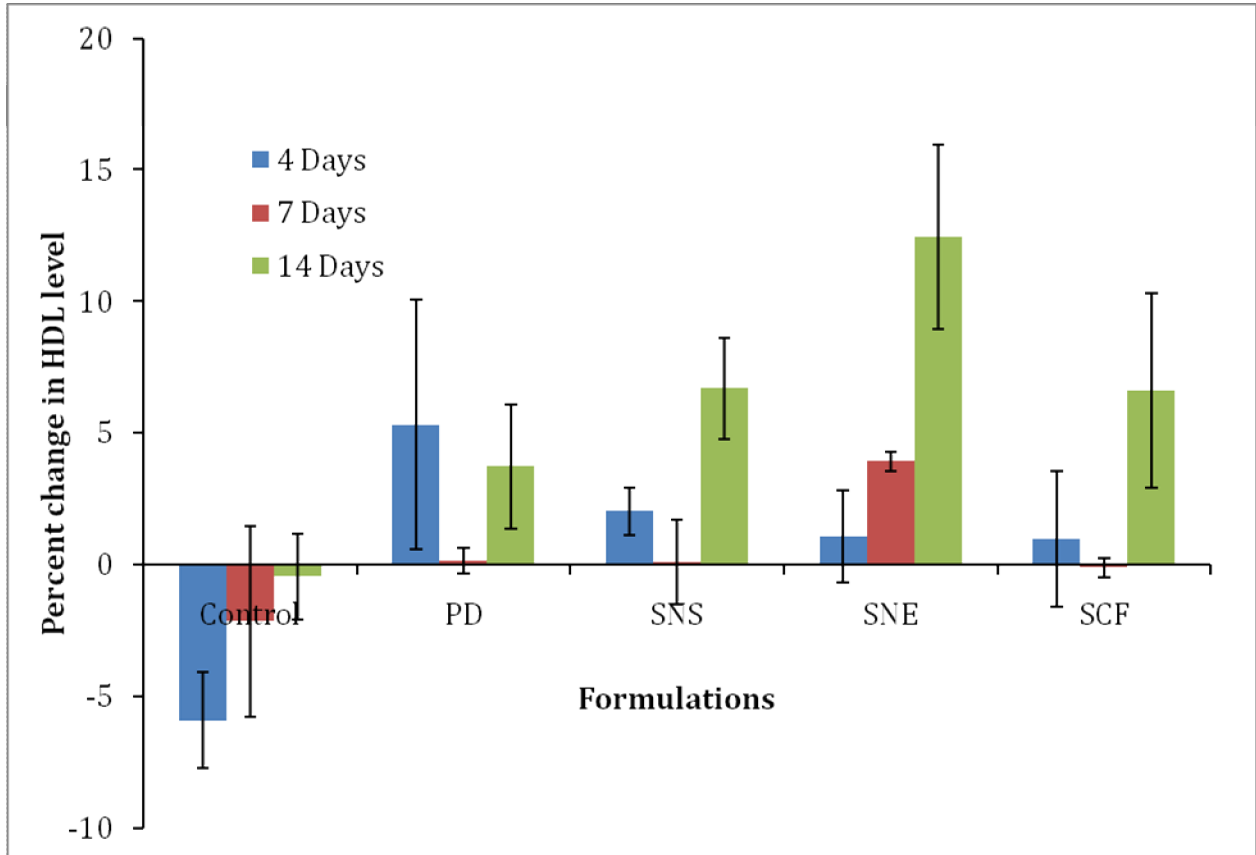
Fig. 8.3. Percent changes in HDL level of experimental groups at different time intervals (n=4)

When the HDL levels of the prepared formulations were compared, increased level was observed for all the formulations (SNS, SNE and SCF formulation) as compared to PD at 14 days. The increase in HDL level was higher at 14 days in all cases while at 4 and 7 days the difference was not significant. At 14 days, 12.43% increase in HDL level was observed for SNE as compared to PD (3.7%), SNS (6.7%) and SCF (6.6%). Thus, there was increase in HDL levels for SNS, SNE and SCF than PD. This increase in HDL level of these formulations might be due to enhanced bioavailability of Simvastatin in case of formulations.

From these results, it was observed that prepared formulations (SNS, SNE and SCF formulation) performed better in controlling hyperlipidemia than plain drug suspension. SNS showed better reduction in TC and TG levels followed by SNE and SCF formulation indicating enhanced hypolipidemic activity. This could be primarily attributed to the improved solubility and dissolution associated with these formulations.

8.2 Pharmacokinetic studies of Simvastatin formulations

8.2.1 Methods:

Simvastatin, a cholesterol-lowering agent, has been widely used in the treatment of hypercholesterolemia, dyslipidemia and coronary heart disease, but it shows low oral bioavailability due to its poor aqueous solubility and extensive metabolism by cytochrome-3A system in intestinal guts and liver. Pharmacokinetic studies were performed in rats in order to investigate the potential of prepared formulation in improving oral bioavailability of Simvastatin. The research protocol of the animal experimentation was approved by the Institutional Animal Ethics Committee of Pharmacy Department, The M.S. University of Baroda, Vadodara, India.

Male Sprague-Dawley rats (250–350 g) were used for the studies and animals were fasted overnight (12h) prior to dosing with free access to water. Rats were divided into four groups namely 1) plain drug suspension (PD), and three test groups 1) Simvastatin nanosuspension (SNS) 2) Simvastatin nanoemulsion (SNE) 3) Simvastatin SCF powder (SCF). The plain drug (PD) and three formulations (SNS, SNE and SCF) were administrated orally at a dose of 20 mg/kg using oral feeding syringe. 1.0mL of blood was withdrawn by retro-orbital puncture into heparinized tubes at specified times intervals. Plasma was separated immediately by centrifugation (10,000×g for 10 min at 4 °C) and stored in polypropylene vials below −20°C until analysis. The analyses of samples of pharmacokinetic studies were performed as per HPLC method given in section 3.5.

8.2.2 Results and discussion:

The plasma concentration- time curve for Simvastatin after oral administration of the plain drug and three formulations (SNS, SNE and SCF) are given in Fig. 8.4. Table 8.3 gives the mean plasma concentration after oral administration of these formulations. The pharmacokinetic parameters of all these formulations were determined by Kinetica software (Kinetica 5.0, Thermo Fisher Scientific). Non compartmental analysis for extra vascular administration was performed and the pharmacokinetic parameters obtained are given in Table 8.4.

Table 8.3: Plasma profiles of Simvastatin formulations in rats following oral administration

Time (h)	PD	SNS	SNE	SCF
		(ng/ml)		
0.5	2.61±1.87	4.79±0.76	6.62±1.28	4.27±1.70
1	6.28±0.88	26.65±2.54	16.74±1.11	12.95±1.40
1.5	11.65±1.43	19.09±1.43	17.63±1.47	9.83±1.31
2	3.16±1.23	7.84±0.88	15.52±1.37	5.29±1.23
3	2.27±0.84	4.31±1.44	10.14±0.55	3.86±1.03
4	1.99±1.08	3.56±0.78	6.54±1.18	3.10±0.68
6	0.74±0.46	2.74±0.56	4.38±0.36	1.94±0.61
8	ND	1.39±0.46	3.30±0.58	0.91±0.36

(n=4), ND-Not detected.
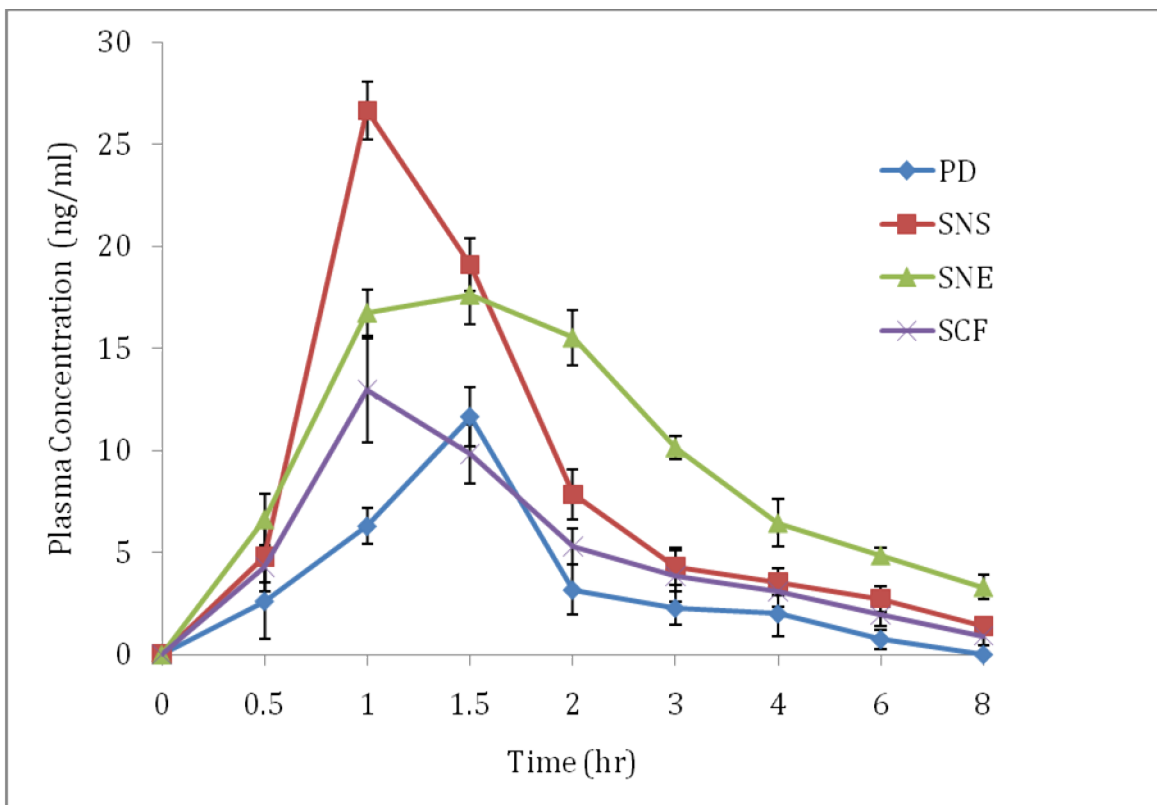
Fig. 8.4: Plasma profiles of Simvastatin formulations in rats following oral administration (n=4)

Table 8.4: Pharmacokinetic parameters after oral administration of Simvastatin formulations

Parameter	Formulation			
	PD	SNS	SNE	SCF
Cmax (ng/ml)	11.65±1.74	26.62±2.50***	17.63±1.43*	13.05±1.25^{ns}
Tmax (h)	1.5	1	1.5	1
AUC$_{last}$ (ng.h/ml)	16.73±6.56	44.11±6.45**	61.75±8.03***	30.29±6.7 ^{ns}
AUC $_{total}$ (ng.h/ml)	21.69±7.45	58.42±7.05**	78.11±13.9***	33.5±8.3 ^{ns}
MRT (h)	3.35±0.75	5.04±1.30 ^{ns}	4.75±0.91 ^{ns}	3.55±0.32 ^{ns}
t$_{1/2}$ (h)	2.35±0.59	4.43±1.46 ^{ns}	3.0±0.95 ^{ns}	2.41±0.26 ^{ns}
F (%)	100	263.6	369.0	181.0

Each value represent the mean + standard deviation (n=4)

Comparison of SNS, SNE and SCF were made with PD

- *P<0.05
- **P<0.01
- ***P<0.0001
- Ns-non significant

After oral administration, nanosized formulations i.e. SNS, SNE exhibited higher plasma level concentration compared to PD. The SCF formulation also showed higher plasma concentration as compared to PD. The AUC$_{last}$ for SNS was found to be 44.11±6.45 ng.h/ml, which was significantly higher than PD which showed AUC$_{last}$ of 16.73±6.56 ng.h/ml (P<0.001, one way ANOVA followed by Bonferroni's multiple comparison test). The AUC$_{last}$

of SNE (61.75±8.03) was also significantly higher than that of PD (P<0.0001), while it was non-significant for SCF (30.29±6.7) formulation. Among all these formulations, SNE showed highest AUC_{last} followed by SNS and SCF formulation. When the C_{max} of these formulations were compared, significant improvement in C_{max} in case of SNS compared to PD was observed (P<0.0001, one way ANOVA followed by Bonferroni's multiple comparison test). The C_{max} value was significantly higher in case of SNE (P<0.001), while there was no significant difference in case of SCF formulation. This improvement in AUC and C_{max} could be explained by the combination of the following effects: firstly, the drug molecules were absorbed rapidly from gastrointestinal wall due to the significantly improved dissolution rate by the reduced particle size with increased surface area and reduced diffusion layer thickness. Secondly, an increase in adhesion surface area between nanoparticles and intestinal epithelium of villi provides a direct contact with the absorbing membranes of the gut (Xia et al, 2010). Similarly, SNS and SNE formulations showed significantly higher AUC_{total} values as compared to the PD (P<0.001). When T_{max} of the prepared formulations was compared with PD, shortest T_{max} was observed in case of SNS which could be due to fastest dissolution rate. As expected, largest T_{max} was observed for plain PD due to its crystalline nature (Sigfridsson et al, 2007).

When $t_{1/2}$ of the prepared formulations was compared with PD, it was observed that there was no significant difference in $t_{1/2}$ of SNS (4.43±1.46), SNE (3.0±0.95) and SCF formulation (2.41±0.26) as compared to PD (2.35±0.59) Similarly, when the mean residence time (MRT) of the formulations was compared with PD, there was no significant difference observed which indicated that their elimination was comparable.

Relative bioavailability or bioequivalence is the most common measure for comparing the bioavailability of one formulation of the same drug to another. The mean responses such as C_{max} and AUC are compared to determine relative bioavailability. The AUC refers to the extent of bioavailability while C_{max} refers to the rate of bioavailability. The relative bioavailability of the SNS and SNE were 263.6 and 369.0 % respectively with respect to plain drug suspension. Thus, there was about 2.6 and 3.7 times increase in bioavailability of Simvastatin for SNS and SNE respectively and it could be attributed to enhanced surface area due to nanosizing and improved dissolution rate. SNS showed highest C_{max} among all

the formulations, indicating higher rate of bioavailability of SNS compared to all other formulations. But SNE showed highest AUC indicating better bioavailability of SNE compared to all other formulations. The relative bioavailability of SCF formulations was also 1.8 times as compared to plain drug which could be attributed to decreased particle size of SCF and physical properties of the formulation. Among all the formulations studied, SNE was the best with nearly 3.7 times increase in bioavailability followed by SNS and SCF. This was attributed to the enhanced permeability by the involved surfactant, uptake of SNE in the intestine and the comparative sustained-release of drug from SNE than SNS. Similar results were obtained for Candesartan (Gao et al. 2011). This indicates that the nanosized formulations such as SNS and SNE have tremendous potential in improving bioavailability of Simvastatin.

If the results of pharmacodynamic studies were compared with pharmacokinetic studies, it was observed that the reduction in TC level was higher in case of SNS and SNE while the relative bioavailability of these formulations was increased similarly. Thus, the results obtained in this pharmacokinetic study are well supported by the pharmacodynamic studies, which showed enhanced hypolipidemic activity of nanosized formulations compared to plain drug as indicated from % protection offered in hyperlipidemia. Thus, it can be inferred that improvement in bioavailability of Simvastatin is possible with nanosizing approaches such as nanosuspension and nanoemulsion.

8.3 Pharmacokinetic studies of Entacapone formulations

8.3.1 Methods

Entacapone is an inhibitor of catechol-O-methyltransferase (COMT), used in the treatment of Parkinson's disease as an adjunct to levodopa/carbidopa therapy and its bioavailability after oral administration is low (29–46%). Pharmacokinetic studies were performed in rats in order to investigate the potential of prepared formulation in improving oral bioavailability of Entacapone. The research protocol of the animal experimentation was approved by the Institutional Animal Ethics Committee of Pharmacy Department, The M.S. University of Baroda, Vadodara, India.

Male Sprague-Dawley rats (200–300 g) were used for the studies and animals were fasted overnight (12h) prior to dosing with free access to water. Rats were divided into four groups namely 1) plain drug suspension (PD), and three test groups 1) Entacapone nanosuspension (ENS) 2) Entacapone nanoemulsion (ENE) 3) Entacapone solid dispersion particles (E-SDP). The plain drug (ENT) and three formulations (ENS, ENE and E-SDP) were administrated by feeding syringe orally at a dose of 10 mg/kg. 1.0mL of blood was withdrawn by retro-orbital puncture into heparinized tubes at specified times intervals (0.5, 1, 2, 4, 6 and 8 hr). Plasma was separated immediately by centrifugation (10,000×g for 10 min at 4 °C) and stored in polypropylene vials below −20°C until analysis. The analyses of samples of pharmacokinetic studies were performed as per HPLC method given in section 3.6.

8.3.2 Results and discussion

The plasma concentration- time curve for Entacapone after oral administration of the plain drug and three formulations (ENS, ENE and E-SDP) are given in Fig. 8.5. Table 8.5 gives the mean plasma concentration after oral administration of these formulations. The pharmacokinetic parameters of all these formulations were determined by Kinetica software (Kinetica 5.0, Thermo Fisher Scientific). Non compartmental analysis for extra vascular administration was performed and the pharmacokinetic parameters obtained are given in Table 8.6.

Table 8.5: Plasma profiles of Entacapone formulations in rats following oral administration*

Time (h)	PD	ENS	ENE	E-SDP
		(ng/ml)		
0.5	407.64±28.87	528.17±38.76	643.87±47.20	1894.48±71.7
1	126.40±5.62	304.87±8.53	506.14±11.43	523.74±4.87
2	52.29±3.44	64.92±4.22	140.08±2.41	190.43±2.98
4	24.27±2.28	34.35±1.89	67.16±1.37	83.85±2.33
6	10.66±1.84	11.32±1.11	22.22±0.55	22.85±1.31
8	0.79±0.38	3.85±0.71	3.93±1.18	0.69±0.42

*(n=4)
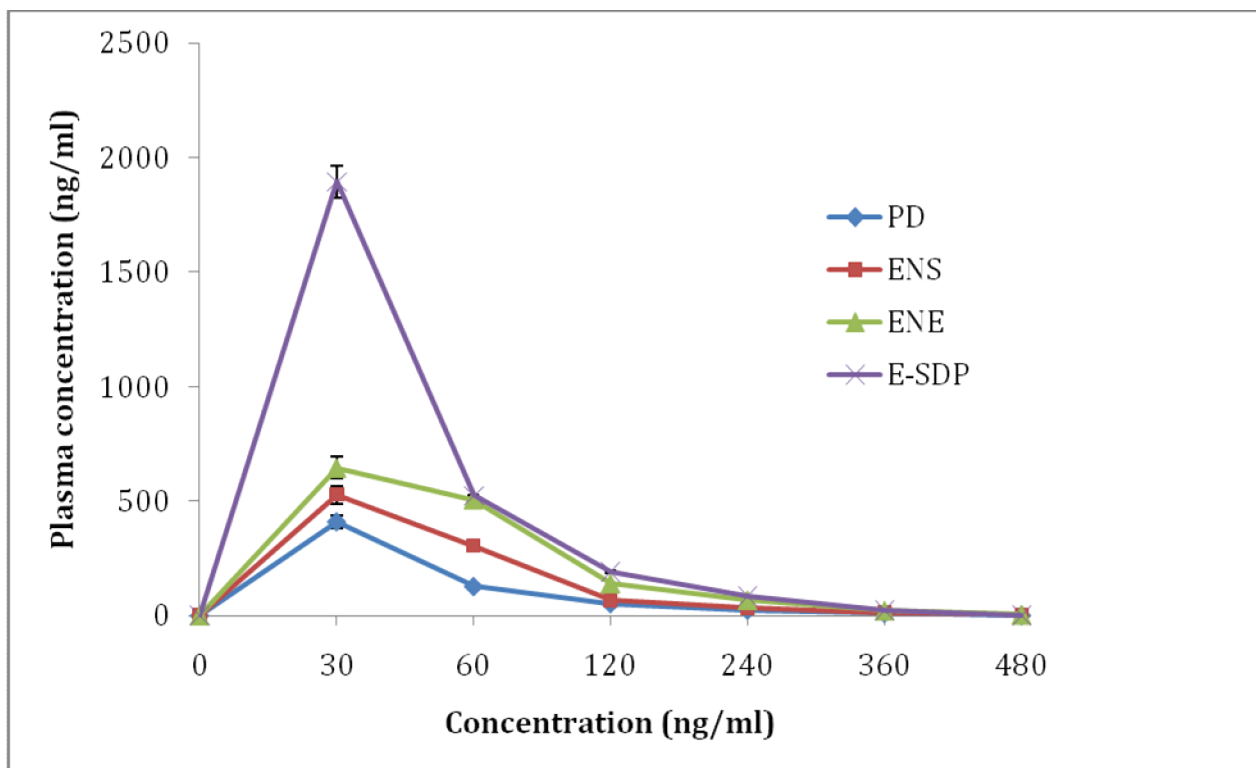
Fig. 8.5: Plasma profiles of Entacapone formulations in rats following oral administration (n=4)

Table 8.6: Pharmacokinetic parameters after oral administration of Entacapone formulations

Parameter	Formulation			
	PD	ENS	ENE	E-SDP
Cmax (ng/ml)	407.64±28.87	528.17±38.76ns	643.87±47.2**	1894.48±71.7***
Tmax (h)	0.5	0.5	0.5	0.5
AUC_{last} (ng.h/ml)	419.58±30.92	641.70±37.59***	1032.61±39.88***	1702.27±47.77***
AUC_{total} (ng.h/ml)	420.71±31.53	648.77±39.30***	1038.61±41.77***	1703.04±48.289***
MRT (h)	1.628±0.05	1.646±0.03ns	1.7817±0.006**	1.384±0.008***
$t_{1/2}$ (h)	0.9702±0.071	1.2636±0.075**	1.055±0.026ns	0.756±0.0574*
F (%)	100	152.9	246.1	405.7

Each value represent the mean + standard deviation (n=3)

Comparison of ENS, ENE and SPD were made with PD

- *P<0.05
- **P<0.01
- ***P<0.0001
- Ns-non significant

After oral administration all nanosized formulations (ENS, ENE and E-SDP) showed higher plasma concentration as compared to PD. The AUC_{last} of ENS (641.70±37.59,), ENE (1032.61±39.88) and E-SDP (1702.27±47.77) were found to be significantly higher as compared to AUC_{last} of PD (419.58±30.92). There was significant enhancement for ENE and E-SDP as compared to PD (P<0.001, one way ANOVA followed by Bonferroni's multiple

comparison test). Similarly, all these nanosized formulations showed significantly higher AUC$_{total}$ values as compared to PD (Table 8.5). The C$_{max}$ of ENE and E-SDP were 643.87±47.2 and 1894.48±71.7 ng/ml respectively, which was significantly higher as compared to AUC$_{last}$ of PD (407.64±28.87) (P<0.001, one way ANOVA followed by Bonferroni's multiple comparison test). However, the difference in ENS and PD was not significant. Overall, these results indicate improvement in bioavailability which was attributed to increased dissolution rate and bioadhesion. Nanosized particles in general possess adhesive properties apart from additional other factors which could enhance the absorption of orally administered nanoparticulate material (Muller et al, 2006). This enhancement could be attributed to adhesion of the particles to the gut wall. The enhancement of Cmax and AUC values might be due to major effect of permeability enhancement. The formulation composition might have attributed to permeation enhancement in case of ENE and E-SDP. The presence of a surfactant in the nanoemulsion system causes changes in membrane permeability by the inhibition of an apocally polarized efflux system, which could lead to enhancement of the oral absorption (Nerulkar et al, 1996). For E-SDP the presence of HPMC and Pluronic F68 might have contributed to enhancement in absorption.

Highest AUC$_{last}$ values were obtained in case of E-SDP formulation of Entacapone and it was significantly higher than that of ENS and ENE (P<0.0001, one way ANOVA followed by Bonferroni's multiple comparison test). The improvement in bioavailability of Entacapone for these formulations was in the order E-SDP>SNE>SNS. Thus, it can be said that nanoemulsion and solid dispersion particles of Entacapone were better formulation approach compared to nanosuspension.

The T$_{max}$ of all these formulations was about 0.5 hr and it might be due to fact that the time intervals considered were not able to detect changes occurring within the short time. The MRT values of ENS was not significantly different than PD but the MRT of ENE (P<0.01) and SPD (P<0.0001) were significantly different from that of PD (one way ANOVA followed by Bonferroni's multiple comparison test). This could be attributed to higher residence of SNE and E-SDP due to their formulation composition. The t$_{1/2}$ values were not significantly different in case of SNE compared to PD, but it was significantly different in case of E-SDP (P<0.05) and ENS (P<0.01 one way ANOVA followed by Bonferroni's multiple comparison test).

The relative bioavailability of the nanosized formulations with respect to PD was calculated to compare the in vivo performance of these formulations. The relative bioavailability of the ENS, ENE and E-SDP were 152.9, 246.1 and 405.7% respectively with respect to PD. Thus, there was 1.5, 2.4 and 4.0 times increase in bioavailability of Entacapone for ENS, ENE and E-SDP respectively and it could be attributed to enhanced surface area due to nanosizing and improved dissolution rate. The enhancement in dissolution rate of Entacapone (at pH 1.2) was also supported by in vitro release studies. In case of E-SDP, complete amorphization occurred, which might have contributed to enhancement in bioavailability as compared to PD and ENS. Other parameters i.e. permeability might have contributed in case of ENE and SPD. Thus, overall it can be concluded that nanosizing of Entacapone by these approaches results in improvement in its oral bioavailability. The E-SDP formulation showed highest improvement as compared to ENS and ENE.

8.4 References

- Ambike AA, Mahadik KR, Paradkar A R. Spray-dried amorphous solid dispersions of Simvastatin, a low Tg drug: In vitro and in vivo evaluations. Pharm. Res. 22, 2005, 990–998.

- Company literature on ZOCOR\ (Simvastatin) Tablets. Merck and Co., Inc, NJ, USA, pp. 1-26.

- Dixit RP, Nagarsenker MS. Formulation and In Vivo Evaluation of Self-Nanoemulsifying Granules for Oral Delivery of a Combination of Ezetimibe and Simvastatin. Drug Dev Ind Pharm. 34, 2008, 1285–1296.

- Elson CE. Tropical oils: nutritional and scientific issues. Crit Rev Food Sci Nutr. 31, 1992, 79-102.

- Gao F, Zhang Z, Bu H, Huang Y, Gao Z, Shen J, Zhao C, Li Y. Nanoemulsion improves the oral absorption of candesartan cilexetil in rats: Performance and mechanism. J Control Rel. 149, 2011, 168–174.

- Muller RH, Runge S, Ravelli V, Mehnert W, Thunemann AF, Souto EB. Oral bioavailability of cyclosporine: Solid lipid nanoparticles (SLN®) versus drug nanocrystals. Int J Pharm. 317, 2006, 82–89.

- Neurkar MM, Burton PS, Borchardt RT. The Use of Surfactants to Enhance the Permeability of Peptides Through Caco-2 Cells by Inhibition of an Apically Polarized Efflux System. Pharm Res. 13, 1996, 528–534.

- Sigfridsson K, Forssen S, Hollander P, Skantze U, de Verdier J. A formulation comparison, using a solution and different nanosuspensions of a poorly soluble compound. Eur J Pharm Biopharm. 67, 2007, 540–547.

- Vogel HG, Vogel WH. Drug Discovery and Evaluation: Pharmacological Assays, Springer-Verlag, Berlin Heidelberg. 1997, pp. 604-611.

- Xia D, Quan P, Piao H, Piao H, Sun S, Yin Y, Cui F. Preparation of stable nitrendipine nanosuspensions using the precipitation–ultrasonication method for enhancement of dissolution and oral bioavailability. Eur J Pharm Sci. 40, 2010, 325–334.

SUMMARY AND CONCLUSIONS

The oral route is by far the most convenient one for drug administration. However, for oral administration, the low concentration gradient between the gut and blood vessel due to the poor solubility of the drug leads to a limited transport, consequently influencing the oral absorption. Recently, drug delivery research mainly focuses on nanotechnology based strategies for drugs with low solubility to improve their bioavailability. Nanoparticulate technology such as pure drug nanoparticles and nanoemulsion has proven its competence for numerous drugs with low solubility in order to improve their therapeutic performance. The ability to formulate poorly-water soluble compounds as nanometer sized particles can have a dramatic effect on performance, such as enhancing bioavailability, eliminating food effects, allowing for dose escalation and hence improving efficacy and safety. Thus, the present investigations focused on nanosizing approaches such as nanosuspension and nanoemulsion.

The present investigation was aimed at the development of nanoparticulate delivery systems for oral administration of Simvastatin and Entacapone to improve their bioavailability. Nanoparticulate delivery systems such as drug nanoparticles and nanoemulsions were prepared and optimized by using factorial design. The drug nanoparticles were prepared by media milling and supercritical method while nanoemulsions were prepared by ultrasonication method.

It was envisaged that drug nanoparticles and nanoemulsions will improve solubility, dissolution rate and permeability which will ultimately increase absorption and hence bioavailability of these poorly water soluble drugs.

9.1 Simvastatin

Nanosuspensions

Simvastatin nanosuspension (SNS) was prepared by media milling method using zirconium oxide beads. The process and formulation parameters were optimized systematically. After preliminary experiments, critical parameters were identified. The important parameters such as media milling volume, surfactant concentration were optimized by factorial design.

The optimized formulation contained 0.5% w/v drug, 1% Tween 80 and 100% milling media volume and milling was carried out for 14 hr. The optimized nanosuspensions were evaluated for particle size, zeta potential, saturation solubility, surface morphology, drug content, in vitro drug release, DSC, XRD and stability studies.

Simvastatin nanosuspension (SNS) showed particle size of 250 ± 09 nm (PI 0.238) and zeta potential was -27.1 ± 3.5 mV. This indicates nanonization of Simvastatin due to media milling and resulted in improved dissolution characteristics. The increase in solubility in case of SNS was almost 3.5 folds higher than the bulk Simvastatin.

The TEM micrographs of SNS confirmed that the milling process was effective in converting bulk Simvastatin particles into the submicron range. Nanosized particles with irregular shape and without any tendency of aggregation were observed indicating change in morphology as that of plain drug which showed needle shaped crystals. XRD and DSC studies showed change in crystallinity of Simvastatin compared to plain drug. In XRD studies, the absence of major peaks of Simvastatin for SNS confirmed formation of amorphous product which might lead to enhanced solubility of the drug in case of SNS. DSC scan of bulk Simvastatin sample showed a single sharp endothermic peak at 140 °C ascribed to the melting of the drug but in SNS, disappearance of melting endothermic peak was observed which indicated substantial crystalline change of Simvastatin due to nanosizing.

Drug content of SNS formulation was found to be 98.53 ± 1.65 % which indicated suitability of method for particle size reduction. The in vitro release of nanosuspension was compared with plain drug. The drug release of 12.35 ± 0.44 % was observed in case of plain drug at 2 hr while the drug release in case of nanosuspension formulation was 39.96 ± 0.34 %. Similarly, at the end of 8 hr, 16.69 ± 0.98 % of drug was released in case of plain drug while the drug release of SNS was 52.4 ± 0.84 %. This increase in release rate can be attributed to increase in the surface area after nanosizing the crystals. The drug release from SNS followed Peppas–Korsmeyer ($r^2 = 0.9711$) and followed fickian diffusion mechanism. The SNS was found to be stable for the period of 3 months at room temperature and cold conditions. Thus, nanosizing approach could play important role in improving solubility of Simvastatin which will ultimately lead to enhancement in its bioavailability.

SCF formulation

Another approach used for size reduction of Simvastatin was supercritical methods. The plain drug particles of Simvastatin were prepared by supercritical antisolvent method using DCM as organic solvent. The process and formulation parameters were optimized to obtain minimum particle size on trial and error basis. The product obtained by supercritical method (SCF formulation) was evaluated for particle size, saturation solubility, surface morphology, flow properties, drug content, in vitro drug release, DSC, XRD and stability studies.

Simvastatin SCF formulation showed particle size of 16.54±0.38 μm (PI 0.546). This indicated reduction in particle size of Simvastatin but nanosizing did not occur. The saturation solubility in case of SCF formulation (0.614 ± 0.078) was slightly higher than plain drug (0.548± 0.062 mg/ml).

The SEM micrographs of SCF formulation confirmed that the particle size was reduced in case of SAS process but there was no conversion of bulk Simvastatin into the nanosized product. The presence of needle shaped crystals was observed. DSC XRD studies were also performed to confirm crystallinity of SCF formulation. In XRD studies of SCF formulation, all the peaks of Simvastatin were retained indicating no change in crystallinity of Simvastatin after SCF processing. This was also confirmed from DSC studies which showed that endothermic peak of Simvastatin was retained in case of SCF formulation.

Drug content of SCF formulation was found to be 97.94±1.65 % indicating suitability of the methods for particle size reduction. The release profile of SCF formulation was compared with plain drug. The drug release of 12.35±0.44 % and 15.8±0.94% was observed in case of plain drug and SCF formulation at 2 hr respectively. At the end of 8 hr, 16.69±0.98 and 18.71±0.95% of drug was released in case of plain drug and SCF formulation respectively. The drug release from SCF followed Korsmeyer-Peppas (r^2=0.9854) and followed fickian diffusion mechanism. This indicates that there was slight increase in drug release from SCF formulation. The product obtained in SCF method was very fluffy with different physicochemical properties and it also showed reduction in particle size compared to plain drug, hence was evaluated for in vivo performance.

Nanoemulsions

The nanoemulsion formulation of Simvastatin was prepared by ultrasonication method. Capryol 90 was selected as oil phase based on solubility of the drug. The process and formulation parameters were optimized systematically, in which initially process parameters such as high speed mixing time, sonication time were optimized and then selection of surfactants was done. After preliminary experiments, important parameters such as oil percentage and ratio of surfactants were optimized by factorial design.

The optimized formulation contained 15% v/v Capryol 90, 2% w/v phospholipon 90, 1% w/v Pluronic F68, 1.8% w/v drug and 85% v/v distilled water. The nanoemulsions were evaluated for particle size, zeta potential, pH, surface morphology, drug content, viscosity, in vitro drug release and stability studies.

The average particle size diameter of the Simvastatin loaded nanoemulsions was found to be 132±9nm. The polydispersity index (PI) of was low (below 0.2) and this unimodal distribution indicates uniformity in globule size.

The TEM image showed that the globules were spherical, possessed diameter ranging from 120-180 nm and had smooth surface. The drug content was found to be 98±1.2 %. The pH of the nanoemulsions was found to be 4.8±0.2. The viscosity of the nanoemulsion was found to be 2.020±0.01 cp. The nanoemulsion formulation was not viscous.

The in vitro release studies showed significant increase in drug release as compared to plain drug suspension. Plain drug suspension (PD) showed only 12.35±0.44% drug release in 2 hr while nanoemulsion (NE) showed 22.37±0.92% drug release which was approximately double. At the end of 8 hr, plain drug suspension showed only 16.69±0.95% drug release while nanoemulsion formulation showed 33.81±0.98% drug release. The drug release from SNE followed Korsmeyer-Peppas (r^2=0.9387) and followed fickian diffusion mechanism. This could be attributed to enhanced solubility and dissolution rate of Simvastatin which in turn can be due to low globule size and surface properties of the nanoemulsion. The nanoemulsion formulation showed physical stability for a period of 3 months at room temperature and cold conditions in terms of drug content and globule size.

Pharmacodynamic studies of Simvastatin formulations

The clinical effects of Simvastatin would be evident by lowering of total cholesterol (TC) level and increment in levels of high-density lipoprotein (HDL). This pharmacodynamic effect is reported to be dose dependent and hence, was used as a basis for the comparison of in vivo performance of the prepared formulations and the plain drug suspension.

Induction of hyperlipidemia was confirmed from the increase TC level and TG levels of control sample. There was significant increase in TC and TG levels after administration of the high fat diet at 4, 7 and 14 days of the treatment in control group. There was reduction in TC level for SNS (7.88±2.43), SNE (9.59±3.55) and SCF (6.74±3.26) formulation as compared to PD at 4 days. At 7 days of administration, SNS showed significant reduction in TC level (23.05±6.73 %) as compared to plain drug suspension (2.39±1.66 %) (P<0.05). SNE also showed significant reduction in TC level (15.34±5.63%) as compared to PD at 7 days of administration (P<0.05) while for SCF formulations reduction in TC level was 8.11±4.20 % at 7 days of administration. At 7 days the percent protection in term of TC reduction offered by SNS (207.8%), SNE (171.8%) was much higher than that of PD (111.3%) and SCF formulation (137.9%). At 14 days also, higher reduction in TC level was observed for SNS, SNE as compared to PD. These results indicate that the prepared formulations (SNS, SNE and SCF) were more efficient in controlling TC level as compared to PD and this can be attributed to enhanced dissolution rate of the formulations leading to improved bioavailability. Among all these formulations, SNS showed higher reduction followed by SNE and SCF formulation.

Similarly, the reduction in TG level in case of all formulations was higher at all intervals as compared to plain drug suspension. SNS showed significant reduction in TG level (7.54%) as compared to plain drug suspension at 4 days of administration (p<0.05). SNE showed significant reduction in TG level (16.70%) as compared to plain drug suspension at 14 days of administration (p<0.05). The reduction in TG levels was higher at 14 days for SNE while it was higher at 4 days for SNS and SCF formulation. Also, there was higher increase in HDL levels for SNS, SNE and SCF than PD. This reduction in TG level and increase in HDL level of these formulations compared to PD could be due to enhanced bioavailability of Simvastatin from the formulations.

Pharmacokinetic studies of Simvastatin formulations

After oral administration, nanosized formulations i.e. SNS, SNE and SCF formulation exhibited higher plasma level concentration compared to PD. The AUC_{last} for SNS was found to be 44.11±6.45 ng.h/ml, which was significantly higher than PD which showed AUC_{last} of 16.73±6.56 ng.h/ml (P<0.001, one way ANOVA followed by Bonferroni's multiple comparison test). The AUC_{last} of SNE (61.75±8.03) was also significantly higher than that of PD (P<0.0001), while it was non-significant for SCF (30.29±6.7) formulations. Among all these formulations, SNE showed highest AUC_{last} followed by SNS and SCF formulation. When the C_{max} was of these formulations were compared, significant improvement in C_{max} in case of SNS compared to PD was observed (P<0.0001, one way ANOVA followed by Bonferroni's multiple comparison test). The C_{max} value was significantly higher in case of SNE (P<0.001), while there was no significant difference in case of SCF formulation.

The relative bioavailability of the SNS and SNE were 263.6 and 369.0 % respectively with respect to plain drug suspension. Thus, there was about 2.6 and 3.7 times increase in bioavailability of Simvastatin for SNS and SNE respectively and it could be attributed to enhanced surface area due to nanosizing and improved dissolution rate. The relative bioavailability of SCF formulations was also 1.8 times as compared to plain drug which could be attributed to decreased particle size of SCF and changed physical properties of the formulation. Among all the formulations studied, SNE was the best with nearly 3.7 times increase in bioavailability followed by SNS and SCF.

The results obtained in this pharmacokinetic study are well supported by the pharmacodynamic studies, which showed enhanced hypolipidemic activity of nanosized formulations compared to plain drug as indicated from % protection offered in hyperlipidemia. Thus, it can be inferred that improvement in bioavailability of Simvastatin is possible with nanosizing approaches such as nanosuspension and nanoemulsion.

9.2 Entacapone

Nanosuspension

Entacapone nanosuspension (ENS) was prepared by media milling method using zirconium oxide beads. In preliminary experiments, milling time, type of milling media, selections of surfactant and drug concentrations were optimized. The important parameters such as media milling volume, surfactant concentration were optimized by factorial design.

The optimized formulation contained 2.0% w/v drug, 1.0% Pluronic F127 and 100% milling media volume and milling was carried out fir 12 hr. The nanosuspensions were evaluated for particle size, zeta potential, saturation solubility, surface morphology, drug content, in vitro drug release, DSC, XRD and stability studies.

Entacapone nanosuspension (ENS) was successfully prepared by milling with particle size of 231 ± 1.2 nm (PI 0.211) after 12hrs. The PDI value of Entacapone nanosuspension was below 0.25 indicating a narrow size distribution of the milled suspension. The zeta potential of the prepared ENS was -22.8 ± 3.5 mV. The saturation solubility of ENS was 2.208±0.125 mg/ml as compared to Entacapone plain drug 0.315±0.036 mg/ml, indicating significant enhancement in solubility. The increase in solubility in case of ENS was almost 7.0 folds higher than the plain Entacapone.

The appearance of ENS was compared with plain drug suspension by TEM and SEM studies. Entacapone plain drug exhibited large aggregates of needle shaped crystals while ENS showed nanosized eclipse shaped particles with smooth surface and particles were non-aggregated. TEM micrographs further confirmed that the milling process was effective in converting the Entacapone plain drug particles into the submicron range. The XRD results showed significant reduction in crystallinity of Entacapone in case of ENS as compared to plain drug. DSC scan of Entacapone plain drug showed sharp endothermic peaks at 155 and 159 °C related to the melting of the drug. This peak was not observed in case of ENS, which indicated significant reduction in crystallinity of the drug. XRD and DSC studies proved change in crystallinity of Entacapone by nanosizing.

Drug content of ENS was found to be 99.03±0.305 %. In vitro release of ENS was studied in pH 1.2 and pH 7.2 phosphate buffer. In 0.1 N HCl, within initial 10 min, 16.33 % of drug was released in case of ENS and the corresponding release for plain drug was 9.17%. Similarly

at 8 hr, 88.23 % of drug was released in case of ENS and the corresponding release for plain drug was 62.12%. At pH 7.2 also, within initial 10 min 12.27 % of drug was released in case of ENS and the corresponding release for plain drug was 10.47%. This increase in drug release could be attributed to the increased saturation solubility and surface area due to nanosizing. The higher release in case of PD could be due high solubility of drug with increased pH. The release profile was fitted in different kinetic model to find out release rate and mechanism. The ENS formulation showed value of 'n' between 0.5-10 indicating anomalous transport mechanisms at both pH conditions. The formulation was found to be stable in term of particle size and drug content for 3 months at room temperature and cold conditions.

Solid dispersion particles by SAS method

Nanosizing of Entacapone plain drug was done by SAS method, but nanonization of the plain drug was not significant, hence solid dispersion particles of Entacapone were prepared by SAS method for improving its dissolution.

Entacapone solid dispersion particles (E-SDP) were prepared by using hydrophilic polymer, HPMC K 15 and Pluronic F68. The precipitation conditions in SAS methods were optimized based on product yield and particle size obtained.

The E-SDPs were evaluated for particle size, zeta potential, surface morphology, drug content, in vitro drug release, DSC, XRD and stability studies.

The particle size of optimized E-SDPs was found to be 560±14 nm (PI 0.492). The results showed the E-SDPs obtained by supercritical antisolvent method had particle size in nanometer range indicating suitability of method for nanosizing. The zeta potential of E-SDPs was found to be -12.3 mV. The incorporation efficiency of E-SDPs was found to be 20.88±2.35 % indicating the SC CO_2-solvent system does not always dissolve the two ingredients to the same extent.

The appearance of E-SDPs was compared with plain drug suspension by TEM studies. Entacapone plain drug exhibited large aggregates of needle shaped crystals. It can be confirmed from TEM studies that morphology of bulk drug was changed by SAS method and the reduction in particle size to nanometer size was observed. The surrounding matrix

around the particles indicates the eroded HPMC matrix. The change in crystallinity of Entacapone in E-SDPs was studied by XRD and DSC studies. In case of E-SPD, all the major peaks associated with plain drug had disappeared indicating complete reduction in crystallinity. In this case, DSC scan of bulk Entacapone sample showed sharp endothermic peaks at 155 and 159 °C related to the melting of the drug. Also these characteristics peaks of Entacapone were not observed for E-SDPs indicating formation of amorphous product. Thus, a combined XRD and DSC study proved that crystallinity of Entacapone was changed by formulating as E-SDPs.

In vitro release of E-SDPs was studied at pH 1.2 and pH 7.2 phosphate buffer. The drug release of Entacapone was significantly improved in case of E-SDPs in 0.1 N HCl. Within initial 10 min, 23.27 % of drug was released in case of E-SDPs and the corresponding release for plain drug was 9.17% which could be attributed to the increased solubility due to nanosizing and solubility enhancing effect of HPMC. At pH 7.2, 20.91 % of drug was released in case of E-SDPs at 10 min while the corresponding release for plain drug was 10.47%. This could be due nanosizing and enhanced hydrophilicity of the formulation. E-SDPs showed value of 'n' of 0.47 indicating diffusion controlled mechanism at pH1.2 while at pH 7.2 value of 'n' of between 0.5-10 indicating anomalous transport mechanisms. The formulation was found to be stable in term of particle size and drug content for 3 months at room temperature and cold conditions.

Nanoemulsion

The Entacapone nanoemulsion (ENE) was prepared by ultrasonication method. Capmul MCM was selected as oil phase based on solubility of the drug. The process and formulation parameters were optimized systematically, in which initially process parameters such as high speed mixing time, selection of surfactants, sonication time were optimized. After preliminary experiments, important parameters such as oil percentage and ratio of surfactants were optimized by factorial design.

The optimized formulation contained 15% v/v Capmul MCM, 0.5% w/v phospholipon 90, 0.5% w/v Pluronic F68, 0.12% w/v drug and 85% v/v distilled water. The ENE were

evaluated for particle size, zeta potential, pH, surface morphology, drug content, viscosity, in vitro drug release and stability studies.

The average particle size diameter of the ENE was found to be 120.8±1.9nm. The polydispersity index (PI) of ENE was 0.144 (below 0.2) and this unimodal distribution indicates uniformity in globule size. The zeta potential of ENE was found to be -20.6±0.8 mV. The drug content was found to be 99.4±0.8 %. The pH of the nanoemulsions was found to be 5.5±0.2 indicating suitability for oral administration. The viscosity of the nanoemulsion was found to be 1.63 ±0.02 cp.

Morphology and droplet size of the ENE was evaluated by TEM. The TEM image showed that the globules were almost spherical, and had diameter ranging from 120-150 nm. The globules were segregated and showed no tendency of aggregation.

The in vitro release profile of ENE and plain drug suspension (PD) was studied at pH 1.2. The in vitro release studies showed increase in drug release for ENE as compared to PD at pH 1.2. Plain drug suspension showed only 25.05±0.44% drug release in 60 min while nanoemulsion formulation showed 31.77±0.92% drug release. At 8 hr, Plain drug suspension showed 62.12% drug release while nanoemulsion formulation showed 80.33±0.92% drug release indicating improved drug release which could be attributed to enhanced solubility of Entacapone and dissolution rate which in turn can be due to low droplet size and surface properties of the nanoemulsion. ENE formulations showed value of 'n' between 0.5-1.0 indicating anomalous transport mechanisms at both pH conditions. ENE showed value of 'n' between 0.5-1.0 indicating anomalous transport mechanisms at pH 1.2. The nanoemulsion formulation found to be stable in term of globule size and drug content for the period of 3 months at room temperature and cold conditions.

.

Pharmacokinetic studies:

After oral administration, all nanosized formulations (ENS, ENE and SDP) showed higher plasma concentration as compared to PD. The AUC_{last} of ENS (641.70±37.59,), ENE (1032.61±39.88) and E-SDP (1702.27±47.77) were found to be significantly higher as compared to AUC_{last} of PD (419.58±30.92). There was significant enhancement for ENE and E-SDP as compared to PD (P<0.001, one way ANOVA followed by Bonferroni's multiple

comparison test). Similarly, all these nanosized formulations showed significantly higher AUC_{total} values as compared to PD. The C_{max} of ENE and E-SDP were 643.87±47.2 and 1894.48±71.7 ng/ml respectively, which was significantly higher as compared to AUC_{last} of PD (407.64±28.87) (P<0.001, one way ANOVA followed by Bonferroni's multiple comparison test). However, the difference in ENS and PD was not significant. Overall, these results indicate improvement in bioavailability which was attributed to increased dissolution rate and bioadhesion. The presence of a surfactant in the nano-formulation causes changes in membrane permeability by the inhibition of an apocally polarised efflux system, which could lead to enhancement of the oral absorption. Thus, formulation composition might have attributed to permeation enhancement in case of ENE and E-SDP.

The relative bioavailability of the nanosized formulations with respect to PD was calculated to compare the in vivo performance of these formulations. The relative bioavailability of the ENS, ENE and E-SDP were 152.9, 246.1 and 405.7% respectively with respect to PD. Thus, there was 1.5, 2.4 and 4.0 times increase in bioavailability of Entacapone for ENS, ENE and E-SDP respectively and it could be attributed to enhanced surface area due to nanosizing and improved dissolution rate. The enhancement in dissolution rate of Entacapone (at pH 1.2) was also supported by in vitro release studies. In case of E-SDP, complete amorphization was observed which might have contributed to enhancement in bioavailability as compared to PD and ENS. Other parameters i.e. permeability might have contributed in case of ENE and E-SPD. Thus, overall it can be concluded that nanosizing of Entacapone by these approaches results in improvement in its oral bioavailability.

9.3 Conclusions:

In the present investigations, nanoparticulate delivery systems such as nanosuspensions, nanoemulsions and SCF formulations by SAS method were prepared for oral administration of Simvastatin and Entacapone to improve their bioavailability. In the in vivo studies, the relative bioavailability of the SNS, SNE and SCF were 263.6%, 369.0% and 181% respectively with respect to plain drug suspension for Simvastatin. Also in pharmacodynamic studies, better reduction in TC levels was observed as compared to plain drug in case of SNS, SNE and SCF formulation. Similarly, the relative bioavailability of the

ENS, ENE and E-SDP were 152.9, 246.1 and 405.7% respectively with respect to PD for Entacapone. The improvement in bioavailability of Simvastatin and Entacapone was supported by the physicochemical characteristics of the nanosized formulations. Enhanced dissolution was observed for these systems compared to conventional drug suspension.

The results of the present investigations conclusively indicate the enhancement in bioavailability of the drugs, Simvastatin and Entacapone, when administered as nanosized formulations through oral route. Hence, the developed nanosized formulations of Simvastatin and Entacapone can be potentially useful in clinical treatment of hypertension and Parkinson's disease respectively. Thus, these formulations hold promise as better alternative to the conventional dosage forms. However, further investigations in human beings under clinical conditions are necessary before they can be commercially exploited.

PRESENTATIONS AND PUBLICATIONS

List of Presentations

1. Sandip Chavhan, Kailash Petkar, Krutika Sawant. "Design, Development and evaluation of novel nanoemulsion for improved biovailability of Simvastatin" presented at 14th Candian Society of Pharmaceutical Sciences (CSPS) Annual Symposium, Montreal, CANADA, 24-28th May 2011.

2. Sandip Chavhan, Heena Soni, Kailash Petkar, Krutika Sawant. "Nanosized particles of simvastatin for enhanced dissolution and hypolipidemic activity" presented at 38th Controlled Release Society (CRS) Annual Symposium, Maryland, USA, 30 July- 03 Aug 2011.

List of Publications

1. Sandip Chavhan, Kailash Petkar, Krutika Sawant. Nanosuspensions in Drug Delivery: Recent advances, Patent Scenario and Commercialization Aspects. Critical Reviews in Therapeutic Drug Carrier Systems, 28(5), 447-488, 2011.

2. Kailash Petkar, Sandip Chavhan, Agatonovik Kustrin, Krutika Sawant. Nanostructured biomaterials in Drug/Gene Delivery: A Review of the State of the Art. Critical Reviews in Therapeutic Drug Carrier Systems, 28(1), 45-114, 2011

3. Sandip Chavhan, Kailash Petkar, Krutika Sawant. "Nanosizing of simvastatin for enhanced dissolution and hypolipidemic activity". Manuscript under preparation.

4. Sandip Chavhan, Kailash Petkar, Krutika Sawant. "Design, Development and evaluation of novel nanoemulsion for improved biovailability of Simvastatin". Manuscript under preparation.

Book Chapter

1. Sandip Chavhan, Kailash Petkar, Krutika Sawant. Nanosizing approaches in Drug Delivery. Accepted for publication in "Clinical Nanomedicine: From Bench to Bench side" 2011, Pan Stanford Publication, USA.

ERRATA

Sr. No.	Page No.	Line	Existing	Corrected